2022

Multiomic Hypotheses Underlying Behavioral Manipulation of Camponotus floridanus ants by Ophiocordyceps camponoti-floridani fungi

Ian Will
University of Central Florida

MULTIOMIC HYPOTHESES UNDERLYING BEHAVIORAL MANIPULATION OF *CAMPONOTUS FLORIDANUS* ANTS BY *OPHIOCORDYCEPS CAMPONOTI-FLORIDANI* FUNGI

by

IAN WILL
M.S. Ludwig-Maximilians-Universität München, 2015

A dissertation submitted in partial fulfillment of the requirements
for the degree of Doctor of Philosophy
in the Department of Biology
in the College of Sciences
at the University of Central Florida
Orlando, Florida

Summer Term
2022

Major Professor: Charissa de Bekker

ABSTRACT

Parasitic manipulation of host behavior lies at the intersection of disease, animal behavior, and coevolutionary processes. In many of these interactions, the underpinning biology is brought into sharp focus as they are obligate relationships, under strong selection to bring about specific changes in host behavior that determine if the parasite will transmit or die. However, experimental and molecular techniques to understand these interactions are still developing and identification of the mechanisms of manipulation is a primary goal in the field. As such, we investigated host-parasite interactions between *Camponotus floridanus* (Florida carpenter ant) and *Ophiocordyceps camponoti-floridani* (Florida zombie ant fungus) from multiple molecular perspectives. By combining genome, gene expression, protein-interaction, and metabolite data from multiple experiments, we analyzed parasitic manipulation in a multiomic framework. We considered the most robust hypotheses of how parasitic manipulation occurs to be those supported by multiomic data. Two major avenues of parasitic influence on host behavior appear to be direct interference with neurotransmission and dysregulation of core cellular pathways that affect behaviors. For example, heightened expression of host dopamine synthesis enzyme genes, predicted binding of secreted parasite proteins to dopamine receptors, and reduced dopamine precursor abundance during displays of manipulated behavior all correlate the dysregulation of dopaminergic processes to manipulation phenotypes. We discuss numerous possible hypotheses, many with multiomic support, some without. We predict that modification of host behavior is a complex and multi-layered process that integrates multiple mechanisms we propose here.

ACKNOWLEDGMENTS

The years of my PhD work have relied upon the collaboration, support, and guidance of many people. **Charissa de Bekker** put much effort into advising me not only for the duration of the work presented here, but she first began mentoring me during my Master's in Germany where she introduced me to fungal fun and invited me to join her new lab team at UCF. And, thank you to my dissertation committee, **Ken Fedorka**, **Anna Savage**, and **Jason Slot** for their encouragement, critical advice, and timely assistance in jumping through those administrative hoops. **Biplabendu Das** and **Thienthanh Trinh** were there with me from the start when we all arrived in Florida confused and alone, as Charissa's first batch of graduate students. We quickly became fast friends and indispensable collaborators. Both of them were key to getting the work done, but also finding that balance with the rest of life. **Jordan Dowell** was an insightful sounding board for experiment discussions – and will continue to be a lasting friend and colleague, whether talking science and institutional reform or bringing the party. **Devin Burris** joined our lab group as an undergraduate honors researcher, pushing forward functional testing of our candidate genes and was a helpful and reliable hand in the lab. **Sophia Vermeulen** helped out with some experiments while still learning the ropes on her own graduate research, and we've become pretty good pals and benchmates along the way. **Andrea Bender** toiled away as an undergraduate technician to set up an expansive library of components that I used for molecular cloning work, and set me up with my first scoby that is still thriving and fermenting. Shout out to the other important, supportive folks that have been especially bright spots during my years here, **Mayer**, **Vero**, **Sarah**, **Alicia**, and other good friends. I am also grateful for my fellowship and financial support from UCF and Charissa's thoughtful inclusion of me in an awarded NSF grant (NSF-CAREER IOS-1941546). I'd also like to recognize the hundreds of ants that gave it up so we could push this work forward.

Thanks everybody.

TABLE OF CONTENTS

LIST OF FIGURES

LIST OF TABLES

CHAPTER ONE: INTRODUCTION

Exploiting more than host resources, certain parasites behaviorally manipulate their hosts to promote transmission. Modifying host behavior to aid the critical step of parasite transmission has evolved across taxa; with the ant-manipulating *Ophiocordyceps* fungi being leveraged as a tractable model to investigate this phenomenon (Moore 2002, 1995; Thomas *et al.* 2010; Lafferty and Kuris 2012; Adamo *et al.* 2013; Lafferty and Shaw 2013; de Bekker *et al.* 2014a, 2018, 2021; Poulin and Maure 2015; Herbison 2017; Hafer-Hahmann 2019; de Bekker 2019). Parasitic manipulation can impact ecosystems by modifying habitat availability, energy flow in trophic systems, or transmission of coinfecting parasites (Lafferty and Morris 1996; Thomas *et al.* 1997, 1999, 2002; Sato *et al.* 2011a, 2011b; Lafferty and Kuris 2012). Although the natural history and impacts of parasitic manipulations have been documented to some extent, the mechanisms and underlying biology have yet to be conclusively established (Herbison 2017; de Bekker *et al.* 2021). Developing a sophisticated understanding of behavioral manipulation biology would likely offer new perspectives on the molecular fundamentals of animal behavior, infection biology, and identification of novel bioactive compounds. Working toward this goal, hypotheses of entomopathogenic manipulation are accumulating from multiple taxa (de Bekker *et al.* 2021). Despite using evidence from phylogenetically distant parasites (e.g., diverse fungi, viruses, and helminth worms), many of these hypotheses are linked by common phenotypes elicited in their insect hosts such as increased locomotor activity, changes in social behavior, and summiting to elevated or exposed positions (de Bekker *et al.* 2018, 2021). To refine, prioritize, and supplement these hypotheses, we investigated manipulation of *Camponotus floridanus* (Florida carpenter ant) by *Ophiocordyceps camponoti-floridani* (Florida zombie ant fungus) with multiple bioinformatic-scale data types ("multiomics").

Ophiocordyceps species manipulate ant behavior and kill their hosts to further the parasite life cycle. Infected ants display hyperactivity, deviation from foraging trails, and a summiting behavior where they latch onto vegetation, suspended there until their death (Pontoppidan *et al.* 2009; Andersen *et al.*

2009; Hughes *et al.* 2011; Mongkolsamrit *et al.* 2012; de Bekker *et al.* 2015; Chung *et al.* 2017; Loreto *et al.* 2018; Andriolli *et al.* 2019; Trinh *et al.* 2021). This behavioral manipulation provides a growth and transmission site that appears to be adaptive for the fungal parasite (Andersen *et al.* 2012; Loreto *et al.* 2014, 2018; Will *et al.* 2022 under review). Parasite-adaptative changes in ant behavior have been hypothesized to operate by release of fungal bioactive compounds and destruction of host tissues (Evans *et al.* 2011a; de Bekker *et al.* 2014b, 2015; Fredericksen *et al.* 2017; Kobmoo *et al.* 2018; de Bekker 2019; Mangold *et al.* 2019; Zheng *et al.* 2019; Loreto and Hughes 2019). These proposed mechanisms span interference with neurotransmission to disruption of behavior-regulating signals to invasion and atrophy of mandible muscles.

Within each of these proposed scenarios of how *Ophiocordyceps* manipulates ant biology, multiple specific molecular mechanisms are plausibly involved. In Chapter 2, we compared two ant-manipulating *Ophiocordyceps* species and their respective *Camponotus* hosts to investigate common patterns in gene expression underlying manipulation. Genes identified through this method reflect shared selection pressures to manipulate ant behavior, although the fungal species we compared occupy distinct clades within the *Ophiocordyceps unilateralis* species complex and their hosts belong to different subgenera (Bolton 1995; Araújo *et al.* 2018). *Ophiocordyceps* species have been often, but not always, reported as host-specific specialists, with one *Ophiocordyceps* species infecting one ant species (Evans *et al.* 2011b; de Bekker *et al.* 2014b; Araújo *et al.* 2018; Sakolrak *et al.* 2018; Lin *et al.* 2020). However, the many homologous genes similarly expressed during manipulation suggest common manipulation mechanisms were conserved or convergently evolved. We published this work in the journal G3: Genes, Genomes and Genetics (Will *et al.* 2020).

To expand upon hypotheses developed from examining genomes and transcriptome expression, we used these data to predict a host-pathogen protein interactome (Chapter 3). Protein-protein interactions (PPIs) between host and parasite could regulate virulence, elicit host responses, and modify host

physiology. We computationally predicted host-parasite PPIs to improve interpretation of possible fungal effectors highlighted in Chapter 2. These predictions also produce new hypotheses about which proteins and functions might have a role in shaping infections and manipulation. Proteome-scale *in silico* predictions of PPIs between species are not yet a routine undertaking and best practices are still developing. As such, we tested two methods. The first method we used was a more "traditional" homology-based approach. By matching proteins from our organisms to known PPIs in other systems, usually single-species self-interactions, we predicted homologous interactions – or "interologs" (Walhout *et al.* 2000). For our study, with two distantly related non-traditional model organisms, few interolog PPIs were identified. We then used a recently published machine learning method (Sledzieski *et al.* 2021). This approach used generalizable protein structure models to make PPI predictions that yielded many more putative interactions for us to analyze.

Finally, in Chapter 4, we generated a new metabolomic dataset composed of three subsets tailored to detection of different compound classes (biogenic amines, polyphenols and flavonoids, and lipids). Here, we collected metabolomic data of healthy and manipulated ants. These data, representing fundamentally different molecules than Chapters 2 or 3 (DNA/mRNA versus untargeted metabolomics) from separate experiments gave us the opportunity to build multiomic hypotheses of manipulation. When multiple signals across molecular levels and experiments could be interpreted as parts of a single hypothesis, we considered these our strongest candidate mechanisms. However we did not wholly discount hypotheses with support from only one data type. We used these metabolomic data in a similar manner as genetic data. That is, we used enrichment and group level analyses as well as highlighted key compounds. However, only a fraction of the data were annotated, and further compound-specific searches may turn up additional informative signals.

Broadly speaking, some of the key molecules or pathways that had multiomic support included those reported in the literature: neurotransmitters and signaling, regulation of foraging behaviors, and

tissue destruction (Lovett *et al.* 2020; de Bekker *et al.* 2021). Even outside of entomopathogenic manipulators, common threads of neuromodulators, altered nutritional signals, and dysregulated immunity have been correlated to locomotor behaviors, summiting, and hyperactivity (Adamo *et al.* 2013; Lafferty and Shaw 2013; Moore 2013; Herbison 2017). Each of these categories contain multiple specific mechanisms we discuss in the following chapters. Those specific, molecule-by-molecule, hypotheses are the ones most amenable to direct experimental testing. We likely can extract more information from the interactome and metabolome datasets with analyses beyond those reported here, but then experimental testing is the next key step. These experiments will be able to use our most robust hypotheses as starting points in choosing which mechanisms might be the most important and experimentally tractable. *Ophiocordyceps-Camponotus* interactions are among the most approachable study systems in parasitic manipulation biology; characterization of these organisms likely will offer generalizable insights to the field overall. As we bring the manipulation mechanisms used by *Ophiocordyceps*, and others, into focus, these findings may help us understand intricately coevolved host-parasite manipulations, the neurobiology of insects and other animals, and the identification of novel bioactive compounds.

CHAPTER TWO: GENETIC UNDERPINNINGS OF HOST MANIPULATION BY *OPHIOCORDYCEPS* AS REVEALED BY COMPARATIVE TRANSCRIPTOMICS

Abstract

Ant-infecting *Ophiocordyceps* fungi are globally distributed, host manipulating, specialist parasites that drive aberrant behaviors in infected ants, at a lethal cost to the host. An apparent increase in activity and wandering behaviors precedes a final summiting and biting behavior onto vegetation, which positions the manipulated ant in a site beneficial for fungal growth and transmission. We investigated the genetic underpinnings of host manipulation by: (*i)* producing a high-quality hybrid assembly and annotation of the *Ophiocordyceps camponoti-floridani* genome, (*ii*) conducting laboratory infections coupled with RNAseq of *O. camponoti-floridani* and its host, *Camponotus floridanus*, and (*iii*) comparing these data to RNAseq data of *Ophiocordyceps kimflemingiae* and *Camponotus castaneus* as a powerful method to identify gene expression patterns that suggest shared behavioral manipulation mechanisms across *Ophiocordyceps*-ant species interactions. We propose differentially expressed genes tied to ant neurobiology, odor response, circadian rhythms, and foraging behavior may result by activity of putative fungal effectors such as enterotoxins, aflatrem, and mechanisms disrupting feeding behaviors in the ant.

Introduction

Transmission from one host to the next is a crucial step in the life cycle of parasites. Certain parasites have evolved to adaptively manipulate the behavior of their animal hosts to aid transmission. Many examples of manipulating parasites and their hosts have been reported across taxa and are active topics of research (Moore 1995, 2013; Thomas *et al.* 2010; Lafferty and Kuris 2012; Poulin and Maure 2015; de Bekker *et al.* 2018; Hafer-Hahmann 2019), with the ant-manipulating *Ophiocordyceps* fungi emerging as a notable model (de Bekker *et al.* 2014a; de Bekker 2019). However, in most parasitic

manipulation systems, including *Ophiocordyceps*-ant interactions, the mechanisms by which the parasite dysregulates animal behavior are largely unknown (Herbison 2017). As such, the study presented here seeks to home in on the major players involved in *Ophiocordyceps* infection and manipulation of carpenter ants by using a comparative transcriptomics framework to identify, compare, and discuss candidate genes underlying manipulation across two different fungus-ant species interactions. The species we compare are *Ophiocordyceps kimflemingiae* and its host *Camponotus castaneus*, on which mechanistic work has previously been performed (de Bekker *et al.* 2014b, 2015; Fredericksen *et al.* 2017; Mangold *et al.* 2019; Loreto and Hughes 2019), and *Ophiocordyceps camponoti-floridani* (Araújo *et al.* 2018) and its host *Camponotus floridanus*. The interactions between the latter pair have not yet previously been investigated.

Ant-manipulating *Ophiocordyceps* infect ants and modify their behavior to complete the parasite life cycle, at a lethal cost to the host. Infected ants display hyperactivity or enhanced locomotor activity (ELA) (Hughes *et al.* 2011; de Bekker *et al.* 2015), deviation from foraging trails (Pontoppidan *et al.* 2009; Hughes *et al.* 2011), and a summiting behavior coupled with biting and clinging to attach themselves to vegetative substrates until death (Pontoppidan *et al.* 2009; Andersen *et al.* 2009; Hughes *et al.* 2011; Mongkolsamrit *et al.* 2012; Chung *et al.* 2017; Andriolli *et al.* 2018; Loreto *et al.* 2018). This final fatal change in behavior is the most tractable readout for manipulation of the host, and provides a growth and transmission site that appears to be adaptive for the fungal parasite (Andersen *et al.* 2012; Loreto *et al.* 2014). Bioactive compounds with neuromodulatory and physiology-disrupting effects (de Bekker *et al.* 2014b, 2015; Kobmoo *et al.* 2018; de Bekker 2019; Loreto and Hughes 2019), and tissue destruction and hypercontraction of jaw muscles (Hughes *et al.* 2011; Fredericksen *et al.* 2017; Mangold *et al.* 2019) have been proposed as possible means of dysregulating host behavior. Moreover, manipulated biting appears to be synchronized by time of day in multiple *Ophiocordyceps*-ant species interactions (Hughes *et al.* 2011; de Bekker *et al.* 2014a, 2015, 2017b; de Bekker 2019). This suggests that

Ophiocordyceps fungi also employ mechanisms to modify host behaviors that operate according to daily rhythms and are under control of the hosts' biological clocks (Hughes *et al.* 2011; de Bekker *et al.* 2014a, 2015, 2017b; de Bekker 2019).

Multiple reports indicate that manipulation of ant behavior only occurs in a host-specific manner, with a single species of *Ophiocordyceps* manipulating a single species of ant (Evans *et al.* 2011; de Bekker *et al.* 2014b; Araújo *et al.* 2018; Sakolrak *et al.* 2018). Part of the mechanisms involved in manipulation of ant behavior might, therefore, be species specific (de Bekker *et al.* 2017a). However, convergently evolved and conserved mechanisms are likely also shared among these specialized *Ophiocordyceps* fungi as they have common evolutionary histories (Araújo and Hughes 2019) and are confronted with similar ecological obstacles (i.e. the modification of ant behavior to attach to elevated transmission sites) (Chetouhi *et al.* 2015; Loreto *et al.* 2018). Investigating these shared mechanisms across *Ophiocordyceps* and their host ant species would elucidate the common elements involved and aid in the identification of candidate genes and compounds that are key to establishing manipulation. Comparative proteomics to understand manipulated phenotypes induced by mermithid worms have demonstrated that such approaches can identify candidate convergent mechanisms of host manipulation across taxa (Herbison *et al.* 2019). As such, we conducted comparative transcriptomics to reveal candidate genes underscoring manipulation that could offer new insights into ant neurobiology and behavior, novel fungal bioactive compounds, and specific understanding of *Ophiocordyceps-Camponotus* interactions. These comparative studies may provide evidence and hypotheses for molecular mechanisms driving comparable manipulation phenotypes in other systems. Baculoviruses that manipulate the behavior of moth larvae also elicit host ELA, climbing, and eventual death at an elevated position, thereby dispersing viral propagules (Kamita *et al.* 2005; van Houte *et al.* 2014a; Han *et al.* 2018). Two primary viral genes have been proposed to be necessary in driving manipulation in this system, ecdysteroid UDP-glucosyl transferase (*egt*) (Hoover *et al.* 2011; Ros *et al.* 2015; Han *et al.* 2015) and

protein tyrosine phosphatase (*ptp*) (Kamita *et al.* 2005; Katsuma *et al.* 2012). Another example of a fatal summiting phenotype as a result of parasitic manipulation is induced by the distantly related *Entomophthora muscae* fungi that infect and manipulate flies (Krasnoff *et al.* 1995; Elya *et al.* 2018). Since *Ophiocordyceps,* Baculovirus, and *Entomophthora* are all presented with the similar challenge of inducing summiting behavior to establish effective parasite transmission, quite plausibly their manipulation mechanisms have convergently evolved.

In the study presented here, we infected *C. floridanus* with *O. camponoti-floridani* and performed RNAseq on both organisms sampled before infection, during manipulated clinging, and after host death. Subsequently, we compared our gene expression data to previous transcriptomics work done in *O. kimflemingiae* and *C. castaneus* (de Bekker *et al.* 2015). Both *Ophiocordyceps* species reside in different clades within the *Ophiocordyceps unilateralis* species complex (Araújo *et al.* 2018), which are genomically vastly different (de Bekker *et al.* 2017a). Furthermore, our approach informs RNAseq of *C. floridanus* with a corresponding and updated genome (Shields *et al.* 2018), unlike the previous work that was constrained to using a *C. floridanus* genome to inform RNAseq of *C. castaneus*. With this framework, we transcriptionally compare fungal parasites and ant hosts, highlighting possible shared mechanisms involved in manipulation. To this end, we also report the first annotated genome assembly of *O. camponoti-floridani* using a long-read short-read hybrid approach. We propose candidate fungal genes and possible scenarios by which they may contribute to infection and manipulation of *Camponotus* hosts. Similarly, we highlight host genes that possibly reflect changes in behavior and challenges to physiology due to fungal infection and manipulation. Our findings include changes in genes associated with ant neurobiology, odor detection, and nutritional status, as well as fungal genes related to toxins, host feeding behavior pathways, proteases, and putative effectors similar to those previously reported in Baculovirus. We propose possible scenarios by which these genes reflect or promote changes in host behavior and physiology as further evidence or new grounds for hypotheses in the field of behavior manipulating

parasitism. We have organized our findings and these scenarios in several comprehensive sections below that discuss principal component analyses (PCA) and weighted gene coexpression network analyses (WGCNA) analyses for ant and fungal data, functional enrichments and differentially expressed genes found in both ant and fungus, and upregulated fungal secondary metabolite clusters.

Methods

Fungal isolation & culture: To sequence the genome and perform infection studies followed by transcriptome sequencing, we isolated and cultured two strains of the fungus *Ophiocordyceps camponoti-floridani*. Strain EC05, used for the de novo genome assembly, was collected from Little Big Econ State Forest in Seminole County, Florida. Strain Arb2 was collected at the University of Central Florida arboretum in Orange County, Florida and used for laboratory infections and RNAseq data. These samples were obtained by permission from the University of Central Florida and the Florida Department of Agriculture and Consumer Services.

Both strains were isolated by surface sterilizing infected *Camponotus floridanus* cadavers in 70% ethanol for 10 sec and aseptically removing ant cuticle with 25 G needles (PrecisionGlide, BD) to extract *O. camponoti-floridani* mycelium. Extracted fungal masses were plunged into a solid medium (7.8 g/L potato dextrose agar [BD], 6 g/L agar [BD], 100 mg/L Penicillin/Streptomycin [Gibco], and 100 mg/L Kanamycin [Alfa Asear]) and maintained at 28°C for 15 days to screen for possible contaminants and indications of sample viability. We placed viable extractions into liquid culture in T25 tissue flasks (CytoOne, USA Scientific) containing Grace's Insect Medium (Unsupplemented Powder, Gibco) supplemented with 10% Fetal Bovine Serum (FBS) (Sterile Filtered US Origin, Gibco). Incubation at 28°C and 50 rpm promoted blastospore growth. Once the culture was established, we reduced FBS to 2.5% for secondary cultures.

Both EC05 and Arb2 nuclear 18S ribosomal short subunit (SSU) sequences matched voucher JA-2017c Flx1 (Araújo *et al.* 2018) with 100% identity, confirming these strains as *O. camponoti-floridani*. We used SSU primers NS1 and NS4 (White *et al.* 1990), which yielded an approximately 1kb PCR amplicon with a Phusion High Fidelity Polymerase (New England Biolabs [NEB]) and the following PCR protocol: initial denaturation at 98°C for 30 sec, 30 cycles of 98°C for 10 sec, 49°C for 30 sec, 72°C for 30 s, and final elongation at 72°C for 10 min.

Whole genome sequencing and assembly: Strain EC05 was used to generate a high-quality draft genome for *O. camponoti-floridani* through a combination of Nanopore long-read and Illumina short-read sequencing. To extract DNA, we disrupted blastospore pellets frozen in liquid nitrogen with a 1600 MiniG tissue homogenizer (SPEX) at 1300 rpm for 30 sec. Samples were processed in 2 mL microcentrifuge tubes (Greiner) containing two steel ball bearings (5/32" type 2B, grade 300, Wheels Manufacturing) and kept frozen throughout disruption. We extracted DNA with 0.9 mL Extraction Buffer (1% SDS [Fisher Scientific], 240 mg/L para-aminosalicyclic acid [ACROS], 484 mg/L Tris/HCl [Fisher Scientific], 365 mg/L NaCl [Fisher Scientific], and 380 mg/L EGTA [MP] at pH 8.5) and 0.9 mL phenol/chloroform (Fisher Scientific). After phase separation, we washed the water phase with chloroform (Alfa Aesar) prior to extracting DNA with isopropanol. Following a 70% ethanol wash and reconstituting in nucleotide-free water (Gibco) we treated the DNA samples with RNase (Thermo Scientific).

A short-read DNA library was prepared with the Nextera DNA Flex Library Prep Kit (Illumina) with an average fragment length of 390 bp. Indexing for paired-end reads was performed with Nextera i5 and i7 adapters (Nextera Index Kit Index – 1 and 2). Short-read sequences were generated by sequencing 300 bp paired-end reads on an Illumina MiSeq (v 3, Miseq Reagent Kit) at the Genomics Service Unit (LMU Biocenter), resulting in 8 GB of fastq data. Reads were then quality filtered and adapter trimmed

using BBduk (Bushnell 2019) as a plugin through Geneious Prime (v 2019.0.3, Biomatters) (trimq = 15, minlength = 75).

To facilitate long-read sequencing, we first size selected genomic DNA for fragments longer than 5 kbp on a Blue Pippin (Sage Science) with 0.75% agarose and a High-Pass protocol. A long-read library was subsequently generated using the SQK-LSK109 Ligation Sequencing Kit (Oxford Nanopore) according to manufacturer's protocols. Sequencing on a PromethION (R9 flowcell, Oxford Nanopore) at the Laboratory for Functional Genome Analysis (LMU Gene Center) generated 105 GB (estimated 180x coverage) of Nanopore sequence data. Sequencing reads were base called with Albacore (v 2.2.5, Oxford Nanopore) and adapters were trimmed with Porechop (Wick 2018). We assembled the initial long-read genome using Canu (v 1.7.1, genomeSize = 45m, default settings) (Koren *et al.* 2017). An overestimation of the genome size allowed us to generate an assembly with good coverage despite the presence of bacterial contaminants (see below). This initial Canu long-read assembly was polished using raw Nanopore read data through Nanopolish (v 0.10.2) (Loman *et al.* 2015), followed by Illumina reads (120x coverage) with three iterations of Pilon (Walker *et al.* 2014) (v 1.23, --fix all) to produce a hybrid assembly. We identified a putative mitochondrion contig by testing for circular sequence structure with Circlator (Hunt *et al.* 2015), MUMmer (Kurtz *et al.* 2004), and Canu (Koren *et al.* 2017).

The assembly contained bacterial contaminant contigs that we removed. We identified contaminant contigs by their: (*i*) low read coverage aligned with Minimap2 (Li 2018) using all EC05 reads (Nanopore average coverage: 553x of *O. camponoti-floridani* genome contigs and 58x of contaminant contigs, and, Illumina: 195x of genome contigs and 15x of contaminant contigs); (*ii*) low RNA coverage with HISAT2 (Kim *et al.* 2015) mapping of Arb2 RNAseq control culture samples (62x of *O. camponoti-floridani* genome contigs and 0.14x of contaminant contigs); and (*iii*) high mapping to known bacterial genomes, *Cohnella* sp. 18JY8-7 (GenBank CP033433.1), *Delftia acidovorans* isolate ANG1 (GenBank CP019171.1), and *Stenotophomonas maltophilia* strain ISMMS2 (GenBank

CP011305.1) (0.08% overlap between *O. camponoti-floridani* genome contigs and these bacteria genomes, and 28.96% overlap of contaminant contigs with these bacteria genomes).

Genome annotation: We predicted genes in the EC05 *O. camponoti-floridani* genome using Augustus (v 3.0.2) trained with BRAKER1 (v 1.1.8) and intron hints from Arb2 transcripts (Stanke *et al.* 2008; Hoff *et al.* 2016). Protein domains predicted by PFAM (v 32) (Finn *et al.* 2014) were used to identify associated GO terms (Ashburner *et al.* 2000; Hunter *et al.* 2009). Protease predictions were made with the MEROPS database and a BLASTp E-value cutoff of 1e-5 (Rawlings *et al.* 2014). We used TMHMM (v 2.0c) to annotate transmembrane domains (Krogh *et al.* 2001). Secretion signals were identified with SignalP (v 4.1) (Almagro Armenteros *et al.* 2019). We predicted small secreted proteins (SSPs) when genes were shorter than 300 amino acids, carried a SignalP secretion signal, and did not have a transmembrane domain outside the first 40 amino acids. We identified genes and clusters predicted to be involved in secondary metabolism using a pipeline based on SMURF (Khaldi *et al.* 2010; de Bekker *et al.* 2015), with parameter d = 3000 bp and parameter y = 6. Transcription factors were identified based on the presence of a PFAM domain with DNA-binding properties using PFAM mappings from (Park *et al.* 2008). For BLAST annotations, we used BLASTp (v 2.7.1) against the NCBI nr database to gather up to 25 hits with E-value ≤ 1e-3. For the final annotation, we passed these hits to the Blast Description Annotator of Blast2GO with default settings (Conesa *et al.* 2005). In addition to searches that returned no results, we considered descriptions starting with “hypothetical protein” or “predicted protein” to lack BLAST annotations. BLASTp searches of the predicted proteins of *O. camponoti-floridani* against the Pathogen-Host Interaction (PHI) database (Urban *et al.* 2017), mitochondrial proteins, fungal secondary metabolite cluster proteins, and the *O. kimflemingiae* genome were conducted using Geneious (v 2019.0.3, Biomatters) with E-value ≤ 1e-3 and bit-score ≥ 50.

We supplemented the published BLAST genome annotations of the latest version of the *C. floridanus* genome (v 7.5) (Shields *et al.* 2018) with PFAM and GO annotations using the InterPro

database (Finn *et al.* 2017) through Blast2GO (Conesa *et al.* 2005). For these additional annotations, we used the longest transcript variant per gene. To allow for comparison of ant RNAseq results of our study to (de Bekker *et al.* 2015), we bridged the current *C. floridanus* assembly to the earlier version (v 1.0) (Bonasio *et al.* 2010) used by de Bekker *et al.* (2015) through BLASTp homology searches with Geneious (v 2019.0.3, Biomatters), taking the top hit after an E-value ≤ 1e-3 and bit-score ≥ 50 cutoff. Annotations from BLAST and further processing for submission to GenBank (NCBI) was done with gffutils (v 0.10.1, Daler) and table2asn (v 1.23.338, NCBI).

Ant collection & husbandry: Ant infections and behavioral observations were done using a wild colony of *C. floridanus*. This colony was collected from the University of Central Florida arboretum in February 2018 and housed in the laboratory. The collected ants consisted of several hundred individuals including minors, majors, and brood. In order to acclimate the ants and entrain their biological clocks to laboratory conditions, we first subjected the colony to two days of constant light and constant 25°C temperature in a climate controlled room. Following this clock "reset" we gave the colony three days of 12 hr – 12 hr light-dark cycles at 25°C to entrain ants to light as a circadian zeitgeber (LD1212, lights begin at zeitgeber time ZT 0). During acclimation, the colony housed in a 9.5 L plastic container (42 cm long x 29 cm wide) lined with talcum powder (Fisher Scientific) and containing aluminum foil wrapped test-tubes (50 mL, Fisher Scientific) with moist cotton to serve as darkened, humid nest spaces. Ants fed *ad libitum* on 15% sucrose solution, autoclaved crickets, and water.

Ant infections: For laboratory infections, we selected minor caste ants from the colony and housed them in two identical containers in each of two climate-controlled incubators. Incubator A (MIR-154, Panasonic) was programmable for light and temperature. Incubator B (I36VL, Percival) was programmable for light, temperature, and relative humidity (RH). Incubator A ran a program with LD1212 and 28°C during the light phase and 20°C during the dark phase. Incubator B maintained humidity at 70% RH, LD1212, and 28°C to 20°C temperature. The light phase of Incubator B included a

4hr increasing ramp step (ZT 0 dark and 20°C transitioning to ZT 4 peak light and 28°C), a 4hr peak light and temperature hold until ZT 8, and 4hr decreasing ramp step until ZT 12 (peak light and 28°C to dark and 20°C). Light, temperature, and humidity for both incubators were verified with a HOBO data logger (model U12, Onset, Bourne, MA) (Appx. AA-B). The incubators were not significantly different for survival of infected ants ($p = 0.072$, log-rank test). Therefore, we chose to consolidate all samples from these incubators for survival and RNAseq analysis.

Each container (33 cm x 22 cm) was lined with talcum and had a thin layer of playground sand on the bottom that we routinely moistened during observations to maintain an elevated humidity inside the ant enclosure. On one end, containers held a 50 mL Falcon tube (Corning) with moist cotton wrapped in aluminum foil and *ad libitum* 15% sucrose and water. On the opposite end, we placed two thin 12 cm high wooden sticks draped with locally collected "Spanish moss" (*Tillandsia usneodies*) and a single "air plant" (*Tillandsia spp.*) (Appx. AC). These plants are common natural substrates for manipulated ants to bite and cling to at local field sites.

We painted ants to distinguish treatment groups (POSCA paint pens, Uni) one to three days in advance of infection by fungal injection (de Bekker *et al.* 2014b). We injected ants without anesthesia using aspirator tubes attached to glass capillary needles (10 µL borosilicate capillary tubes, Fisher Scientific), pulled using a PC-100 Narishige instrument. Needle placement for injection was on the ventral side of the thorax, sliding under the prosternum. The night before injection, we removed sugar and water from ants to be infected to ease the procedure. We timed injections to begin at ZT 0 and not last more than 3.5 hr. Ants that survived the first 3 hr post-injection were placed into the experiment. Control ants were not injected. Sham treatment ants were injected with 1 µL of Graces-2.5% FBS. Infected ants were injected with 1 µL of 3.5×10^7 blastospores/mL in Graces-2.5% FBS, harvested during log-phase growth ($OD_{660nm} = 0.984$, approximately 1.8×10^7 cells/mL based on estimates with *Saccharomyces*

cerevisiae). Blastospores were harvested immediately preceding injection, washed twice in deionized water, and re-suspended in Graces-2.5%FBS.

Incubator A contained 18 control, 13 sham, and 33 infected ants. Incubator B contained 12 control, 13 sham, and 30 infected ants. After 14 days post injection (dpi), we observed aggressive patrolling and cleanup of dead and dying ants. Therefore, we chose to separate infected ants from non-infected groups to reduce the chances of interference with cadavers or the progress of manipulation. Control ants and sham ants were removed from the experiment boxes and rehoused in similar containers directly next to their original box for the remainder of the experiment.

Observations of infection progression and sample collection: We made daily observations for manipulated ant phenotypes and survival at ZT 0, 2, 4, 6, 8, and 23 with sporadic opportunistic surveys for manipulated ants. We additionally began observations at ZT 20 starting 18 dpi. We considered ants to be manipulated when they displayed clasping or biting onto any substrate. Individuals that ceased to move nor responded to agitation by air puffs were considered dead. Live manipulated ants collected for RNAseq were recorded as dead for survival analysis. We analyzed survival data using the R package survival (Therneau 2015) and visualized curves with survminer (Kassambara *et al.* 2019).
Upon visible behavioral manipulation, we froze whole-ant samples for RNAseq directly in liquid nitrogen. We sampled healthy live control ants at ZT 21, which corresponds to the time of observed manipulation in our study. Healthy controls, rather than sham-injected ants, were collected to better match the previous study on *O. kimflemingiae* and *C. castaneus*, which we reference for comparative transcriptomics (de Bekker *et al.* 2015). Upon flash freezing, we stored ants in pre-chilled 2 mL microcentrifuge tubes (USA Scientific) at -80°C until RNA extraction. In total, we analyzed 13 ants for RNAseq: live manipulated n = 5, dead manipulated n = 5, healthy control n =3. To obtain fungal control samples of strain Arb2 (n = 3), blastospore cultures were harvested at ZT 21 after a constant light and 28°C synchronization treatment for two days, followed by an entrainment period for five days at LD1212

and 28°C to 20°C. During this time, light and temperature of culture conditions were validated with a HOBO data logger (Appx. AB). Fungal control cultures were grown to a late-log phase (OD_{660nm} = 1.7) before harvesting by pelleting 1 mL of culture per sample and snap-freezing in liquid nitrogen. Any collections made during subjective dark were done under red-light (730 nm wavelength).

RNAseq data generation and analysis: All frozen samples for RNAseq were disrupted in the same manner as fungal genomic DNA samples (see above) prior to RNA isolation. For ant samples, we first decapitated frozen cadavers in petri dishes chilled with liquid nitrogen and then proceeded to frozen tissue disruption using individual heads. We extracted RNA with a RNAqueous Micro kit (Life Technologies) according to the manufacturer's protocol, without DNase treatment. We isolated mRNA with poly-A magnetic beads (NEB) from 500 ng total RNA for each sample. Subsequently, we converted purified mRNA to 300 bp fragment DNA libraries with the Ultra II Directional kit (NEB) and indexed samples for multiplexing (NEB).

All libraries were sequenced on an Illumina HiSeq as 100 bp single-end reads at the Laboratory for Functional Genome Analysis (LMU Gene Center), resulting in 27M to 56M reads for each sample. We trimmed reads using BBduk (Bushnell 2019) as a plugin through Geneious Prime (v 2019.0.3, Biomatters) to remove adapters and for quality (qtrim = rl, trimq = 10, minlength = 25). Our choice for a Q10 quality trim and minimum 25 bp length of RNAseq reads yielded a sufficient number and quality of reads while reducing risk of introducing biases from read processing (Williams *et al.* 2016).

For mixed transcriptome libraries (infected ants with host and parasite reads), we conservatively separated transcript sequences by first discarding all reads from the mixed sample that mapped to one organism's genome before proceeding to analyze the other organism's transcriptome (Fig. 1). That is, we mapped to the host genome and then aligned the unmapped reads to the parasite genome, and *vice versa*. This method removes reads that map ambiguously to both the host and parasite from analysis. However,

we estimate this to be only ≤ 0.04% of reads based on these organism's transcriptomes in control conditions (Fig. 1). All transcript mapping steps were done with HISAT2 (Kim *et al.* 2015).

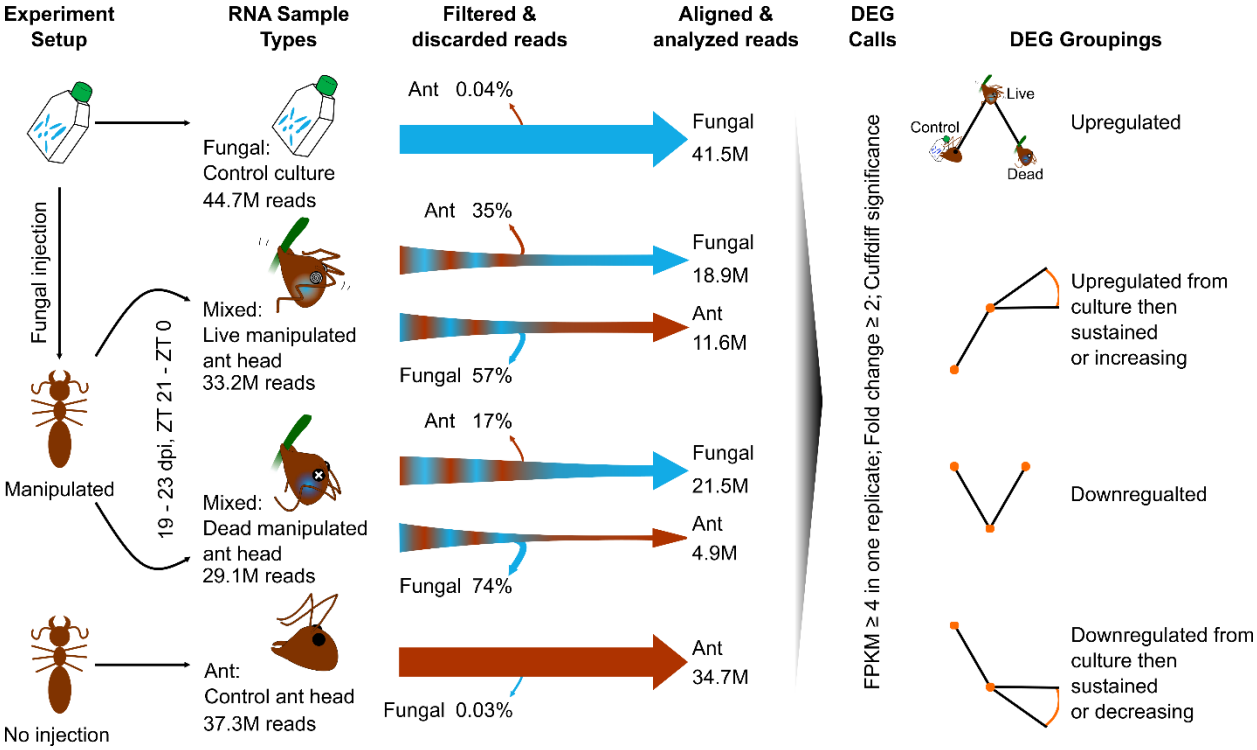

Figure 1. RNAseq experimental overview.

Manipulated ant, ant control (no injection), and fungal control (blastospore culture) samples were processed for RNAseq. Manipulated ants contained mixed RNA of both the parasite and host. We observed and collected manipulation samples 19 – 23 dpi and between ZT 21 to ZT 0. Control ants and fungal culture samples were collected at ZT 21. To minimize possible bias from read counts of transcripts from mixed samples that map to either organism, we first filtered reads through either the host or parasite genome before aligning remaining reads to the other genome for gene expression analysis. DEGs were identified with Cuffdiff significance and expression cutoffs imposed for comparability to de Bekker *et al.* (2015). DEGs were then grouped by expression pattern over the course of the different sample points. All RNA samples taken from ants were extracted from whole heads. Read counts are the mean value per sample type.

We normalized and analyzed whole transcriptome gene expression levels with Cuffdiff with default settings (Trapnell *et al.* 2012). We used Cuffdiff significance calls (q ≤ 0.05, test = OK,

significant = yes) to identify differentially expressed genes (DEGs) between sample groups. To consider DEGs biologically relevant to our analyses, we required genes to have an expression level of ≥ 4 RPKM in one replicate, and a minimum of two-fold change between sample types. This methodology allows us to have the most comparability to published RNAseq data from *O. kimflemingiae* and *C. castaneus* (de Bekker *et al.* 2015)

We used unsupervised PCAs to describe the variation among control, live manipulated, and dead manipulated samples (R Core Team 2014; RStudio Team 2015). We ranked genes within a principal component (PC) by loading values to investigate the top 20 that explain the most variation within a PC. All gene RPKM transcription values were first $log2(X + 1)$ transformed for every gene with at least one sample replicate with RPKM ≥ 4. Plots were generated using R package ggplot (Wickham 2016).

Using a WGCNA we produced modules of coexpressed genes and associated them with control, live manipulated, and dead manipulated ants. Although our sample size is below an ideal replicate number, we applied this analysis for a coarse evaluation of possible gene modules associated with manipulation. Data were filtered (RPKM ≥ 4) and $log2(X + 1)$ transformed before analysis. We processed all samples together in the R package WGCNA (v 1.67) (Langfelder and Horvath 2008; R Core Team 2014; RStudio Team 2015). We applied a signed-hybrid network type, a soft power threshold equal to nine (fungus) or 12 (ant), minimum module size of 30, and default settings. Our categorical trait data were entered as either 0 (sample was not that type) or 1 (sample was that type) for control, live manipulation, and dead manipulated. For correlation of ant and fungal modules, eigengene values for ant modules were calculated with the moduleEigengenes function of the package and used as trait data for fungal module correlations. R package WGCNA was also used to generate a sample dendrogram to assess clustering of biological replicates (function hclust, with method = “average”).

We performed enrichment analyses on gene sets identified by PCA, WGCNA modules, and DEG groupings by using a hypergeometric test with Benjamini-Hochberg correction to correct for multiple

testing (minimum number of genes with annotation term = 5, corrected p-value ≤ 0.05) (R Core Team 2014; RStudio Team 2015).

Data availability: The version of the *Ophiocordyceps camponoti-floridani* genome assembly in this paper (JAACLJ010000000) has been deposited on Genbank under accession JAACLJ000000000. Read data for that assembly are available under BioProject PRJNA596481. Read data for transcriptomics are available under BioProject PRJNA600972. Supplemental files have been uploaded to figshare. RNAseq data, WGCNA modules, and enrichment analyses can be found in supplemental files File S1 (ant data) and File S2 (fungus data). Additional results and discussions are presented in Appx. C.

Results & discussion

Manipulated behavior of *Camponotus floridanus* after laboratory infections: We set out to identify parasite and host genes involved in manipulated biting and clinging behavior observed in *Ophiocordyceps*-infected *Camponotus* ants. To this end, we infected *C. floridanus* with *O. camponoti-floridani* to compare gene expression levels in this host-parasite interaction with those published for *C. castaneus* and *O. kimflemingiae* (de Bekker *et al.* 2015).

All manipulated *C. floridanus* ants (n = 11) clung to plants with their legs, with two individuals additionally biting the plant. This lab-infected manipulation phenotype well-approximated wild manipulations (Fig. 2). Live manipulated ants commonly displayed subtle tremors, feeble clasping motions, and low responsiveness to puffs of air. If these ants fell from their manipulation perches, they continued clasping motions but otherwise did not right themselves or move (n = 2). Overall survival was significantly different based on treatment (p = 0.00059, log-rank test), with the 95% confidence interval of infected ants lower and not overlapping with sham treated or control ants by 21 dpi (Fig. 2). Manipulated clinging and biting behavior displayed by *O. camponoti-floridani* infected *C. floridanus* ants occurred within a stereotypic dpi-window with apparent time of day synchronization. Infected ants

displayed manipulated behavior starting 19 dpi, with the last manipulation at 23 dpi (Fig. 2). All observed manipulations occurred pre-dawn from at least as early as ZT 20 until ZT 23 (i.e., 4 hr to 1 hr before lights-on). When we captured the onset of manipulated clinging and allowed the ant to progress to death, the time between manipulation and death was 0.5 hr to 2 hr (n = 3, of six dead manipulated ants). In previous infection studies with *O. kimflemingiae*, manipulations of *C. castaneus* occurred 16 through 24 dpi and shortly after subjective dawn (ZT 3), which was the first daily observation period of that study (de Bekker *et al.* 2015). Infected *C. castaneus* usually died at least 5 hr after manipulation. Such stereotypic patterns have also been reported for other ant-manipulating *Ophiocordyceps*, both in the laboratory (Sakolrak *et al.* 2018) and in the wild (Hughes *et al.* 2011).

Our opportunistic preliminary field observations have found live manipulated *C. floridanus* one to three hours after solar noon (n = 4). This is out of phase from our laboratory observations for this species, as well as those made for *O. kimflemingiae*-infected *C. castaneus* (de Bekker *et al.* 2015). Differences in abiotic factors, such as light, temperature, and humidity, across labs and field observations could have led to these phase shifts (Hughes *et al.* 2011; Andriolli *et al.* 2018; Cardoso Neto *et al.* 2019). Therefore, rather than selecting a ZT at which to sample infected *C. floridanus* for RNAseq, we sampled based on behavioral phenotypes comparable to infected *C. castaneus*: immediately upon observing manipulated clinging behavior or death after manipulation. We expect sampling according to phenotype instead of daily timing to have produced more comparable gene expression profiles across the two species-interaction studies. A role for light-cues in the summiting aspect of *Ophiocordyceps* manipulation of ants has previously been proposed (Chung *et al.* 2017; Andriolli *et al.* 2018). Insect manipulating baculovirus strains also induce summiting behavior in silkworm hosts, with an apparent phototactic element in coordinating manipulation (Kamita *et al.* 2005; van Houte *et al.* 2014a; Han *et al.* 2018). Baculovirus may only require light before, but not during summiting (Han *et al.* 2018). Such light-

coordinated behavior, rather than direct phototaxis, possibly underlies the pre-dawn summiting we observed in the laboratory.

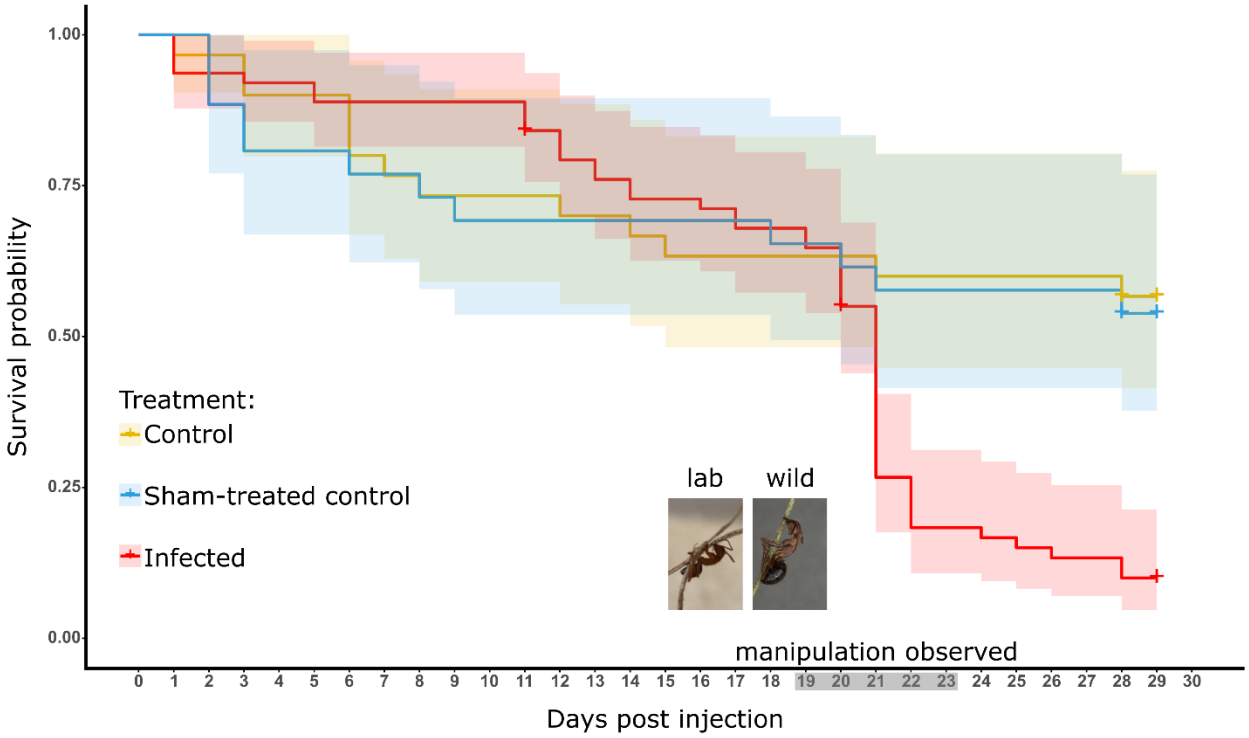

Figure 2. Survival curves of infection experiment ants.

We introduced three treatment groups in the infection experiments, ants not injected (yellow, control n = 30), injected with media-only (blue, sham-treated control n = 26), or injected with the O. camponoti-floridani (red, infected n = 63). Shaded regions around survival data indicate 95% confidence intervals. Treatment had a significant effect on survival (p = 0.00059, log-rank test). Manipulations were observed only in infected ants, 19 to 23 dpi (gray axis shading). Crosses indicate censorship events when ants were removed from the experiment and no longer contributed to analysis. The photo inserts show a live lab infected ant (left) and a wild manipulated cadaver (right).

***De novo* hybrid assembly of the *Ophiocordyceps camponoti-floridani* genome:** The reliable alignment and separation of mixed sequencing reads to determine relative abundances of both host and parasite transcripts requires high-quality reference genomes of both organisms (Fig. 1). A recently updated genome of *C. floridanus* is publicly available (Shields *et al.* 2018). To generate a high-quality *O.*

camponoti-floridani genome, we combined Nanopore long-reads and Illumina short-reads data in a hybrid assembly.

After polishing and contaminant removal steps, our *de novo* hybrid assembly contained 13 contigs encompassing 30.5 Mbp, with a N50 of 3.8 Mbp and 53x Nanopore coverage (Table 1). Pezizomycotina telomeric repeats, TTAGGG (Podlevsky *et al.* 2008), are present on nine of the contigs, three of which are bounded on both ends by repeats and therefore should represent whole chromosomes of 5.6 Mbp, 3.8 Mbp, and 2.5 Mbp in length.

Table 1. *O. camponoti-floridani* genome assembly.

Assembly characteristic	Value	Annotation	Number of genes
contigs	13	BLAST	6291
size (Mbp)	30.5	PFAM	5460
N50 (Mbp)	3.8	GO	3515
largest contig (Mbp)	5.6	SignalP	801
predicted genes	7455	SSP	271
BUSCO%	99.7	TMHMM	1372
GC%	48.4	2° metabolism	111
Telomeric repeat areas	12	MEROPS	243
		transcription factor	206

One of the 13 contigs represents a putative mitochondrial genome of 272,497 bp. We identified this mitochondrial contig by *(i)* its high read coverage (735x) compared to the genome average (53x), *(ii)* its

low GC content (27%) compared to the total assembly (48%), *(iii)* the presence of homologs to known mitochondrial proteins on this contig but nowhere else in the genome (BLASTp of ATP6, COB, COX1, and NAD1 of *Aspergillus niger*) (Joardar *et al.* 2012), and *(iv)* its circular sequence structure. The genome assembly appeared nearly complete with 99.7% of pezizomycotina benchmarking universal single-copy orthologs (BUSCOs) (v 3, using OrthoDB v. 9) (Simão *et al.* 2015) (Table 1) (GenBank Accession JAACLJ000000000).

Genome annotations identified 7455 gene models (Table 1). Most genes received functional annotations based on PFAM domains (73%) or BLAST descriptions (86%). We also identified 801 putatively secreted proteins containing a SignalP domain (11%) and 271 small secreted proteins (SSPs, 3.6%). Only 19% of the SSPs carried known PFAM domains and only 37% returned BLAST descriptions. With many SSPs lacking clear functional annotations, these SSPs may contain a pool of novel bioactive compounds secreted by *O. camponoti-floridani*.

RNAseq identifies differentially expressed genes associated with manipulation: To discover candidate fungal and ant genes that underpin the manipulated behavior of *O. camponoti-floridani*-infected *C. floridanus* hosts, we sequenced the transcriptomes of samples obtained before, during, and after manipulation. Ant heads collected during and after manipulation contained mixed transcriptomes of both host and parasite (Fig. 1). The average number of aligned reads for each fungal and ant transcriptome fell between 11.6M and 41.5M, except for the ant transcriptome of the dead manipulated samples (i.e. after manipulation), which resulted in only 4.9M aligned reads (Fig. 1). For both fungal culture and healthy ant head control samples, 93% of the RNAseq reads aligned to their respective reference genomes (Shields *et al.* 2018). We aligned 57% and 74% of reads obtained from live manipulated or dead manipulated ant heads to the *O. camponoti-floridani* genome, respectively. In contrast, these samples only resulted in 35% and 17% of reads that aligned to the *C. floridanus* genome (Fig. 1) (Shields *et al.* 2018). These findings corroborate previous findings in other *Ophiocordyceps*-ant interactions that the fungus has colonized the

ant head by the time of manipulation and rapidly destroys host tissue for its own growth as the host dies (Hughes *et al.* 2011; de Bekker *et al.* 2015).

To validate differential expression analysis between our biological sample groups, we first determined if the variation between replicates within these groups was smaller than the variation between them. Unsupervised dendrograms based on replicate ant and fungal gene expression profiles indeed clustered biological replicates together (Appx. B). However, the fungal profile of live manipulation sample 4 (L4) was placed ambiguously relative to live and dead manipulated samples (Appx. BA). Regardless, we did not exclude sample L4 as an outlier, as we are not confident about the confines of typical disease progression and gene expression during this time point. As these samples were selected on observed behavioral phenotype, the transcriptional state of genes essential for manipulation is plausibly shared despite differences in other genes.

We included all samples to identify differentially expressed genes correlated to control (fungal culture and healthy ants), live manipulation, and dead manipulation samples, finding 1431 ant and 2977 fungal genes differentially expressed between at least one pair of sample conditions. To identify genes that are plausibly involved in *Ophiocordyceps* manipulation of ant behavior, we performed various complementary gene expression analyses for both fungal and ant genes, which are detailed below.

Principal component analyses identify host changes linked to manipulation: Through PCAs we identified the genes that contributed the most to the transcriptome variations between our biological groups. An unsupervised PCA of all normalized ant transcriptome data distinguished host gene transcription prior to infection (control), during manipulation (live manipulation), and after (dead manipulated) (Fig. 3A). Principal Component 1 explained 47% of the variation between host transcriptional profiles over progression of the infection from healthy to manipulated to dead ants. To identify the major contributors to PC1, we ranked and plotted ant genes by their PC1 loading values (Fig. 3B, Appx. D). The top 20 genes of PC1 included genes putatively related to odor detection (pheromone-

binding protein Gp-9-like and a pheromone-binding protein (PBP)/general odorant-binding protein (GOBP) family PFAM domain-containing gene), nutrition and energy balance (alpha-amylase 1, alpha-amylase A-like, and an apolipophorin-III precursor PFAM domain-containing gene), and muscle tissue (myogenesis-regulating glycosidase-like and muscle actin). These genes were also found to be differentially expressed between sample types and are further highlighted in the DEG section below.

PC2 largely described the variation between healthy control ants and live manipulated hosts, explaining 18% of sample variation in total. The top 20 PC2 genes shared PBP/GOBP domain genes with PC1. However, the PC2 top 20 also included putative DEGs involved in insect immunity (defensin and a von Willebrand factor type C domain-containing gene) and insect starvation response-mediated by juvenile hormone (JH) (cytochrome P450 4C1-like) (Fig. 3C, Appx. E).

Principal component analyses identify fungal effectors produced during infection: A PCA of all normalized fungal transcriptome data generated a PC1 explaining 71% of the transcriptional variation. PC1 indicated a large separation between transcription profiles prior to infection (control) and after (live or dead manipulated) (Fig. 3D). Fungal gene expression profiles from live and dead manipulated ants were less different from each other, as indicated by the partial overlap of their 95% confidence ellipses (Fig. 3D). The second principal component (PC2, 13%) primarily described the difference between replicate L4, and other fungal samples, which the sample dendrogram also indicated (Appx. B). Major elements of PC1 likely indicated genes linked to infection, manipulation, and killing of the host.

The top 20 of all fungal genes, as determined by their PC1 loading values (Fig. 3D, Appx. F), peaked during live manipulation in both *O. camponoti-floridani* and *O. kimflemingiae* (de Bekker *et al.* 2015). Although significantly higher expressed compared to culture, their expression relative to dead host samples was not always significantly different. This set of 20 genes contained multiple candidates of interest identified in secondary metabolite clusters and as DEGs. These genes, discussed in more detail in the sections below, included multiple members of a putative aflatrem biosynthesis pathway (cluster 18)

and a putative enterotoxin that was extremely highly upregulated in both *O. camponoti-floridani* and *O. kimflemingiae*.

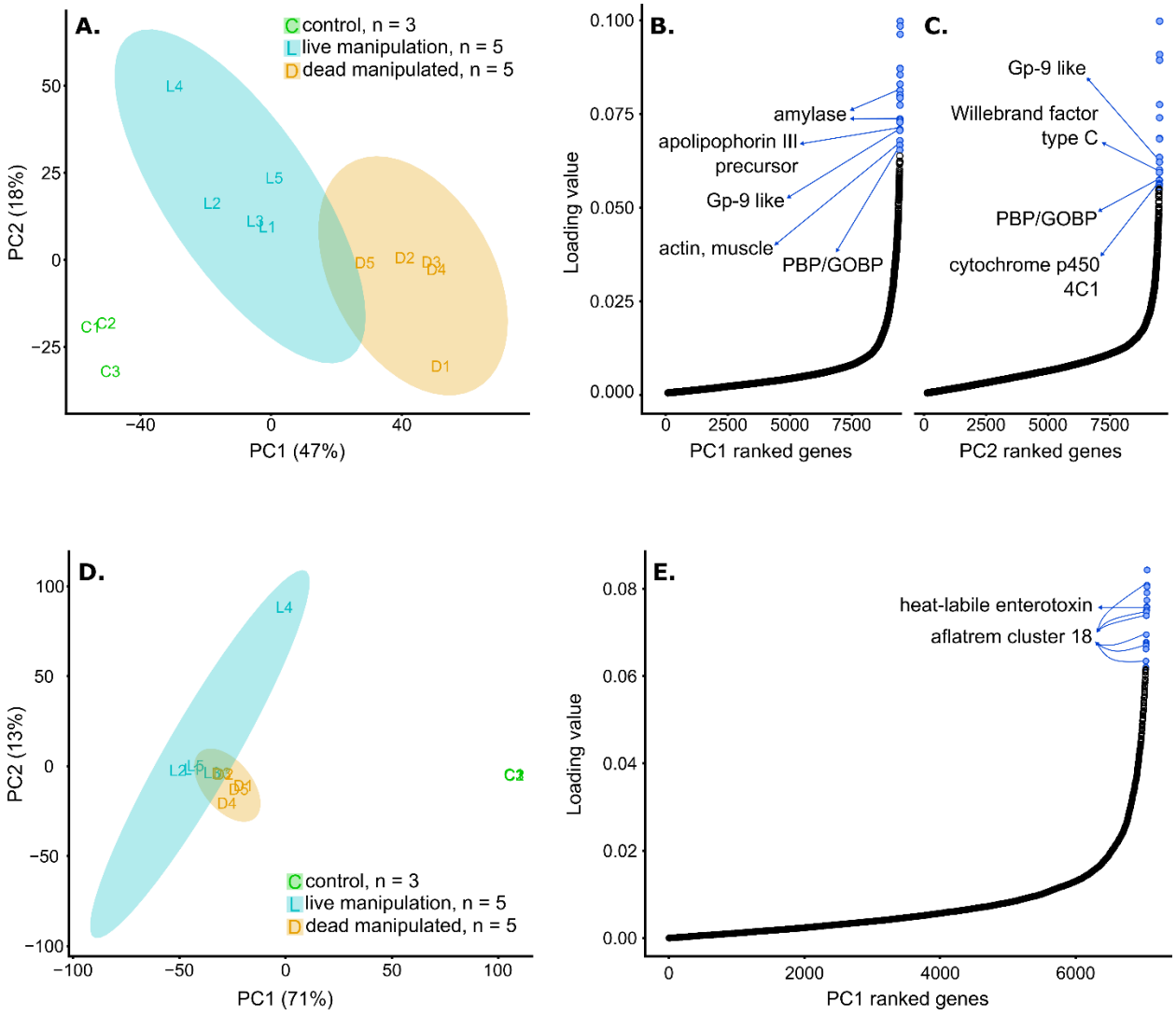

Figure 3. **Principal component analyses and principal component loading value plots of RNAseq data.** Analyses are based on normalized ant (A, B, C) and fungal (D, E) gene expression values. PCA plots (A, D) show the relationship between samples that serve as controls (green) and those that were collected during live manipulation (blue) and after host death (orange). Shaded regions indicate 95% confidence ellipses. A) Replicates of host gene expression vary across PC1 as the state of the host progresses from healthy control ants to live manipulated hosts to dead manipulated hosts killed by the fungus. PC2 primarily describes the variation between healthy controls and live manipulated ants, but all biological groups vary along this axis. B, C) All ant genes ranked

by loading values in PC1 (B) or PC2 (C). Most genes have low loading values, however a relatively high-loading value subset contribute the most to PC1 or PC2. Of these high value genes, the top 20 include genes that may play key roles during infection and manipulation (blue). D) Gene expression of the fungal parasite interacting with the ant host is clearly distinguished from that of fungal culture control samples by PC1. E) All fungal genes ranked by loading values in PC1. The top 20 fungal PC1 genes are highlighted and include toxin related genes (blue).

Weighted gene coexpression network analysis correlates parasite gene expression during manipulation to host gene networks: We also analyzed ant and fungal RNAseq data using a WGCNA to describe coexpressed gene networks (modules) correlated with control, live manipulated, and dead manipulated samples. This analysis shows which genes may be expressed in concert with each other and how those networks correlate to the manipulation state of the host or coexpressed networks in the parasite. We then characterized these networks based on annotation enrichment analyses.

For ant gene coexpression patterns, the WGCNA generated 22 modules, which we named A1 – A22. Expression of four modules, A4, A5, A6, and A10, were significantly positively correlated with live manipulation ($p \leq 0.05$, Fisher's asymptotic test on Pearson correlation values) and either had a negative or no significant correlation with control and dead samples (Appx. G). Four additional modules, A14, A15, A17, and A18, were significantly negatively correlated to live manipulation. Of these modules, A17 and A18 were also positively correlated to healthy control ants. Taken together, the WGCNA identified eight ant gene modules with significant correlations to the time of live manipulation that highlight transcriptional responses to fungal infection and manipulation (File S1).

To investigate general functions of the ant gene modules, we performed enrichment analyses of annotated PFAM domains and GO terms present in those modules. In module A4, genes putatively involved in proteasome activity and odorant detection (i.e., PBP/GOBP PFAM domain) were overrepresented (File S1). These gene functions were also highlighted by the ant PCA above (Fig. 3B-C). Reduced detection of odor cues and related social interactions have been hypothesized to play a role in the early stages of manipulation that precede biting by *Ophiocordyceps*-infected carpenter ants (de

Bekker *et al.* 2015). Modules A5, A6, and A10 were enriched for annotations related to gene and DNA regulatory processes (File S1).

In the ant modules negatively correlated to live manipulation, we detected gene modules associated with neuronal function. A14 and A15 had a 7 transmembrane receptor (rhodopsin family) PFAM enrichment related to light sensing and cellular signaling (Appx. H). This suggests a loss in light sensitivity as a mechanism to promote light-seeking behavior, which has previously been hypothesized to occur in manipulated ants prior to biting to assure light levels that promote fungal growth and transmission (Andriolli *et al.* 2018). Module A15 additionally contained an overrepresentation of genes with a 7 transmembrane domain (sweet-taste receptor) related to glutamate or GABA receptors and neurotransmitter gated ion channels (i.e., putative acetylcholine, glycine, and glutamate receptors) (File S1). Both modules were also predominantly enriched for transmembrane transport, ion regulation, and cell signaling activity annotations, with multiple immunoglobulin domain enrichments (File S1). Although, the underlying genes for these enrichments were generally not DEGs. The immunoglobulin domain overrepresentations contained a variety of genes putatively encoding cell-surface binding proteins related to neuronal development, maintenance, and activity, such as IgLON family proteins with additional light sensing or circadian, olfaction, and memory related functions (Appx. I). These multiple signals tied to the ant's neurobiology in modules A14 and A15 suggest disrupting neuronal function underscores manipulated behavior (Fig. 4). Genes from enriched annotations point to mechanisms dysregulating light responsiveness and neurotransmitters related to behavior and muscle activity (Fig. 4, Appx. H, Appx. I).

The WGCNA for fungal gene coexpression patterns generated 13 modules, F1 – F13, and correlated them to the three possible sample types – control culture, live manipulation, and death after manipulation (File S2). Three modules, F1, F2, and F4, were significantly positively correlated with live manipulation. F1 and F2 were additionally negatively correlated with fungal growth in control culture

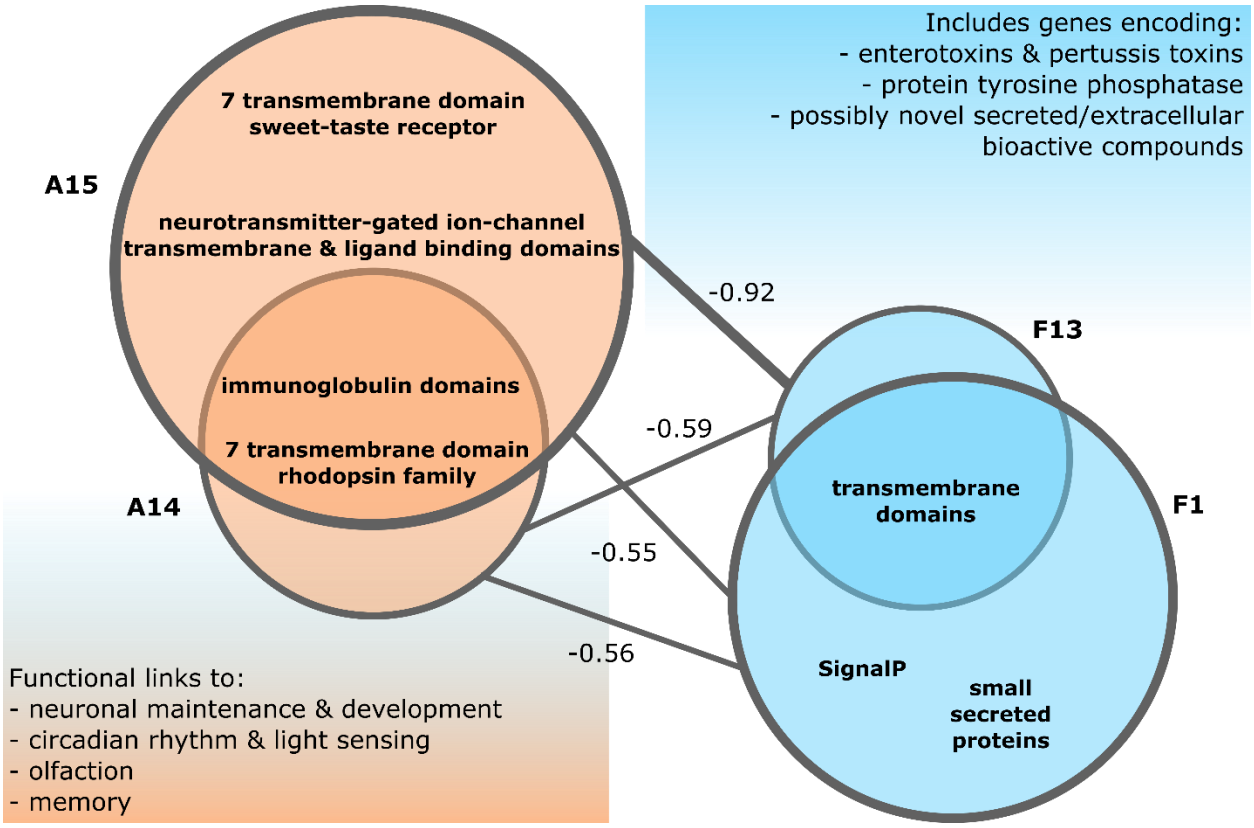

Figure 4. Ant WGCNA modules correlated with fungal modules suggest interference with neuronal function. A14 and A15 are enriched for PFAM domains that suggest neuronal functions, which are negatively correlated to fungal modules F1 and F13 that are enriched for extracellular and secretion signals. These fungal modules also contain putative effectors discussed in greater detail in following sections, such as enterotoxins or protein tyrosine phosphatase (PTP). Pearson correlation values shown by lines connecting modules.

(Appx. J). Subsequently, we performed an additional WGCNA with all 13 fungal modules against the eight ant modules that had significant correlations to live manipulation of the host to describe possible behavioral changes and responses to infection. We used these eight ant modules as a new set of trait data (i.e., eigengenes) to correlate our fungal modules to (Fig. 5). Using this strategy rather than separately associating fungal and ant gene networks to the broader categories of our biological groups, we aimed to make a more detailed connection between fungal gene expression and the corresponding transcriptional changes in the host.

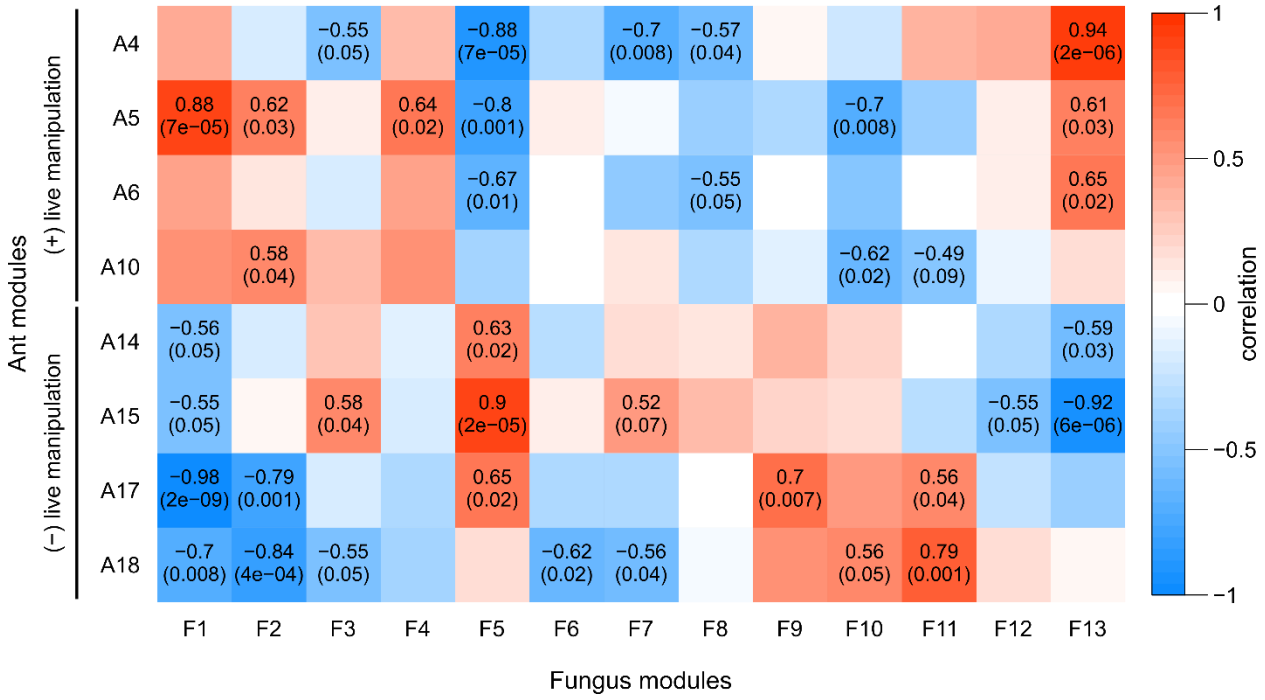

Figure 5. WGCNA of fungal and ant modules correlated to each other.

Fungal gene expression (columns) show correlation (color and top number in each cell) and p-value (in parentheses) of gene modules to selected ant modules that are either positively or negatively correlated to samples during live manipulation (rows). Pearson correlation and p-values (Fisher's asymptotic test) are shown only for significant module to module correlations. Modules F1, F2, and F13 are enriched for secretion signals or transmembrane domains and therefore may contain extracellular fungal effectors. Modules A14 and A15 have PFAM domain overrepresentations suggesting a role in neuronal function and development.

Fungal modules F1, F2, and F13 appeared to be major contributors to fungal effects on the ant host as these modules were positively correlated to activation of manipulation-associated ant modules and negatively correlated to ant modules deactivated during manipulation (Fig. 4, Figure 5). Putatively secreted genes (i.e., SignalP and SSP annotations) were overrepresented in F1 and F2, as were transmembrane domains (TMHMM) in modules F1 and F13. These enrichments suggest that these fungal modules are involved in extracellular interactions with the host. Oxidation-reduction related annotations and transcription factors were also overrepresented in module F2. Oxidation-reduction terms are a

hallmark of parasite-host interactions and were overwhelmingly found in *O. kimflemingiae – C. castaneus* interactions (de Bekker *et al.* 2015). Although fungal modules F1 and F13 did not harbor any other annotation enrichments, they indicated an increase of putatively secreted effectors and virulence related activity in *O. camponoti-floridani* in correspondence to the changing expression of ant gene networks correlated with manipulation. Notably, F1 and F13 negatively correlated with ant modules A14 and A15, which in turn appear to be associated with neuron function (Fig. 4). Therefore, modules F1 and F13 possibly contain extracellular fungal effectors that dysregulate neuron function and health (Fig. 6).

Differentially expressed ant genes during infection and manipulation: To consider genome-wide enrichment patterns in ant gene expression in relation to infection, manipulation, and host death, we divided our RNAseq data into subsets representing different interpretations of gene function that may underlie host responses and effects of fungal activity (Fig. 1). Genes that were significantly upregulated from control ants to live manipulation and then downregulated once the ant died may indicate specific responses to infection and active behavioral manipulation by the parasite (120 genes, File S1). We also analyzed genes that were upregulated during live manipulation from control and then had sustained or increased transcription until the ant died (88 genes, File S1). Being upregulated, these genes plausibly play a role during manipulation but may also be more generally associated with infection or host death. Similarly, we considered differentially expressed gene sets that were downregulated at live manipulation relative to both healthy ants and dead hosts (6 genes, File S1), and those holding or dropping further in dead hosts (529 genes, File S1). We collected our samples for the dead manipulated time point under frequent observation, such that these ants should reflect a manipulated ant transcriptome just as the host dies. As many significant transcriptional effects would likely lag behind the moment of presumed death, we expect to have captured the state of a moribund ant as it dies. To propose host changes that could be underlying the manipulated behaviors in *C. floridanus*, we closely investigated the functional annotations of these DEG sets and compared them to those previously found for manipulated *C. castaneus*.

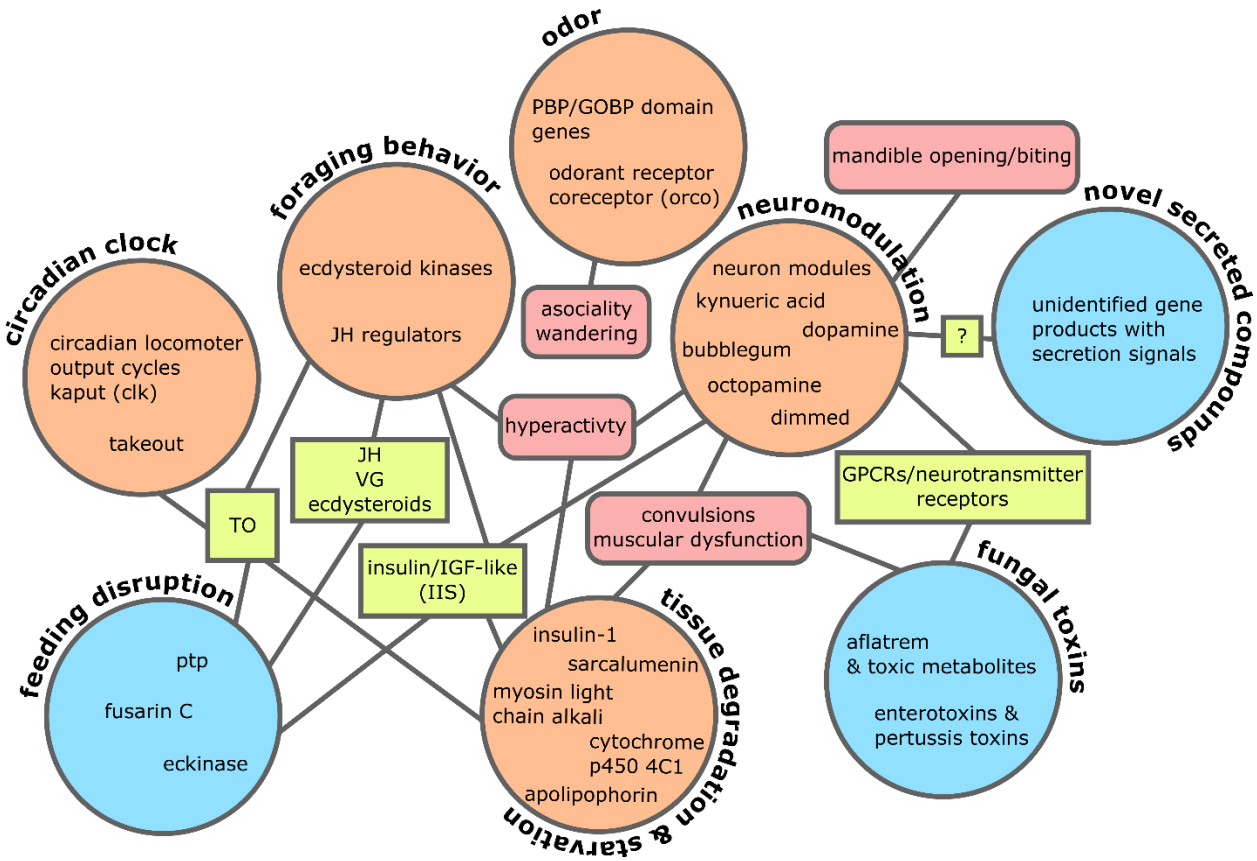

Figure 6. Major themes and candidate manipulation mechanisms.

These genes and pathways are possible players in manipulation, emerging from RNAseq of *O. camponoti-floridani-C. floridanus* and comparisons to published *O. kimflemingiae-C. castaneus* interactions (de Bekker *et al.* 2015). Ant DEGS and proposed mechanisms (orange circles) are connected to fungal counterparts (blue circles) via shared molecular players (yellow rectangles) and phenotypes (red rounded-rectangles).

Host gene expression patterns related to tissue destruction and nutrition. The destructive invasion and consumption of host tissues by *Ophiocordyceps* may have implications for behavior beyond mere host death. Notably, the ants' muscles are affected, leading to muscle atrophy and hypercontraction that have been suggested to have a role in the locked biting position of manipulated ants (Hughes *et al.* 2011; Fredericksen *et al.* 2017; Mangold *et al.* 2019). In line with this aspect of the disease, a putative sarcalumenin gene was downregulated during live manipulation in both *C. floridanus* and *C. castaneus* (3-fold and 8-fold decrease from control to live manipulation, respectively) (de Bekker *et al.* 2015).

Sarcalumenin has been shown to interact with calcium and regulate muscle excitation and fatigue in mammalian systems (Zhao *et al.* 2005; O'Connell *et al.* 2008). Additionally, an essential component of myosin motor proteins, a myosin light chain alkali (Yamashita *et al.* 2000), was downregulated in both species of ant hosts during live manipulation (4-fold and 2-fold decrease from control to live manipulation in *C. floridanus* and *C. castaneus*, respectively). A gene BLAST annotated as "actin, muscle", was a DEG in both ant species, and we found additional muscle genes downregulated in *C. floridanus* (Appx. C). Taken together, gene expression levels in heads of both host species during manipulated biting and clinging show hallmarks of muscle tissue destruction and dysregulation (Fig. 6).

Over the course of infection by *Ophiocordyceps*, ant hosts are expected to lose energy stores to the parasite. The expression of genes related to nutritional balance will likely reflect this change in physiology. Moreover, starvation often induces hyperactivity in animals exhibited by increased levels of locomotion behavior (Yang *et al.* 2015), which in some cases could be adaptive for the host (Hite *et al.* 2019) or reflect parasitic manipulation. Indeed, we found DEGs putatively related to primary metabolism and nutrition in *Ophiocordyceps*-infected ants, which we frequently observed to display elevated bouts of locomotion prior to death (i.e. ELA). Two putative apolipophorin genes (apolipophorin and an apolipophorin III precursor domain containing gene) were significantly downregulated over the course of infection and manipulation in both *C. floridani* and *C. castaneus* (between 2-fold to 9-fold decrease from control to live manipulation) (de Bekker *et al.* 2015). Apolipohorin III has immune functions that operate in a trade-off manner with metabolism of high fat diets in insects (Adamo *et al.* 2010).

Beyond signs of a diminishing lipid metabolism (Appx. C), we detected differential cytochrome p450 4C1 expression, which has been implicated in starvation responses in cockroaches and responds to JH treatments in females (Lu *et al.* 1999). In cockroaches, starvation upregulated this gene, while we detected thirty putative cytochrome p450 4C1 genes downregulated from control to live manipulation in *C. floridanus*, with three significantly downregulated homologs in *C. castaneus* (de Bekker *et al.* 2015)

(Appx. C). An alpha amylase A-like gene, involved in the degradation of complex sugars (Da Lage 2018), was additionally downregulated over the course of infection (286-fold decreases from control to death in *C. floridanus* and 12-fold in *C. castaneus*). This indicates a reduction of starch metabolism in the likely starving host. Also tied to nutritional state, we observed a putative *insulin-1* gene downregulated in both species of ant hosts (3-fold and 6-fold decrease from control to live manipulation in *C. floridanus* and *C. castaneus*, respectively).

Insulin/insulin-like growth factor (IGF) signaling (IIS) pathways have been implicated in behavior, division of labor, and establishment of reproductive caste and associated behaviors in ants and bees (Ament *et al.* 2008; Chandra *et al.* 2018). Juvenile hormone and vitellogenin (VG) appear to play an important role in IIS pathways and behavior, although typically the strongest effects are observed during development and early life (Bloch *et al.* 2000; Brent *et al.* 2006; Lengyel *et al.* 2006; Nelson *et al.* 2007; Ament *et al.* 2008, 2010; Velarde *et al.* 2009; Penick *et al.* 2011; Dolezal *et al.* 2012; Libbrecht *et al.* 2013; Corona *et al.* 2013, 2016; Das 2016; Chandra *et al.* 2018; LeBoeuf *et al.* 2018; Opachaloemphan *et al.* 2018). Nutritional status, energy demands, and behaviors such as foraging appear to be interlinked in these eusocial insects. In our transcriptome dataset, we found two JH activating genes (juvenile hormone acid O-methyltransferases) and two deactivating genes (juvenile hormone epoxide hydrolases) that were significantly downregulated in live manipulated ants compared to healthy controls (Shinoda and Itoyama 2003; Zhang *et al.* 2005). A similar gene expression pattern was found for a homologous JH epoxide hydrolase in *C. castaneus* (de Bekker *et al.* 2015). *Ophiocordyceps*-induced changes in ant behavior could be partially due to, or reflected in, the dysregulation of ant JH levels (Fig. 6) and IIS functions (Appx. C).

Ecdysteroids can indirectly influence insect development and behavior by interacting with JH (Libbrecht *et al.* 2013). Modification of ecdysteroids has been implicated in the behavioral manipulation of moth larvae by baculovirus to assure that they remain in an elevated position (Hoover *et al.* 2011; Ros

et al. 2015; Han *et al.* 2015). We detected an enrichment of genes putatively encoding ecdysteroid kinases in the subset of ant genes that were downregulated from control to live manipulation and remained lowly expressed or decreased further into host death. The modification of ecdysteroids could, thus, also be involved in *Ophiocordyceps* manipulation of ant behavior to induce climbing behavior, and perhaps be a more general mechanism underlying summiting in parasite-manipulated insects. Possible fungal effectors interacting with these JH or ecdysteroid pathways are discussed in more detail in the differentially expressed fungal gene section below (Fig. 6).

Shifts in circadian rhythms and clock-controlled genes that regulate behavior. The cooption and manipulation of circadian rhythms have been proposed as an underlying mechanism for synchronized biting and the disruption of exploratory foraging behaviors in manipulated *Camponotus* (de Bekker *et al.* 2015, 2017b; de Bekker 2019). Healthy ants display daily regimented foraging behaviors controlled by the molecular clock. These behaviors are seemingly disrupted and replaced by manipulated climbing, biting, and clinging behaviors that in turn take place in a synchronized manner (Hughes *et al.* 2011; de Bekker *et al.* 2015). As controls and manipulated ants were time-matched within this study and within de Bekker *et al.* (2015), differential expression of clock-related genes is likely due to infection by *Ophiocordyceps* and not an artifact of time of day during sampling. In line with the circadian clock hypothesis, we found that the core clock gene, circadian locomotor output cycles kaput (*clk*) (Darlington *et al.* 1998), was significantly downregulated from healthy control to live manipulated ants in both *C. camponoti-floridani* (10-fold decrease) and *C. castaneus* (3-fold decrease) (de Bekker *et al.* 2015). Additionally, a gene putatively encoding the clock-controlled Takeout (TO) protein showed a similar gene expression pattern, again both in *C. floridanus* and *C. castaneus* (3-fold and 4-fold decreases from control to live manipulation, respectively) (de Bekker *et al.* 2015). Takeout is a JH interacting protein involved in insect foraging behaviors and starvation response (Sarov-Blat *et al.* 2000; Meunier *et al.* 2007; Schwinghammer *et al.* 2011) and has been proposed as a possible target for parasitic disruption of

insect locomotor activity and behavior (van Houte *et al.* 2013). We have found more evidence for this hypothesis and further discuss possible fungal effectors dysregulating *to* in the fungal DEG section below (Fig. 6).

Dysregulation of odor detection. Odor detection is at the basis of social organization and behavior in ants, mediated by multiple odorant receptors and odorant binding proteins. Pheromone binding proteins are a subset of odorant binding proteins specialized in binding pheromones and as such play a vital role in an individual's response to external stimuli (van den Berg and Ziegelberger 1991; Chang *et al.* 2015). We found 16 odor receptor and binding protein genes differentially expressed in *C. floridanus* (File S1, Appx. C), 13 of which were differentially expressed between controls and live manipulation, six being downregulated and seven upregulated.

One of the odorant receptors, putatively encoding an odorant receptor coreceptor (Orco), is highly conserved in insects and has a central role in odor detection (Jones *et al.* 2005; Stengl and Funk 2013; Zhou *et al.* 2014; Lin *et al.* 2015). Dysregulation of *orco* in ants has been linked to changes in overall sensitivity to odorants, and affects behavior such as time spent outside the nest, ability to detect prey, and aggression towards conspecifics (Yan *et al.* 2017; Ferguson *et al.* 2020). One of two putative *orco* genes in *C. floridanus* was significantly upregulated in the ant during live manipulation compared to control (3-fold increase). Its homolog in *C. castaneus* was significantly downregulated (4-fold decrease) (de Bekker *et al.* 2015). However, up- or downregulation of *orco* may lead to similar phenotypes as both agonist and antagonist effects on Orco are reported to produce similar changes in *C. floridanus* nestmate recognition (Ferguson *et al.* 2020). Similarly, in both ant host species, multiple genes putatively encoding PBP Gp9 were differentially expressed during manipulation (de Bekker *et al.* 2015) (Appx. C) and have been implicated in mediating fire ant colony social dynamics (Ross 1997; Ross and Keller 1998; Krieger and Ross 2002; Gotzek and Ross 2007; Gotzek *et al.* 2007). *Ophiocordyceps* infected individuals may be unable to properly communicate with nestmates and recognize organizational signals due to disrupted

odorant reception. This dysregulation could be facilitating the wandering behaviors we observed in infected individuals and prove to be parasite-adaptive if infected ants are thereby more commonly positioned in suitable fungal transmission sites (Fig. 6).

Dysregulation of neurotransmitter signaling. Dysregulation of neurotransmitter and neuron-modulating compounds are a plausible parasite strategy to manipulate host behavior. We identified a suite of ant neuron regulating and neurotransmitter receptor genes in the WGCNA modules that were negatively correlated to samples collected at live manipulation (see above and Figure 4). Closely inspecting DEGs, we also identified putative ant neuromodulatory compounds that were differentially expressed over the course of infection.

Dysregulation of kynurenic acid, an anticonvulsant and neuroprotective neuroinhibitor, has been implicated in mammalian neurodegenerative disease, changes in activity levels, and reduced motor coordination (Yu *et al.* 2004b, 2006). A putative kynurenine/alpha-aminoadipate aminotransferase, which promotes the synthesis of kynurenic acid, was upregulated in the ant during live manipulation (3-fold increase from control to live manipulation in *C. floridanus* and 33-fold increase in *C. castaneus*) (de Bekker *et al.* 2015). Additionally, metabolomics on manipulated *C. castaneus* identified that *O. kimflemingiae* secreted the neuroprotectant ergothionine (Loreto and Hughes 2019). Indeed, neural tissues appear to be among the last host tissues to be severely degraded (Hughes *et al.* 2011; Fredericksen *et al.* 2017). The preservation of neural tissue by compounds such as parasite ergothionine or host kynurenic acid is potentially critical for manipulation by fungal effectors operating via changes in ant biogenic amines and the disruption of neuron functions (Fig. 6).

Biogenic monoamines have neuromodulatory roles in insects, and changes in monoamine activity and synthesis may underlie manipulated phenotypes in ants. Acting through G-protein coupled receptors (GPCRs), octopamine functions as a neurotransmitter in insects modulating learning and memory, foraging behavior, starvation-induced locomotion activity, insulin levels, olfactory decision making,

aggression, and social interactions (David and Verron 1982; Schulz *et al.* 2002; reviewed in Roeder 2005; Yang *et al.* 2015; Li *et al.* 2016). Such processes may serve as targets for *Ophiocordyceps* to induce behavioral modifications such as ELA (Hughes *et al.* 2011; de Bekker *et al.* 2015). Moreover, parasitoid venom-induced hypokinesia in cockroaches has been linked to modulation of octopamine activity levels, most likely through manipulation of octopamine receptors (Libersat and Gal 2014). Consistent with this scenario, we identified octopamine receptors that were differentially expressed between live manipulated and control ants. In *C. floridanus*, a putative octopamine receptor beta-2R was downregulated during manipulation (2-fold decrease from control to live manipulation), while beta-3R was found to be upregulated in *C. castaneus* (6-fold increase from control to live manipulation) (de Bekker *et al.* 2015). This suggests that octopamine responsiveness is dysregulated in *Ophiocordyceps*-infected ants, although the specific mechanisms used by different fungal species may differ.

Dopamine, another biogenic monoamine, also functions as a neurotransmitter in insects and regulates motor neuron activity, locomotion behavior, and biting behavior, among other processes, sometimes in a clock-controlled fashion (Cooper and Neckameyer 1999; Ceriani *et al.* 2002; Szczuka *et al.* 2013; reviewed in Yamamoto and Seto 2014). Tyrosine 3-monooxygenase drives the rate-limiting step in dopamine synthesis (Daubner *et al.* 2011). We found homologous genes putatively encoding for this enzyme to be significantly upregulated during manipulation in *C. floridanus* (4-fold increase from control to live manipulation) and *C. castaneus* (3-fold increase) (de Bekker *et al.* 2015). In addition, a putative DOPA decarboxylase, which catalyzes the final step of dopamine synthesis (Daubner *et al.* 2011) was significantly upregulated in *C. floridanus* during manipulation (3-fold from control to live manipulation). Changes in dopamine levels may also be implicated in immune function, as a precursor to melanin, which is a component of ant immunity (Ratzka *et al.* 2011). However, dysregulation related to both octopamine and dopamine in ants during manipulation indicated a role for biogenic monoamines in producing the observed behaviors (Fig. 6).

In addition to neuroprotective agents and biogenic monoamines, we identified two more differentially expressed genes that could be involved in aberrant neuronal functioning in manipulated individuals. Both *C. floridanus* and *C. castaneus* exhibited reduced expression of a putative *dimmed*-like transcription factor in live manipulated ants compared to the healthy controls (6-fold and 9-fold decrease, respectively) (de Bekker *et al.* 2015). The downregulation of *dimmed* resulted in the dysregulation of neuropeptide secretion and IIS-responsive neuronal maintenance in *Drosophila* (Hamanaka *et al.* 2010; Luo *et al.* 2013; Liu *et al.* 2016). A putative *bubblegum* gene was also downregulated in *C. floridanus* during manipulation (5-fold decrease from control to live manipulation) as was the homolog in *C. castaneus* (4-fold decrease) (de Bekker *et al.* 2015). In *Drosophila*, *bubblegum* mutants displayed neurodegeneration, retinal degeneration, and reduced locomotor activity (Min and Benzer 1999; Sivachenko *et al.* 2016).

Differentially expressed putative fungal effector genes: As for the ant gene expression data, we divided the fungal data into subsets representing different interpretations of gene function in relation to manipulation (Fig. 1). Fungal genes that were significantly upregulated from culture to live manipulation and then downregulated once the host died likely played a role in infection and/or behavioral manipulation (307 genes, File S2). For enrichment analysis, we further narrowed this set of upregulated genes to the top 50th percentile of genes with the largest downregulation in dead hosts (168 genes, File S2). Genes in this 50th percentile were tightly regulated relative to the manipulation event and, therefore, possibly the most manipulation specific genes in our dataset. We also considered genes that were upregulated from culture to live manipulation and then had sustained or increased transcription in the dead host (1088 genes, File S2). Being upregulated, these genes plausibly play a role in infection or manipulation. They may also play a role in fungal activities associated with host death, such as killing the host and consuming dead host tissues. Similarly, we considered differentially expressed gene sets that were downregulated at live manipulation relative to both culture and dead hosts (61 genes, File S2), a 50th

percentile strongly down subset (33 genes, File S2), and downregulated from culture and holding or dropping further in dead hosts (867 genes, File S2). These gene sets could either indicate genes not important for manipulation, or the reduced transcription of inhibitors. The two fungal species shared more homologs in upregulated (29%) than downregulated (18%) DEGs. Upregulated DEGs also contained more hits for pathogenicity in the Pathogen-Host Interaction database (Urban et al. 2017) (S3 File). This suggested that upregulation during manipulation contains proportionally more genes with conserved function and fitness constraints, i.e. involvement in infection and manipulation.

Over 25% (239 genes) of genes with SignalP secretion signals were upregulated from culture to living manipulated ants. Similarly, 22% (195 genes) were upregulated in the putative secretome of *O. kimflemingiae* (de Bekker *et al.* 2015). The increased activation of the *Ophiocordyceps* secretome during manipulation by both species suggests a critical role for secreted compounds in modifying host behavior. This is in line with microscopy evidence demonstrating that fungal cells do not grow invasively into the ant's brain (Hughes *et al.* 2011; Fredericksen *et al.* 2017), but rather likely manipulate behavior peripherally by secreting neuroactive compounds. Yet, only 54% of the *O. camponoti-floridani* secretome upregulated from culture to manipulation had PFAM annotations (Appx. K), leaving about half of these potential key players without an assigned putative function.

Ophiocordyceps upregulated GPCR-interfering toxins during manipulation. Many cellular receptors, including neurotransmitter receptors, are GPCRs that could serve as targets for fungal ADP-ribosylating toxins (Fig. 6). Heat-labile enterotoxins are in this class and have been described for pathogens such as *Escherichia coli*, *Cordyceps bassiana*, and *Metarhizium robertsii* (reviewed in Lin *et al.* 2010; Mannino *et al.* 2019). Heat-labile enterotoxins of *E. coli* transfer an enzymatic domain into host cells to modify GTP-binding proteins and interfere with GPCRs and subsequent intracellular signaling through increased cyclic AMP levels. This process eventually leads to cell dysfunction and apoptosis (reviewed in Lin *et al.* 2010; Mangmool and Kurose 2011). Other microbial toxins that disrupt GPCRs or

intracellular signaling showcase pathogenic effects that suggest toxins could benefit *Ophiocordyceps* in infecting and manipulating host ants. Heat-stable bacterial enterotoxins dysregulate pheromone production in insect fat bodies (Wiygul and Sikorowski 1986, 1991). The ADP-ribosylating mosquitocidal toxin of *Bacillus sphaericus* acts on G proteins and has lethal effects on mosquitoes (Thanabalu *et al.* 1991). Cytotoxic necrotizing factor-1 interacts with GTPases and contributes to *E. coli* invasion of central nervous tissues and crossing of the blood-brain-barrier in mammals (Khan *et al.* 2002).

The *O. camponoti-floridani* genome contains 35 predicted heat-labile enterotoxin genes based on the PFAM annotation Enterotoxin_a, which was enriched among upregulated genes during manipulation (Fig. 7). This group of upregulated enterotoxins also resulted in enrichment of the GO terms "multi-organism process," "interspecies interactions between organisms," "toxin activity," and "pathogenesis" (File S2). Thirty putative enterotoxins carried SignalP secretion domains, 10 of which were upregulated from culture to live manipulation, and then six were sharply downregulated in the dead host. The most strongly upregulated enterotoxin in *O. camponoti-floridani* displayed a >12,000-fold increase in transcripts from culture. The putative ortholog in *O. kimflemingiae* displayed a marked > 3,000-fold upregulation (de Bekker *et al.* 2015). Moreover, this enterotoxin gene appears to be exclusively conserved in ant-manipulating *Ophiocordyceps* species (de Bekker *et al.* 2017a), suggesting a potential specialized role in facilitating ant manipulation. This enterotoxin gene was also present in the manipulation associated fungal WGCNA module F2 with seven other enterotoxins. Module F1 contained an additional three enterotoxin genes.

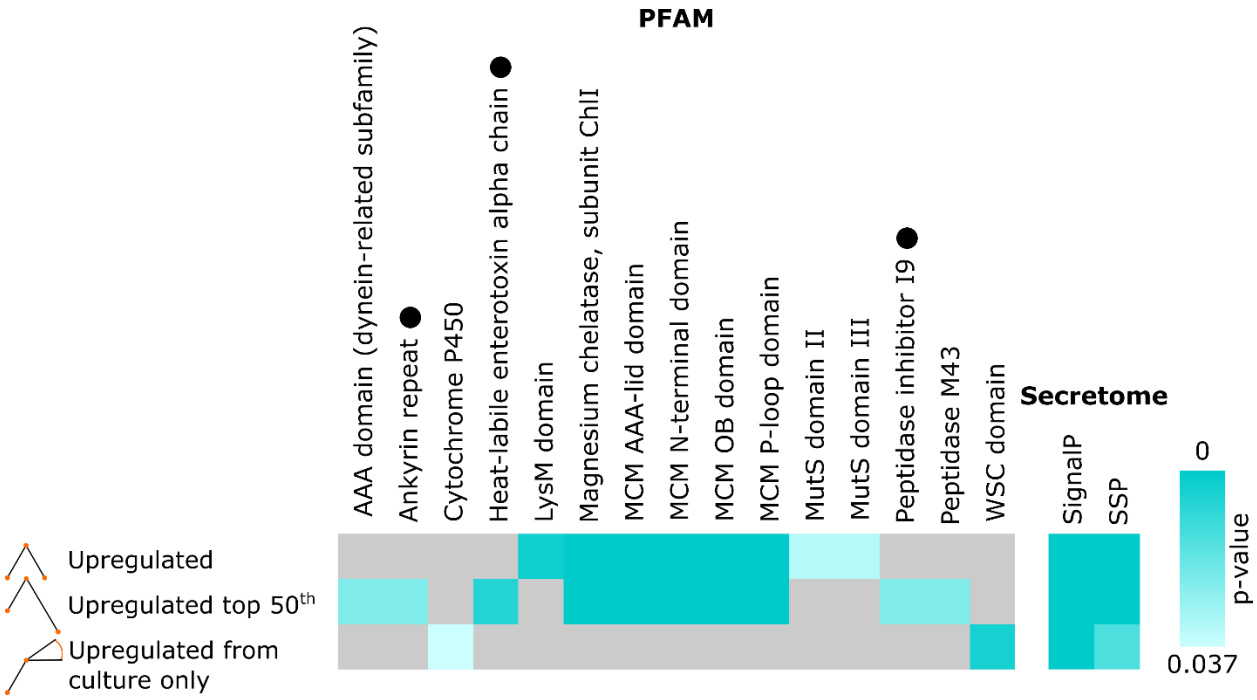

Figure 7. PFAM and secretion signal domain enrichments in DEG sets with increased transcription during live manipulation.

"Upregulated" refers to genes with peak transcription during live manipulation. "Upregulated top 50th" refers to the subset of upregulated genes with the strongest subsequent downregulation in dead manipulated samples. "Upregulated from culture only" are genes with increased transcription from culture to live manipulation, but exhibited no change or increasing transcription with host death. PFAMs associated with genes that have possible roles in manipulation include: Heat-labile enterotoxin alpha chain, Ankyrin repeat, and Peptidase inhibitor I9 (indicated by black dots), and Peptidase M43 (File S3).

Ant-infecting *Ophiocordyceps* genomes are enriched for heat-labile enterotoxins compared to generalist fungal pathogens and have been suggested to play a major role in *Ophiocordyceps* pathogenesis. For example, *O. kimflemingiae* has 36 putative enterotoxins, *Ophiocordyceps australis* has 20, and *Ophiocordyceps polyrhachis-furcata* has 22 (Wichadakul *et al.* 2015; de Bekker *et al.* 2017a), while the generalist entomopathogens *C. bassiana*, *M. robertsii*, and *Isaria javanica* have 13, six, and five enterotoxins, respectively (Xiao *et al.* 2012; Mannino *et al.* 2019; Lin *et al.* 2019). The number of putative enterotoxin genes, their notable upregulation, and membership in manipulation associated gene

modules strongly suggest a role for these toxins during *Ophiocordyceps* infection and manipulation (Fig. 6).

Other putative ADP-ribosylating toxins were also upregulated in *O. camponoti-floridani* at the time of manipulation relative to growth in culture and in dead hosts. This included two *Bordetella pertussis* toxin A genes that were also identified in the manipulation correlated fungal WGCNA module F1. These genes carried Ankyrin repeat domains, which contributed to the enrichment for this PFAM annotation among genes upregulated during manipulation (Fig. 7). One of these pertussis toxins was upregulated in both fungal species over the course of infection (i.e., 4-fold increase from culture to live manipulation in *O. camponoti-floridani*, and 538-fold in *O. kimflemingiae*). The active sites of pertussis toxins are similar to heat-labile enterotoxins and also act via GPCR interference (Locht *et al.* 1986), and therefore may have comparable effects on host physiology.

Fungal serine proteases are upregulated during manipulated biting behavior. Fungal subtilases are subtilisin-like serine proteases that have been implicated in entomopathogenic interactions by degrading insect cuticle (chitin). During infection, *Metarhizium anisopliae* produces increased levels of serine protease Pr1, leading to host death. Additionally, Pr1 overproducing strains of *M. anisopliae* decrease host-feeding and injections of Pr1 are toxic (St Leger *et al.* 1996). Often, these proteases contain a peptidase inhibitor I9 domain, which is present in propeptides and assists folding and activation once cleaved (reviewed in Figueiredo *et al.* 2018).

Inhibitor I9 domain encoding genes were found to be enriched among genes upregulated during manipulation (Fig. 7). Two of these three I9 containing genes were subtilases with MEROPS S8A annotations similar to Pr1 found in *C. bassiana* and *M. anisopliae* (Joshi *et al.* 1995). We found six S8A annotated *O. camponoti-floridani* genes upregulated during manipulation relative to culture (some lack I9 domains, Appx. C), one of which was found in WGCNA module F1. Similarly, six serine proteases were upregulated during manipulation in *O. kimflemingiae* (de Bekker *et al.* 2015). If *Ophiocordyceps* fungi

employ these subtilases for virulence in general or use them for manipulation specifically is not clear. However, the highly species-specific ant manipulating *Ophiocordyceps* carry fewer subtilases (*O. camponoti-floridani* n = 16, *O. kimflemingiae* n = 18, and other *Ophiocordyceps* species n < 20) compared to generalist entomopathogenic fungi (*C. bassiana* n = 43, *Cordyceps militaris* n = 26, *M. anisopliae* n = 55, and *Metarhizium acridum* n = 43) (Gao *et al.* 2011; Zheng *et al.* 2011; Xiao *et al.* 2012; de Bekker *et al.* 2015; Wichadakul *et al.* 2015). A larger repertoire of proteolytic enzymes may facilitate infection of various host species and is thought to be associated with a broader host range in fungal entomopathogens (Xiao *et al.* 2012; Lin *et al.* 2019). The relatively low number of subtilases in *Ophiocordyceps* genomes corroborates their high species-specificity (de Bekker *et al.* 2014b; Araújo *et al.* 2018; Sakolrak *et al.* 2018).

A putative fungal eckinase may modulate host ecdysteroids. We have uncovered evidence for changes in ant JH, IIS pathways, and ecdysteroids being linked to modified behavior. One possible scenario is that fungal effectors are targeting these elements of host physiology directly. Ecdysteroids have been implicated in viral manipulation of caterpillars that display a summit disease phenotype. Baculovirus secretes an enzyme, EGT, which inactivates an ecdysone molting hormone and alters larval feeding behavior and development (O'Reilly 1995). In certain species of caterpillar, *egt* is implicated in driving fatal summit disease, while it only alters pre-molting climbing behavior in others (Hoover *et al.* 2011; Ros *et al.* 2015; Han *et al.* 2015). Moreover, the entomopathogenic fungus *Nomuraea rileyi* appears to attack host ecdysteroid pathways by secreting an enzyme that disrupts larval development (Kiuchi *et al.* 2003; Kamimura *et al.* 2012).

In *O. camponoti-floridani*, we detected a phosphotransferase gene with eckinase and SignalP domains that was significantly higher expressed during manipulation than in culture (2-fold increase). This gene was also present in WGCNA module F2. Eckinase activity helps mediate the balance of active

free ecdysteroids and inactive storage forms (Sonobe *et al.* 2006). As such, *O. camponoti-floridani* could be utilizing a similar strategy as baculovirus or *Nomuraea* to modify its host, targeting ecdysteroid levels with an ecdysteroid modulating enzyme (Fig. 6).

Upregulated protein tyrosine phosphatase implicated in insect hyperactivity and ELA. Also implicated in baculovirus infection, PTP has a suggested role in ELA phenotypes of infected caterpillars (Kamita *et al.* 2005; Katsuma *et al.* 2012), but not summiting (van Houte *et al.* 2014b). Whether enzymatic activity of PTP is needed for modifying caterpillar behavior appears to differ by the study system used (Katsuma *et al.* 2012; van Houte *et al.* 2012). However, when enzymatic activity is critical, PTP has been hypothesized to act via changes of TO or the cGMP-dependent serine/threonine protein kinase, Foraging (For) (van Houte *et al.* 2013). The protein For underlies feeding behaviors in ants and other insects (Osborne *et al.* 1997; Ben-Shahar *et al.* 2002, 2003; Lucas and Sokolowski 2009; Ingram *et al.* 2011) and serves as an intriguing candidate for fungal disruption. Circadian expression and phototactic effects of *for* have previously been shown (Ben-Shahar *et al.* 2003; Ingram *et al.* 2011). Therefore, if fungal PTP could dysregulate activity of For in ants, this would be a plausible strategy for the parasite to alter when and how long the ant host leaves the nest to engage in foraging behaviors and locomotor activity. Similarly, disruption of TO, which is downregulated in manipulated *Camponotus*, could dysregulate foraging behavior (Fig. 6).

What function PTP may have for fungal manipulation of *Camponotus* ants is uncertain at this time. However, *O. camponoti-floridani* has seven putative *ptp* genes, of which five were upregulated from culture during manipulation, with three of those putatively secreted. We found four *ptp* genes in manipulation WGCNA modules F1 (n = 1) and F2 (n = 3), and two of these upregulated *ptp* genes in *O. camponoti-floridani* (365- and 8-fold increase from culture to manipulation) have homologs in *O. kimflemingiae* that were upregulated in similar fashion (28- and 2-fold increase) (de Bekker *et al.* 2015).

Fungal secondary metabolites involved in manipulation and infection: We identified 25 secondary metabolite clusters in the *O. camponoti-floridani* genome and determined the bioactive compounds they produce from the annotated PFAM domains of their backbone genes. The genomes of *O. kimflemingiae* and *O. polyrhachis-furcata* contain comparable numbers of annotated clusters, 25 and 24, respectively (de Bekker *et al.* 2015; Wichadakul *et al.* 2015). Notably, 23 of the *O. camponoti-floridani* clusters contain genes with homologs identified previously in *O. kimflemingiae* as secondary metabolite cluster genes (de Bekker *et al.* 2017a). Their gene expression patterns and functional annotations offer insights into the possible fungal secondary metabolites involved in manipulation and infection as discussed below and Appx. C.

Cluster 18, Manipulation-related aflatrem-like indole-diterpene alkaloid production. Metabolite cluster 18 putatively produces an alkaloid that appears to be a mycotoxin. The entirety of this eight-gene cluster demonstrated a striking upregulation during infection (Fig. 8A), as did the homologous cluster in *O. kimflemingiae* (de Bekker *et al.* 2015). Additionally, six cluster 18 genes were found in fungal manipulation WGCNA module F2. These clusters are highly similar in gene composition and organization between the two *Ophiocordyceps* species(Fig. 8B) (de Bekker *et al.* 2015). Previously, de Bekker *et al.* 2015 identified one possible product of this cluster to be an ergot alkaloid based on a tryptophan dimethylallyltransferase (TRP-DMAT) backbone gene of the cluster (> 12,000 fold increase from culture to live manipulation in *O. camponoti-floridani*, 5,900 fold in *O. kimflemingiae*).

However, homology searches indicated that cluster 18 is more likely to produce an aflatrem-like indole-diterpene alkaloid (Fig. 8B). Aflatrem is a neurotoxic tremorgen that causes “stagger disease” in poisoned hosts and is closely related to other mycotoxins such as paxilline or lolitrem (Gallagher and Hawkes 1986). By interfering with big potassium (BK) channels, and, gamma amino butyric acid (GABA)-ergic and glutamatergic processes, aflatrem can induce muscle tremors, changes in activity level, and confusion (Valdes *et al.* 1985; Gant *et al.* 1987; Yao *et al.* 1989; Knaus *et al.* 1994).

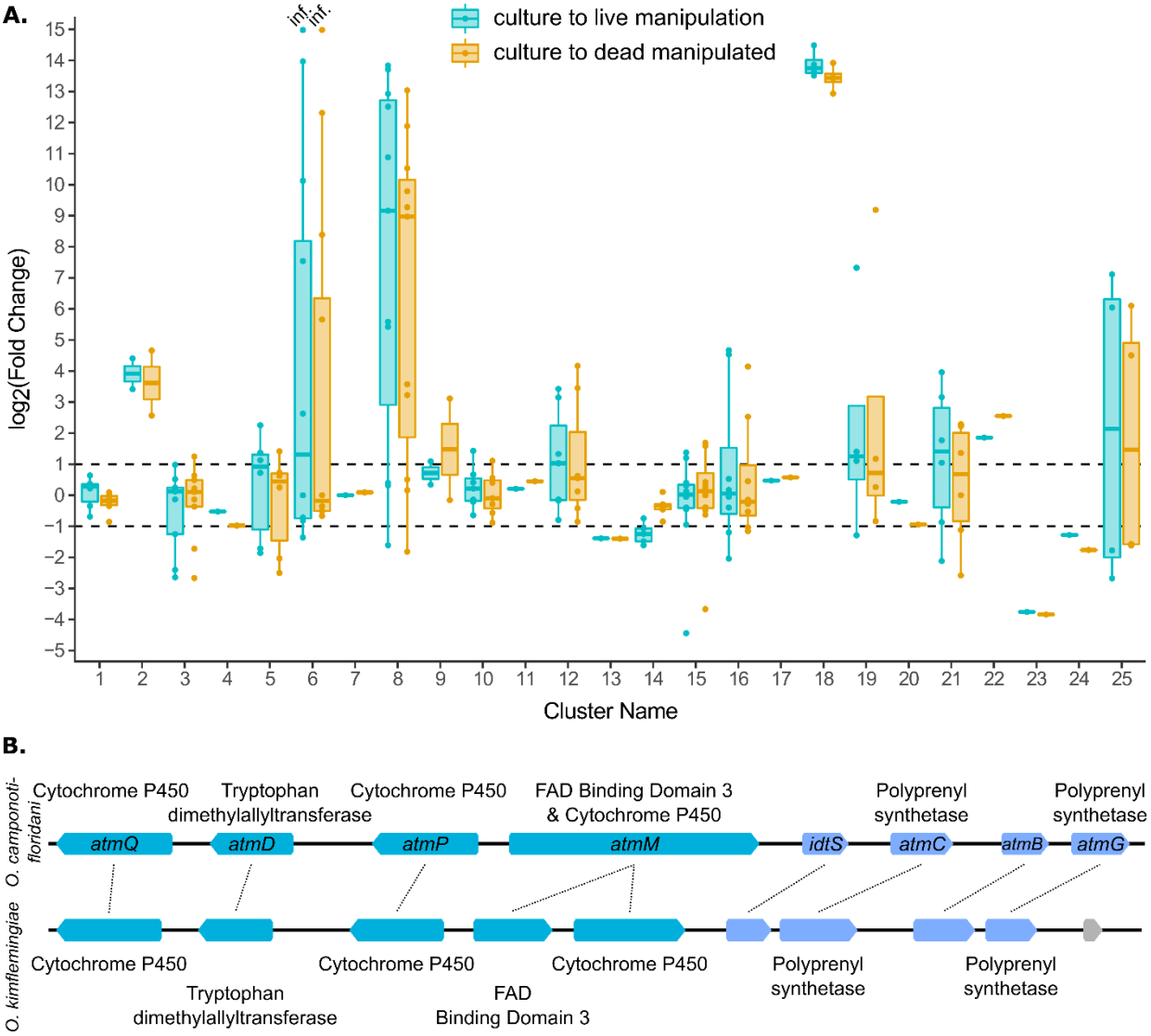

Figure 8. Changes in expression of secondary metabolite cluster genes relative to control conditions.

A) Fold change of secondary metabolite cluster genes transcripts during live-manipulation (blue) and in dead-manipulated samples (orange) relative to control culture. Dots represent fold change of a single gene within a metabolite cluster. Dashed lines indicate a 2-fold change in transcript abundance (i.e. log2(Fold Change) = ±1). Clusters 2, 6, 8, 12, and 18 are possibly involved in pathways producing entomopathogenic compounds similar to aflatoxin, fusarin C, aflatoxin, citrinin (File S3), and aflatrem, respectively. Many genes of these clusters also displayed notable increases in transcript levels relative to culture. Points labeled "inf." in cluster 6 have infinite fold increases due to culture RPKM values equal to 0. B) Schematic of cluster 18 genes (top) and corresponding homologs in O. kimflemingiae (bottom). PFAM annotations are labeled outside the depicted loci and, for O. camponoti-floridani, BLASTp hits for aflatrem synthesis proteins are indicated inside. Teal indicates cluster genes

identified bioinformatically, blue genes are selected cluster-adjacent genes based on their similar expression, putative function, and proximity to the main cluster (not represented in [A]). The locus in gray is unrelated to the cluster. Image modified from output generated by Geneious Prime (v 2019.0.3, Biomatters).

Ophiocordyceps infected ants display comparable symptoms such as convulsions (Hughes *et al.* 2011), muscle hypercontraction (Mangold *et al.* 2019), and atypical exploratory behaviors (de Bekker *et al.* 2014b) (Fig. 6).

Adjacent to secondary metabolite genes in cluster 18, we identified additional putative cluster members based on similar expression patterns, functional annotations related to secondary metabolism, and proximity (approximately within 3 kbp of another cluster gene, i.e., double the distance between any genes in the original cluster). Among these genes, we identified an upregulated terpene cyclase *atmB*-like gene. This gene has a homolog in *O. kimflemingiae* annotated as *paxB* (the corresponding paxilline synthesis gene compared to aflatrem), which suggests that aflatrem or a similar indole-diterpene is synthesized by cluster 18 (Fig. 8B).

We subsequently performed a BLASTp of translated Aspergillus flavus aflatrem synthesis genes (atmA, atmB, atmC, atmD, atmG, atmM, atmP, and atmQ) (Nicholson et al. 2009) against the entire *O. camponoti-floridani* genome. All proteins except AtmA scored BLASTp hits with the lowest E-value hits in or adjacent to cluster 18. All putative aflatrem synthesis homologs were present in a single cluster of the O. camponoti-floridani genome, while these genes are split between two genomic sites in A. flavus (Nicholson et al. 2009).

Despite not detecting any homologous proteins to AtmA in the *O. camponoti-floridani* genome, there is an upregulated gene in the cluster-adjacent set that has a BLAST annotation corresponding to *idtS*, but otherwise lacks a GO or PFAM annotation (Fig. 8B). Described in the lolitrem-producing fungi *Epichloë* and *Neotyphodium* as necessary for indole-diterpene synthesis (Schardl et al. 2013), the molecular role of IdtS is not entirely clear. Similarly, the role of AtmA in aflatrem synthesis has not yet

been fully elucidated (Nicholson et al. 2009). The *O. camponoti-floridani idtS* homolog may work in concert with the indole-diterpene synthesis genes identified in cluster 18, although we currently do not fully understand its function.

Aflatrem gene cluster synteny and upregulation during manipulation were well conserved between *O. camponoti-floridani* and *O. kimflemingiae* (Fig. 8B), suggesting an important role for this mycotoxin in facilitating manipulation. Metabolite clusters are suggested to reflect ecological and evolutionary pressures and allow insight into possible critical functions for the life history of a fungus (Slot *et al.* 2019). Possible fitness benefits are suggested by these genes being clustered at a single genomic site and their high degree of conservation between *O. camponoti-floridani* and *O. kimflemingiae*. Such organization may allow these fungi to better regulate aflatrem genes in tandem and maintain them as a physically linked genetic unit, unlike *A. flavus* for example, which carries these genes at two distinct sites.

Clusters 8 and 2, Putative aflatoxin production during infection and manipulation. Aflatoxin is a potent mycotoxin and carcinogen with lethal effects on insects (Trienens and Rohlfs 2011). We predicted the polyketide metabolite clusters 8 and 2 to contribute to production of a secondary metabolite in the same class or sharing structural similarity to aflatoxin. We hypothesized this based on homology to known aflatoxin genes in the *Ophiocordyceps* genome and a number of those genes belonging to these metabolite gene clusters. The polyketide synthase (PKS) backbone gene in these clusters having a starter unit:acyl carrier protein transacylase (SAT) domain that facilitates the first step in the synthesis of aflatoxins (Brown *et al.* 1996). Upregulation of most genes in putative aflatoxin-like clusters 8 and 2 during live manipulation suggests a role for this mycotoxin during the final stages of infection (eight of 11 and two of two genes upregulated, respectively) (Fig. 8A). Five genes from cluster 8 were in the manipulation associated WGCNA module F2. The PKS backbone of cluster 8 was upregulated during manipulation in both *O. camponoti-floridani* and *O. kimflemingiae* (i.e., 43-fold increase from culture to

live manipulation in *O. camponoti-floridani*, 4,350-fold in *O. kimflemingiae*). The PKS backbone of cluster 2 was also upregulated (11-fold increase from culture to live manipulation). However, the cluster 2 backbone homolog in *O. kimflemingiae* were downregulated during this time.

Using the *Aspergillus parasiticus* aflatoxin gene cluster (Yu *et al.* 2004a), we performed a BLASTp search of 25 proteins against the *O. camponoti-floridani* genome. All but two genes (*aflI* and *aflX*) had at least one *O. camponoti-floridani* homolog. The PKS backbone of cluster 8 is homologous to *aflC*, the PKS of the *A. parasiticus* cluster (E-value = 2.61e-98). Additionally, cluster 8 contained the top BLASTp hit for *aflJ*. Furthermore, *aflD* returned a low E-value hit within the cluster (1.94e-06), but fell short of our bit score 50 cutoff (46.21). Although these results do not demonstrate that cluster 8 produces aflatoxin, they do suggest a role in generating a similar compound.

The PKS backbone of cluster 2 is also a putative homolog to AflC (E-value = 1.38e-93) and the clusters' O-methyltransferase was the top BLASTp hit for AflP, which generates the penultimate product in aflatoxin synthesis (Yu *et al.* 2004a). Although our bioinformatic approach only identified these two genes in cluster 2, similarly regulated adjacent genes could generate products consistent with the aflatoxin synthesis pathway. In proximity to cluster 2, the *O. camponoti-floridani* genome contains an upregulated gene encoding a protein homologous to AflQ, known to play an important role in the final step of aflatoxin synthesis (Yu *et al.* 2004a). We also identified a possible homolog to *aflT* (E-value = 4.22e-38), which is known to be involved in aflatoxin synthesis (Yu *et al.* 2004a). A homolog of *A. parasiticus* Velvet-complex member *laeA* is also adjacent to the cluster, which functions as a regulator of the aflatoxin-intermediate sterigmatocystin (Bok and Keller 2004). The top BLASTp hit for AflR, which is a transcription factor involved in aflatoxin synthesis and interacts with LaeA in a regulatory feedback loop (Yu *et al.* 2004a; Bok and Keller 2004) was found on the same contig, albeit distantly from cluster 2. Also possibly interacting with LaeA, two velvet domain containing genes were upregulated from culture

to manipulation, one of which has a similarly upregulated homolog in *O. kimflemingiae*. The homologs of *alfC*, *alfP*, *alfT*, and a velvet transcription factor were also found in fungal WGCNA module F2.

Taken together, metabolite clusters 2 and 8 and their homologs in *O. kimflemingiae* suggest that both species of *Ophiocordyceps* have the capacity to produce an aflatoxin-like compound. However, contrasting transcriptomics data for cluster 2 across these species indicated that the regulation of aflatoxin production during infection and manipulation might be different across these species.

Cluster 6, Fusarin C as a possible virulence or behavior modifying factor. Fusarin C is the likely product of cluster 6, consisting of nine genes, two of which were upregulated during live manipulation (Fig. 8A). Three other genes in this cluster were also present in WGNCA modules F1 (n = 1) and F2 (n = 2). Fusarin C is a carcinogenic mycotoxin and although produced by the entomopathogen *Metarhizium anisopliae*, insecticidal or antibacterial activity appears to be absent without culturing additives (Krasnoff *et al.* 2006). Additionally, insects possibly resist some effects of fusarin C by detoxification pathways that respond to xenobiotic and toxic challenges (Gelderblom *et al.* 1988; Gui *et al.* 2009; Rohlfs and Churchill 2011). However, fusarin C may have non-lethal effects as suggested by its apparent mycoestrogen activity, demonstrated in mammalian cells (Sondergaard *et al.* 2011). Estrogens could be involved in the production of ecdysteroids and VG with effects on development, reproduction, and diapause in insects (reviewed in Das 2016). Speculatively, exogenous estrogen activity from fusarin C produced by *Ophiocordyceps* could, thus, be disrupting ant physiology and behavior (Fig. 6).

Four genes appear necessary for fusarin C synthesis in *Fusarium fujikuroi*: *fus1*, *fus2*, *fus8*, and *fus9* (Niehaus *et al.* 2013). All four homologs in cluster 6 represented the top or sole BLASTp result in the *O. camponoti-floridani* genome. Two additional fusarin C cluster proteins, Fus3 and Fus4 (Niehaus *et al.* 2013), also had top BLASTp hits in cluster 6. Only *fus4* (seven-fold increase from culture to live manipulation) and *fus9* (0 RPKM to 2 RPKM) homologs were upregulated during manipulation, while the other cluster genes were either not differentially expressed or downregulated. *Ophiocordyceps*

kimflemingiae and *O. polyrhachis-furcata* also contain clustered homologs of the necessary fusarin C synthesis genes (de Bekker *et al.* 2015; Wichadakul *et al.* 2015). In the *O. kimflemingiae*, all but the *fus1* homolog were upregulated during live manipulation relative to both culture and dead hosts (de Bekker *et al.* 2015).

Similar to our findings for aflatoxin, the presence of homologous fusarin C clusters among *Ophiocordyceps* species suggests that all utilize fusarin C-like mycoestrogens, but when this metabolite is produced or used may differ between species. Possibly, fusarin C has a role earlier in infection when subtler behavioral changes such as altered locomotor activity manifest. Changes in ecdysteroid or VG related behaviors, such as time spent foraging or nest occupation, may be plausible effects of the introduction of such a mycoestrogen and the underlying synthesis genes may no longer be strongly expressed during the final manipulation stage in all *Ophiocordyceps*.

Conclusion

A growing body of literature has proposed possible fungal effectors of the ant-manipulating *Ophiocordyceps* based on genomic, transcriptomic, and metabolomic analyses (de Bekker *et al.* 2014b, 2015, 2017a; Wichadakul *et al.* 2015; Kobmoo *et al.* 2018). Although phylogenetic and experimental evidence indicate that *Ophiocordyceps*-ant interactions are species specific (Kobmoo *et al.* 2012; de Bekker *et al.* 2014b; Araújo *et al.* 2018; Sakolrak *et al.* 2018), we hypothesized that *Ophiocordyceps* species share mechanisms to infect and manipulate their hosts as they face similar host and transmission related challenges (Chetouhi *et al.* 2015; Loreto *et al.* 2018). Indeed, we have found transcriptomic and genomic signals during *Ophiocordyceps camponoti-floridani* manipulation in line with previous work on *O. kimflemingiae* and other species, indicating several possible common contributors to infection and manipulation. Not only did these putative mechanisms of infection and manipulation emerge from

comparisons across species of both parasite and host, they were consistent among the analyses that we employed (PCA, WGCNA, and DEG analysis).

Gene expression changes related to neuron function in manipulated ants could be an effect of secreted fungal compounds (Fig. 6). Neurotransmitter receptors present one of many possible GPCR targets for fungal ADP-ribosylating toxins. Additionally, a putative aflatrem alkaloid toxin may be attacking the host nervous system, inducing stagger disease-like symptoms. A wealth of unannotated putative secreted proteins also offers candidate manipulation genes that may act on the nervous system, or other aspects of host biology.

Behavior regulating pathways involving players such as TO, CLK, JH, ecdysteroids, and IIS may be intertwined with each other and respond to fungal disruption via mechanisms such as PTP, eckinases, or fusarin C (Fig. 6). In particular, foraging behaviors may be modified and result in ELA and wandering behaviors of manipulated ants that facilitate dispersal of infected hosts to transmission sites. In line with dysregulation of task performance, changes in ant odorant reception and chemical communication with nestmates could contribute to similar asocial wandering phenotypes.

Taken together, we propose several fungal candidate manipulation genes and possible ant behavioral pathway responses that could drive manipulated climbing, biting, and clinging behaviors in *Ophiocordyceps*-manipulated individuals. However, the candidates that we identified must still be functionally tested for a more precise understanding of how, and if, they play a critical role in the manipulation of host behavior. Similarly, follow-up metabolomic approaches would validate the production of secondary metabolites by the putative gene clusters we propose here. Investigating potential protein-level mimicry by the parasite to interfere with host processes and physiology may be fruitful as well (Hebert *et al.* 2015). The comparison of multiple *Ophiocordyceps* and their respective ant hosts could identify possible species-specific mimicry that would indicate tight coevolutionary relationships and precise mechanisms of manipulation. Such studies could eventually be expanded to other parasitic

manipulation systems since we find signatures of potentially convergently evolved mechanisms across manipulators (i.e., baculovirus). As such, our study provides a springboard towards deeper functional and evolutionary understandings of the molecular mechanisms underlying host manipulation. In turn this could offer additional insights into novel bioactive compounds and the neurobiology of animal behavior in general.

Acknowledgements

We thank the Laboratory for Functional Genome Analysis and Genomics Services Unit at the Ludwig Maximilians Universität for sequencing support. We also thank Hannah Christensen for isolating the Arb2 fungus and Sara Linehan for preliminary field observations, who with Andrea Bender and Brianna Santamaria assisted with behavioral observations. The Genetics Society of America and the Mycology Society of America both supported dissemination and this work with funding awards. The published version of this Chapter with supplemental data files was authored by Ian Will, Biplabendu Das, Thienthanh Trinh, Andreas Brachmann, Robin A. Ohm, and Charissa de Bekker (Will *et al.* 2020).

CHAPTER THREE: BIOINFORMATIC PREDICTIONS OF PROTEIN-PROTEIN INTERACTIONS MEDIATING INFECTION AND PARASITIC BEHAVIORAL MANIPULATION OF *CAMPONOTUS FLORIDANUS* (FLORIDA CARPENTER ANT) BY *OPHIOCORDYCEPS CAMPONOTI-FLORIDANI* (FLORIDA ZOMBIE ANT FUNGUS)

Abstract

Parasitic fungi are known to produce a number of effector proteins that can modulate virulence, alter host physiology, and trigger host responses. Some effectors act via protein-protein interactions (PPIs) between host and parasite. Cross-species PPIs between *Ophiocordyceps camponoti-floridani* and *Camponotus floridanus* could underly infection and parasitic behavioral manipulation in this host-pathogen relationship. The fungal parasite *Ophiocordyceps* induces a summit disease phenotype in *Camponotus* ants, and ultimately kills the host once it has attached to a locally elevated transmission position. Bioinformatic prediction of PPIs offer a high-throughput method to produce mechanistic hypotheses. Homology based approaches use the similarity of proteins to known PPI partners to make predictions in new datasets. Alternatively, machine learning approaches train models on known PPIs, but are not limited to only predicting orthologous interactions (interologs) in new datasets. Here, we compare both methods in predicting host-pathogen interactions between two non-traditional model species. Finding the D-SCRIPT machine learning approach to be the most promising, we further analyzed predicted PPIs to identify overrepresentation of functional annotations in PPI proteins hypothesized to mediate *Ophiocordyceps-Camponotus* interactions. Proteases, G-protein coupled receptors, transcription factors, and undescribed small secreted proteins appear to be key elements in the PPIs we predicted. These hypothesized interactions may include drivers of infection and manipulation of ant hosts, whether by increasing, decreasing, or modulating host protein activity.

Introduction

Fungal parasites have been shown to use a diverse array of molecules to defend themselves, promote infection, and modify their hosts. Often termed "effectors," these molecules are critical players in host-parasite dynamics that include both widely shared and highly specific mechanisms (Hogenhout *et al.* 2009; Win *et al.* 2012; Beckerson *et al.* 2019; Wang *et al.* 2021). Effector biology discussions frequently center on parasite proteins that can interact with host nucleic acids, carbohydrates, lipids, small metabolites, and other proteins. Such proteins have been suggested to play key roles in fungal infections of insects (Xiao *et al.* 2012; Wang and Wang 2017; Cen *et al.* 2017; Wang *et al.* 2021). Here, we focus on exploring possible protein effectors and protein targets between a behavior manipulating entomopathogenic fungus (*Ophiocordyceps camponoti-floridani*: Florida zombie ant fungus) and its insect host (*Camponotus floridanus*: Florida carpenter ant).

Manipulated host ants succumb to a summit disease, affixing themselves to locally elevated positions and dying at these locations to promote fungal growth and transmission (Andersen *et al.* 2009; Lovett *et al.* 2020; de Bekker *et al.* 2021). Behavioral changes preceding this final summit may be host-adaptive responses, parasite-adaptive manipulations, or general symptoms of disease that include: hyperactivity, uncoordinated foraging, decreased nestmate communication, and convulsions (Pontoppidan *et al.* 2009; Andersen *et al.* 2009; Hughes *et al.* 2011; de Bekker *et al.* 2015; Trinh *et al.* 2021). Identifying host-parasite protein-protein interactions (PPIs) can offer fundamental insights into the molecular basis of how these organisms interact and how the resulting infection and modified behavioral phenotypes are produced.

Proteome-scale bioinformatic prediction of PPIs has largely been employed to describe protein interaction networks within a single organism, such as in the *C. floridanus* host species (Gupta *et al.* 2020). However, multiple works have also made PPI predictions in cross-species host-pathogen relationships (Ma *et al.* 2019; Loaiza *et al.* 2021; Sledzieski *et al.* 2021). Using bioinformatic approaches

can offer rapid, large-scale predictions of PPIs prior to labor and resource intensive functional gene assays or laboratory screens (e.g., yeast-two-hybrid). Predicting PPIs is typically done using either an interolog or machine learning method. Interologs are orthologous interactions conserved across species. That is, each protein in one PPI have orthologs in the second interolog PPI (Walhout *et al.* 2000). While a useful tool for predicting PPIs, detecting an interolog in a new system requires that a reference PPI has already been established in previous systems. This direct one-to-one dependency on previous works offers some confidence in the clear matching to known interactions but is also directly constrained by available data. To produce more predictions, interologs can be supplemented by homologous domain-domain interactions in absence of full protein homology (Loaiza *et al.* 2021). Alternately, interologs can be conservatively filtered by domain-domain interactions as a second prediction criterion (Gupta *et al.* 2020). Machine-learning methods offer more flexibility. As these methods require training data of known PPIs, they still depend on established interactions, but can predict novel PPIs that are not exactly orthologous to known interactions (Chen *et al.* 2019; Sledzieski *et al.* 2021). However, many models form predictions directly from protein sequence data and perform most robustly when tested on sequences from the same species they were trained on. Bypassing, at least in part, species-specific patterns in protein sequences, D-SCRIPT is a machine learning tool that trains models on putative protein structure rather than primary sequence data (Sledzieski *et al.* 2021). This cross-species generalizability of D-SCRIPT predictive power is an important step for researchers working on non-model or multi-species systems that lack experimentally supported PPIs. Notably, fungi secrete a range of taxonomically distinct undescribed small secreted proteins (uSSPs) that are often hypothesized to be effectors in host-pathogen interactions (Cheng *et al.* 2014; Feldman *et al.* 2020; Fischer and Requena 2022). Bioinformatic techniques hinging upon well described protein annotations or subject to strong species-specific biases can only have limited success in assigning uSSPs to PPIs.

Studies of parasitic manipulation by the ant-manipulating *Ophiocordyceps* have produced a number of hypotheses of possible molecules and pathways underlying infection and manipulation: neuro-modulators and -protectants, insect hormones, circadian rhythms and light-sensing, and muscular hyperactivity (de Bekker *et al.* 2014a; Kobmoo *et al.* 2018; de Bekker 2019; Mangold *et al.* 2019; Zheng *et al.* 2019; Loreto and Hughes 2019; Will *et al.* 2020; Trinh *et al.* 2021; de Bekker and Das 2022). Among these, PPIs may mediate important host-pathogen interactions. Hypothesized *O. camponoti-floridani* effectors that could participate in cross-species PPIs include: bacterial-like putative enterotoxins, protein tyrosine phosphatases, peptidases (such as S8 subtilisin-like serine proteases), and various uSSPs. The highlighting of these proteins as possible important players is based on strong gene upregulation during active manipulation of the ant, conservation between *O. camponoti-floridani* and another ant-manipulator – *Ophiocordyceps kimflemingiae*, and in the case of the protein tyrosine phosphatase, hypothesized links to behavioral changes in caterpillars by certain baculoviruses (Kamita *et al.* 2005; Katsuma *et al.* 2012; de Bekker *et al.* 2015, 2017; Will *et al.* 2020).

To predict possible *Ophiocordyceps-Camponotus* PPIs, we (*i*) made a comparison of interolog and D-SCRIPT machine learning methods, (*ii*) divided predicted PPIs into subsets we consider most likely to include the highest concentration of PPIs relevant to infection and manipulation, and (*iii*) preformed enrichment analyses of functional annotations with both host and parasite proteins in those PPIs. We collected a diverse interolog reference set of PPIs across different species and multiple databases. As we sought to predict interologs in non-model cross-species data, we anticipated that a large PPI reference set from many taxa would improve our ability predict PPIs. For example, although we were predicting PPIs between eukaryotes, proteins with functional domains largely known from prokaryote toxins (i.e., enterotoxins) have been hypothesized to participate in *Ophiocordyceps* virulence and manipulation. For the machine learning approach, we used the pre-trained D-SCRIPT model, which has predicted PPIs in insect and fungus model organisms (Sledzieski *et al.* 2021). We emphasized analysis of

PPIs involving putatively secreted fungal proteins that were upregulated during manipulation of the ant. These fungal proteins were plausibly produced and exported to the host environment during manipulation, making these PPIs possibly most relevant to understanding manipulation of host behavior. Using enrichment analyses on both *Ophiocordyceps* and *Camponotus* proteins from these PPIs, we put forward hypotheses and observations relating infection and manipulation to proteins involved in oxidation-reduction, proteolysis, receptor signaling, and gene regulation.

Methods

Analytical framework and tools used in both interolog and D-SCRIPT PPI discovery approaches: For both methods of predicting PPIs between *C. floridanus* and *O. camponoti-floridani* we first tested each putatively secreted or transmembrane (i.e., extracellular) *Ophiocordyceps* protein for a possible interaction with all *Camponotus* proteins (i.e., the proteome) (Fig. 9). We annotated *Ophiocordyceps* proteins as putatively secreted (hereafter, simply "secreted") if they passed the multiple methods used in Beckerson *et al.*, 2019. Proteins that were not annotated as secreted, but did have at least one putative transmembrane domain, were considered transmembrane proteins. We retrieved protein sequence information from high-quality genome assemblies integrating long-read technology for both *O. camponoti-floridani* and *C. floridanus* (GenBank accessions GCA_012980515.1 and GCA_003227725.1, respectively) (Shields *et al.* 2018; Will *et al.* 2020). We focused our analyses on PPIs involving fungal proteins encoded by differentially expressed genes (DEGs) upregulated during manipulation (Will *et al.* 2020). The fungus upregulated these DEGs from control culture to manipulation of the ant. Although host-pathogen PPIs are likely to be important throughout the course of infection, gene expression data were not available for intermediate infection time points.

We speculated that predicted cross-species PPIs would be most likely to indicate specific host-parasite interactions when the *Ophiocordyceps* proteins were upregulated, secreted, and predicted to only

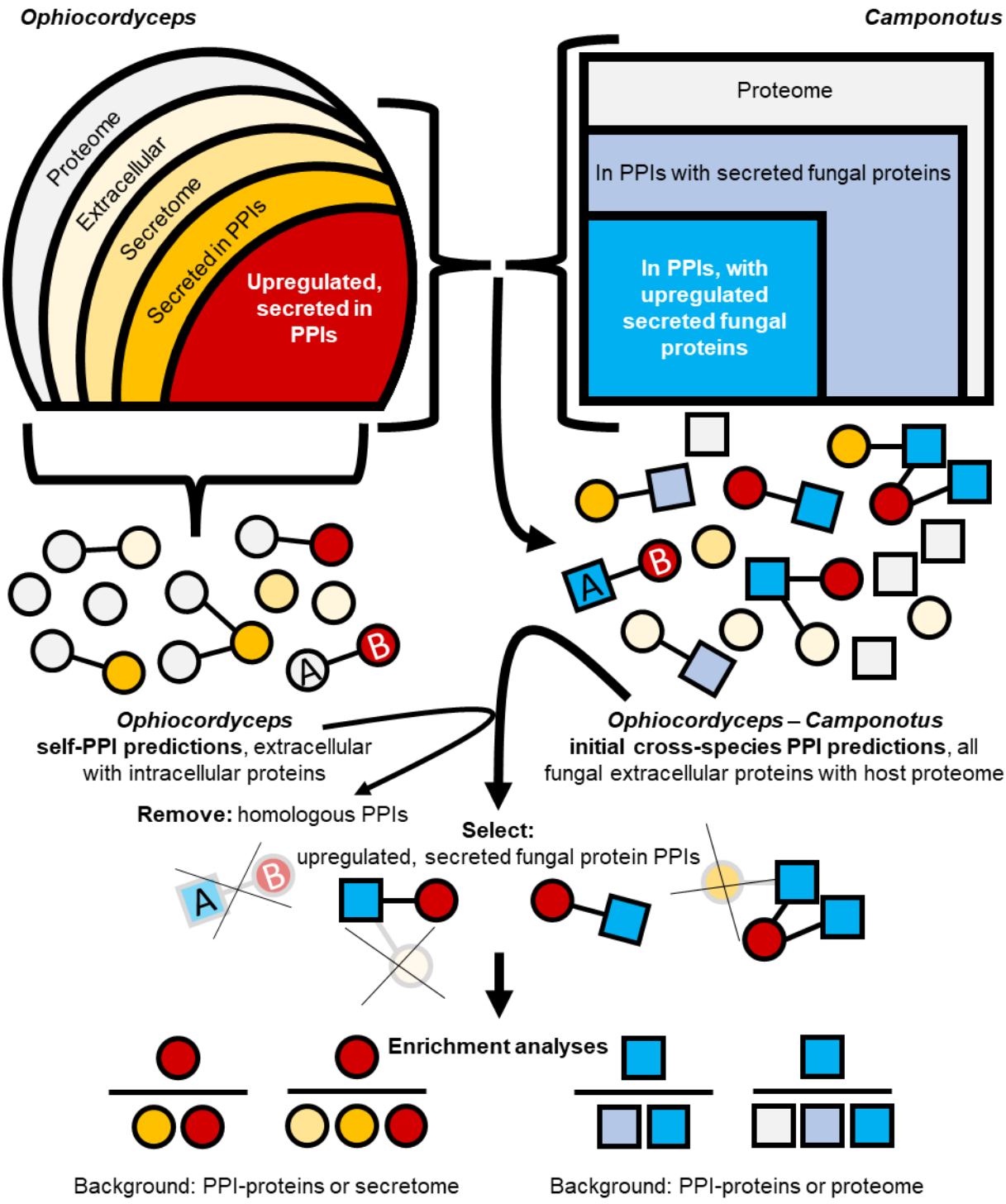

Figure 9. Conceptual framework for PPI testing, selection, and analysis.

With either the interolog or D-SCRIPT methods, we first tested every extracellular *O. camponoti-floridani* protein

with every *C. floridanus* protein in the host proteome. We filtered predicted PPIs to focus on PPIs with fungal proteins that were secreted (rather than transmembrane) and upregulated during manipulation. We removed PPIs from cross-species predictions if the ant protein was homologous to a fungal protein found in an *Ophiocordyceps* self-interaction PPI. Finally, we analyzed host and parasite proteins from these PPIs with hypergeometric enrichment analyses. We tested two background proteins sets for each organism, either all proteins in PPIs, or, the broader set of the secretome (*Ophiocordyceps*) or full proteome (*Camponotus*). Fungal proteins are shown as circles and ant proteins as squares. Proteins are color-coded by functional subset, with *Ophiocordyceps* upregulated, secreted proteins in cross-species PPIs as red and their interacting *Camponotus* proteins in bright blue. Other extracellular fungal protein categories are shades of orange. Other host proteins in PPIs are blue-gray. All other proteins of either organism are gray. Proteins "A" are *Ophiocordyceps* and *Camponotus* homologs to each other, and protein "B" is a single fungal protein.

bind *Camponotus* proteins and not any of the fungus's own proteins. If the parasite protein was predicted to bind one of *Ophiocordyceps*' own intracellular proteins as well as a *Camponotus* protein homologous to that intracellular protein, that PPI may be a conserved PPI not directly related to infection and manipulation of the host. Thus, to identify self-interacting *Ophiocordyceps* PPIs, we tested extracellular *Ophiocordyceps* proteins with intracellular *Ophiocordyceps* proteins. Any predicted cross-species PPI that had a homologous predicted fungal self-interaction PPI was not included in our primary analyses (Fig. 9). To search for reciprocal homologs (putative orthologs) between *Ophiocordyceps* and *Camponotus* proteins, we used Proteinortho (v 5.0) with default settings (Lechner *et al.* 2011).

We performed hypergeometric enrichment analyses on proteins from the final set of PPIs. The test set in every case was either the fungal or ant proteins found in the predicted non-homologous PPIs between the secreted, upregulated *Ophiocordyceps* proteins and the entire *Camponotus* proteome. Background protein sets were selected to answer subtly different questions (see Results) (Fig. 9). We compared fungal proteins to a background of either all secreted fungal proteins in a PPI, or to the fungal secretome (Fig. 9). We compared ant proteins to a background of either all ant proteins in a PPI, or, the ant proteome (Fig. 9). For the enrichment analyses we examined GO terms, PFAM domains, and weighted gene co-expression network analysis (WGCNA) module membership for both organisms (Will

et al. 2020). These WGCNA modules were correlated to sample types (controls, live manipulated ants, and moribund manipulated ants at death) and directly, module-to-module, between *Ophiocordyceps* and *Camponotus* (Fig. 5) (Will *et al.* 2020). We reference their assigned names that follow the basic patterns of ant-module-1 (A1) and fungus-module-1 (F1), where the number has no special meaning other than to uniquely identify the module. For *Camponotus* only, we also tested for enrichments with RNAseq DEG data (upregulated or downregulated from healthy controls to live manipulated ants) (Will *et al.* 2020). For *Ophiocordyceps* only, we tested for enrichment of uSSP annotations (Will *et al.* 2020). The uSSP annotations were added in place of GO terms and PFAM domains for proteins that we annotated as secreted here and were previously annotated as small secreted proteins without any BLAST description, GO term, or PFAM domain (Will *et al.* 2020). We performed hypergeometric enrichment analyses with the R package timecourseRNAseq (v 0.0.9000) using default settings (significant enrichment at FDR ≤ 0.05) in R studio (v 2021.09.2) with R (v 4.1) (RStudio Team 2015; R Core Team 2021; Das 2022). We plotted GO terms in semantic space to cluster related terms based on R code generated from REVIGO but did not remove any GO terms (R package ggplot2) (Supek *et al.* 2011; Wickham 2016).

Interolog PPI reference list creation: For the interolog approach to predict PPIs between *C. floridanus* and *O. camponoti-floridani*, we first constructed a large reference list of publicly available PPIs from many databases. In total, we gathered over 3 million unique PPIs. We extracted Uniprot protein identifiers (IDs) for the proteins listed in these PPIs or converted database-specific IDs to Uniprot IDs when ID cross-references were available. From these IDs, we collected sequence data for 160,583 UniprotKB protein entries listed as "active" (Bateman *et al.* 2021). The PPIs we included were either experimentally validated or hypothesized interologs, across different kingdoms of life. We gathered all available PPIs from: Biogrid (v 4.3.196), the Database of Interacting Proteins (DIP) (v 20170205), the Drosophila Interactions Database (DroID) (v 2018_08), the Host-Pathogen Interaction Database (HPIDB) (v 3.0), IntAct (accessed 2021-Apr-29), iRefWeb (accessed 2021-May-20), and the Molecular Interaction

database (MINT) (accessed 2021-Apr-25) (Hermjakob *et al.* 2004; Salwinski *et al.* 2004; Chatr-aryamontri *et al.* 2007; Turner *et al.* 2010; Murali *et al.* 2011; Ammari *et al.* 2016; Oughtred *et al.* 2021). We used R package RpsiXML (v 2.36.0) to parse PSI-MI files when needed (Zhang *et al.* 2021). While these databases contained many redundancies, we kept only a unique list of PPIs based on Uniprot IDs.

Interolog PPI prediction between *Ophiocordyceps* and *Camponotus*: We searched for orthology between the proteomes of our study organisms and the 160,583 protein sequences in the reference PPIs with Proteinortho. With these data, we predicted a PPI between *Ophiocordyceps* and *Camponotus* for every reference PPI where one protein had an ortholog in the fungus and the other in the ant. We did not employ additional domain-interaction or cellular-localization (other than secretion signals in the fungus) filtering steps with the PPI lists we generated. Although such steps can improve the accuracy of PPI predictions in some cases, known domain interactions only explain a minority of PPIs (ca. 4% to 20% of PPIs) (Pawson and Nash 2003; Itzhaki *et al.* 2006; Schuster-Böckler and Bateman 2007). As our task was to make an initial survey of possible PPIs between host and parasite, we did not wish to unnecessarily constrain the possible PPI predictions at this early stage.

D-SCRIPT machine learning based PPI predictions: We used the D-SCRIPT (v 0.1.5) default pre-trained model and settings to make PPI predictions between *O. camponoti-floridani* and *C. floridanus* (Sledzieski *et al.* 2021). D-SCRIPT assigns each tested protein interaction an edge value, essentially a confidence score to rank possible PPIs with default threshold for positive prediction ≥ 0.5, on a scale of zero to one. We tested every PPI combination between extracellular *O. camponoti-floridani* proteins and all proteins of *C. floridanus*. We used proteins shorter than 2,000 amino acids due to computational constraints. Limiting the length of input proteins removed six extracellular (0.3%) and 63 (1.1%) intracellular *Ophiocordyceps* proteins and 299 *Camponotus* proteins (2.4%).

Creation of a training PPI dataset to build a new D-SCRIPT model: Although D-SCRIPT has been engineered to make robust predictions across taxa, the human protein trained model slightly

underperformed when predicting PPIs in the fungus *Saccharomyces cerevisiae* (Sledzieski *et al.* 2021). Additionally, the cross-species aspect of our work may present a more challenging case compared to within-species PPI predictions. As such, we sought to train a model tailored to fungal-insect host-parasite interactions on combinations of *S. cerevisiae*, *Drosophila melanogaster*, and diverse host-pathogen PPIs from STRING and the HPIDB. We only used HPIDB interactions that were experimentally supported (n = 45,737 PPIs with 15,742 unique proteins). We selected only STRING PPIs that had some experimental support ("experiments score" > 0) and were overall a high-confidence interaction ("combined score" ≥ 700). These quality filters substantially reduced the number of PPIs retrieved from the total list of PPIs available on STRING. We retrieved 100,392 yeast PPIs (5.4% of all *S. cerevisiae* PPI entries) composed of 4,525 unique yeast proteins. We also retrieved 26,334 fly PPIs composed of 4,339 unique fly proteins (0.7% all *D. melanogaster* PPI entries). We removed sequences over 800 amino acids to reduce computational load as done in Sledzieski *et al.* 2021. Also following Sledzieski *et al.* 2021, we removed redundant homologous PPIs to avoid over-fitting the model to common PPIs. We grouped all proteins into homologous groups by a 40% homology threshold using CD-Hit (Huang *et al.* 2010). Per PPI that spanned a connection between two groups of clustered homologous proteins, only one representative PPI was kept between those groups, leaving 54,066 non-redundant PPIs composed of 15,447 unique proteins. The D-SCRIPT model also requires false "PPIs" to learn cases where proteins do not interact. Under the assumption that true PPIs are rare, we randomly combined proteins from the training data to create a set of false PPIs in ten-fold excess of the true PPIs (Sledzieski *et al.* 2021). We again filtered out redundant PPIs relative to other random PPIs and the 54,066 true PPIs to generate the putatively false random PPIs for training (n = 540,660). We split the final training data into five randomized blocks, each containing a 10:1 false:true PPI ratio, for a five-fold cross-validation of model training.

None of these training attempts created satisfactory models despite substantial efforts testing a variety hyperparameter setting combinations (i.e., epochs, batch size, learning rate, projection dimensions,

and hidden dimensions) and modifications to the input PPI set. However, D-SCRIPT had a major code bug that was recently discovered to prevent accurate training with the version we used, which has been remedied only with the February 2022 release, v 0.1.8. The prediction functions of D-SCRIPT were not impacted by this bug.

Results

Overview of interolog based PPI predictions: We anticipated that the highest signal (true PPI) to noise (false-positive PPI) ratio would be in a conservative PPI set of upregulated, secreted *O. camponoti-floridani* proteins that bind *C. floridanus* proteins, but do not engage in PPIs within the fungus (Table 2). We predicted 92 PPIs composed of eight fungal proteins interacting with 89 ant proteins. This number of PPIs suggests that such host-parasite interactions are rare, or our methods and available PPI interolog data were insufficient to identify most interactions. We also tested for PPIs using more relaxed criteria, but consistently found only few plausible interactions (Table 2). As a means of gauging if our interolog approach could consistently identify proteins likely to engage in PPIs, we constructed a *C. floridanus* PPI list of self-interacting ant proteins from the whole ant proteome (Table 2). We compared these PPIs to an initial interolog list that was used to construct a published high-quality *C. floridanus* PPI network (Gupta *et al.* 2020). We used the same large reference PPI list as for the cross-species PPI predictions. In the earlier work we compare to, the authors used only DroID (v 2014_10) and DIP, a much more focused database survey, and a different *C. floridanus* genome assembly (Bonasio *et al.* 2010; Gupta *et al.* 2015, 2020) than our work, which is based on a more recent genome (Shields *et al.* 2018). The preliminary orthology-only *C. floridanus* PPI network from Gupta *et al.* 2020 contained 51,866 PPIs composed of 6,274 proteins from 5,295 gene loci. Our *C. floridanus* PPI had 115,906 PPIs composed of 9,920 proteins from 6,277 unique gene loci. Based on orthology between the two *C. floridanus* genome assemblies using Proteinortho, our 6,277 genes contained 74% of the 5,295 genes found in Gupta *et al.*

2020. This suggests that our implementation of interolog PPI predictions could identify many plausible interactions with typical single-species data. We attribute the higher number of predicted PPIs in our case to the much broader survey of possible interologs and the slightly greater number of gene models in the genome that we used.

Table 2. Interolog PPI sets overview.

We searched for interolog pairs that matched a *O. camponoti-floridani* protein to any *C. floridanus* protein. We then created PPI subsets based on fungal gene expression, extracellular signals, and homologous interaction between extracellular and intracellular fungal proteins. We additionally drafted a *Camponotus* self-interaction network as an approximate method of benchmarking our approach relative to a previously published *C. flordianus* PPI network (Gupta *et al.* 2020).

PPI set	**Predicted PPIs**	***Ophiocordyceps* proteins**	***Camponotus* proteins**
Camponotus (*C.*) & self	115,906	NA	9,920 (all isoforms) & 6,277 (unique loci)
Ophiocordyceps (*O.*)-extracellular & self-intracellular	58,839	2,847	NA
O. & *C.*	20,705	965	3,964 (all isoforms) & 3,904 (unique loci)
O.-extracellular & *C.*	2,107	156	1,262 (all isoforms) & 1,258 (unique loci)
O.-extracellular & *C.*, no homologous *O.* self PPIs	388	51	326 (all isoforms) & 325 (unique loci)
O.-secreted & *C.*, no homologous *O.* self PPIs	320	31	279 (all isoforms) & 278 (unique loci)
O.-secreted, upregulated & *C.*, no homologous *O.* self PPIs	92	8	89 (either)

Overview of D-SCRIPT machine learning based PPI predictions: We generated 22,972,653 possible PPIs to test by combining 1,881 *Ophiocordyceps* extracellular proteins with 12,213 *Camponotus* proteins. D-SCRIPT PPI predictions that fell below the 0.5 edge value threshold were typically far below this cutoff, suggesting that this edge value was robust against selecting most putatively false PPIs (Fig. 10A). Of the ca. 23 million PPIs tested with D-SCRIPT, 0.41% were positive predictions (n = 94,215 PPIs) (Table 3). This is in line with the 0.95% PPIs that D-SCRIPT previously predicted as true from a 50 million PPI test-set with single-species data (Sledzieski *et al.* 2021).

We found *Ophiocordyceps* transmembrane proteins to often be more promiscuous binding partners than secreted proteins and involved in possibly less informative predicted PPIs. For example, the extracellular proteins with the two highest number of predicted interactions with the host were a *Ophiocordyceps* transmembrane Sec61 subunit (n = 1392 PPIs) and maltose permease (n = 983 PPIs) (Fig. 10B). The Sec61 protein transporter plays a role in translocating proteins to the endoplasmic reticulum and the maltose permease is involved in sugar transport (Cheng and Michels 1989; Osborne *et al.* 2005); both of these functions appear to be more indicative of core cell functions and possible spurious PPI predictions. In total, secreted *Ophiocordyceps* proteins had fewer predicted interactions (range = 1 to 644, median = 15) than transmembrane *Ophiocordyceps* proteins (range = 1 to 1392, median = 21). Similarly, the resulting binding partners in *Camponotus* had fewer interactions with secreted fungal proteins (range = 1 to 94, median = 3) compared to fungal transmembrane proteins (range = 1 to 252, median = 4) (Fig. 10B). Also, as secreted proteins would be wholly contained in the host-environment, we inferred that these proteins would more often be effector candidates. These PPIs involving only secreted *Ophiocordyceps* proteins included 23,629 predicted PPIs (Table 3).

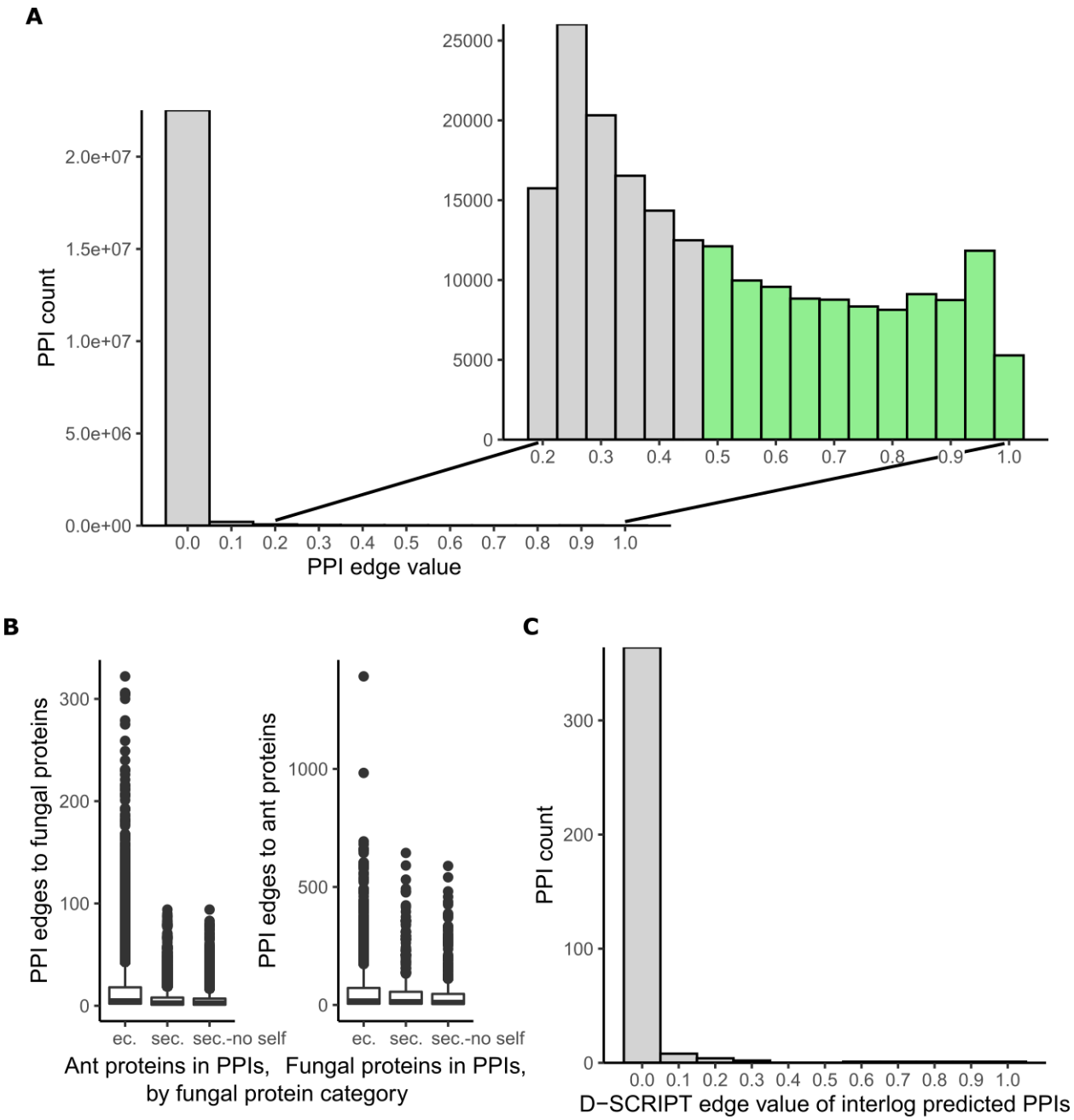

Figure 10. Metrics of D-SCRIPT PPI predictions.

A) D-SCRIPT edge values for tested protein pairings between extracellular fungal proteins and the ant proteome. D-SCRIPT edge values indicate the confidence of the model prediction for a given PPI to be true. We used the default edge value cutoff of ≥ 0.5 (green). These positive predictions comprised 0.41% of the ca. 23 million protein combinations tested. D-SCRIPT assigned most negative predictions with decisively low values far below the 0.5 threshold. B) Predicted number of PPIs per protein. PPI networks between extracellular fungal proteins ("ec.") and host proteins had the most connected proteins (i.e., protein nodes with the most PPI edges). Removing PPIs

involving fungal transmembrane proteins left only secreted proteins ("sec.") and further filtering out homologous PPIs across species ("sec.-no self") reduced connectivity. Note the difference in scale between ant protein connectivity (maximum > 300) and fungal protein connectivity (> 1,000). C) Interolog predicted PPIs largely have low D-SCRIPT edge values. The two methods that we used to predict PPIs did not agree well, with only five interologs with secreted fungal proteins having D-SCRIPT edge values above the 0.5 threshold.

Table 3. D-SCRIPT PPI sets overview.

We tested every combination of an extracellular *O. camponoti-floridani* (*O.*) protein (n = 1,881) to every *C. floridanus* (*C.*) protein (represented by the single longest isoform, n = 12,213) (except any proteins > 2,000 amino acids long). Predicted PPIs were all combinations returned with an edge value of ≥ 0.5. We then created PPI subsets based on fungal gene regulation, extracellular signals, and homologous interaction between extracellular and intracellular fungal proteins. For the *Ophiocordyceps*-self interaction set, the extracellular proteins were tested against all remaining intracellular proteins (n = 5,505).

PPI set	**Predicted PPIs (% of protein combinations tested)**	***Ophiocordyceps* proteins**	***Camponotus* proteins**
Ophiocordyceps (*O.*)-extracellular & *Camponotus* (*C.*)	94,215 (0.41%)	1358	5740
O.-extracellular & self-intracellular	65,809 (0.64%)	1275-extracellular 3326-intracellular	NA
O.-extracellular & *C.*, no homologous self PPIs	82,702 (0.36%)	1349	5613
O.-secreted & *C.*	23,629 (0.33%)	402	3289
O.-secreted & *C.*, no homologous self PPIs	20,779 (0.29%)	398	3143
O.-secreted, upregulated & *C.*	6,792 (0.30%)	130	2230
O.-secreted, upregulated & *C.*, no homologous self PPIs	6,011 (0.26%)	129	2083

To remove possibly spurious predictions with homology to PPIs within *Ophiocordyceps*, we used D-SCRIPT to test for fungal self-interacting PPIs. This produced 65,809 PPIs from a possible 10,354,905 combinations (0.64%) using extracellular *Ophiocordyceps* proteins combined with the fungus's own 5,505 intracellular proteins (Table 3). For all fungal intracellular proteins in a self-interacting PPI, we found their *Camponotus* orthologs with Proteinortho. When preparing PPI test sets for enrichment analysis, we removed cross-species PPIs where the fungal secreted protein was predicted to bind both an *Ophiocordyceps* intracellular protein and that protein's *Camponotus* homolog. Removing these homologous PPIs led to minor changes in the enrichment results that did not shift our fundamental interpretation of the study (File S3).

In total, the most stringently selected set of protein interactions tested were upregulated, secreted *Ophiocordyceps* proteins in combination with the *Camponotus* proteome (n = 2,271,618 possible PPIs) that resulted in 6,792 predicted PPIs (Table 3). Then, we removed the 781 PPIs that were predicted to also have within-*Ophiocordyceps* interactions. The remaining 6,011 PPIs involved 129 unique *Ophiocordyceps* proteins and 2,083 unique *Camponotus* proteins (Table 3) (File S3).

Comparison of interolog and D-SCRIPT methods: discussion and rationale for using D-SCRIPT predictions: We found little overlap in the PPI predictions of the interolog and D-SCRIPT approaches. There were no common predicted PPIs that involved fungal proteins upregulated during manipulation. Irrespective of fungal gene expression, D-SCRIPT predicted five PPIs that were also found in the interolog set. These PPIs were composed of three unique *Ophiocordyceps* proteins and five unique *Camponotus* proteins. A single fungal DnaJ and TPR domain containing protein was predicted to interact with three ant proteins, putatively annotated as another DnaJ and TPR protein, Lsm-4, and a heat shock protein 90 domain containing protein. Proteins with DnaJ and TPR domains can function as chaperones in cooperation with other heat shock proteins (Hennessy *et al.* 2005; Kravats *et al.* 2017) or can be involved in the spliceosome, which Lsm proteins are also involved in (Korneta *et al.* 2012). A fungal SEL-1-like

protein was predicted to interact with a host protein ubiquitination enzyme, which is in line with SEL-1's function to assist processing of misfolded proteins for ubiquitination and degradation in the endoplasmic reticulum (Christianson *et al.* 2008). We additionally found a fungal carboxylesterase interacting with an ant carboxylesterase, specifically annotated as acetylcholinesterase, which does not appear to be firmly grounded in abundant supporting evidence. The other four PPI interactions did have evidence supporting the binding and functional relationships of the proteins. However, we considered these predicted cross-species PPIs to reflect cases where secretion signals were conflated with membrane and organelle trafficking signals, leading to spurious misidentifications of cross-species PPIs. Although we sought to remove functionally identical PPIs between *Ophiocordyceps* and *Camponotus* by removing homologous interactions, this likely was not successful in every case. We suspected this to be more likely than the parasite using proteins with these specific functions in the course of infection and manipulation.

To compare D-SCRIPT and interolog PPIs more broadly, we retrieved the D-SCRIPT edge value for every interolog PPI. Overall, positive interolog based predictions had low D-SCRIPT edge values (median edge value = 0.004), meaning that D-SCRIPT predicted that these were unlikely to be true PPIs (Fig. 10C). Given the general disagreement between our methods, either one or both approaches were performing poorly in detecting cross-species PPIs. Possibly, these different approaches could have been complementary, identifying distinct sets of PPIs based on their different methods of analysis. However, the interolog PPI predictions did not appear to be the most efficient dataset to analyze given that (*i*) it returned very few PPIs overall (difficult to perform enrichment analyses), (*ii*) would be more biased towards intracellular networks based on the available reference PPI data (increased probable false-positives), and (*iii*) have limited or no success in predicting PPIs with proteins such as uSSPs that lack homology to well-described proteins (decreased true-positives). Thus, we continued all further analyses with the D-SCRIPT data only.

Enrichment signals among *Ophiocordyceps* proteins involved in PPIs: We conducted enrichment analyses on the test set of the 129 upregulated, secreted *Ophiocordyceps* proteins from the cross-species specific PPIs (Fig. 9). We used two possible background data sets for these enrichment analyses (Fig. 9). In the first case, we analyzed the test set against a background of all secreted fungal proteins that had predicted PPIs with host proteins, regardless of their expression pattern (n = 398 proteins) (Table 4) (Fig. 9). Here, we asked if this upregulated test set was functionally distinct from other secreted *Ophiocordyceps* proteins predicted to bind host proteins. In the second case, we analyzed the same test set against the entire *Ophiocordyceps* secretome (n = 586) (Table 4) (Fig. 9) to ask if the upregulated test set of host-binding proteins was functionally distinct from all proteins *Ophiocordyceps* could secrete.

In both cases, our analyses returned the same enriched annotations. We found one PFAM domain, three WGCNA modules, no GO terms, and no uSSP enrichment (Table 4). The enriched PFAM domain was a "peptidase S8 domain," suggesting upregulated serine protease activity. Five fungal peptidase S8 proteins were predicted to interact with 34 host proteins across 39 PPIs. Among these host proteins, there were seven kinesin-like proteins (motor proteins), five nuclear pore proteins, and a pro-resilin that is an insect cuticle and connective tissue protein (Burrows and Sutton 2012). We also found fungal WGCNA modules F1, F2, and F3 to be enriched. Modules F1 and F2 were previously described to have significant positive correlations to manipulation and F3 was significantly negatively correlated to control samples (with modest positive correlation to manipulated ants and recently dead manipulated ants). All three modules also had significant direct correlations to ant WGCNA modules (Will *et al.* 2020). Modules F1 and F2 were enriched for extracellular signals and carried many secreted enterotoxin- or ADP-ribosylating toxin-like genes (n = 5 and 8, modules F1 and F2, respectively). These two modules also contained all the protein tyrosine phosphatase genes found among manipulation-associated fungal modules (n = 1 and 3, modules F1 and F2, respectively). Module F1 was directly correlated to ant

modules A14 and A15, which were enriched for proteins with putative neuronal functions (Fig. 4). In turn, these ant modules were also significantly negatively correlated to manipulation. Module F2 also contained a secreted putative eckinase. F2 had other non-secreted hallmarks of pathogenic activity characterizing it as a possibly infection and manipulation specialized gene network. It was enriched for oxidation-reduction functions that are involved in many processes, including host-pathogen interactions. Additionally, module F2 carried many putative secondary metabolite biosynthesis genes, including most for the synthesis of a putative aflatrem-like toxin. Module F3 was largely enriched for transcription factors and cellular signal transduction processes.

Table 4. Annotation enrichments of PPI proteins.

The PPIs used for enrichment analysis were all those involving an upregulated, secreted *Ophiocordyceps* protein and any *Camponotus* protein. Proteins form those interactions were tested for functional enrichments relative to two possible backgrounds sets, per host and parasite. We found no enrichment signal for uSSPs in the fungus. *Ophiocordyceps* abbreviated as *O.* and *Camponotus* as *C.* Upregulated DEGS are abbreviated as UP and downregulated DEGs as DN.

Test proteins (n)	**Background proteins (n)**	**GO**	**PFAM**	**WGCNA**	***C.* DEG**
O. (129)	*O.*-secreted, in PPIs (398)	0	1	3	NA
	O. secretome (586)	0	1	3	NA
C. (2,083)	*C.*, in PPIs with *O.*-secreted (3,143)	25	0	4	none
	C. proteome (12,213)	50	106	9	UP, DN

Enrichment signals among *Camponotus* proteins involved in PPIs: We applied the same approach to the *Camponotus* proteins found to be in cross-species PPIs as we did for the fungus. In this case, we compared the 2,083 host proteins to two possible reference backgrounds: (*i*) all *Camponotus* proteins that were involved in a PPI with a secreted fungal protein, regardless of the parasite gene expression (n = 3,143 host proteins) or (*ii*) the full host proteome, which encompasses every protein that

possibly could have bound an *Ophiocordyceps* protein (n = 12,213 host proteins) (Table 4) (Fig. 9). Given the large difference in background for these reference sets, the enrichments signals had marked differences. In the first comparison, against a background of ant proteins predicted to bind fungal proteins, 25 GO terms, no PFAM domains, 4 WGCNA modules, and no DEG classifications were enriched (Table 4) (Fig. 11). In the second comparison, against a background of all ant proteins, 50 GO terms, 106 PFAM domains, 9 WGCNA modules, and both up- and down-regulated DEGs were enriched (Table 4) (Fig. 12). As GO term and PFAM domain enrichments often indicated similar functions, we present results largely from the GO term perspective, as both analyses had enriched GO terms and fewer terms overall compared to PFAM domains. We do highlight PFAM domains for emphasis or to discuss biologically interesting results not well captured by GO terms alone. In most cases, the second analysis with more enriched annotations included the annotations from the first analysis.

We detected the enrichment of oxidation-reduction functions among *Camponotus* proteins in PPIs in both enrichment analyses (three or six supporting GO terms) (Fig. 11, 12, File S3). Altogether, 159 host proteins had oxidation-reduction annotations, forming 321 PPIs with 48 parasite proteins. These fungal proteins included cytochrome P450s, oxidases and oxidoreductases, amidases, peptidases, and an enterotoxin. A plurality of the host proteins were encoded by cytochrome P450 genes (70 unique genes, 15 putative subtypes). This abundance of cytochrome P450, a hemoprotein, also contributed to the enrichment of "heme-binding" and "iron ion binding" GO terms and the PFAM domain "cytochrome P450" (Fig. 11, 6). These *Camponotus* cytochrome P450 proteins paired with 10 unique *Ophiocordyceps* genes, consisting of uSSPs and fungal cytochrome P450s. Another ant protein with oxidation reduction function was a putative delta-1-pyrroline-5-carboxylate dehydrogenase. This enzyme catalyzes synthesis of glutamate, an amino acid with roles in metabolism and a key excitatory neurotransmitter of insect motoneurons (Johansen *et al.* 1989; Krnjević 2010; Pflüger and Duch 2011; Srivastava *et al.* 2012; Tiwari *et al.* 2013). We predicted this enzyme to bind a fungal uSSP. Other notable contributors to the host

enrichment of oxidation reduction related functions were peroxiredoxins, laccases, dehydrogenases, and a vat-1 synaptic vesicle membrane-like protein (File S3).

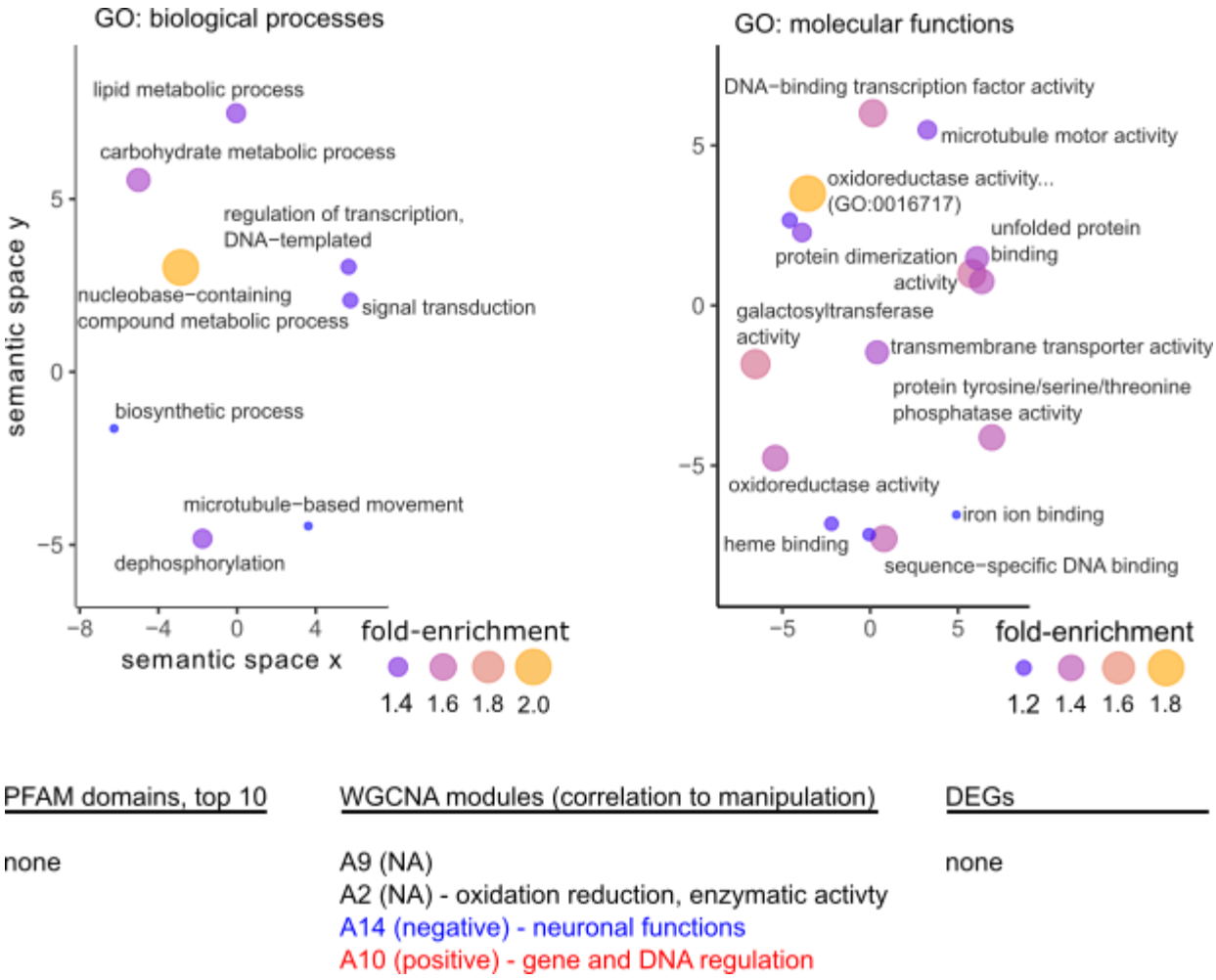

Figure 11. Enrichments found for *C. floridanus* proteins in PPIs with upregulated secreted fungal proteins against a background of *C. floridanus* proteins in PPIs, irrespective of fungal gene expression.

GO terms are plotted in semantic space to cluster terms by functional similarity. Some labels were omitted for readability and when not relevant to our discussion of the results. WGCNA modules are ordered by fold-enrichment and colored if they were negatively (blue) or positively (red) correlated to manipulation.

Host proteins contributing to an enrichment of the PFAM "ligand-gated ion channel" domain (against the proteome background) also had putative links to glutamate. Three out of the five host proteins had BLAST descriptions or additional PFAM domains indicating they were glutamate receptors (File S3). Three fungal proteins interacted with the five host proteins to form eight PPIs. None of the fungal proteins had annotations, with two of them being uSSPs. All three fungal proteins were highly connected to many host proteins (> 200 each).

Only in the analysis compared to the whole ant proteome, we detected GO term enrichments for "G protein-coupled receptor (GPCR) activity" and "GPCR signaling pathway." We predicted 71 GPCR related PPIs with 16 unique *Ophiocordyceps* proteins (File S3). All but two receptor proteins carried the PFAM domain "7 transmembrane receptor (rhodopsin family)." We found 33 unique receptor protein genes, with a range of putative ligands: 11 neuropeptides (n = 12 receptors), four biogenic monoamines (dopamine, serotonin, octopamine, tyramine) (n = 11 receptors), acetylcholine (n = 2 receptors), a spider venom toxin protein (alpha-latrotoxin) (n = 1 receptor), and opsin blue- and ultraviolet-sensitive receptors (n = 2 receptors). Fourteen of these 33 *Camponotus* receptors (or receptor subunits) belonged in ant WGCNA modules A14 and A15 (see above) (Fig. 4, 5). Few of the encoding host genes were DEGs during manipulation. The only upregulated gene was a putative G-protein alpha subunit – a key component of GPCR signaling function. We also found a downregulated receptors for neuropeptides (putative pyrokin-1 and gonadotropin-releasing hormone II), a biogenic monoamine (octopamine beta 2R), and acetylcholine (muscarininc gar-2). The host proteins were predicted to bind 16 fungal proteins that included five uSSPs, a carboxylesterase, a glycosyl hydrolase, a CAP cysteine-rich secretory protein, and a protein tyrosine phosphatase. Most of these proteins were previously assigned to fungal module F2 (n = 9) but included some in modules F1-4 (see above) (Fig. 4, 5).

The GO term "signal transduction" was enriched in the analysis with the conservative background of only PPI ant proteins (Fig. 11). Often, but not always, involved in GPCR signal

transduction, small GTP-binding, ras-like, or ras-related proteins made up 14 of 15 proteins in this set (all with PFAM domain "Ras family") (Chiariello *et al.* 2010; Xu *et al.* 2017; Dohlman and Campbell 2019), with the remaining one annotated as a G kinase-anchoring protein. We predicted that these 15 ant proteins interact with 17 fungal proteins across a total of 65 PPIs. Six of these *Ophiocordyceps* proteins were uSSPs, the rest included the two M43 peptidases and the same CAP and glycosyl hydrolase proteins reported above for GPCR interactions. Most of the uSSPs also overlapped with those found in the GPCR PPIs. Fungal modules F1, F2, and F3 were again the primary WGCNA modules of these fungal interactors (n = 4, 5, and 7, respectively) (Fig. 4, 5).

Against the full proteome background, we found 28 ant proteins that shared the enriched GO term "structural constituent of cuticle" (and PFAM domain "insect cuticle protein"). We predicted these ant proteins interacted with 22 fungal proteins to form 138 PPIs. We found the same M43 peptidases, CAP protein, glycosyl hydrolase, and four of the uSSPs above. We additionally identified a carboxylesterase (the same protein as predicted in the GPCR results), a disintegrin/reprolysin-like peptidase, a S8 subtilisin-like serine peptidase, another uSSP, and an unannotated secreted protein (larger than an uSSP).

Two forms of peptidase activity were enriched against the total ant background, "cysteine-type peptidase activity" and "threonine-type endopeptidase activity." All seven host cysteine peptidases were "Cathepsin propeptide inhibitor domain (I29)" or "Papain family cysteine protease" PFAM domain proteins, linking them to lysosomal functions (Turk *et al.* 2012). These proteins interacted with six fungal proteins, forming 18 PPIs. The fungal proteins include a vacuolar protease A (analogous to animal lysosomal proteases), a cerato-platanin-like protein, a tyrosinase, and an uSSP. Six host threonine endopeptidases, all related to proteasome function (PFAM domain "proteasome subunit"), were predicted to interact with two fungal proteins to generate nine PPIs. The two fungal proteins were an endothiapepsin-like protein and the same vacuolar protease as above.

Multiple enrichments that can be associated to gene transcription and regulation were enriched in both analyses, regardless of background. We found 188 host proteins annotated for "DNA binding," "DNA-binding transcription factor activity," and "sequence-specific DNA binding" GO terms. "DNA helicase activity" and "mRNA binding" GO terms were additionally enriched in the analysis against the whole proteome, leading to a total of 204 host proteins. These proteins similarly contributed to the high enrichment of PFAM domains such as "helix-loop-helix DNA-binding domain," "zinc Finger C4 type," "'paired box' domain," and "bZIP transcription factor" (Fig. 12). These 204 host proteins interacted with 43 fungal proteins to generate 922 PPIs. These fungal proteins included five uSSPs that were also found in the PPIs reported above, three that were not, and various hydrolases, oxidoreductases, peptidases, and carboxylesterases. Among the 204 host proteins, we found transcription factors and regulators with many functions, such as: Jim Lovell (graviotaxis, locomotion), Mushroom body large type Kenyon specific protein 1 (e.g., ecdysteroid signaling, elevated in worker bees, learning and memory), Gooseberry (e.g., neuromuscular junction homestasis), Hairy and hairy/enhancer-of-split related (e.g., neuronal fate and proliferation, juvenile hormone signaling modulation), steroid and ecdysone receptors and induced proteins (e.g., development and reproductive/caste behaviors), Dead ringer (e.g., glial cell development and neural organization, modulation of pro-locomotor neuron cell fate), Achaete-scute complex proteins (e.g., neurogenesis and sensory organ development), Forkhead (e.g., development, cell cycle, neuroimmune signaling), photoreceptor specific nuclear receptor (light sensing), CLOCK (circadian clocks), and various histone proteins (Häcker *et al.* 1995; Shandala *et al.* 2003; Velarde *et al.* 2006; García-Bellido and De Celis 2009; Marie *et al.* 2010; Tang *et al.* 2012; Bjorum *et al.* 2013; Cheng *et al.* 2015; Ables *et al.* 2015; Saha *et al.* 2016; Guo *et al.* 2018; Kumagai *et al.* 2020). These 41 proteins account for 198 of the 922 gene regulation PPIs, interacting with 28 fungal proteins covering a similar breadth of protein types as the 43 fungal proteins overall.

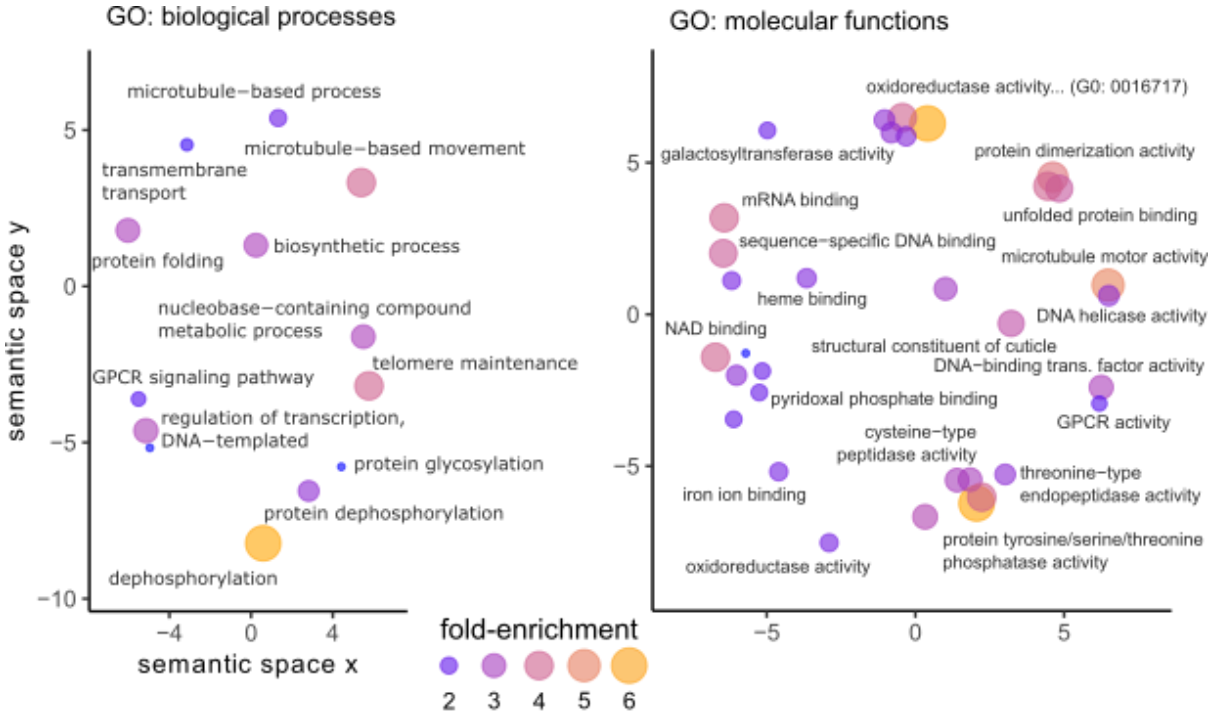

PFAM domains, top 10	WGCNA modules (correlation to manipulation)
PF03953 Tubulin C-terminal domain	A8 (NA)
PF00225 Kinesin motor domain	A10 (positive) - signal transduction and transcription
PF00010 Helix-loop-helix DNA-binding domain	A9 (NA)
PF00118 TCP-1/cpn60 chaperonin family	A11 (NA)
PF00170 bZIP transcription factor	A1 (NA)
PF07716 Basic region leucine zipper	A14 (negative) - neuronal function
PF00105 Zinc finger, C4 type (two domains)	A13 (NA) - ion channels and immunoglobulins
PF00292 'Paired box' domain	A4 (positive) - proteosomes and odor detection
PF00989 PAS fold	A3 (NA) - translation, mitochondrial metabolism,
PF02801 Beta-ketoacyl synthase, C-terminal domain	and juvenile hormone binding

PFAM domains, other notable	DEGs
PF00135 Carboxylesterase family	Upregulated
PF00379 Insect cuticle protein	Downregulated
PF00001 7 transmembrane receptor (rhodopsin family)	
PF00503 G-protein alpha subunit	
PF00102 Protein-tyrosine phosphatase	
PF00060 Ligand-gated ion channel	
PF00069 Protein kinase domain	

Figure 12. Enrichments found for *C. floridanus* proteins in PPIs with upregulated secreted fungal proteins against the *C. floridanus* proteome background.

GO terms are plotted in semantic space to cluster terms by functional similarity. Some labels were omitted for readability and when not relevant to our discussion of the results. WGCNA modules and PFAM domains are ordered by fold-enrichment. WGCNA modules are colored if they were negatively (blue) or positively (red) correlated to manipulation.

Of the seven general functional categories reported above (oxidation-reduction, ligand-gated ion channel, GPCR signaling, signal transduction, cuticle, peptidase, and transcription and DNA-binding enrichments), we predicted 1,551 PPIs of 457 host proteins and 77 parasite proteins (Fig. 13). Over half

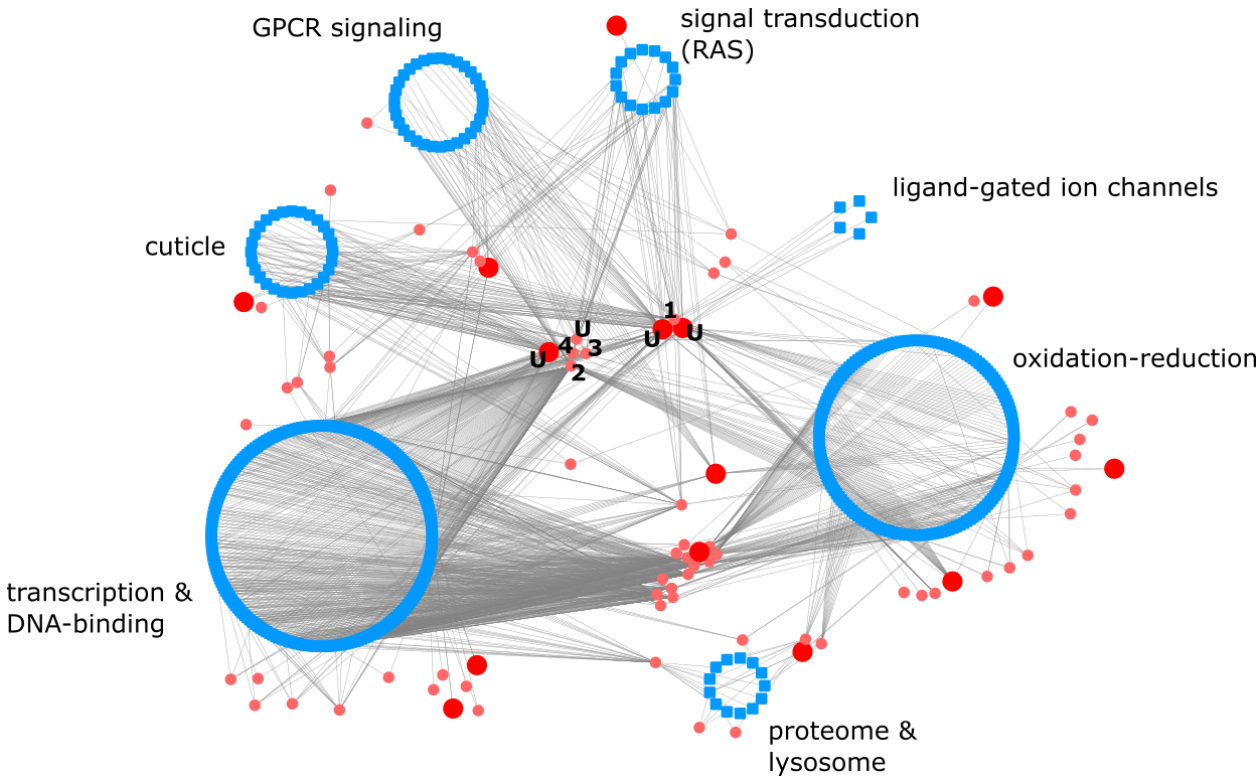

Figure 13. PPI network with host proteins contributing to selected GO term enrichments.
Host proteins (blue squares) are clustered by their general GO term functional category and connected to their fungal PPI partners that are either secreted proteins (small pink circles) or uSSPs (large red circles) that were found to be upregulated during *Ophiocordyceps* manipulation of carpenter ant behavior. Eight fungal proteins are the most highly connected between host enrichment groups (center of figure, fungal proteins 1-4 and U), with each fungal protein having at least one PPI with a host protein in six or more of the functional categories. These proteins were an oxidase (1), carboxylesterase (2), CAP protein (3), glycosyl hydrolase (4), or four unannotated proteins (U). Many

other proteins only interacted with one of the selected host protein clusters, but may have PPI connections with host proteins outside of those depicted here.

of the fungal proteins interacted with host proteins in multiple enrichment categories (n = 41 fungal proteins). The most connected fungal proteins among these selected PPI networks, were also highly promiscuous across all PPIs (much greater than the median secreted fungal protein connectivity of 15 PPIs). Three fungal proteins interacted with six of seven host protein enrichment categories (not with the peptidase group). Two of these fungal proteins were uSSPs and one was a putative oxidase (n = 482, 355, 280 PPIs, respectively). An additional five fungal proteins interacted with those host proteins except ones in the ligand-gated ion channel category. These five fungal proteins were also highly connected across the study: an uSSP (n = 591 PPIs), carboxylesterase (n = 395), glycosyl hydrolase (n = 263), unannotated protein (n = 110), and CAP cysteine-rich secretory protein (n = 95) (Fig. 13). Taken together, this suggests that most fungal proteins of interest were predicted to bind multiple host proteins, with a few predicted across a wide range of proteins in different biological pathways (Fig. 13). Although many uSSPs were shared in the PPIs contributing to the enrichment terms reported above, such proteins, as a class, were not prone to bind more host proteins than other fungal proteins (Fig. 14).

In the analysis that used ant proteins in PPIs as the background (n = 3,143), two ant WGCNA modules were enriched that had significant correlations to manipulation. Module A14 was negatively correlated to manipulation and included many genes putatively associated with neuronal function, including the GPCRs discussed above (Fig. 4, 5). Module A10 was positively correlated to manipulation and contained enrichment signals for gene regulatory processes (Fig. 15, 11). Including those enrichments, the analysis against the full proteome background also detected ant module A4 that had a positive correlation to manipulation (Fig. 5, 12). This module contained enrichment signals for both proteasomes and odor detection. Also in this wider analysis, there was an enrichment for host DEGs, both upregulated and downregulated (Fig. 12).

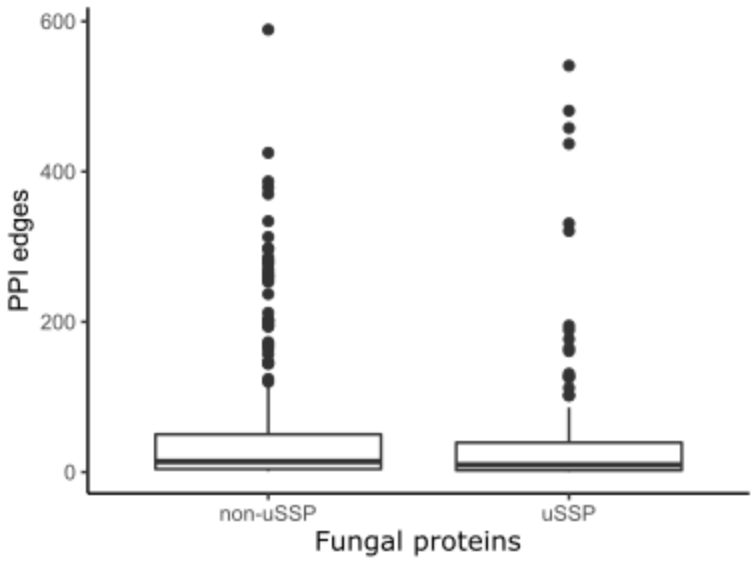

Figure 14. Secreted fungal proteins other than uSSPs ("non-uSSP") and uSSPs-only have similar connectivity to host proteins.

Each point represents a single fungal protein, and the PPI edges count shows how many host proteins that fungal proteins was predicted to bind.

Targeted searches for previously hypothesized effector proteins and putative host partners:

Previously, possible *O. camponoti-floridani* effector proteins were proposed based on their upregulation during manipulation, conservation of sequence and regulation between fungal species, and hypothesized biological activities (Will *et al.* 2020). We searched for possible PPIs involving a selection of these proteins. A sharply upregulated enterotoxin (GenBank KAF4589869.1) with strong homology between *O. camponoti-floridani* and *O. kimflemingiae* was never predicted in a PPI (maximum edge value = 0.09). Although, we did predict two other upregulated enterotoxins to be involved in 16 PPIs, most often binding host nuclear pore proteins. A hypothesized protein tyrosine phosphatase effector (GenBank KAF4589831.1) was involved in 101 PPIs. Most predicted interaction partners were other phosphatases, kinases, myosins, and tubulins. We investigated two uSSPs hypothesized to have effector functions. One uSSP (GenBank KAF4585483.1) was predicted to interact with two host T-complex proteins (chaperone

and folding). The other uSSP (GenBank KAF4591615.1) was never predicted to bind a host protein (maximum edge value = 0.07).

Discussion & conclusion

The molecular interactions between host and parasite during manipulation of *C. floridanus* by *O. camponoti-floridani* likely include protein effectors and protein targets. Bioinformatically predicting possible cross-species PPIs in non-model systems presents a special challenge with approaches still improving. As such, we piloted two methods of predicting interactions, a homology-based interolog approach and D-SCRIPT machine learning model. The interolog method yielded few PPIs and we chose not to deeply analyze those results as the machine learning approach appeared to be more reliable. We used the pre-trained human protein-based model of D-SCRIPT to predict cross-species PPIs from combinations of putatively extracellular fungal proteins and the host ant proteome. Although a code bug prevented us from training a model tailored to our input data, D-SCRIPT's strength is its generalizability. D-SCRIPT models are trained on existing PPI data, but are not wholly constrained by direct protein homology, as interolog searches are. Rather, the machine learning approach infers structural relationships between proteins without relying on protein-wide homology. This flexibility allows D-SCRIPT to extend predictive power across organisms and beyond previously documented PPIs. Our results support this, as D-SCRIPT predicted over 200-fold more PPIs than the interolog method. This is not to say more is always better, as the balance of true and false positives must be taken into account. However, the interolog method only predicted 31 secreted fungal proteins to interact with the host, which is much lower than what some other host-pathogen PPI prediction studies have found (Ma *et al.* 2019; Loaiza *et al.* 2021). D-SCRIPT predicted 398 fungal proteins to interact with host proteins.

We used multiple metrics to annotate the putative fungal secretome (Beckerson *et al.* 2019). However, these secretion signals are not foolproof and can be difficult to disentangle from

organelle/membrane trafficking intracellular “secretion” functions. For example, we found fungal proteins in PPIs that are often associated with the endoplasmic reticulum (e.g., cytochrome P450s) or the fungal vacuole (vacuole protein A). Whether or not these fungal proteins are being exported to the host environment and have functions there is unclear. As we are generating hypotheses that will need future functional validation, we analyzed and considered the possibility of PPIs involving such proteins here.

To focus our investigation on the strongest candidate proteins for PPIs, we removed PPIs that were homologous interactions both within *Ophiocordyceps* and between host and parasite. We suspected that such interactions would more likely contain spurious PPI predictions that related to core cell functions such as protein chaperoning and folding and intracellular transport. However, the possibility remains that for such PPIs, transcriptional/translational regulation and post-translational modifications could allow *Ophiocordyceps* to control the activity of the effector protein within itself. If so, some parasite effectors may target well-conserved biological processes and pathways that might be overlooked in this subset of PPIs. But, we chose to be conservative in this respect. Similarly, we focused our analyses on fungal proteins upregulated during manipulation of the host. Possible PPIs of biological importance may not always include fungal proteins upregulated during host manipulation, but we suspected that most manipulation related PPIs would be. RNAseq data collected in future experiments at finer timescales of *Ophiocordyceps* infection would allow greater exploration of PPIs during the course of infection.

Given the various caveats in data selection and inevitable noise in using large bioinformatic datasets, we focused most of our interpretation on group level trends (i.e., enriched annotations). Specific searches and interpretations need to bear in mind that benchmarking tests with this D-SCRIPT model showed ca. 36% recall and 80% precision (Sledzieski *et al.* 2021). That is, for a given true PPI, D-SCRIPT will detect it only 36% of the time. And, of the predicted PPIs D-SCRIPT reports, only 80% of those will indeed be true PPIs. Therefore, searching for a specific PPI hypothesized *a priori*, will often lead to no PPI found. If a PPI is predicted, it is likely a true PPI, but still 20% of the time it may be

incorrect. This, at least in part, likely explains why some of our targeted PPI searches (e.g., enterotoxin KAF4589869.1) yielded no results. Although, the possibility that this protein does not in fact bind host proteins remains.

In many PPIs that we investigated in more depth, we found reoccurring fungal interaction partners. Differentiating true and false signals ultimately would require functional validation. However, very broadly associated fungal proteins perhaps indicated extreme cases related to model training and so may not yield the strongest first hypotheses of possible effector proteins. For example, in nearly 400 PPIs, we found a fungal carboxylesterase that could either indeed be a broadly targeted protein or many of these predicted PPIs could be erroneous results stemming from the particular qualities of this protein. Carboxylesterases can have a range of substrates and hydrolyze ester or amide (peptide) bonds using a well-conserved mechanism and set of amino acid residues shared with serine hydrolases, peptidases, and lipases (Hosokawa 2008; Wang *et al.* 2018). Furthermore, carboxylesterases are often localized in the endoplasmic reticulum and involved in detoxification functions (Hosokawa 2008; Wang *et al.* 2018). Given this protein could have an endoplasmic reticulum trafficking secretion signal, a broad substrate repertoire, and key amino acid residues shared with other enzymes, this protein could be a prime example of a difficult situation for our methods to disentangle true and false host-pathogen PPIs. We also predicted a highly connected glycosyl hydrolase (capable of trimming oligosaccharides on glycoproteins, which include a diverse range of proteins) in many PPIs. Like the carboxylesterase, in some cases this could reflect core cell functions (i.e., post-translation modification and degradation) (Vandenborre *et al.* 2011). A CAP cysteine-rich secretory protein was also found in a wide range of interactions. Proteins with CAP domains have been implicated as fungal effectors in multiple systems and have diverse functions. However, they may function more often by binding sterols or other lipids than by protein binding (Darwiche *et al.* 2016). Given that carboxylesterases and hydrolases could cleave proteins or attached modifications and CAP proteins have known effector functions, these proteins could plausibly contribute

to fungal virulence and manipulation of *Camponotus*. It is, however, the degree of connectivity of these, and other, proteins that warrants closer scrutiny. Although *Ophiocordyceps* effectors could indeed bind many host proteins across different pathways, as has been observed in other systems and may even be the norm (Hogenhout *et al.* 2009; Win *et al.* 2012). Still, protein-specific hypotheses will require deeper analysis to assess the biological plausibility of their predicted interactions. Taken superficially, if *Ophiocordyceps* releases these and many other protein effectors that each dysregulate hundreds of different host proteins, this might lead to a degree of physiological chaos at odds with the apparently fine-tuned aspects of manipulation phenotypes, such as timed-summiting or species-specificity (Evans *et al.* 2011b; de Bekker *et al.* 2014b, 2015; Araújo *et al.* 2018; Sakolrak *et al.* 2018; Will *et al.* 2020; Lin *et al.* 2020). However, we cannot yet discount widespread dysregulation as part of the parasite strategy. But more realistically, our predicted PPIs might contain false-positives and every "true" interaction might not be relevant in every context. Predicted protein binding does not indicate that all such interactions occur in a dynamic changing physiological environment. In and around the cell, protein localization, transcriptional control, post-translation modification, competing PPIs, and biochemical environment changes (e.g., pH) could affect the likelihood of a predicted PPI to actually occur. The cellular environments within *Ophiocordyceps* fungal cells and *Camponotus* insect cells could plausibly differ in many ways shaping protein activity.

Fungal PPI proteins were enriched for S8 peptidase domains, indicating proteolytic functions. Multiple host kinesin motor proteins were in PPIs with these *Ophiocordyceps* proteins. Kinesins are involved in mitotic and intracellular transport processes – with key functions in vesicle transport towards the periphery of neurons (Klinman and Holzbaur 2018). Defects in kinesin activity can lead to dysregulated receptor and neurotransmitter release at synapses, thereby contributing to impaired neurological functions (Klinman and Holzbaur 2018). Zika viruses has been hypothesized to interfere with human kinesin to lead to blindness and microcephaly (Liu *et al.* 2021). From these predicted S8

peptidase-kinesin interactions, we infer that the fungus may be dysregulating core host cell processes, possibly with impaired neuron signaling and neurotransmitter release underlying modified behavioral phenotypes. We also predicted these peptidases to interact with multiple *Camponotus* nuclear pore proteins. Although some components of the nuclear pore undergo proteolytic post-translation modification to remove sumoylation (Hang and Dasso 2002; Zhang *et al.* 2002), these peptidases are in a different family than S8 peptidases. If some of the S8 peptidase-nucleopore proteins interactions are genuine, this could mean the parasite alters transport of molecules in and out of the host nucleus. Speculatively, this could even allow increased entry of fungal transcription factor-binding proteins proposed here. Furthermore, fungal PPIs were enriched for WGCNA modules associated with manipulation. Assuming "guilt-by-association," in some cases this could indicate these PPIs are related to infection and manipulation processes even if we yet lack clear mechanistic hypotheses of how (e.g., PPIs with uSSPs) (Stuart *et al.* 2003; Carlson *et al.* 2006; Gillis and Pavlidis 2012). The relative lack of enrichments among fungal proteins compared to ant proteins could relate to the background protein sets tested. If these background PPI and secretome proteins were already functionally specified toward host-pathogen and infection processes, the upregulated PPI proteins might not represent a highly distinct subset.

We predicted over 300 PPIs that contributed to an enrichment of oxidation-reduction processes among the host proteins. Oxidation-reduction processes can be involved in a range of metabolic, development, and host-pathogen interaction pathways that have been previously hypothesized to play a role in *Ophiocordyceps* infections (Dubovskii *et al.* 2010; de Bekker *et al.* 2015; Iwanicki *et al.* 2020; Will *et al.* 2020). Nearly half of the host proteins were putative cytochrome P450s. In insects, cytochrome P450 proteins are often involved in hormone metabolism (e.g. ecdysone and juvenile hormone), stress response, xenobiotic detoxification processes, and cuticular development (Scott and Wen 2001; Sztal *et al.* 2012; Iga and Kataoka 2012; Su *et al.* 2021; Xing *et al.* 2021). In turn, we predicted that many of

those host cytochrome P450s interacted with fungal cytochrome P450s. Although cytochrome P450 proteins often act independently, homo- and hetero-dimer formation of cytochrome P450 proteins can modulate protein function in positive, negative, and substrate-specific manners (Kandel and Lampe 2014). Host cytochrome P450s possibly also interacted with fungal uSSPs. In what way these undescribed proteins may be modulating host protein activity remains to be functionally tested.

Another ant protein with oxidation-reduction function was a glutamate synthesis enzyme that we predicted to be in a PPI with a fungal uSSP. We cannot yet conclude what the functional outcome of this interaction would be from these data. However, manipulated ants show tremors and additional locomotor activity in the final stages of *Ophiocordyceps* infection. As glutamate functions as an excitatory neurotransmitter at insect neuromuscular junctions (Johansen *et al.* 1989; Pflüger and Duch 2011), the fungus may upregulate host glutamate synthesis with this PPI. Three "ligand-gated ion channel" domain host proteins had BLAST descriptions or additional PFAM domains indicating they were glutamate receptors (File S3). Again, unannotated fungal proteins interacted with these receptors, not clearly indicating how they might be modifying receptor activity, but increased activation seems most consistent with observed phenotypes. All three of these fungal proteins had hundreds of predicted PPIs, perhaps resulting from an overestimation of their binding partners. As such, these preliminary hypotheses should be taken cautiously.

Also implicated in neurotransmission, we detected over 30 ant GPCR or receptor subunits in PPIs with fungal proteins. Most receptors were from the rhodopsin/A family and included receptors related to biogenic monoamines, acetylcholine, and neuropeptides. These receptors offer a wide range of hypothetical links to manipulated ant behavior. The monoamine neurotransmitters dopamine, serotonin, octopamine (analogous to vertebrate norepinephrine), and tyramine have been implicated in modulating locomotor, foraging, learning, social, reproductive, and aggressive behaviors in many insects, and have been tested in social insects, including ants (Adamo 2008; Aonuma and Watanabe 2012; Adamo *et al.*

2013; Kamhi *et al.* 2017; Verlinden 2018; Finetti *et al.* 2021). We additionally detected two muscarinic acetylcholine receptors associated with sensory and motoneurons in non-insect animals (Stankiewicz *et al.* 199AD; Lee *et al.* 2000; Tsentsevitsky *et al.* 2017). In bees, excessive activation of acetylcholine receptors can cause changes in locomotor, navigational, foraging, and social behaviors (Grünewald and Siefert 2019). The neuropeptide receptors had a range of putative ligands. Allatostatin can act as a feeding behavior modulator, sometimes via juvenile hormone inhibition (Aguilar *et al.* 2003; Hergarden *et al.* 2012). Gondaotropin-releasing hormone, or in insects more likely adipokinetic hormone or corazonin, can affect vitellogenin levels, locomotor, feeding, or reproductive behaviors (Sakai *et al.* 2017). Cholecystokinin-like peptides have been linked to feeding, hyperactivity, aggression, and locomotion, possibly in a octopamine-responsive manner (Nässel and Williams 2014). Also linked to feeding and locomotion, we found a CCHamide-2 receptor (Ren *et al.* 2015). We found four receptors that may respond to pyrokinin, pheromone biosynthesis activating neuropeptide (PBAN), and/or capa type neuropeptides that have been implicated in pheromone biosynthesis, muscle contraction, and developmental processes (Jurenka and Nusawardani 2011; Choi *et al.* 2012; Ragionieri *et al.* 2017). An orphan receptor, GPCR 52, is responsive to anti-psychotic drugs, implicated in models of depression and neurodegenerative disease (e.g., Huntington's), and is coexpressed in neurons with dopamine receptors, where it can interact with dopamine signaling pathways with effects on locomotion (Komatsu *et al.* 2014; Yao *et al.* 2015; Mantas *et al.* 2021). Two of the three predicted fungal binding partners for this receptor were uSSPs – possibly offering insights to the unknown endogenous ligand of GPCR 52. From a different family of GPCRs (secretin/family B), a latrophilin/CIRL-like receptor is a GPCR that gets its name from a sensitivity to alpha-latrotoxin in black widow venom. This receptor has been implicated in mechanosensation, interneuronal adhesion, neurological disorders, hyperactivity, and increased nighttime activity (Moreno-Salinas *et al.* 2019). We also predicted PPIs involving a putative host G(i) subunit alpha, which serves an important role as a component of GPCRs and was the sole upregulated host gene

in this category. Most GPCR genes were not DEGs, but host pyrokin, gondaotropin-releasing/adipokinetic hormone, octopamine, and acetylcholine receptors were downregulated during manipulation.

The various fungal proteins predicted to bind these GPCRs included five uSSPs upregulated during manipulation. All five were in WGCNA modules F1-3, which have associations with manipulation. Three of these uSSPs are conserved with *O. kimflemingiae*, from which we infer common functional roles in both host-parasite interactions. Given that these fungal proteins lack annotations, we cannot yet determine if they might be agonists or antagonists and if they bind the ligand-site or elsewhere on the receptor. As these uSSPs were not predicted to be specific to only binding these host proteins, their interaction with the receptors may be less likely mediated by specific receptor-ligand binding sites than more generic contact sites elsewhere on the host protein.

Capable of mediating GPCR-dependent or GPCR-independent signal transduction, GTP-binding signaling molecules were enriched in host PPI proteins (Chiariello *et al.* 2010; Xu *et al.* 2017; Dohlman and Campbell 2019). These host proteins were predicted to interact with many of the same fungal proteins as the GPCR and GPCR-subunits above. These fungal proteins were mostly members of infection and manipulation associated WGCNA modules. Although that association does not inform us of exactly how these molecules could act as effectors, it does suggest that many of them would have a role during host-pathogen interactions.

During manipulation, the fungus secretes proteins predicted to bind host cuticle and connective tissue proteins. *Ophiocordyceps* would have direct access to internal host connective tissues, the endocuticle layer (once the epidermis is breached), and the cuticular lining of the gut and trachea (Davies 1988; Burrows and Sutton 2012). In termites, the endocuticle of worker heads is especially thick compared to other castes, possibly linked to protective and sensory functions (Ye *et al.* 2021). The gene expression data we used to select upregulated fungal DEGs came from heads of infected minor worker

caste ants (Will *et al.* 2020). The fungus could be degrading cuticular proteins for nutrition, detaching muscles, or in preparation for emerging hyphae to grow out of the host cadaver. Although we have observed *Ophiocordyceps* hyphae to largely grow from host cadaver joints and orifices, the fungus possibly degrades some host cuticular proteins to fully emerge. If the fungus and ant share homologous extracellular chitin-associated proteins (in their cell walls and cuticle, respectively), we cannot fully discount that some of these secreted fungal proteins may be cell wall modifying proteins. To test for this as we continue analyses, we may expand the homologous PPI data filter between *Ophiocordyceps* and *Camponotus* to include all fungal-self PPIs, and not only the extracellular set tested against the intracellular set. Supplementing published descriptions of fungal invasion, degradation, and atrophy of manipulated ant mandible muscles (Hughes *et al.* 2011; Fredericksen *et al.* 2017; Mangold *et al.* 2019; Zheng *et al.* 2019), future investigations documenting fungal growth and host tissue destruction at different stages and in body compartments could be very insightful. Such data could allow us to better understand how the fungus may be controlling, or not controlling, its effects on host muscle. The predicted fungal interactors with host proteins included multiple proteases: a M43-like metalloprotease, S8 subtilisin-like serine protease, and disintegrin/reprolysin-like metalloprotease. S8 proteases degrade insect cuticle and can be found in many fungi (St Leger *et al.* 1996; Arnesen *et al.* 2018). A reprolysin-like (or disintegrin in snake venom) and a serine protease has been found in parasitoid wasp venom and hypothesized as candidates involved in immune suppression and virulence, but not necessarily by proteolytic activity (Andrews and Berndt 2000; Parkinson *et al.* 2002a, 2002b). We also detected unannotated secreted proteins in cuticular protein PPIs that could have similar or different functions.

Enrichments of host peptidases could have indicated ant degradation of fungal secreted proteins. However, upon closer inspection these PPIs could also plausibly include spurious predictions based on protein complexing relationships rather than true cross-species interactions. The enriched host proteins have canonical functions tied to proteosome and lysosome function, which are involved in protein

degradation. Some of the fungal proteins (e.g, vacuolar protease A) predicted to interact with these host proteins have organelle-associated protein-degradation functions as well – possibly indicating that these proteins might have analogous roles and protein-complex relationships in their respective organisms. This does not discount that such parasite proteins may have true host-pathogen interactions outside of these PPIs (the putative vacuolar protease A was predicted in over 100 PPIs). Some of the fungal proteins do not have a clear protein degradation function and might indeed be true targets of host proteases: a putative creato-platanin-like protein, tyrosinase, and uSSP. Fungal creato-platanins, best described in phytopathogens, interact with carbohydrates and chitins and may relate to fungal virulence and growth or host detection of pathogens (Gaderer *et al.* 2014). In one case, a fungal creato-platanin from a human pathogen was reported to have proteolytic activity, but these conclusions remain uncertain (Cole *et al.* 1989; Gaderer *et al.* 2014). As such, we hypothesize that the PPI reflects host immunity and degradation of this fungal protein. Fungal tyrosinases can initiate the conversion of tyrosine or L-DOPA toward melanin, with roles in virulence and stress responses (Halaouli *et al.* 2006). Although typically intracellular proteins, extracellular fungal tyrosinases have been reported (Selinheimo *et al.* 2006; Gasparetti *et al.* 2012). Whether the fungus might use such tyrosinases to deplete host tyrosine or L-DOPA, produce melanin, or other functions is unclear. In any case, it appears that the host is degrading a secreted fungal tyrosinase.

Ophiocordyceps could possibly interfere with *Camponotus* gene regulation with proteins that bind host transcription factors and DNA- or mRNA-binding proteins. Such an approach may be metabolically favorable for the parasite as it could dysregulate host function upstream of more costly metabolic steps, using the host's own cells to dysregulate behavioral pathways. Some of the fungal proteins in these PPIs were uSSPs that will require experimental validation to see if and how these proteins might modulate function of the host proteins. However, a number of parasite proteins were hydrolases; we suggest that these most plausibly could cleave host proteins and post-translation

modifications. Especially in cases when a peptide bond within the main protein is broken, we expect this would reduce functionality of the host protein – which, depending on the role of that protein, could increase or decrease transcription of host genes. Among the ca. 200 host proteins in this category, our preliminary survey found many with behavioral and activity effects via changes in locomotion, feeding/foraging behavior, graviotaxis, light perception, circadian clocks, development and social caste related hormones, and neuronal maintenance. A deeper investigation of the specific PPIs in this group to find the pairs most plausibly interacting and producing biologically relevant changes will allow us to propose specific hypotheses for further testing.

We detected an enrichment of host PPI proteins in WGCNA modules that have been previously correlated to *Ophiocordyceps*-manipulated *Camponotus*. In particular, a module enriched for neuronal processes and GPCRs contained many of the discussed GPCRs in PPIs with fungal proteins. Another host module correlated to manipulation was enriched for gene regulatory processes – which we now propose are targets for fungal disruption. Additionally, both upregulated and downregulated host DEGs were enriched in predicted PPIs (relative to the whole ant proteome). These *Camponotus* genes that showed large changes in transcription at manipulation and were predicted to interact with *Ophiocordyceps* proteins possibly indicate host responses to fungal interference (e.g., homeostatic responses to fungal modulation of functional protein levels).

Although we were unable to test a machine learning model tailored to our data and questions, the structure-based predictions produced by D-SCRIPT appear to have identified many plausible cross-species PPIs. Now that the code bug preventing model training has been fixed, we may return to training these models and possibly improve D-SCRIPT's predictive capabilities for insect-fungal host-pathogen PPI modeling. To benchmark these models we can follow the canonical steps of cross validation and testing them on known PPIs outside of their training set. For example, D-SCRIPT was trained on human proteins, but tested on fly, yeast, bacterium, and nematode PPIs. As our model would be trained on fly

and yeast, a fair comparison may be the nematode PPI set. Furthermore, we can produce single-species PPI networks for both *O. camponoti-floridani* and *C. floridani* separately. With the ant PPI predictions, we can compare our results to a published interolog-based *C. floridanus* PPI network. As interologs can often work well for single-species PPIs, we would expect a well predicted PPI set from D-SCRIPT to largely agree with the interolog approach. A final validation would be to use GO term semantic similarity of PPIs against negative predictions, for both organisms. Semantic similarity uses the hierarchical structure of GO terms to quantify relatedness of GO term functions. With this test, we would assume many single-species PPIs are cooperative interactions, leading to both proteins having related GO terms and therefore a higher semantic similarity than randomly assigned PPIs (Gupta *et al.* 2020). By testing if D-SCRIPT predicted PPIs within a single-species have significantly higher shared semantic similarity than presumably false PPIs, we can evaluate if the model is performing well.

The bioinformatic prediction of host-pathogen PPIs between *O. camponoti-floridani* and *C. floridanus* with D-SCRIPT offers a rich dataset. However, due to the unfamiliar terrain of leveraging this approach between non-model species, specific hypotheses must be carefully vetted. In doing so, we should seek a balance of biological plausibility based on previous knowledge of protein and cellular function, but also, consider that undescribed or unusual mechanisms may underly the molecular interactions of this parasitic manipulation system. Weighing these possibilities will also have to contend with fewer available cross-species PPI datasets compared to single-species data – let alone for entomopathogenic parasitic manipulators. Another way we can better understand these PPI predictions is through network analyses and clustering PPIs into groupings not only determined by functional annotations, but PPI edge relationships. These types of analyses may offer insights by allowing us to infer functional relationships by shared expression and protein interaction partners. Our enrichment analyses focus on host and parasite proteins separately; yet the actual unit of biological interest are the interactions. Developing a framework to characterize the PPI itself, and not only the constituting proteins, could allow

us to reach more meaningful conclusions. There are also many ways in which to subset and analyze these data, each asking subtly different questions. We have focused here on upregulated, secreted fungal proteins and all host proteins. However, examining fungal proteins regardless of gene regulation during manipulation or including transmembrane proteins could be fruitful to gain a broader sense of possible host-pathogen interactions. Our efforts here focused on finding putative fungal effectors and their targets potentially underlying parasite-induced host behavioral outputs. In addition to searching for effector proteins, as we have begun here, we can also search for previously hypothesized host-targets driving manipulation phenotypes. A host-centric approach using ant gene expression data to subset PPI predictions could also improve our understanding of how the host counteracts fungal infection and manipulation. Host-adaptive PPIs could include functions such as detection of the parasite (e.g., pathogen associated molecular patterns, PAMPs) or degradation of fungal effectors.

Taken together, we consider two general types of PPIs to have the most supporting data and interesting links to manipulated phenotypes. We hypothesize PPIs involving host GPCRs and transcription factors, with reported links to behavior, to underly aspects of infected and manipulated ant phenotypes. From PPIs involving these host proteins, we aim to further investigate predicted interacting fungal uSSPs and other proteins with few conflicting interpretations regarding their extracellular secretion or biological plausibility to act on those host proteins. Additionally, to estimate where, structurally, fungal proteins are binding host proteins we can use D-SCRIPT's contact map outputs. These contact maps show the predicted residues that mediate the PPI binding. This information allows for better estimations of the likelihood of interaction and the type of interaction (e.g., if the fungal protein binds allosterically, in an active/ligand-binding site, etc.). For orphan receptors, this may even let us hypothesize about the identity of unknown endogenous ligands. Putting our predicted PPIs in context of what other host-parasite systems, especially with entomopathogens, have found or predicted, will also enable us to put forward a

top selection of hypotheses. Ultimately, even our most robust hypotheses will require functional testing and real-world validations to move forward.

Acknowledgements

We would like to thank Samuel Sledzieski for answering questions regarding D-SCRIPT implementation and Shishir Gupta for an updated link to *Camponotus* Cflo_N gene identifiers. We expect future dissemination of this work to be coauthored by Ian Will, Biplabendu Das, William Beckerson, and Charissa de Bekker. Supplemental data files are available upon request.

CHATPER FOUR: METABOLOMIC CHARACTERIZATION OF BEHAVIORALLY MANIPULATED ANTS & MULTIOMIC INTEGRATION OF DATA

Abstract

Parasitically manipulated *Camponotus floridanus* ants show multiple diseased behaviors and a fatal summiting phenotype when infected by *Ophiocordyceps camponoti-floridani* fungi. Altered host behavior as a response to and driven by parasites occur in a broad swath of taxa. In many cases, such as this interaction, the underlying mechanisms have not yet been clearly characterized. The drastic phenotypic changes observed could in some cases reflect large physiological changes within cells, spanning different molecular levels from nucleic acids to metabolites. Here, we link existing genomic and transcriptomic data to a new metabolomic dataset we produced to hypothesize on the mechanisms of manipulated "zombie ants" from a multiomic perspective. Multiple lines of evidence point toward dysregulation of neurotransmitters and neuronal signaling. We propose that these processes are altered during infection and manipulation based on: neurotransmitter synthesis and receptor gene expression, altered metabolite abundances, parasite suppression of a connected immunity pathway, and plausible behavioral ties to known effects of these neurotransmitters in ants and other insects. We additionally report signals for fungal metabolic activity during manipulation and possible alterations of host pathways related to detoxification and hormone metabolism.

Introduction

Host-parasite interactions can take on many forms as two (or more) organisms compete in tightly interlinked biological relationships over individual, ecological, and evolutionary time. Hosts infected or threatened by parasites can show altered phenotypes that can be adaptive for the host or pathogen. In the

latter case, parasite-adaptive changes in host behavior may be specifically promoted by the parasite and are often referred to parasitic behavioral manipulation. Examples of apparent parasitic manipulations of host behavior and physiology occur in a broad range of host and parasite taxa, although the underpinning mechanisms are still being revealed (Thomas *et al.* 2010; Moore 2013; Heil 2016; Libersat *et al.* 2018).

In many parasitic manipulations, insect hosts succumb to summit disease, where the manipulated individual occupies an elevated location and dies in a stereotypical manner (Lovett *et al.* 2020; de Bekker *et al.* 2021). These final, elevated, and exposed summit positions are thought to be adaptive for the parasite by aiding transmission either by direct dispersal of the parasite or trophic transmission. Although, deeper understanding of the fitness cost and benefits for both host and parasite may reveal that such behaviors could also be sometimes adaptive for hosts, at the individual or group level (perhaps especially so for eusocial animals, such as ants). Even if hosts are not the ultimate drivers of these phenotypes, they may already demonstrate behaviors that can be easily coopted for manipulation. In these cases, the parasite may benefit by taking advantage of and influencing host processes and symptoms without relying on costly mechanisms to "rewire" their hosts (Adamo 2019; Lovett *et al.* 2020). Molecular descriptions of hosts displaying apparent manipulations may offer a glimpse into how parasites (or hosts) modulate animal behavior, the coevolution of specialized host-parasite relationships, and undescribed neurmodulatory properties of certain proteins and metabolites.

The ant-manipulating *Ophiocordyceps* have been leveraged in laboratory studies to better understand the mechanistic basis of behavioral manipulation of infected ants. Manipulated ants display a summiting behavior, latching and biting onto their final summit perches until their death. Preceding this final fatal change in behavior, infected ants also deviate from foraging trails and increase locomotor activity, reduce nestmate communication, and tremor (Pontoppidan *et al.* 2009; Andersen *et al.* 2009; Hughes *et al.* 2011; de Bekker *et al.* 2015; Sakolrak *et al.* 2018; Trinh *et al.* 2021). Investigations of infected-host responses, genomes, transcriptomes, and metabolomes continue to accumulate and help

bring the most robust mechanistic hypotheses into focus. The range of hypotheses touch upon mechanisms involving: neuromodulators and effector proteins, circadian rhythms and phototropism, insect hormones and behavioral profile regulators, neuroprotectants, and muscular hyperactivity (de Bekker *et al.* 2014a; Kobmoo *et al.* 2018; de Bekker 2019; Mangold *et al.* 2019; Zheng *et al.* 2019; Loreto and Hughes 2019; Will *et al.* 2020; Trinh *et al.* 2021; de Bekker and Das 2022). Previous metabolomic works with *Ophiocordyceps kimflemingiae* infecting host ants or isolated tissue, have already identified many metabolites associated with manipulation. The metabolomic profile of the *O. kimflemingiae-C. castaneus* interaction also differs from infections where either the parasite or host was a exchanged for a different species (de Bekker *et al.* 2014b; Zheng *et al.* 2019; Loreto and Hughes 2019). Here, we continue to add to these works in a multiomic approach to present a new, more in-depth, metabolomic analysis of *Camponotus floridanus* (Florida carpenter ants) manipulated by *Ophiocordyceps camponoti-floridani* (Florida zombie ant fungi) interpreted in the context of existing transcriptomic and genomic data for both these organisms (Will *et al.* 2020).

As the key processes of manipulation could involve specialized and general mechanisms, host and parasite effectors, or changes from the genetic to chemical level, multiomic approaches can cast a sufficiently broad net to best detect these processes. To supplement existing transcriptomic data, we collected metabolite data using liquid chromatography-tandem mass spectrometry (LC-MS/MS). In this work we focused on altered metabolic pathways supported by a combination of metabolite and gene signals. Following this framework of using multiple data types and highlighting points of overlap as the strongest evidence, we applied multiple analytical tests to the metabolomic data presented here. To evaluate if individual metabolite features distinctly associated with healthy or manipulated ants, we assessed these data by their differential abundances, principal component analyses (PCAs), and decision trees. This approach follows the intuition that every analysis is subject to its own particular biases but data

that represent substantial biological changes are more likely to be selected by multiple complementary tests.

We also selected groups of features for metabolic pathway enrichment analyses based on either those tests or by constructing network modules of correlated features. Grouping metabolite features in networks based on concentration changes from healthy to manipulated ants is built upon a prediction that such metabolites may be biochemically linked in shared pathways. For example, in the simplest cases, a precursor becoming reduced in concentration as the derivative increases, or multiple metabolites that change concentration in sync to mount a unified response. These network approaches may capture the biological complexity in systems where phenotypes or molecular processes are the result of many elements (e.g., genes or metabolites) creating an overall signal. Furthermore, assumptions of group-level activity and interconnected regulation can lead to inferences about the function of unidentified elements (as many untargeted metabolomic data features are) (Stuart *et al.* 2003; Carlson *et al.* 2006). However, this "guilt by association" paradigm has faced criticism for over-extension and under-validation (Gillis and Pavlidis 2012). To balance caution with exploration, we primarily used network modules as a way to subset our large dataset for metabolic pathway enrichment analyses, rather than making predictions about the functions of individual unknown features.

Our study compared whole head samples of healthy *C. floridanus* ants and ants manipulated by *O. camponoti-floridani*. Sampling whole heads allowed direct comparison to Will *et al.* 2020 transcriptomic ant-head data. Although metabolomic signals will be homogenized, whole heads will contain the chemical profiles of ant neural tissue, muscle, and hemolymph in addition to fungal cells that all may contain metabolites of interest (Hughes *et al.* 2011; de Bekker *et al.* 2014b, 2015; Fredericksen *et al.* 2017; Mangold *et al.* 2019; Zheng *et al.* 2019; Loreto and Hughes 2019). We have not incorporated isolated *in vitro* fungal control samples as was done for transcriptomic analysis in Will *et al.* 2020. Fungal metabolite production can be highly reflective of culture conditions (VanderMolen *et al.* 2013) and,

unlike transcriptomic analyses, we would not be able to discern the origin of metabolites in mixed-organism manipulated ant samples. As such, analyses of isolated fungal samples would not have been an effective allocation of resources given the relatively high number of samples needed to obtain reliable metabolomic data. Instead, we used the transcriptomic data to propose links of altered metabolite abundances during manipulation to either the host or parasite.

By analyzing our metabolomic data in light of previous genomic and transcriptomic data, we have arrived at three major branches of metabolism showing notable multiomic signals altered during manipulation. Metabolism of the biogenic amine neurotransmitters dopamine, serotonin, and octopamine appear to change, with connections to insect immunity. Glutamate metabolism could relate to alterations of ant neuronal and muscular activity, while the fungus increases production of 4-aminobutyric acid (GABA) for its metabolic demands. The excitatory neuromodulator, acetylcholine, appears to have been elevated in manipulated ants as they attached to their final summiting position, but swiftly depleted once summiting is completed and used for increased fungal cell membrane metabolism via conversion to choline. We additionally found more ambiguous signals for the production of an unexpected neuroprotectant peptide (carnosine), reduced insect hormone biosynthesis, and fluctuations in drug metabolism and detoxification pathways.

Methods

Ant collection & husbandry: We used a single laboratory-housed wild-caught colony of *C. floridanus* to produce all samples. This colony was collected in March 2021 in the University of Central Florida arboretum. Following collection, we housed the ants indoors under 48 h constant light to prepare them for circadian entrainment to laboratory conditions. Follow the “circadian reset,” we transferred the colony to climate-controlled incubators (I36VL, Percival) cycling 12 h-12 h, light-dark, 28 C°-20 C°, 65% RH-80% RH daily cycles. Climate conditions cycled in a ramping manner, with a 4 h ramp from

lights-on to a 4 h hold at peak day conditions to a 4 h ramp to lights-off. We validated climate conditions with a HOBO data logger (model U12). This colony had several hundred individuals including minors, majors, and brood. The ants resided in a 9.5 L plastic container (42 cm long × 29 cm wide) lined with talcum powder (Fisher Scientific) and contained aluminum foil wrapped test-tubes (16 mm x 125 mm, Fisher Scientific) with moist cotton to serve as darkened, humid nest spaces. Ants fed *ad libitum* on 15% sucrose solution, water, and sporadic frozen *Drosophila* feedings. The colony housed together under these conditions for approximately six weeks before individuals were removed for experimental infection by *O. camponoti-floridani*.

Fungal strain OJ2.1 collection, culture, and storage: *O. camponoti-floridani* strain OJ2.1 was used to infect all ants in this work. We isolated this fungal strain using mycelium extracted from the abdomen of a fresh, manipulated *C. floridanus* cadaver. This cadaver was found in the Ocala National Forest, FL (29° 13' 41.7" N, 81° 41' 44.9" W). The isolation procedure, short ribosomal subunit genetic validation, and culturing followed the protocols detailed in Will *et al.* 2020. Cell stocks of secondary blastospore culture supplemented to 15% glycerol were frozen at -80 C° in cryotubes (Fisher Scientific).

Experimental infections of ants: Using stored cryostocks of *Ophiocordyceps* cells, we inoculated new shaking cultures to grow blastospores for ant infections. We cultured cells for 10 days, filtered, harvested, and brought the blastospore cells to a working concentration of approximately 10^7 cells/mL (optical density 660 nm = ca. 0.4) in Graces medium supplemented with 2.5% fetal bovine serum (GF), as described in Will *et al.* 2020.

Also 10 days before infection, we separated ants from their colony into boxes per treatment group. For the *Ophiocordyceps*-infection treatment, we gathered 41 ants and 10 additional caretaker ants with painted abdomens (Testors paint), which did not receive the treatment but assisted the 41 injected ants with recovery. Healthy nestmates in small colony contexts do not attack or discriminate against *Ophiocordyceps* infected individuals during the early stages of infection before manipulation; but rather

continue to exchange food and care as normal (Gracia *et al.* 2018; Trinh *et al.* 2021). One day before infection treatments, we removed the sugar and water from the ant box to reduce the amount of fluid in the ants and ease the injection procedure. Due to experimenter mishandling that lead to widespread death, our sham-infection treatment followed the *Ophiocordyceps* experimental infection by two-weeks. Ants from the same colony were used for the sham treatment (n = 30 with 8 painted caretakers).

Ants were either anesthetized by placing their plastic box on top of ice prior to injection, or directly injected at room temperature. We injected each ant with 0.5 μL *Ophiocordyceps* blastospores (infection, n = 41) or 0.5 μL of GF (sham, n = 30) as detailed in Will *et al.* 2020. We placed the treated ants and their painted caretaker ants in plaster-lined boxes with biting structures (*Tillandsia usneoides* tied to wooden sticks with twine) and returned them to the climate-controlled incubator.

Observation and sample collection for LC-MS/MS: After three days post injection (dpi) we removed dead ants and then painted caretaker ants at 10 dpi. Previous work has observed *C. floridanus* to destroy and interfere with manipulated nestmates presumably as a component of their social immunity and nest hygiene; as such, we removed these healthy caretaker ants well before manipulated behavior was expected (Diez *et al.* 2014; Will *et al.* 2020; Trinh *et al.* 2021). Also beginning 3 dpi, we screened the ants for manipulations and deaths multiple times per day. We checked for manipulation and mortality at zeitgeber-time (ZT)-0, the beginning of subjective day, and ZT-6, the mid-point of subjective day. Starting 15 dpi, we began more frequent opportunistic checks as behavioral manipulations of *C. floridanus* had been observed starting 19 dpi in the laboratory (Will *et al.* 2020). After discovering the first manipulation at 21 dpi, we made multiple daily checks beginning at ZT-20 and ending at ZT-14. Previous laboratory *O. camponoti-floridani* manipulations synchronized to the ants' subjective pre-dawn hours and we selected our observation times to improve the odds of collecting manipulations close to their beginning (Will *et al.* 2020). We screened non-manipulated mortalities for fungal infection by crushing tissue from the dead ant in 50 μL of water, briefly touchdown centrifuging, and examining 15 μL of the

supernatant on a microscope. Notable levels of fungal cells were always and only seen in the *Ophiocordyceps* treatment ants. We analyzed and plotted survival data using the R packages survival and survminer in R (v 4.1) with R Studio (v. 2021.09.2) (RStudio Team 2015; Therneau 2015; Kassambara *et al.* 2019; R Core Team 2021).

We collected live manipulated ants displaying characteristic summiting biting and/or latching behavior for LC-MS/MS immediately upon discovery (n = 20). We subsequently collected dpi-matched sham ants at a 1:1 ratio with manipulations at ZT-21.5, as this was the most common time at which manipulated ants were found and collected (n = 20). Manipulated ants found after death were recorded for survival statistics but not used in the LC-MS/MS analyses (n = 3). We created three blank-collection samples at the beginning, middle, and end of manipulated ant sampling, i.e., after the first, 10^{th}, and 20^{th} manipulated ants were found (n = 3). For manipulated ant collection, we clipped the biting substrate just above and below the manipulated ant and submerged the ant in liquid nitrogen briefly until frozen. The sample was then placed in a pre-chilled, autoclaved 2 mL microcentrifuge tube (USA Scientific) and stored in liquid nitrogen or at -80 C°. We collected sham ant samples in a similar manner, plucked from the experiment box with forceps. We made blank-collection samples by briefly touching the forceps to the floor of the sham treatment housing boxes, submerging them in liquid nitrogen, and swirling them in a microcentrifuge tube. We cleaned all tools and surfaces with 70% ethanol and deionized water before sampling and between sample types.

We prepared collected samples for LC-MS/MS processing by isolating ant heads and creating 10 two-head pools from ants in chronological order per treatment (healthy sham or *Ophiocordyceps* manipulations). Each frozen ant was quickly processed on a plastic petri dish (USA Scientific) on a bed of dry ice. Using sharp forceps, we removed biting substrate from the ant's mandibles if needed, snapped the head off, and placed it in a new pooled-sample microcentrifuge tube. For blank-collection samples, we dragged the forceps along the petri dish and swirled the forceps inside the original collection tube. We

cleaned the tools and petri dish with 70% ethanol and deionized water between pools and used a new petri dish between sample types. All samples and tubes were kept constantly chilled on dry ice or in liquid nitrogen.

LC-MS/MS processing of ant head samples: All samples were sent on dry ice to the West Coast Metabolomics Center (WCMC, University of California, Davis) for LC-MS/MS processing. The WCMC processed samples in three LC-MS/MS protocols broadly tailored toward different chemistries: "biogenic amines," "polyphenols and flavonoids," and "complex lipids." The WCMC manually separated the two individual ant heads from each pool, using one for polyphenols and the other for a biphasic extraction used for biogenic amines and lipids. Blank-collection samples were shared across the three LC-MS/MS chemistries. The WCMC produced quality-control (QC) pool samples consisting of all samples used per protocol and additional blank-extraction controls. These WCMC control samples were run at the beginning and every ten samples thereafter per protocol. All LC-MS/MS protocols collected MS/MS data in a top-four data-dependent-acquisition (DDA) mode. We report below all available WCMC protocol information returned with our data.

Samples for biogenic amines were processed for use in hydrophilic interaction chromatography (HILIC) with quadrapole time of flight (Q-TOF) mass spectrometry. Homogenized ant head samples were extracted with a methanol and methyl-tert-butyl ether protocol (Matyash *et al.* 2008) and the aqueous phase used for biogenic amines LC-MS/MS and the organic phase used for lipids (see below). Extractions were mixed with internal standards for normalization according to WCMC protocols to a final volume of 100 μL (File S4). Biogenic amine HILIC LC-Q-TOF in electrospray ionization (ESI) positive and negative mode materials and methods were as follows: Agilent 6530 Q-TOF (ESI positive) and Agilent 6550 Q-TOF (ESI negative) spectrophotometers; Waters Acquity UPLC BEH Amide VanGuard (1.7 μm, 2.1 mm × 5 mm) pre-column; Waters Acquity UPLC BEH Amide (1.7 μm, 2.1 mm × 5 mm) column; 40 C° column temperature; ultrapure water with 10 Mm ammonium formiate, 0.125% formic acid, pH 3

mobile phase (A); acetonitrile:ultrapure water 95:5, with 10 mM ammonium formiate, 0.125% formic acid, pH 3 mobile phase (B); 1 μL injection volume; 4 C° injection temperature; 0.4 mL/min flow rate; 0 min 100% (B), 0–2 min 100% (B), 2–7 min 70% (B), 7.7–9 min 40% (B), 9.5–10.25 min 30% (B), 10.25–12.75 min 100% (B), 16.75 min 100% (B) elution gradient; 4.5 kV capillary voltage; 45 eV collision energy; 3 Da precursor isolation width; 60 – 1200 Da scan range; 2 spectra/sec spectral acquisition speed; 10,000 mass resolution.

Samples for lipids were processed for use in charged surface hybrid (CSH) chromatography with Q-TOF mass spectrometry. The organic phase per biphasic extraction also used for biogenic amines (see above) was taken for lipids LC-MS/MS and mixed with internal standards according to WCMC protocols (File S4) to a final resuspension volume of 110 μL. Lipid CSH LC-Q-TOF in ESI positive and negative mode materials and methods were as follows: Agilent 6546 Q-TOF spectrophotometer; Waters Acquity UPLC CSH C18 (1.7 μm, 2.1 mm x 100 mm) column; 65 C° column temperature; acetonitrile:water 60:40, 10 mM ammonium formiate, 0.1% formic acid mobile phase (A); isopropanol:acetonitrile 90:10, 10 mM ammonium formiate, 0.1% formic acid mobile phase (B); 1.7 μL (ESI positive) and 5 μL (ESI negative) injection volume; 4 C° injection temperature; 0.6 mL/min flow rate; 0 min 15% (B), 0–2 min 30% (B), 2–2.5 min 48% (B), 2.5–11 min 82% (B), 11–11.5 min 99% (B), 11.5–12 min 99% (B), 12–12.1 min 15% (B), 12.1–15 min 15% (B) elution gradient; 3.5 kV capillary voltage; 60 – 1200 Da scan range; 10,000 (ESI positive) and 20,000 (ESI negative) mass resolution.

Samples for polyphenols were processed for use in pentafluorophenyl (PFP) chromatography with QExactive HF (QE) mass spectrometry. Homogenized ant head samples were extracted in a similar fashion as described above and resuspended in a final 100 μL volume of 7% acetonitrile and internal standards (File S4). Polyphenol PFP LC-QE in ESI positive and negative mode materials and methods were as follows: Thermo Scientific Q Exactive spectrophotometers; Kinetex PFP column (1.7 μm, 2.1 mm × 30 mm); ultrapure water, 0.1% formic acid mobile phase (A); acetonitrile, 0.1% formic acid mobile

phase (B); 5 µL injection volume; 0.4 mL/min flow rate. All QC pools were reported to fail upon injection and therefore not used in data filtering procedures.

Metabolomic data processing, quality filtering features: The WCMC performed initial processing steps on all samples to produce metabolomic feature lists consisting of mass/charge ratio (*m/z*), retention time (rt), and value of quantification ion peaks. They aligned raw data with MS-DIAL (v 4.7.0) (Tsugawa *et al.* 2015), subtracted signals detected in the blank-extractions produced in the core facility, removed duplicate signals and isotopes, normalized samples by internal standards, and assigned compound and adduct annotations based on manual MS/MS matching in Massbank, Metlin, and NIST14 databases and, for lipids, with LipidBlast (v 68) (Kind *et al.* 2013). The resulting data consisted of several thousand features per dataset: biogenic amines (5605 total with 141 annotated), polyphenols (6178 total with 158 annotated), and lipids (7021 with 517 annotated) (File S5).

We applied additional feature quality control and data reduction methods to create a final list of metabolite features to investigate. Features that had greater than 50% missing values within both sham and infection treatments were removed. Similarly, we removed features with both median peak values (sham and infection) less than double that of median blank-collection peaks. Following removal based on missingness and peak values, we removed features that we determined to have signals too variable for robust analysis based on their coefficient of variation (CV%, or relative standard deviation). For the biogenic amines and lipid datasets that had successful QC pool data returned, we applied a CV% maximum threshold to remove peaks that varied greatly due to technical variation between QC pool injections. We selected the CV% threshold as the lowest (i.e., strictest) value between 30% and a data-dependent value determined from the distribution of CV% values. We calculated this data-dependent value as the 75^{th}-quartile + 1.5*interquartile-range (IQR), as is used to identify extreme values or outliers in data distributions. For the lipids, the 1.5*IQR method produced CV 25% as the cutoff, removing 5.7% of features. For biogenic amines, the 1.5*IQR CV% was greater than 30%; therefore, 30% was used,

removing 6.6% of features. As the QC pools failed for polyphenols, we ranked each feature by its lowest CV% (i.e., from either CV%-sham or CV%-infection) and removed the highest 6.1% of features. This 6.1% value was the mean of the removal rates of the biogenic amine and lipid datasets. Although we cannot fully discount biological variation in biogenic amine peak values within a treatment, by selecting the lowest CV% per feature (whether from the sham or infection treatment), we sought to remove only features that had high CV% regardless of treatment. After all these filtering steps, we continued with 3268 biogenic amine features (58% of initially collected), 4878 polyphenol features (79% of initial), and 6305 lipid features (90% of initial).

We further applied a putative adduct calling step to consolidate unannotated features that may represent different adducts of the same compound. Per LC-MS/MS dataset, we divided features by treatment and ESI mode, and processed each of these subsets with Binner (v 1.0.0) (Kachman *et al.* 2020). Briefly, Binner compares metabolite features "binned" by rt and calls putative adduct relationships between these features based on a table of possible adducts, feature *m/z*, and correlation of peak values across samples. Data were split by treatment to avoid possibly conflating signals for different compounds found in only one of the treatments as adducts of each other. Data were natural log transformed, no additional deisotoping step was preformed, the mass tolerance was set to 0.005 Da (biogenic amines and lipids) or 0.003 Da (polyphenols), and default settings were used elsewhere. For biogenic amines and polyphenols, we searched for adducts used in KACHMAN *et al.* 2020. For lipids, we supplemented this adduct table with an additional adduct set publicly available online (Fiehn Lab 2020). We then reunited data subsets to create feature lists that included all peaks that were labeled as primary ions or remained unannotated in either treatment group. In effect, this step only removed peaks that were determined to be putative adduct peaks in both treatments, resulting in the final processed datasets for analysis of: 2955 biogenic amines (90% of QC filtered peaks remained), 4315 polyphenols (88% of QC filtered peaks), and 4924 lipids (78% of QC filtered peaks) (File S6).

Metabolomic data analysis, selecting significant features and feature-groups: To select features of interest, we applied three statistical approaches to home in the most relevant feature sets for interpretation. For features with values equal to zero, we imputed zeros as 20% of the minimum value measured for that feature. Each analysis we preformed was done independently per biogenic amines, lipids, and polyphenols. We determined if a feature represented a differentially abundant metabolite (DAM) with a t-test (corrected FDR, $p \leq 0.05$) and minimum ±1.5-fold change in abundance between sham and infection treatments. Principal component analyses always indicated that only PC1 separated samples by treatment type (see Results). As such, we noted features ranked in the upper 50% of PC1 absolute loading values. Given that our choice of threshold was defined as half of the data, we did not rely on this test solely as merit for discussing a feature, but rather as a way to add confidence to results of other analyses. Both t-tests and PCAs were performed through the MetaboAnalyst interface (v 5.0) (Pang *et al.* 2021). Finally, we selected features "confirmed" as "important" by Boruta (v 7.0.0, R package) random-forest based analyses with 900 maxRuns and 70,000 ntree settings (Kursa and Rudnicki 2010). Boruta offers an improvement over standard random-forest analyses for high dimensional data such as in metabolomics, increasing the stability and robustness of the features selected (Acharjee *et al.* 2020).

Additionally, we created co-abundance network modules of metabolite features per LC-MS/MS dataset using the weighted gene co-expression network analysis (WGCNA) method (Langfelder and Horvath 2008). Although the WGCNA was developed primarily for gene expression data, this technique has been used and evaluated for metabolomic data as well (Bartzis *et al.* 2017). Heightened activity in a metabolic pathway could lead to many compounds increasing. But simultaneously, their precursors may become depleted. Therefore, correlations within a network could be both positive and negative. As such, we constructed unsigned WGCNA modules. All WGCNA modules were constructed on feature data without imputing zeros, based on the biweight midcorrelation to compare between treatment types (e.g., corFnc="bicor", robustY=F, maxPOutlier=0.05) (R package WGCNA, v 1.67). In cases where zeros were

present, the analysis defaulted to the Pearson correlation for that feature. We obtained similar network modules when the Pearson correlation was used for all features (data not shown). Soft power thresholds were selected according to program recommendations as follows: biogenic amines – 3, polyphenols – 10, and lipids – 11.

We analyzed different groups of selected features for metabolic pathway enrichments. We formed feature groups that combined data across all three LC-MS/MS datasets based on individual feature selection analyses (t-test, PCA, and Boruta) or their presence only in manipulation samples. Network modules were only analyzed in the context of the LC-MS/MS dataset they belonged to and if the module was correlated to treatment (Student correlation $p \leq 0.05$). We preformed Mummichog analyses on these feature groups (Li *et al.* 2013), as further described in Results & Discussion. This process matched 1,523 unique metabolite features to 6,725 KEGG annotated compounds. For enrichment analyses combining features across datasets, we additionally used a technique based on gene set enrichment analysis (GSEA) ranking features by t-scores returned by t-tests (Subramanian *et al.* 2005). In network module pathway enrichment analyses, only Mummichog was used as it sets a hard threshold to define a group of interest versus the background. Membership within or out of a network module was simply defined and could be used for this division. All enrichment analyses were conducted through the MetaboAnalyst interface with the following settings: Mixed ion mode, 3 ppm mass tolerance, retention time included, primary ions not enforced, all adducts tested, default currency metabolites, and conducted once for both the *Drosophila melanogaster* and *Saccharomyces cerevisiae* Kyoto Encyclopedia of Genes and Genomes (KEGG) metabolic pathway and compound databases (Kanehisa and Goto 2000). As we sought to characterize the composite metabolome of manipulated ant heads containing both insect and fungal tissue, we chose both a well-studied insect and fungal model organism to improve our odds of matching annotations. We did not use results from one database or the other to discriminate between a host (ant) or parasite (fungus) signal. Neither of the databases would represent the full metabolic repertoire of their respective model

organisms and combining them could offer more complete data for comparison. Furthermore, we wished to consider the possibility that due to the relationship of the host and parasite, either organism may be producing metabolites canonically associated with the other as part of its strategy in this antagonism.

Depending on the comparison and input data, we evaluated significantly enriched pathways based on one of the p-values reported by MetaboAnalyst: raw hypergeometric/Fisher's exact test (FET), gamma-null adjusted, or combined using the Fisher method. In the study-wide comparison between treatment groups, running Mummichog and a GSEA as a joint analysis, the Fisher's combined p-value was used. For other analyses in cases where our input list of selected features was less than 50% of the total feature list, enriched pathways were selected by the gamma-null adjusted p-value (< 0.05). For feature groups that were greater than or equal to 50% of the total features analyzed, the gamma-null p-values did not yield results promoting further investigation and discussion ($n = 2$ network modules). As the gamma-null distribution is determined by resampling of the input data based on the number of selected features, cases where the selected features already constitute the majority of data imposes a high bar for detection of significant pathways. In such cases, the raw FET p-value was used to identify possible enriched pathways, which were still subject to other threshold metrics we employed. In a final dissemination of this work, we intend to apply a sub-clustering step to separate these two large network modules into smaller modules more amenable to evaluation by the gamma-null p-value. A preliminary test of this approach did not change the core biological interpretation. Pathway enrichments were only considered for discussion with a minimum of three selected features in the pathway, 1.25-fold enrichment, and three differentially expressed genes (DEGs, see below) encoding associated enzymes to discard weak signals that would likely be difficult to interpret biologically in a multiomic pathway-level context. For cases when a pathway was selected using both *D. melanogaster* and *S. cerevisiae* KEGG databases, a mean p-value and fold-enrichment is reported. For a few enriched pathways that plausibly could have an important role in mediating this host-parasite interaction, we did not have any

accompanying compound annotations for individual features. In such cases, we retrieved Mummichog matches between "empirical compounds" and KEGG compounds with R package keggrest (v 1.34.0) for discussion (Tenebaum and Maintainer 2021). Mummichog is not a feature annotation tool meant to confidently pair a feature to a single best annotation, and we use it here as such only sparingly to gain a tentative glimpse of the finer scale changes within an enriched pathway of interest.

Multiomics integration of genomic and transcriptomic data: We interpreted results of this work's LC-MS/MS data in light of previously collected transcriptomic RNAseq data when possible (Will *et al.* 2020). That RNAseq data was collected with a similar experimental framework, including comparisons of gene expression of both *C. floridanus* and *O. camponoti-floridani* between a control (uninfected ant or fungal culture) and living manipulated ant samples. As quality genomes were available for both organisms (Shields *et al.* 2018; Will *et al.* 2020), RNAseq reads could be mapped and assigned to each organism from mixed organism tissue samples collected from manipulated ant heads. Identification of DEGs (Cuffdiff analysis $q < 0.05$, minimum two-fold change, minimum 4 RPKM in one sample type) and relevant statistics are reported in Will *et al.* 2020. For each enriched metabolic pathway, we retrieved gene sequence data for enzymes associated with that pathway in KEGG (by enzyme nomenclature EC number). For each enzyme EC, we extracted the first representative gene listed for both *D. melanogaster* and *S. cerevisiae*. We searched for reciprocal best matches to those genes in both the *C. floridanus* and *O. camponoti-floridani* genomes using Proteinortho (v 5) with default settings (Lechner *et al.* 2011). While this non-exhaustive approach would not identify every possible *C. floridanus* or *O. camponoti-floridani* gene with homology to known enzymes of interest, it did assist with initially selecting pathway enrichments for deeper analysis. Per pathway, we required that at least three DEGs combined from both transcriptomes of the ant and fungus had homologs to the enzymes associated with that pathway. This selection criterion followed the pathway-level thinking to require at least three contributing metabolite features matched by Mummichog to consider an enrichment result for discussion. For other protein

homology searches we used BLASTp with default settings (Altschul *et al.* 1990). For protein sequence alignment, we used the MAFFT plugin (v 1.4.0, Biomatters) through Geneious (v 2022.0.2, Biomatters) with default settings (Katoh *et al.* 2002).

Results & discussion

Infection mortality and observations of manipulation: Similar to previous laboratory infections with *O. camponoti-floridani* (Will *et al.* 2020), manipulated *C. floridani* in this study were found and collected between 4 hr before to 0.5 hr after dawn, beginning approximately three weeks after infection (Fig. 15). Sham treatment ants showed no mortality until 29 dpi, whereas infection treatment

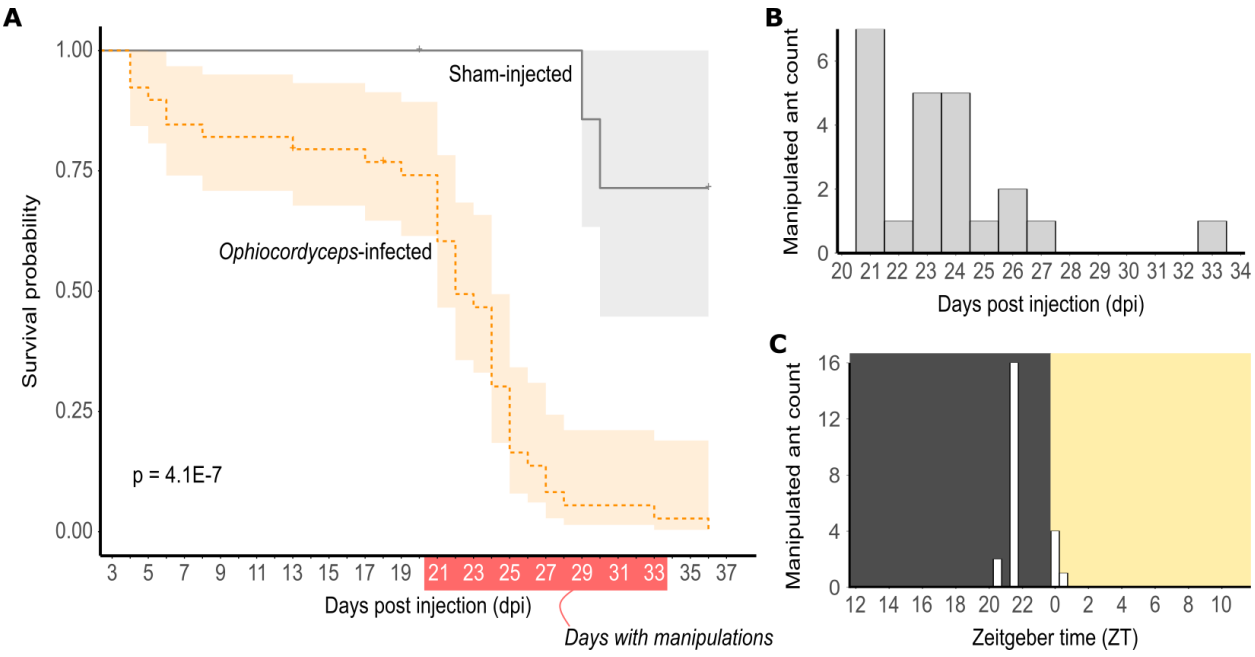

Figure 15. Ant manipulations occur at stereotypical days and times.
A) *O. camponoti-floridani* infection leads to significantly increased mortality compared to sham treatment (p = 4.1E-7, log-rank test). B) Manipulated ants most often appeared 20-27 dpi, but as late as 33 dpi. C) Manipulated ants were collected near dawn, most often at ZT 21.5, 2.5 hr before lights turned on.

ants began to die immediately once we started recording deaths on 4 dpi. This difference in survival was markedly different between treatments (p = 4.1E-7, log-rank test) (Fig. 15). In total, three sham treatment ants died out of the 28 that survived through 3 dpi. Twenty-three infected ants were manipulated out of the 39 that survived through 3 dpi. The other 16 infected ants died with visible blastospore loads but without observed behavioral manipulation.

Metabolomic feature selection and grouping for pathway enrichment analyses: To construct a set of features for study-wide pathway enrichment analysis, we characterized features by their: differential abundance (DAMs), contribution to PCA clustering (PC1 loading values), and importance for navigating decision trees (Boruta) between healthy and manipulated ants. Combining all three LC-MS/MS datasets, approximately 60% of features were DAMs, with most DAMs increasing in abundance in manipulated ants compared to healthy controls (Fig. 16A, Table 5). Separation of treatment groups by PCA only clearly clustered along PC1 (ca. 60% to 80%), with PC2 (ca. 4% to 9%) and other PCs (not shown) describing little of the variation between treatments (Fig. 16B). Using the Boruta selection method, we found ca. 40% of features to be selected as important for distinguishing treatment types (Table 5). We performed pathway analyses with a group of features that satisfied at least two of following criteria: (*i*) it was a DAM, (*ii*) it was among the highest 50% of absolute PC1 loading values, or (*iii*) it was "confirmed" by Boruta. Most features that satisfied at least two requirements (n = 6,468 features, 53% of a total 12,194 features), in fact satisfied all three (n = 4,656, 72% of features passing two criteria) (Fig. 15C, Table 5, File S6). The feature group passing at least two filters contained 347 of the 760 features given compound annotations by the WCMC. The many features passing our filters is likely due to a combination of metabolites related specifically to infection processes and general aspects of fungal metabolism, as *O. camponti-floridani* cells were only present in manipulated ants. For this set of features passing at least two selection filters, we jointly analyzed them with Mummichog and a GSEA in MetaboAnalyst for enriched KEGG pathways. We detected eight significantly enriched pathways that

passed our p-value, minimum metabolite feature, fold-enrichment, and DEG thresholds (Table 6, File S7).

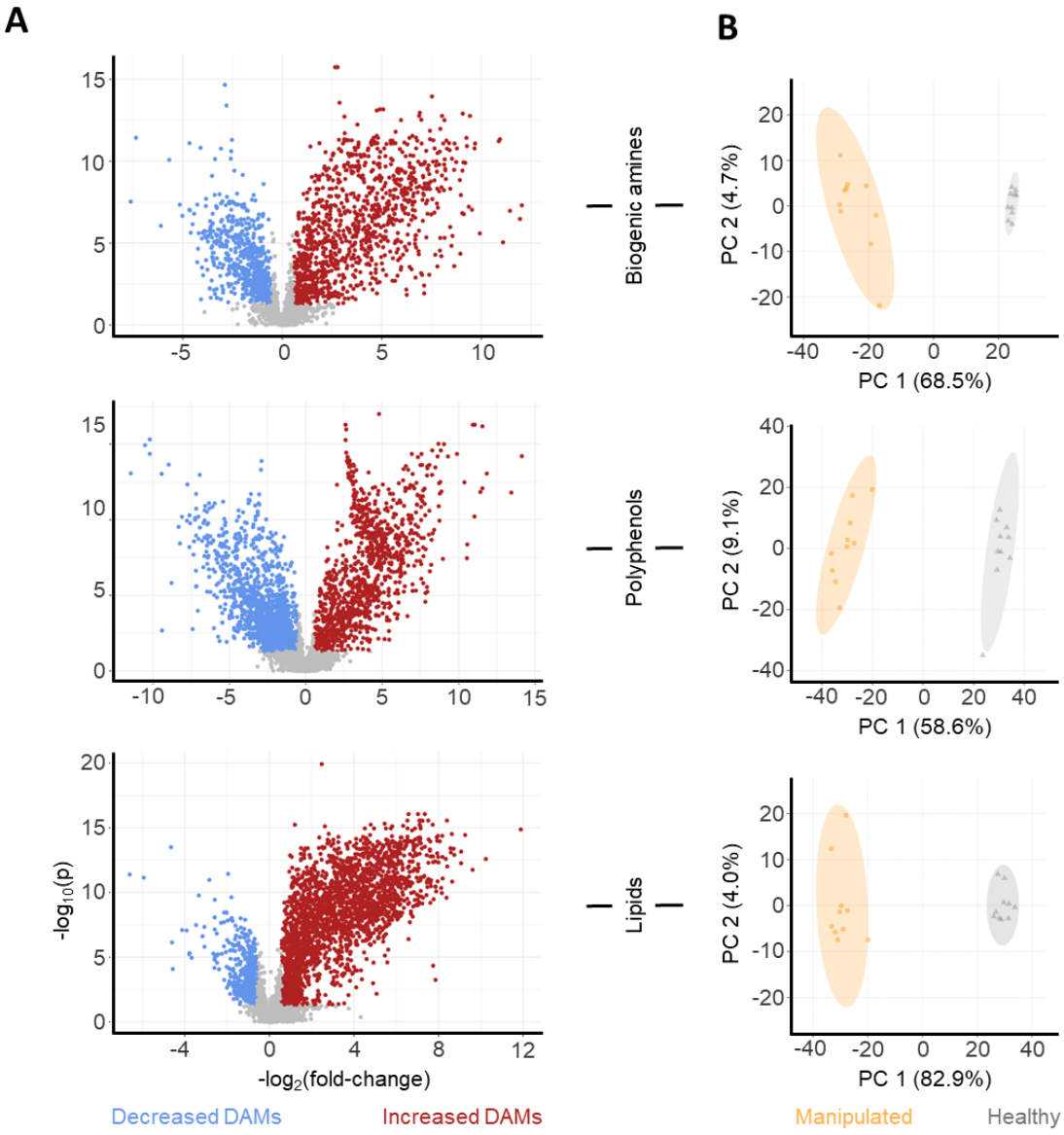

Figure 16. Feature selection overview.

A) Volcano plots per dataset show DAMs that increased (red) or decreased (blue) at manipulation according to a 1.5-fold change and $p \leq 0.05$. B) PCAs for each dataset show distinct clustering of samples between manipulated (orange) and healthy ants (gray) along PC1. C) Features that passed at least two selection criteria (bold) were used for study-wide pathway analyses.

Table 5. Number of features that were selected by different analyses.

Most DAMs in the biogenic amines and lipids datasets increased during manipulation, whereas the polyphenol DAMs more often decreased. We also selected features in top 50% of PC1 from PCAs, these statistics are not reported in the table as they are half of the total features per dataset by definition.

Dataset	Total features	Total DAMs	Increased DAMs	Decreased DAMs	Boruta confirmed	Passing 2+ selection filters
Biogenic amines	2955	1774	1129	645	1226	1535
Polyphenols	4315	2641	1141	1500	1619	2262
Lipids	4924	2995	2390	605	2477	2671
Total	12194	7410	4660	2750	5322	6468

Table 6. All KEGG pathways enriched across analyzed feature sets.

KEGG pathways that were found enriched in Mummichog or GSEA analyses also were required to show a minimum 1.25-fold enrichment, three feature matches contributing to that enrichment, and three DEGs that were homologous to representative enzyme genes within that pathway. We chose these additional selection criteria to focus on pathways that would be most likely to be robust hits amenable to a metabolite-gene multiomic interpretation. Each pathway is listed alphabetically once in the table, with all network modules (or the study-wide feature set that passed at least two selection filters) that were enriched for that pathway.

Enriched KEGG metabolic pathway	Feature sets					
Alanine, aspartate and glutamate metabolism	P13					
Amino sugar and nucleotide sugar metabolism	A1	P1	P2	P3	P18	study-wide
Aminoacyl-tRNA biosynthesis	L3	P2	P11			
Arginine and proline metabolism	A1	P2				
Arginine biosynthesis	A1					
Ascorbate and aldarate metabolism	A1	P13				
beta-Alanine metabolism	P2	study-wide				

Enriched KEGG metabolic pathway	Feature sets					
Biosynthesis of unsaturated fatty acids	L2	L10	P3	study-wide		
Butanoate metabolism	P2					
Citrate cycle (TCA cycle)	A5	P3	P13			
Cyanoamino acid metabolism	A1					
Cysteine and methionine metabolism	L1	P1	P18			
Drug metabolism - cytochrome P450	L3	P3				
Drug metabolism - other enzymes	A1	study-wide				
Fatty acid degradation	P3					
Folate biosynthesis	P2					
Fructose and mannose metabolism	P2	P18				
Galactose metabolism	A1	P18	study-wide			
Glutathione metabolism	A1					
Glycerolipid metabolism	P2					
Glycerophospholipid metabolism	P2	study-wide				
Glycine, serine and threonine metabolism	A5	P2	P11			
Glycolysis or Gluconeogenesis	P3					
Glyoxylate and dicarboxylate metabolism	P13					
Histidine metabolism	A1					
Inositol phosphate metabolism	P2					
Insect hormone biosynthesis	A1	P3				
Lysine biosynthesis	A1					
Lysine degradation	P2					
Metabolism of xenobiotics by cytochrome P450	A1	P2				
Nicotinate and nicotinamide metabolism	P2					
Pantothenate and CoA biosynthesis	A1	P18				
Pentose and glucuronate interconversions	A1	P18				
Pentose phosphate pathway	A1	L1	P1	P2	P3	P18
Phenylalanine metabolism	A1	P2				
Propanoate metabolism	A5					
Purine metabolism	L1	P1	P18			
Pyrimidine metabolism	A1	P11	study-wide			
Pyruvate metabolism	P13					
Starch and sucrose metabolism	A1	P3	P18			
Sulfur metabolism	P2					

Enriched KEGG metabolic pathway	Feature sets		
Taurine and hypotaurine metabolism	L1	P1	
Tyrosine metabolism	P2	P3	
Ubiquinone and other terpenoid-quinone biosynthesis	P3		
Valine, leucine and isoleucine degradation	A5	P18	study-wide
Vitamin B6 metabolism	A5		

Many metabolite features in our dataset were uniquely represented in manipulated samples: 454 features were never detected in healthy sham treatment ants and 1,781 additional features either were detected in less than 50% of the sham treatment ants and/or their median peak value was not at least double that of blank-collection controls (2,235 features total). These features may represent compounds tightly regulated and scarce in the healthy ant or uniquely produced by the fungus. We predicted that this feature set might have been enriched for hallmarks of infection and manipulation processes. However, no significant pathway enrichments were returned from our Mummichog and GSEA analyses. This could indicate that these metabolites are not linked by common metabolic pathways and/or many of these metabolites were not well annotated in the KEGG databases (e.g., species-specific metabolites).

To search for finer-scale patterns between healthy and manipulated *Camponotus*, we used the WGCNA-based approach to cluster metabolite features that change abundance levels between treatments in tightly correlated manners. Compounds shifting abundance in tandem between healthy and manipulated ants can, in some cases, suggest linked biological functions and activity in the same metabolic processes. We detected three biogenic amine, eight polyphenol, and five lipid network modules that were significantly correlated to treatment (Fig. 17). A total of six biogenic amine (A1-A6), 19 polyphenol (P1-P19), and 10 lipid (L1-L10) networks were created in total. Biogenic amine network modules A1-A6 are distinct from ant transcriptome gene WGCNA modules A1-A22 from Chapter 2 (Will *et al.* 2020). As we created these network modules based on changes in feature abundances between only two conditions (i.e., healthy versus manipulated), these simple network modules largely reflect

compounds that have similar absolute fold-change values as ants become manipulated. One of the ways to leverage WGCNAs is to find hub features that are highly interconnected within a network that sometimes can be reflective of the core functions of that module. However, due to our sparse annotation

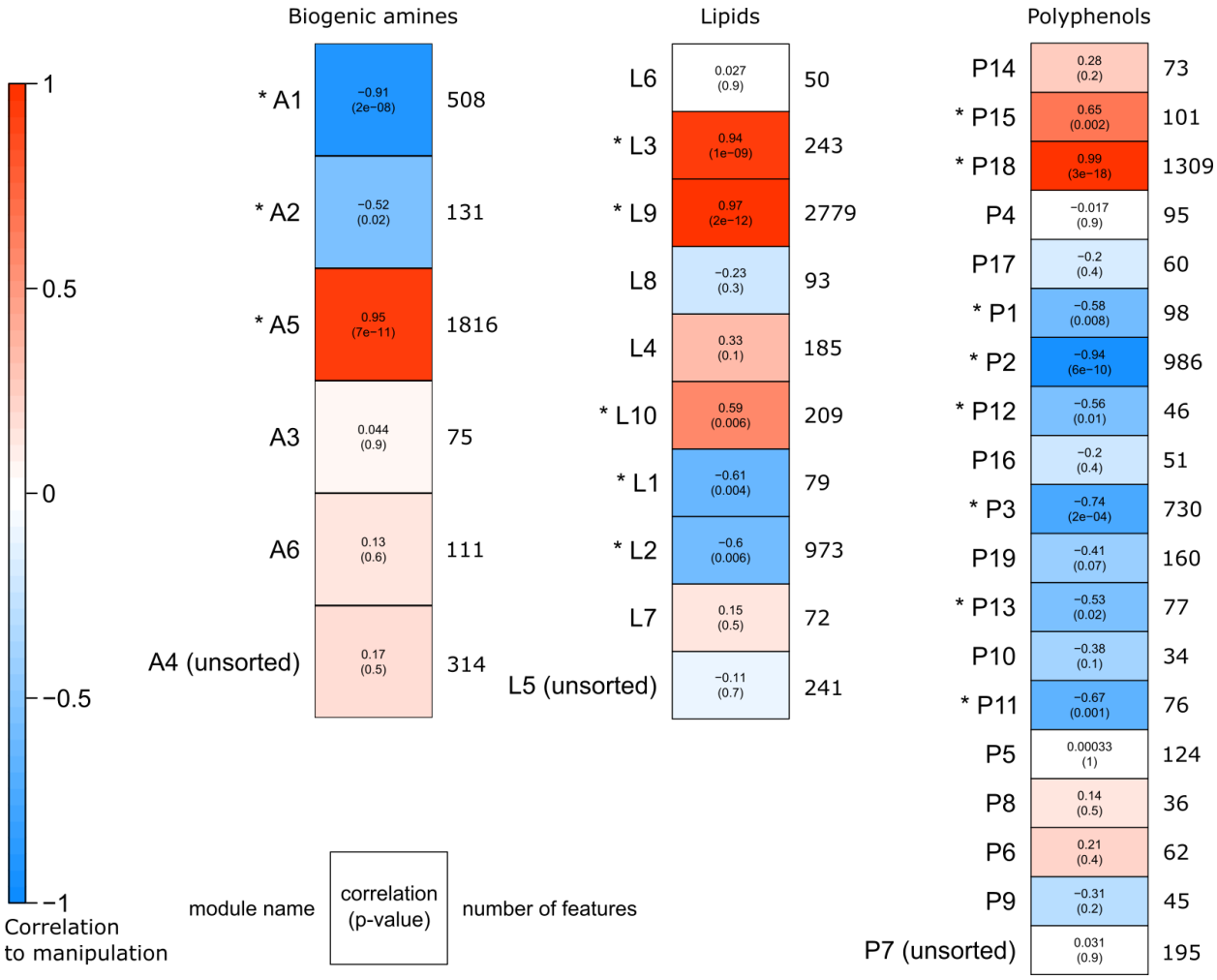

Figure 17. WGCNA network modules of metabolite features and their correlation to manipulation.
In total we detected three, five, and eight significantly correlated (Student correlation $p \leq 0.05$, denoted with *) network modules to manipulation in the biogenic amines, lipids, and polyphenol datasets, respectively. Network modules were constructed as unsigned, meaning the direction of the correlation describes the network as a whole, although some features may be anti-correlated within the module. “Unsorted” modules contain all features that were not successfully correlated to other features in a network.

data, we were not able to consistently compare hub features. As such, we considered all available annotations within a network module and Mummichog pathway enrichments. Across all network modules significantly correlated to the transition from healthy to manipulated ants, 46 unique KEGG pathways were enriched, which included the eight found across the study-wide data passing at least two selection filters (Table 6, File S7).

Among the enzyme homologs used to select pathway enrichments, most ant and fungal DEGs were downregulated from the healthy ants to manipulation (ant: 142 of 157, 90%, fungus: 166 of 268, 62%). In both cases, these numbers of downregulated DEGs were much greater than the transcriptome-wide DEG ratios during manipulation for ant (72% downregulated) and fungus (41% downregulated) (binomial exact test, p = 2E-8 and 6E-12, respectively). The metabolic pathway DEG estimates are based on a coarse analysis using homology to a constrained subset of well-annotated fly and yeast enzymes listed in KEGG; however, this sample of genes could plausibly be a proxy for broader patterns among metabolism-related DEGs. In *Camponotus* hosts, the significant and severe downregulation of genes related to these metabolic pathways may indicate a general slowing of metabolism in a weakened host, terminally infected and manipulated in the last hours of life. The smaller number of upregulated DEGs might therefore contain some of the most informative signals, as their activity goes against the general trend. In the fungal parasite, the significant reduction of gene expression of these pathways could more plausibly reflect a state of *O. camponoti-floridani* metabolism tuned to late infection and manipulation processes. By the time of manipulation, the fungus has been engaged with host immunity and modulation of behavior and has access to host metabolites to scavenge. Genes related to those functions may be upregulated while genes related to non-critical metabolic pathways may be downregulated. Furthermore, many fungal proteins important for manipulation may not be enzymes involved in major metabolic pathways, but rather are extracellular effectors (e.g., involved in protein-protein interactions), post-translational regulators, and others.

The biogenic monoamine neurotransmitters dopamine, serotonin, and octopamine are known to modulate ant activity and may be proximate drivers of diseased behaviors: A combination of pathway enrichments, annotated DAMs, and DEGs suggest that shifts in metabolism associated with neurotransmitters relate to behavioral alterations in *C. floridanus* infected and manipulated by *O. camponoti-floridani*. The monoamine neurotransmitters dopamine, serotonin, and octopamine (analogous to vertebrate norepinephrine) have been implicated in modulating locomotor, foraging, learning, social, reproductive, and aggressive behaviors in many insects, and have been tested in social insects, including ants (Adamo 2008; Aonuma and Watanabe 2012; Adamo *et al.* 2013; Kamhi *et al.* 2017; Verlinden 2018). Serotonin, octopamine, and melanin derived from L-DOPA (or tyrosine and dopamine) have roles in insect immunity as well (Geun *et al.* 2009; González-Santoyo and Córdoba-Aguilar 2012). Administration of dopamine and serotonin to *Formica polyctena* wood ants have produced altered behaviors in the laboratory, such as aggressive mandible-opening and biting behaviors (Szczuka *et al.* 2013). In the field, *Pogonomyrmex barbatus* harvester ant dopamine levels positively correlated with foraging trips, as seen both by dopamine supplementation and inhibition (Friedman *et al.* 2018). Similarly, pharmacological depletion of serotonin led to reduced and impaired trail-following foraging behavior in *Pheidole dentata* ants (Muscedere *et al.* 2012). Although clear signs of increased aggression with octopamine treatment was not found in *F. polyctena* (Szczuka *et al.* 2013), in another species, *Formica aquilonia*, there is evidence for octopamine increasing aggressive behaviors (Yakovlev 2018). Octopamine additionally appears to modulate the social behavior of trophallaxis in *Camponotus fellah*, while serotonin had no significant effect (Boulay *et al.* 2000). As such, the exact effects of these neurotransmitters can differ by species and social or physiological context. However, many of these observed behaviors exhibited with higher neurotransmitter levels are relatable to the disease phenotypes observed in *Ophicordyceps* infected ants. Observations of *Ophiocordyceps*-infected ants include changes in behavior leading to increased walking, deviation from foraging trails, and reduced nestmate

communication (Pontoppidan *et al.* 2009; Andersen *et al.* 2009; Hughes *et al.* 2011; de Bekker *et al.* 2015; Trinh *et al.* 2021). Furthermore, WGCNA modules of gene expression negatively correlated between the ant and fungus were enriched for host neuronal function and parasite manipulation-associated secreted proteins. This correlation suggested parasite effectors promote the downregulation of host gene modules related to neuronal maintenance, circadian rhythm, olfaction, and memory (Will *et al.* 2020). We also reported many predicted protein-protein interactions involving secreted fungal proteins and host receptors for dopamine, serotonin, and octopamine that overlap with proteins in those WGCNA gene modules (Chapter 3). Although we did not identify dopamine, serotonin, or octopamine in our metabolomic data, we did measure features annotated as biosynthetically related compounds.

Changes in dopamine metabolism possibly modified ant behaviors and shifted host-pathogen immunological interactions during manipulation. A combination of metabolomic and transcriptomic data indirectly suggest increased dopamine metabolism in manipulated ants. The metabolomic signals consisted of changes in neurotransmitter precursor abundances and enrichment of pathways in metabolite network modules correlated to manipulation. Phenylalanine and tyrosine are precursors in synthesis pathways for dopamine and octopamine. KEGG pathway "phenylalanine metabolism" was enriched in both network modules A1 and P2 ($p = 0.026$ and 0.028, fold-enrichment = 1.5 and 1.9, respectively), both of which were negatively correlated to manipulated ant samples. Additionally, KEGG pathway "tyrosine metabolism" was enriched in modules P2 and P3 ($p = 0.030$ and 0.024, fold-enrichment = 1.4 and 1.6, respectively), both also negatively correlated to manipulation. Moreover, module P2 also contained the most informative compound annotations regarding dopamine metabolism.

The immediate precursor to dopamine, L-3,4-dihydroxyphenylalanine (L-DOPA), was 2.8-fold reduced in abundance in manipulated ants ($p = 0.008$, and in the top-50% of PC1) (Fig. 18). L-tyrosine was also annotated in this module and is the precursor to L-DOPA and tyramine. The latter can be converted into the neurotransmitter octopamine. L-Tyrosine was a DAM with a 2.1-fold decrease in

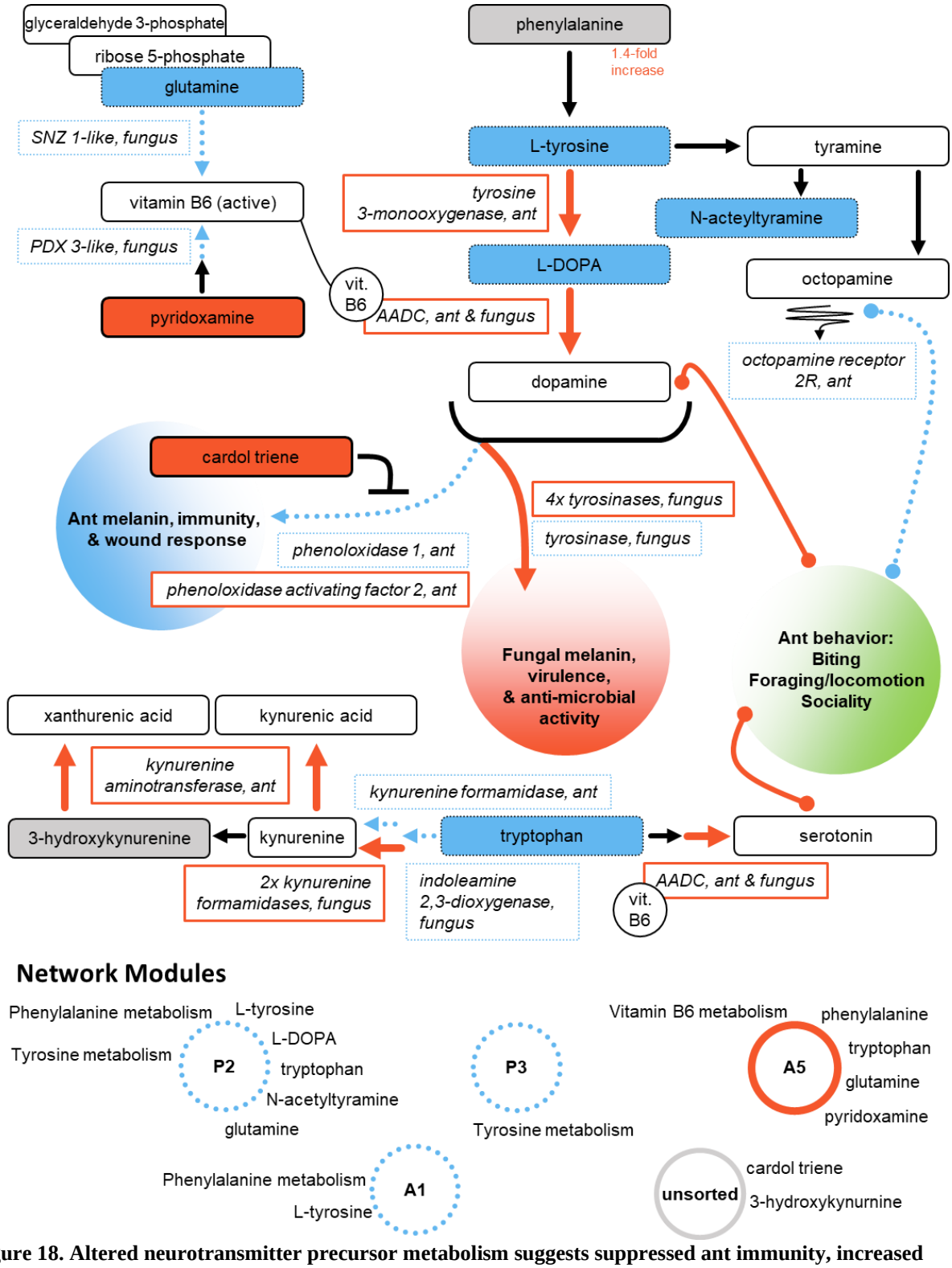

Figure 18. Altered neurotransmitter precursor metabolism suggests suppressed ant immunity, increased dopamine and serotonin, and reduced octopamine during infection and manipulation.

Cardol triene may produced by the fungus to suppress ant immunity and thereby also increase availability of tyrosine and L-DOPA for dopamine synthesis. L-amino acid decarboxylase (AADC) catalyzes the final step of dopamine and serotonin synthesis and is upregulated by manipulated ants. A reduction of L-DOPA and tryptophan suggest that these compounds are being converted into dopamine and serotonin, respectively. The activity of AADC may also be modulated by altered vitamin B6 levels. Upregulation of an ant kynurenine aminotransferase possibly increases or maintains (if the kynurenine precursor is reduced) kynurenic acid levels. The possible of reduction of octopamine concentration follows the reasoning that it requires L-tyrosine for its synthesis, which is reduced during manipulation, and there is no compensatory upregulation of enzyme genes in the octopamine pathway to compete with upregulated dopamine biosynthesis. Dysregulated ant behavior during infection and manipulation may arise due to this altered neurotransmitter metabolism. Network modules from which discussed feature annotations or enriched pathways reside are given at the bottom of the figure. Increases are indicated by solid lines and red color, decreases by dotted lines and blue color, metabolites are in rounded rectangles, genes are in rectangles, annotated metabolites that were not DAMs have gray color, compounds with white color were not identified in the LC-MS/MS data, and hypothesized functional links are given in the shaded circles. Metabolic steps that did not have DEG are shown as black arrows when useful for context but are omitted elsewhere. A squiggled arrow indicates metabolite interaction with a receptor.

abundance ($p = 1E-4$, and Boruta confirmed). An annotation for tyrosine was also present in the network module A1, however, we did not identify this metabolite feature as a DAM ($p = 0.154$, 1.2-fold reduction). Outside of network modules A1, P2, and P3, we also detected phenylalanine, the precursor to tyrosine. Phenylalanine showed a modest increase in abundance during manipulation just below our 1.5-fold change threshold for classification as DAM ($p = 0.019$, 1.4-fold increase) (Fig. 18). Decreases in L-tyrosine and L-DOPA could be difficult to interpret alone, however in combination with RNAseq data, we found evidence for increased dopamine synthesis that can explain the depletion of these dopamine precursors.

During manipulation, both ant hosts and fungal parasites upregulated an aromatic L-amino acid decarboxylase (AADC) gene (Fig. 18). This enzyme catalyzes the final step of L-DOPA conversion to dopamine and the conversion of L-5-hydroxytryptophan to serotonin (Dakshinamurti *et al.* 2017). A tyrosine 3-monooxygenase, which catalyzes the rate-limiting conversion of L-tyrosine to L-DOPA, was

upregulated by manipulated ants. The ant homolog to Henna (i.e., DTPHu phenylalanine 4-monooxygenase), which converts phenylalanine to L-tyrosine and, primarily in the periphery, tryptophan to the serotonin precursor in *D. melanogaster*, was not differentially expressed (Neckameyer and White 1992; Coleman and Neckameyer 2005; Neckameyer *et al.* 2007). This consistent expression may help explain the modest accumulation of phenylalanine during manipulation while its derivatives were found at lower concentrations.

Additionally, this phenylalanine feature resided in module A5, which was positively correlated to manipulation and was enriched for the pathway "vitamin B6 metabolism" ($p = 0.026$, fold-enrichment = 1.5) that could indicate changing AADC enzymatic activity (Fig. 18, upper left). One of the many functions of vitamin B6 is as a co-factor for AADC and therefore it may participate in the modulation of dopamine and serotonin production. Largely, insects cannot synthesize active vitamin B6 *de novo* but rather metabolize B6 vitamers obtained by diet and symbiotic microbes to meet their vitamin B6 demands (Michalkova *et al.* 2014; Douglas 2017). In addition to the overall enrichment of the vitamin B6 pathway, network module A5 had two compound annotations that further specifically suggest changes in vitamin B6 metabolism. Pyridoxamine is a vitamer form of vitamin B6 and was annotated in network module A5 as an increased DAM ($p = 4E-7$, 3.5-fold increase, passing all selection criteria) (Fig. 18). Pyridoxamine is not the active B6 vitamer used as a co-factor for AADC, but is converted to the active pyridoxal 5'-phosphate vitamer by two additional enzymatic steps (Dakshinamurti *et al.* 2017). Negatively correlated to pyridoxamine in network module A5, glutamine, one of three substrate molecules needed for the fungus to form active vitamin B6 *de novo* (Raschle *et al.* 2007), was reduced during manipulation ($p = 7E-6$, 3.3-fold decrease, passing all feature selection criteria). Similarly, L-glutamine was also detected in network module P2 as a DAM reduced in abundance ($p = 8E-10$, 3.9-fold decrease, passing all feature selection criteria) (Fig. 18). In *O. camponoti-floridani*, putative homologs to yeast SNZ-1 (synthase domain) and SNO-1 (glutaminase domain) genes, which encode proteins that come together to catalyze

de novo synthesis of active vitamin B6 (Rodríguez-Navarro *et al.* 2002), showed mixed DEG profiles during manipulation. The SNZ-1-like gene was upregulated while the SNO-1-like gene did not significantly change in expression (Fig. 18). If vitamin B6 synthesis was reduced in the fungus, one might predict that glutamine levels would increase, which we did not find. This reduction of glutamine could be related to other biological processes, such as glutamate metabolism (see below). Consistent with insects lacking a *de novo* pathway (Douglas 2017), no homologs to these genes were found in the ant genome, nor were any *D. melanogaster* representatives of this enzyme group listed in the KEGG database. In *O. camponoti-floridani*, a putative homolog of the yeast PDX3 gene (a pyridoxamine 5'-phosphate oxidase) that converts a pyridoxamine 5'-phosphate intermediate to active vitamin B6 was also downregulated during manipulation (Fig. 18). Taken together, the fungus may be scavenging host vitamin B6 and reducing its own synthesis of active vitamin B6 as evidenced by downregulated SNZ-1 and PDX3-like genes and an accumulation of the precursor vitamer pyridoxamine. Possibly, the accumulating pyridoxamine is available to the ant host, and her sustained expression of a pyridoxamine 5'-phosphate oxidase homolog (not a DEG, albeit with a 1.4-fold increase) continues to produce active vitamin B6. Speculatively, if substrate availability limited ant synthesis of active vitamin B6, the availability of pyridoxamine could even lead to elevated vitamin B6 levels. In scenarios where active vitamin B6 is more abundant in ant tissues, it may be working in concert with elevated AADC to substantially increase dopamine production. Alternatively, if vitamin B6 is scarce, upregulated AADC could represent a homeostatic response to insufficient dopamine production, at least in part (Fig. 18).

Dopamine and its precursors can also be converted into melanin, a key compound for insect wound response and immunity (González-Santoyo and Córdoba-Aguilar 2012; Sugumaran and Barek 2016; Wang *et al.* 2017). Fungi can also synthesize melanin for use in host-pathogen interactions and against competing microbes (Nosanchuk and Casadevall 2006; Nosanchuk *et al.* 2015). We found evidence that this pathway for melanin production is reduced in the ant during manipulation and,

possibly, increased in the fungus (Fig. 18). The production of a fungal-derived compound may inhibit tyrosinases necessary to convert dopamine-pathway metabolites to melanin and hence simultaneously steer these metabolites toward dopamine production. This metabolite feature was annotated as cardol triene (i.e., 5-(8,11,14-pentadecatrienyl)resorcinol) and was a DAM only detected in manipulated ant samples ($p = 0.0037$, median peak value = 28,520, detected in 6 of 10 manipulation samples, in the top 50% of PC1) (Fig. 18). As cardol triene was never detected in healthy ants, it plausibly is produced solely by the fungus, although we cannot discount the possibility that production of this metabolite is produced by ants facing infection and completely absent in healthy individuals. Detecting this feature in only 60% of manipulation samples could indicate that carol triene levels are tightly regulated. Cardol triene has been shown to inhibit tyrosinase oxidation of L-DOPA (Zhuang *et al.* 2010). In insects, phenoloxidases are a type of tyrosinase and are key enzymes that begin the conversion of dopamine and L-DOPA to pro-immune melanin production pathways (Gorman and Arakane 2010; González-Santoyo and Córdoba-Aguilar 2012; Wang *et al.* 2017). In addition to possible chemical inhibition of phenoloxidase activity by fungal cardol triene, the ant showed mixed gene expression signals plausibly consistent with a faltering melanin-immune response. A homolog to phenoloxidase-1 was downregulated in the manipulated ant, which could lead to a reduction in melanin production for immunity (Fig. 18). A gene annotated as phenoloxidase activating factor-2 was upregulated in manipulated ants, possibly as an attempt to increase phenoloxidase activity and bolster the suppressed immune response (Piao *et al.* 2005). Entomopathogen infections suppress phenoloxidase activity in mosquitoes and the inhibition of protein processing of inactive pro-phenoloxidase to active phenoloxidase by oosporein has been hypothesized as a mechanism of fungal interference with insect host immunity (Feng *et al.* 2015; Ramirez *et al.* 2018). In addition to suppressing host melanin production, the fungus may be converting L-DOPA or related compounds into fungal melanin precursors, as four upregulated and one downregulated putative tyrosinases were found during manipulation (Fig. 18). Three of the upregulated fungal tyrosinases are putatively secreted and

may possibly interact with host tyrosine and its derivatives. One appears to even be targeted by ant protein-degradation pathways (Chapter 3). The sum result of this proposed redirection of dopamine precursors could weaken host immunity, bolster parasite pathogenicity, and drive altered host behavior by increased dopamine concentration (Fig. 18).

Altered serotonin biosynthesis during manipulation could be linked to manipulated behaviors. In consideration of the proposed changes in dopamine metabolism, which is linked to serotonin biosynthesis by the shared upregulated AADC enzyme (Fig. 18), we additionally searched our datasets for signals tied to serotonin metabolism. In polyphenol network module P2, which contained L-tyrosine, L-DOPA, and the tyrosine and phenylalanine metabolism pathway enrichments discussed above, we detected a tryptophan signal that was 2.2-fold reduced (not a DAM with $p = 0.283$, selected by Boruta) (Fig. 18). Tryptophan was also detected in network module A5, which carried the phenylalanine feature annotation and pathway enrichment of vitamin B6 metabolism. This measurement of tryptophan from the biogenic amine dataset also did not qualify as a DAM, however it showed a possible marginal increase, rather than decrease, in abundance ($p = 0.208$, 1.3-fold increase). Given that neither tryptophan signal was a DAM and their fold-changes trend in opposite directions, we cannot offer a concrete conclusion on the relative abundance of tryptophan during manipulation. However, given that reduced tryptophan feature was selected by the Boruta analysis, the upregulation of AADC, and the plausible behavioral link to changing serotonin levels during infection, we propose here a hypothetical scenario interpreting the tryptophan signals as a putative decrease in abundance (Fig. 18). Depletion of tryptophan with the simultaneous upregulation of ant AADC suggests increased serotonin production. Furthermore, a stably abundant feature annotated as 3-hydroxykynuerine (a tryptophan derived compound) could indicate that the reduction of tryptophan does not reflect widespread increasing metabolism in a competing non-serotonergic pathway. We detected two features annotated as 3-hydroxykynuerine that were not DAMs nor correlated with other features in network modules. Although, tryptophan can be metabolized into

many possible compounds, upwards of 95% of tryptophan is metabolized in the kynurenine degradation pathway in mammals, which can have immune- and neuromodulatory effects (Rossi *et al.* 2019; Platten *et al.* 2019). Further supporting that there was no overall increase of kynurenine pathway metabolism, expression of the rate-limiting enzyme to enter this direction of tryptophan metabolism is constant in the ant and downregulated in the fungus (indoleamine 2,3-dioxygenase in the fungus). Genes for kynurenine 3-monooxygenase that catalyzes the production of 3-hydroxykynuerine were also not DEGs in either organism (Fig. 18). However, we did find two upregulated genes encoding enzymes involved in kynurenine and kynurenic acid synthesis. The host upregulated a putative kynurenine/alpha-aminoadipate aminotransferase that catalyzes synthesis of kynurenic acid and xanthurenic acid. Kynurenic acid particularly can have neuroprotectant effects, but has also been associated to neurological disease (Yu *et al.* 2004b, 2006; Han *et al.* 2008; Colín-González *et al.* 2013; Rossi *et al.* 2019). Additionally, *Ophiocordyceps* upregulated two kynurenine formamidases, the much more highly expressed of which we predicted to be secreted. The fungus may be using this enzyme exported to the host environment to promote synthesis of kynurenine, the precursor for kynurenine aminotransferase mediated synthesis of kynurenic acid. In contrast, *Camponotus* downregulated a kynurenine formamidase homolog. Taken together, we infer that reduced tryptophan abundance represents a metabolic shift towards serotonin synthesis rather than broadly upregulating the alternative pathway of kynurenine metabolism; but certain key elements of the kynurenine pathway may become more active during manipulation without drawing more heavily on available tryptophan (Fig. 18).

Mixed signals in octopamine metabolism and reception indicated a possible reduction of octopamine during manipulation. With data supporting changing dopamine and serotonin metabolism, we also investigated octopamine metabolism, which shares a common precursor with dopamine through L-tyrosine. In addition to the proposed L-tyrosine depletion feeding into dopamine synthesis, L-tyrosine can also be converted to tyramine – the precursor to octopamine. However, unchanging gene expression in the

ant for tyrosine decarboxylase indicates this was not happening at an accelerated pace (Fig. 18). Perhaps, given the upregulation of the rate-limiting tyrosine 3-monooxygenase that converts L-tyrosine to L-DOPA, the tyramine and octopamine pathway was being outcompeted for L-tyrosine substrate. In line with this scenario, we did observe reduction of N-acetyltyramine, a product synthesized from tyramine (Fig. 18). Arylalkylamine N-acetyltransferases, and specifically in *D. melanogaster*, dopamine N-acetyltransferase converts tyramine, dopamine, and serotonin to N-acetylated forms, generally along melanin pathways related to immunity, cuticle sclerotization, or melatonin (Hintermann *et al.* 1995; Dempsey *et al.* 2014, 2015; Wu *et al.* 2020). The putative ant homolog to dopamine N-acetyltransferase was not a DEG, further suggesting that tyramine nor these other neurotransmitters were converted to non-neurotransmitter acetylated forms more than in healthy individuals. Given that levels of N-acetyltyramine were reduced but the enzyme for this conversion did not change in expression suggested that either tyramine was being depleted for reasons other than N-acetyltyramine synthesis, or, N-acetlyyramine was being consumed at an accelerated pace. As the gene for conversion of tyramine to octopamine was not differentially expressed in the ant, it appears plausible that levels of octopamine would have also decreased if the availability of tyramine was reduced (Fig. 18). However, the ant significantly downregulated a gene putatively encoding octopamine receptor 2, which could be more reflective of a homeostatic response to accumulating octopamine levels (Fig. 18). In consideration of the reduced L-tyrosine and N-acetyltyramine levels, with upregulated tyrosine 3-monooxygenase, we propose a reduction in octopamine as the more likely scenario.

Glutamate and GABA in the context of ant neuromodulation and fungal growth metabolism: In insects and other animals, glutamate and GABA are well documented neuromodulators with notable roles at the insect neuromuscular junction, among their other metabolic functions (Johansen *et al.* 1989; Krnjević 2010; Pflüger and Duch 2011; Wolstenholme 2012; Tiwari *et al.* 2013; Rashmi *et al.* 2018). In *C. floridanus*, multiple genes putatively encoding receptors containing domains associated with

GABA or glutamate response were negatively correlated to manipulation by a two WGCNA gene modules (Will *et al.* 2020). Additionally, a putative biosynthetic gene cluster for an aflatrem-like compound in *O. camponoti-floridani* displayed a strong upregulation during manipulation of host ants (Will *et al.* 2020). Aflatrem has been shown to cause tremors, confusion, and changes in activity levels in mammals by mechanisms including disruption of GABAergic and glutamatergic neuronal activity (Valdes *et al.* 1985; Gant *et al.* 1987; Yao *et al.* 1989; Knaus *et al.* 1994). However, these possible disruptions of ant neuronal function, do not appear to be clearly tied with dramatic changes in compound abundances or metabolic enzymes. Glutamic acid (the conjugate acid of glutamate) did not qualify as a DAM, although it displayed marginal reduction in concentration short of our 1.5-fold change threshold ($p = 0.007$, 1.4-fold decrease) (Fig. 19). This glutamate feature was grouped in network module A5, which included a pathway enrichment for the "citrate cycle" ($p = 0.051$, fold-enrichment = 1.4), to which glutamate and GABA metabolism is associated with by succinate and α-ketoglutaric acid (Watford 2008; Michaeli and Fromm 2015; Rashmi *et al.* 2018). We detected an increase of succinate ($p = 0.002$, 2.1-fold increase) (Fig. 19). Within network module A5, there were multiple reduced DAMs with biosynthetic connections to glutamate: glutamine ($p = 1.8E-6$ and 6.2E-11, 3.3- and 3.8-fold decrease, in network module A5 and also P2, respectively), proline ($p = 0.001$, 1.9-fold decrease), ornithine ($p = 3.1E-5$, 2.2-fold decrease), putrescine ($p = 0.001$, 1.9-fold decrease), and N-acetylglutamic acid ($p = 0.022$ and 7.3E-6, 2.0- and 1.8-fold decrease, in network modules A5 and also P18, respectively).

Cytidine has been associated with reduced glutamate and glutamine with anti-depressive neurological effects in certain contexts (Yoon *et al.* 2009). Cytidine was an increased DAM during manipulation that was only detected reliably in manipulated ant samples ($p = 7.4E-8$, 19.8-fold increase, passing all selection criteria). To what degree this elevated cytidine content is available to host cells or is an aspect of the proliferating fungal cell population (e.g., nucleic acid metabolism) is unclear. Cytidine can also be interconverted with uridine, an increased DAM in manipulated ants ($p = 3.0E-7$, 5.4-fold

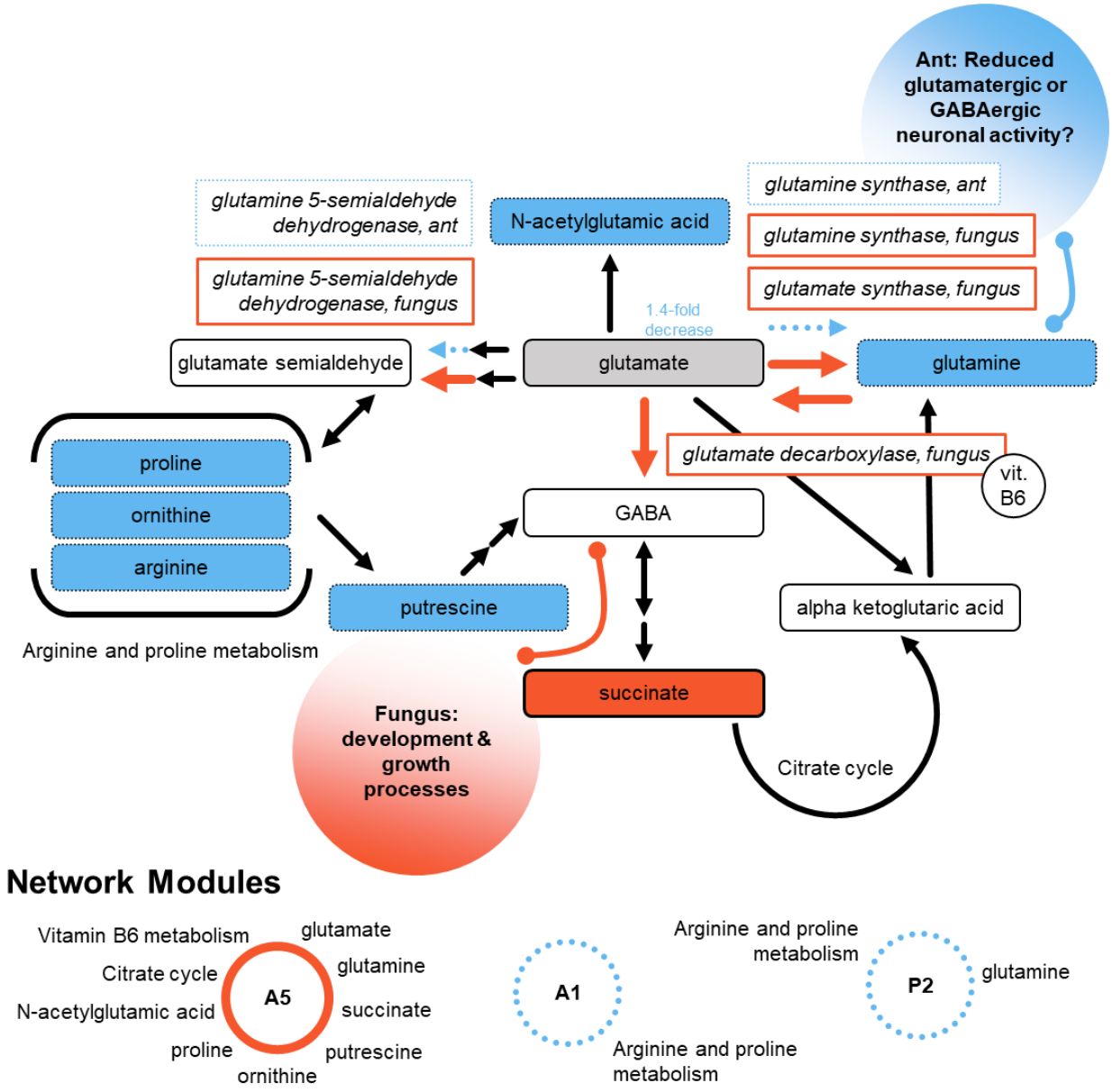

Figure 19. Changes in glutamate and GABA metabolism suggest increased GABA biosynthesis in the fungus that may be used for growth and development metabolism; while a wide-spread reduction of these compounds in the manipulated ant could relate to neuronal and behavioral activity.

Network modules from which discussed feature annotations or enriched pathways reside are given at the bottom of the figure. Increases are indicated by solid lines and red color, decreases by dotted lines and blue color, metabolites are in rounded rectangles, genes are in rectangles, annotated metabolites that were not DAMs have gray color, compounds with white color were not identified in the LC-MS/MS data, and hypothesized functional links are given in the shaded circles. Metabolic steps that did not have DEG are shown as black arrows when useful for context but are omitted elsewhere.

increase, passing all selection criteria), which in combination with choline has shown some neuroprotective effects, likely related to phosphatidylcholine synthesis (Baumel *et al.* 2021).

Furthermore, in *Camponotus*, a putative glutamine synthase (converting glutamate to glutamine) was a downregulated DEG during manipulation. Ant glutamate synthase (reversely converting glutamine to glutamate) and a glutamate decarboxylase (converting glutamate to GABA) were not DEGs but had marginal 1.5-fold reductions. Glutamate decarboxylase is also an enzyme requiring vitamin B6 as a co-factor (Strausbach and Fischer 1970; Huang *et al.* 2016). Ant enzymes associated with the GABA shunt pathway to convert GABA to citrate cycle derivatives (e.g. succinate) were also not DEGs, but had marginal ca. 1.6-fold decreases in expression (Carillo 2018). Possibly altering glutamate metabolism in the host, we predicted an undescribed secreted fungal protein to bind a host enzyme that converts glutamate semialdehyde to glutamate (Chapter 3). Glutamate semialdehyde can also be interconverted to compounds that have become scarcer during manipulation – proline, ornithine, and putrescine (Fig. 19). Network modules A1 and P2 were enriched for the "arginine and proline metabolism" pathway related to these compounds. We additionally predicted three highly promiscuous undescribed fungal proteins to interact with host glutamate receptors, among their many other predicted interactions (Chapter 3). How or if these protein interactions shape manipulation processes will remain unclear until the fungal protein functions can be identified. Taken together, in the ant, there appears to be a general holding or slight reduction in biosynthetic activity and compound abundances related to glutamate and GABA, with possible fungal interference (Fig. 19). Although, this could have physiological, neuronal, and behavioral repercussions in the ant – the metabolomic signals may be at least as indicative, if not more so, of fungal metabolism once put into the context of gene expression data.

In the fungal transcriptome, multiple putative genes for glutamate-related enzymes were DEGs during manipulation. Among these genes, a putative glutamate decarboxylase, which converts glutamate to GABA, was upregulated. Additionally, both a glutamine synthase and a glutamate synthase were

upregulated, suggesting heightened metabolic activity interconverting glutamate and glutamine (Fig. 19). Given the reduced levels of glutamine, the mostly consistent levels of glutamate, upregulation of the putative fungal glutamate decarboxylase, and increase of succinate – the fungus appears to be increasing GABA production by converting glutamine to glutamate to GABA, which may in turn to be converted to succinate (Fig. 19). Broadly, GABA can be used by various fungi in nitrogen metabolism, conidiation, and development processes (Kumar and Punekar 1997). For example, in *Trichoderma atroviride*, GABA and glutamate decarboxylase appear to be important players in normal fungal growth. Deletion of glutamate decarboxylase and reduction of GABA decreased the growth and germination rates and produced atypical highly-branched hyphal morphologies (Nižňanský *et al.* 2013). As *O. camponoti-floridani* proliferates in the terminally manipulated host, soon needing to rapidly colonize the host cadaver in a hyphal growth stage, GABA-dependent growth processes may be already upregulated at the time of manipulation, a few hours before host death. The fungus may also be using an upregulated putative glutamine 5-semialdehyde dehydrogenase that catalyzes one of two steps to convert glutamate into glutamate semialdehyde, which in turn can be used to synthesize amino acids that were reduced in manipulated ants (Fig. 19). Meanwhile, the ant downregulated a homolog to this gene.

Altered glycerophospholipid metabolism suggested increased fungal cell membrane activity and ant accumulation of the excitatory neurotransmitter, acetylcholine: The KEGG pathway "glycerophospholipid metabolism" was enriched in module P2 and in study-wide features passing at least two selection filters ($p = 0.024$ and 0.030, fold-enrichment = 1.9 and 1.4, respectively). We found evidence for two possible major effects, changes in cell membrane composition and the accumulation of acetylcholine. Of our annotated features, metabolic signals centered on choline offered the most insight into altered glycerophospholipid metabolism. Glycerophospholipids and choline-containing compounds have been associated with neurodegenerative disease, such as Alzheimer's or Parkinson's, and insect host-pathogen responses (Walter *et al.* 2004; Hoxmeier *et al.* 2015; Alecu and Bennett 2019). Choline is a

key component involved in the synthesis of phospholipids associated with forming cell membranes, especially as incorporated through phosphatidylcholine (Li and Vance 2008). Although, in fungi and insects, phosphatidylethanolamine is also a major cell membrane component (Batrakov *et al.* 2001; Dawaliby *et al.* 2016; Cassilly and Reynolds 2018). Using the lipids dataset we compared peak values of phosphatidylethanolamines (n = 95 features) and phosphatidylcholines (n = 85 features) and found phosphatidylethanolamines to indeed be abundant in our insect and fungal tissue samples. Within healthy sham ants, phosphatidylethanolamines were significantly more abundant than phosphatidylcholines, but only slightly, at 1.10-fold higher (t-test, p = 0.017, t = -2.657). Within manipulated ants, there was no significant difference (t-test, p = 0.739, t = -0.339, phosphatidylethanolamines 1.05-fold higher). As both phospholipid types were nearly equally abundant, we considered changes of specific metabolite features of either class could reflect important processes during manipulation.

Choline was a DAM increasing during manipulation (p = 1.7E-11, 20.0-fold increase, passing all selection criteria) (Fig. 20). We also observed other DAMs related to choline within the glycerophospholipid metabolism pathway. Glycerophosphocholine, a choline precursor was increased at manipulation and detected in two datasets (p = 3.4E-11 and 1.2E-7, 5.9- and 7.7-fold increase, passing all three selection criteria). We also detected two DAMs interconnected between choline and phosphatidylethanolamine: ethanolamine (p = 5.2E-5, 2.1-fold increase, also Boruta confirmed) and ethanolamine phosphate (p =1.6E-9, 5.5-fold decrease, passing all selection criteria) (Fig. 20). Three putative *Ophiocordyceps* phospholipase C genes were DEGs, two upregulated and one downregulated (Fig. 20). Broadly, phospholipid C proteins cleave phospholipids and have been implicated in cell signaling, pathogenicity, and cell membrane metabolism (Pokotylo *et al.* 2013). When cleaving either phosphatidylcholine or phosphatidylethanolamine they can produce an intermediate 1,2-diacyl-sn-glycerol product. Additionally, the fungus expressed a putative diacylglycerol cholinephosphotransferase

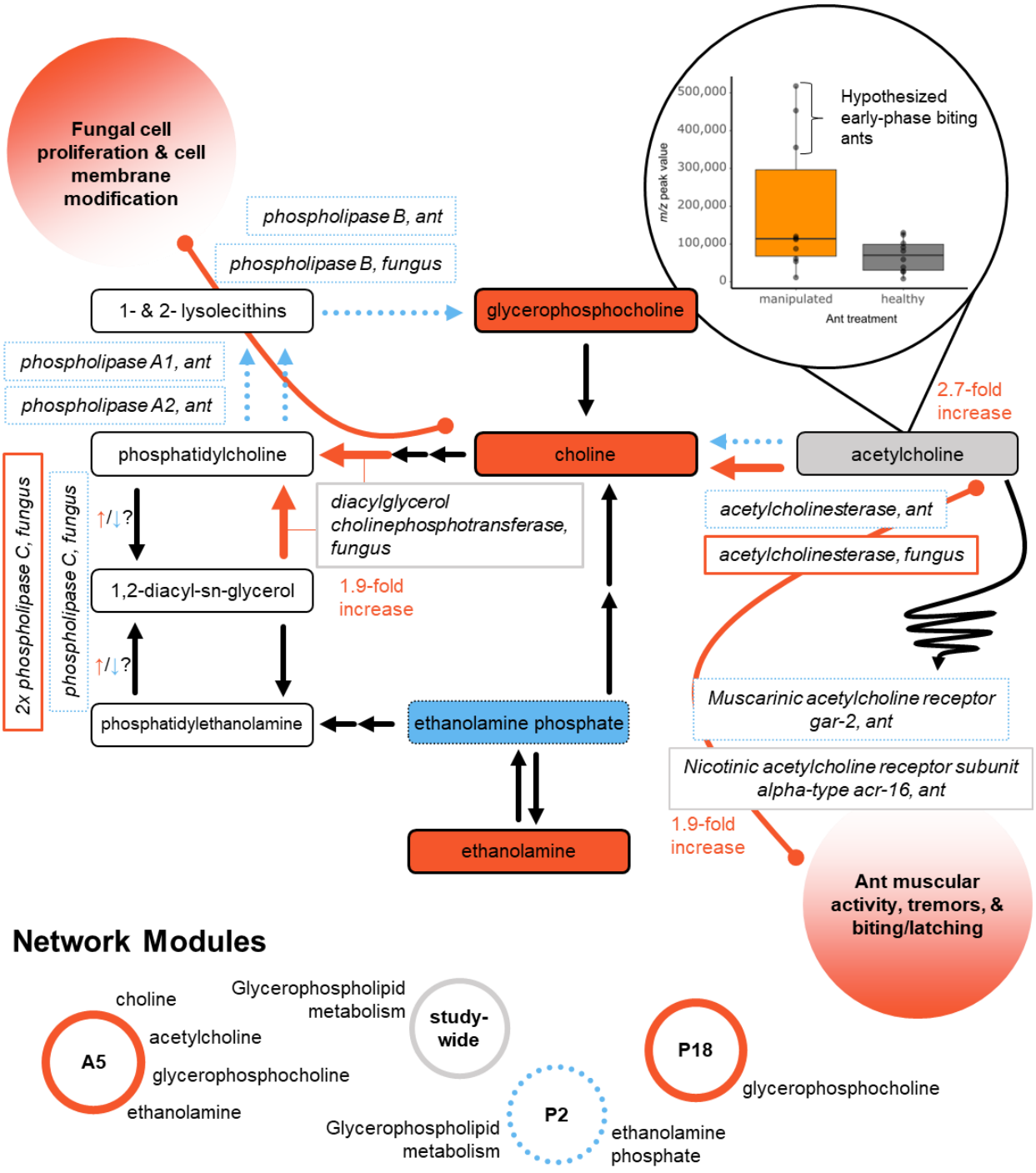

Figure 20. Changing glycerophospholipid metabolism during manipulation primarily indicate altered acetylcholine levels in the ant and cell membrane metabolism in the fungus.

Manipulated ant samples appeared to have two distinct groups, one with high acetylcholine and one with levels similar to healthy ants. In manipulated ants, the putative acetylcholinesterase and two acetylcholine receptor genes

were downregulated, suggesting acetylcholine levels were accumulating. We hypothesize that increased acetylcholine in manipulated ants is associated with the increased muscular activity during early manipulation (e.g., tremors, biting, and latching behavior). Once the ant is secured in a summited position and the mandible muscles (and associated neurons) are further degraded, the fungus may be scavenging and converting the available acetylcholine to choline, thereby rapidly reducing acetylcholine levels. The fungus may be converting choline to phospholipids, such as phosphatidylcholine to remodel and build cell membranes. Network modules from which discussed feature annotations or enriched pathways reside are given at the bottom of the figure. Increases are indicated by solid lines and red color, decreases by dotted lines and blue color, metabolites are in rounded rectangles, genes are in rectangles, annotated metabolites or genes that were not DAMs or DEGs have gray color, compounds with white color were not identified in the LC-MS/MS data, and hypothesized functional links are given in the shaded circles. Metabolic steps that did not have DEG are shown as black arrows when useful for context but are omitted elsewhere. A squiggled arrow indicates metabolite interaction with a receptor.

gene 1.9-fold higher during manipulation, nearly qualifying as a DEG. This enzyme combines 1,2-diacyl-sn-glycerol and CDP-choline to produce phosphatidylcholine. Phosphatidylcholine could then be converted to glycerophosphocholine within two metabolic steps, but this pathway appeared to be downregulated. Three genes putatively encoding the enzymes driving this conversion were downregulated in the ant (phospholipases A1, A2, and B). In the fungus, a phospholipase B-like gene was also downregulated (Fig. 20). The net effect appears to be catabolism of phosphatidylethanolamines and synthesis of phosphatidylcholines leading to a minor compositional shift overall- but perhaps including specific and important changes we cannot yet identify (Fig. 20).

Choline can also be metabolized into acetylcholine, the most abundant excitatory neurotransmitter in insects (Gauthier 2010). In bees, excessive activation of acetylcholine receptors can cause changes in locomotor, navigational, foraging, and social behaviors (Grünewald and Siefert 2019). We propose a scenario of increased acetylcholine in the manipulated ant during the initial stages of summiting and biting – while the ant is highly active. Shortly thereafter, once the ant has been locked into position and its mandibular muscles further degraded, fungal scavenging and metabolism of acetylcholine may outpace ant production of acetylcholine and lead to globally reduced levels. Acetylcholine was

detected but did not qualify as a DAM ($p = 0.142$). Although it did show a 2.7-fold mean increase at manipulation overall, manipulated samples appeared to have two distinct peak value groups. Three manipulated ants had 5.5-fold higher acetylcholine peak values than the other seven (Fig. 20). Comparing treatments with a median-based fold-change gave a 1.6-fold increase during manipulation. Possibly, this pattern could reflect rapid changes in physiology during manipulation as the ant climbs and bites onto a summiting substrate. Mandibular muscles have been shown to become hypercontracted during manipulated biting (Mangold *et al.* 2019) but also already begin to show signs of atrophy and degradation induced by the fungus (Hughes *et al.* 2011; Fredericksen *et al.* 2017). One scenario reconciling the available data would be elevated acetylcholine levels related to heightened locomotor activity and biting behavior (muscle hypercontraction), but then a reduction as acetylcholine-producing neurons and the mandibular adductors are quickly destroyed and the ant becomes unable to release herself. Importantly, glutamate is the direct primary excitatory neurotransmitter at insect neuromuscular junctions, but acetylcholine has fast-acting regulatory effects on motor behavior (Johansen *et al.* 1989; Gauthier 2010; Pflüger and Duch 2011). The variation within our manipulated samples might therefore represent how far along this sequence of muscular hyperactivity to degradation a manipulated ant was. Acetylcholinesterase is the enzyme that mediates the conversion of acetylcholine to choline and has been a target of enzyme-inhibiting insecticides (Fournier *et al.* 1992; Colovic *et al.* 2013; Singh *et al.* 2017). Putative homologs to this enzyme were DEGs in both the fungus and ant, with opposite changes in expression (Fig. 20). In the ant, the acetylcholinesterase-like gene was downregulated, consistent with increased acetylcholine levels. Additionally, the ant downregulated a putative muscarinic acetylcholine receptor gar 2 that has been found in sensory and motor neurons of *C. elegans* (Lee *et al.* 2000). Nearly a DEG as well, a putative ant nicotinic acetylcholine receptor acr-16 subunit gene was expressed 1.9-fold lower during manipulation. Possibly, this represents a homeostatic response to the proposed elevated acetylcholine levels present during the onset of manipulated summiting and biting. In contrast, the fungus upregulated a putative

acetylcholinesterase that would increase choline levels, which we detected. A shift in metabolism to increased choline production in the fungus could indicate higher demand for membrane phospholipids due to cell proliferation and remolding the cell membrane. Modification of the cell membrane could be necessary to accommodate transmembrane proteins or secretory activity involving organelle membranes such as in the endoplasmic reticulum (van der Veen *et al.* 2017; Shyu *et al.* 2019). Although, the fungus also downregulated one of two choline transporter genes annotated in its genome. The competing choline-acetylcholine metabolism between the ant and fungus may further explain the high variation in the manipulated sample acetylcholine feature peak values.

Hypotheses with mixed or constrained multiomic evidence: *Carnosine production may have been catalyzed by the fungal parasite to alleviate the physiological stress of manipulation and infection on host ants.* Within network module P2 and study-wide features passing at least two selection filters, we detected an enrichment signal for the "beta-alanine metabolism" pathway ($p = 0.025$ and 0.002, fold-enrichment = 1.8 and 1.5, respectively). Two amino acids participating in this pathway were reduced DAMs in manipulated ants, β-alanine ($p = 0.012$, 1.6-fold decrease) and histidine ($p = 1.3E\text{-}5$, 4.5-fold decrease, passing all selection criteria). We also observed increased carnosine ($p = 6.4E\text{-}10$, 4.1-fold increase, passing all selection criteria), which is a dipeptide formed from β-alanine and histidine. Carnosine and it's analogs are primarily known from vertebrates, with rare observations in mollusks (Boldyrev *et al.* 2013; Pan *et al.* 2021). Indeed, within healthy ant samples, the signal for carnosine was detected at nearly the same levels of our mock blank-collection samples (only 1.2-fold higher). In vertebrates, carnosine is found largely in muscle and the olfactory bulb where it has protective effects for both muscular and neuronal function by possible pH buffering and antioxidant properties (Bellia *et al.* 2011; Dolan *et al.* 2019; Wang-Eckhardt *et al.* 2020; Jukić *et al.* 2021). Neither the *O. camponoti-floridani* nor *C. floridanus* genomes had robust homology to carnosine synthase genes that encode the enzyme for the formation of carnosine. However, the fungal genome contains more likely candidates.

Carnosine synthases possibly originated from an ancestral gene containing two ATP-grasp domains and a C-terminal D-alanine-D-alanine ligase domain (Drozak *et al.* 2010). In the fungal parasite, there are seven genes containing both of these domains, four of which include the two ATP-grasp and one D-alanine-alanine ligase composition. No ant genes include both domains. However, a lack of strong homology between these fungal genes and animal carnosine synthases leaves the mechanism of production of carnosine in *C. floridanus* manipulated by *O. camponoti-floridani* an open question (Appx. L). We also cannot discount a possible endosymbiont or microbiome resident being involved in this process. Regardless of which organism produced carnosine, it may use β-alanine and histidine to form carnosine as a protective agent against the physiological stresses of hyperactive muscular activity (increased locomotion, tremors, biting) and/or buffer the CNS against excessive damage until the host has been successfully behaviorally manipulated.

Reduced insect hormones biosynthesis during manipulation. Both network modules A1 and P3 were enriched for the KEGG pathway "insect hormone biosynthesis" ($p = 0.006$ and 0.009, fold-enrichment = 1.8 and 3.2, respectively). This pathway term combines two primary arms of insect hormones metabolism, one for the canonical juvenile hormone III, and the other, for ecdysteroids. These hormones play a role in insect development and behavior, and have been considered in hypotheses of behavioral manipulation of ants infected by *Ophiocordyceps* and caterpillars infected by baculovirus (Hoover *et al.* 2011; Ros *et al.* 2015; Han *et al.* 2015; de Bekker *et al.* 2015; Will *et al.* 2020). Across the board, we found reduced compound abundances and downregulated genes related to metabolism of these hormones. Previous works suggest that manipulation correlates to reduced activity of ecdysteroids that inhibits caterpillar development to promote summiting disease (O'Reilly and Miller 1989; Han *et al.* 2015). On the other hand, increased juvenile hormone has correlated with adult ant foraging and higher activity that plausibly relate to manipulated ant behavior (Norman and Hughes 2016). Our metabolomic data contain signals for reduced ecdysteroid abundance, which is supported by transcriptomic data. Our

data also have reduced signals for both a precursor of juvenile hormone and inactive derivative. Similarly, gene expression data showed the downregulation of both juvenile hormone promoting and deactivating enzymes. Although there appears to be a change in juvenile hormone metabolism, it remains unclear whether there is an increase or decrease in active juvenile hormone titers.

Within network modules A1 and P3, the Mummichog compound matches producing the enrichment signal were reduced during manipulation. We used Mummichog matches in lieu of WCMC annotations as we lacked any features annotated as compounds found in the KEGG insect hormone biosynthesis pathway (see caveats for this approach in Methods). In network module A1, four possible compounds in this pathway were Mummichog matched, some by multiple metabolite features: ecdysone (two features), 3-dehydroecdsyone, 20-hydroxyecdysone, farnesoic acid (three features), and (10S)-juvenile hormone III diol (two features). Each compound had at least one representative feature significantly reduced during manipulation, with none more abundant (for full reporting see File S8). In network module P3, eight metabolite features were implicated in this pathway, five were reduced in abundance during manipulation, and four of those were simultaneously matched by Mummichog to other compounds. The five significantly reduced features putatively related to insect hormone biosynthesis are given here with their alternative matches : 3-dehydroecdysone, cholesterol (or lathosterol, ergosterol, 5,7,24(28)-ergostatrienol, 5-dehydroepisterol, and 3-keto-4-methylzymosterol), ecdysone (or KEGG glycan G01391), 7-dehydrocholesterol (or zymosterol and ergosta-5,7,22,24(28)-tetraen-3beta-ol), and another 7-dehydrocholesterol feature (or zymosterol and 4alpha-carboxy-5alpha-cholesta-8,24-dien-3beta-ol) (File S8).

Cholesterol and 7-dehydrocholesterol have a variety of metabolic roles, including the early steps of ecdysteroid synthesis. With fewer conflicting compound matches and more specific to ecdysteroid synthesis, we putatively detected the active ecdysteroids ecdysone and 20-hydroxyecdysone hormones and the inactive 3-dehydroecdysone that interconverts with ecdysone. In baculoviruses, an ecdysteroid

UDP glucosyltransferase has been proposed to inhibit normal function of 20-hydroxyecdysone in larval molting behavior and promote summit disease possibly through increased lifespan, in some, but not all species of pathogen and host (Hoover *et al.* 2011; Ros *et al.* 2015; Han *et al.* 2015). A homolog of ecdysone 20-monoxygenase, which catalyzes the conversion of ecdysone to 20-hydroxyecdysone, in the ant was downregulated during manipulation; but it was never expressed above 4 RPKM to qualify as a DEG (1.7 RPKM maximum in healthy ants) (Petryk *et al.* 2003). A putative ecydsteroid kinase DEG upregulated in *O. camponoti-floridani* may also interact with ecdysones to deactivate them into an ecdysteroid 22-phosphate form (Sonobe *et al.* 2006). The reduction in ecdysteroid concentration and synthesis and increased deactivation that we suggest here is consistent with the baculovirus manipulation hypotheses.

Our data also have Mummichog matches with reduced signals for farnesoic acid, which is synthesized into juvenile hormone, and a deactivated-form of juvenile hormone, (10S)-juvenile hormone diol. Two putative juvenile hormone acid O-methyltransferases used in the conversion of farnesoic acid to the immediate precursors of juvenile hormone, were downregulated during manipulation (Shinoda and Itoyama 2003; Van Ekert *et al.* 2015). Although a downregulation of farnesoic acid conversion would predict an accumulation of farnesoic acid, we rather observed a reduction. This can be explained by the downregulation of a homolog to the aldehyde dehydrogenase catalyzing the production of farnesoic acid, which under some conditions can be a rate determining step (Rivera-Perez *et al.* 2013). This gene was downregulated 1.9-fold in the ant (nearly a DEG). Contrastingly, juvenile hormone degradation may also have been slowed as seen by the downregulation of two putative juvenile hormone epoxide hydroxylase and three juvenile hormone esterase genes (originally annotated as venom carboxylesterase-6) (Zhang *et al.* 2005; Leboeuf *et al.* 2016; Das and de Bekker 2022). Juvenile hormone epoxide hydroxylases are responsible for the generation of the diol form of the hormone, which was reduced during manipulation. Intertwined with ecdysone and juvenile hormone functions, we also detected a possible downregulation of

vitellogenin production in the ant (Corona *et al.* 2007; Kohlmeier *et al.* 2018; Wu *et al.* 2021). Manipulated ants had reduced expression of a putative viteollgen-1 gene, although never above 4 RPKM to qualify as a DEG (3.2 RPKM maximum, in healthy ants). The wholesale reduction in enzyme expression and insect hormone metabolite abundance during manipulation could contribute to the changing behavioral profile of the sick ant – regardless of if these reductions are highly targeted by the fungus or simply the symptoms of a terminally diseased ant.

Three pathway enrichments suggested changes in detoxification and drug-related metabolism. Pathway "drug metabolism – P450" was enriched in network modules L3 and P3 (p = 6.7E-4 and 0.024, fold-enrichment = 10.0 and 1.4, respectively), "drug metabolism – other enzymes" in A1 and the study-wide data (p = 0.006 and 0.030, fold-enrichment = 2.1 and 1.5, respectively), and "metabolism of xenobiotics by P450" in A1 and P2 (p = 0.012 and 0.29, fold-enrichment = 1.6 and 1.5, respectively). Each of these KEGG pathway annotations contain multiple distinct metabolic pathways pertaining to the detoxification metabolism specific drugs or compounds. Altered drug metabolism pathways could reflect antagonist host-pathogen interactions employing metabolites with similar structure as the drugs and toxins specifically described in the KEGG pathways. As with the insect hormone biosynthesis pathway discussed above, our data had no metabolite features annotated with compounds found in these pathways. Therefore, we investigated the tentative Mummichog compound matches to offer insights to the specifics of these pathways. Across all three pathways, matched compounds were diffusely populated across multiple drug-specific sub-pathways and in all cases either reduced in abundance or not significantly changed. Given this trend we cannot offer compound-specific biological interpretations for these pathway enrichments or why such metabolites would be found reduced during manipulation.

However, outside of these network modules enriched for drug and xenobiotic metabolism, an increased DAM matched to aflatoxin B1-exo-8,9-epoxide by Mummichog as its only compound match. This feature was only detected in manipulated samples (p = 2.4E-14, median peak value = 749,741, passing all three

selection criteria). We single out this compound match as it is a derivative of aflatoxin B1, a well-recognized mycotoxin produced by fungi with insecticidal properties (Yu *et al.* 2004a; Trienens and Rohlfs 2011). Two other features matched aflatoxin B1-exo-8,9-epoxide, one a decreased DAM and the other not differentially abundant. Given that the increased DAM was only detected in manipulated ants, it appears as the most sensible feature match to a degradation product of a specialized fungal metabolite. In the *O. camponoti-floridani* genome, multiple genes putatively related to mycotoxin and secondary metabolite production were identified and many were upregulated during manipulation (Will *et al.* 2020). Whether this aflatoxin derivative reflects this hypothesized fungal toxin production during infection of the ant host remains unclear.

Common metabolites between Ophiocordyceps-Camponotus *manipulations in two species pairings.* Previous LC-MS/MS studies with *O. kimflemingiae* have identified many metabolites associated with infection of *C. castaneus* and proposed links between these compounds and manipulation (de Bekker *et al.* 2014b; Zheng *et al.* 2019; Loreto and Hughes 2019). In addition to common metabolic threads between species, species-specific response have also been recorded. Laboratory co-culture of *O. kimflemingiae* with brains from different ant species showed distinct metabolic profiles reflecting the ant species tissue and host-specific fungal secretions, although shared metabolites were also found (de Bekker *et al.* 2014b). Ergothioneine, an amino acid produced by some fungi, but not animals, has been detected in mixed ant-fungal tissue from manipulated ant brains and muscles (Zheng *et al.* 2019; Loreto and Hughes 2019). Corroborating these findings, we detected two ergothioneine signals (biogenic amine and polyphenol datasets) that were wholly absent in the healthy ants or with peak values near that of blank-collection samples ($p = 7.3E-15$ and $4.6E-12$, passing all selection criteria). In addition to fungal metabolism, ergothioneine has been discussed as a possible neuroprotectant to preserve the ant brain until manipulated summiting and biting are complete (Loreto and Hughes 2019). Supporting this line of reasoning, ergothioneine in the ant brain was not detected at elevated levels in moribund ants infected by

the generalist entomopathogen *Cordyceps bassiana* that consumes hosts more quickly, without inducing summit disease, and appears to occupy the ant head capsule to a lesser extent than *Ophiocordyceps* (Fredericksen *et al.* 2017; Loreto and Hughes 2019).

Previous work with *O. kimflemingiae* and this work with *O. camponoti-floridani* have found adenosine and adenosine-phosphate (AMP) to be differentially abundant between manipulation and healthy and/or generalist-infected ants (Zheng *et al.* 2019; Loreto and Hughes 2019). We found two features annotated as adenosine, one which was not differentially abundant and one that was a reduced DAM in manipulated samples (p = 6.6E-4, 2.5-fold decrease). In contrast, previous works found adenosine to increase in abundance in both manipulated ant brains and mandible muscles (Zheng *et al.* 2019; Loreto and Hughes 2019). We also found decreased AMP (p = 0.003, 2.1-decrease, Boruta confirmed) in the head, as was found in manipulated *C. castaneus* (Zheng *et al.* 2019; Loreto and Hughes 2019). In *O. kimflemingiae* infection, a role for adenosine mediated neuromodulation was hypothesized, as was changing AMP levels possibly reflecting changes in mitochondrial activity (Zheng *et al.* 2019; Loreto and Hughes 2019). Cyclic AMP is involved in many pathways, including as a secondary messenger in G-protein coupled receptor signaling, which we hypothesized to be implicated in manipulation (e.g., via enterotoxin-like proteins or undescribed secreted proteins) (Will *et al.* 2020) (Chapter 3). If changing abundance of AMP reflects upon the cyclic form as well, this could relate to dysregulation of receptor signaling. Metabolically related to adenosine, hypoxanthine and inosine were also proposed to have links to energetic and neurological processes in manipulated ants (Zheng *et al.* 2019; Loreto and Hughes 2019). As in those studies, we also detected increased levels of hypoxanthine during manipulation, two of three features annotated as hypoxanthine increased at manipulation (p = 0.007 and 7.7E-6, 1.6-fold increase or absent in sham, the latter of which passed all selection criteria). We also detected one inosine and two inosine-monophosphate features increased in manipulated ants (p =

0.002, 3.8E-7, and 1.4E-5, 1.9-, 2.8-, 2.5-fold increase, all also Boruta confirmed). This could indicate the conversion of AMP and adenosine to hypoxanthine primarily via inosine intermediates.

Conclusion

Infection and behavioral manipulation of hosts can involve many interacting molecular and cellular processes. As we better characterize these host-parasite interactions we can also gain insights into specialist co-evolutions, the mechanistic basis of animal behavior, and the discovery of new bioactive compounds. To unravel the mechanistic complexity of infection and manipulated host behavior, we require functional tests built upon robust hypotheses. Towards this goal, we studied parasitic manipulation of *C. floridanus* by *O. camponoti-floridani*, combining metabolomic, transcriptomic, and genomic data to develop a set of hypotheses regarding molecular processes during manipulation. We put forward these hypotheses with the goal to explain the data as reflections of behavioral manipulation and infection, although non-manipulative explanations may exist.

We found evidence for altered biogenic monoamine neurotransmitter production during infection and manipulation that may be proximate causes of manipulated behavior. In total, we propose a scenario where the manipulated ant has elevated production of dopamine and serotonin with a decrease of octopamine. The fungus may have simultaneously suppressed the host's melanin and immunity pathways while metabolizing dopamine and its precursors for fungal melanin production. Ants infected by *Ophiocordyceps* display enhanced locomotion/activity levels, reduction of social behaviors, and a final summit latching behavior – elements of these behaviors have already been associated with neurotransmitter signaling in ants. Intriguingly, aquatic gammarid crustaceans manipulated by acanthocephalan worms display a phototactic summiting and clinging phenotype in the water column sometimes associated with increased serotonin, decreased octopamine, and suppressed phenoloxidase-mediated immunity – essentially, parts of the same pattern we propose in manipulated *Camponotus*

(Helluy and Holmes 1990; Lefèvre *et al.* 2009; Helluy 2013; Herbison 2017). Manipulators of vertebrate behavior may also leverage serotoninergic and dopaminergic processes to alter fish and mouse behaviors related to escape responses, locomotion, and aggression (Shaw *et al.* 2009; Prandovszky *et al.* 2011; Adamo *et al.* 2013; Lafferty and Shaw 2013). How much of the alteration of neurotransmitter metabolism may be a general response to fungal infection and how much results from specific manipulation by *Ophiocordyceps* is difficult to pinpoint at this time. However, cardol triene appears to be a fungal derived compound that could suppress ant immunity and increase substrate availability for dopamine production. Also, *Ophiocordyceps* upregulated three putatively secreted tyrosinases that possibly interact with host dopamine/melanin precursors. Although less typically reported than their intracellular counterparts, extracellular fungal tyrosinases have been found in another fungus as well (Selinheimo *et al.* 2006; Gasparetti *et al.* 2012). Vitamin B6 metabolism and, therefore, AADC enzymatic activity to synthesize dopamine and serotonin might be also altered during manipulation. Dopamine, serotonin, and octopamine receptors appear to be directly targeted by secreted fungal effector proteins as well (Chapter 3).

Glutamate and GABA are also important neurotransmitters, insect neuromuscular modulators, and components of metabolism more broadly. Glutamate and many of the compounds that are biosynthetically linked to glutamate and GABA are reduced during manipulation. Manipulated ant gene expression suggests that glutamate conversion into GABA remains steady, while two alternative branches of glutamate metabolism are downregulated. These transcriptomic data possibly signifying increased substrate availability for GABA production or homeostatic attempts to maintain glutamate levels amid widespread depletion of glutamine and other compounds. The fungus meanwhile appeared to be increasing consumption of glutamate, including by upregulation of a gene putatively encoding a glutamate decarboxylase (also a vitamin B6 dependent enzyme) to produce GABA. We consider it most likely that the fungus is using GABA and glutamate derivatives for its own metabolic demands during growth and development. Although, we cannot discount it exporting GABA into the host environment.

Changing glycerophospholipid metabolism during manipulation, largely centered on choline, suggested dysregulation of acetylcholine levels in the ant and fungal biosynthesis of cell membrane components. Manipulated ants reduced expression of acetylcholinesterase, and three metabolomic manipulation samples had notably higher acetylcholine concentrations than the rest. We propose this division could indicate differences between ants earlier and later in their respective infection progression. High acetylcholine could contribute to summiting and wandering behavior (i.e., increased locomotion), tremors, and the hypercontracted biting that locks manipulated ants into place. Once established at a summiting location, rapid destruction of neurons by the fungus may limit ant production of acetylcholine. Upregulated fungal acetylcholinesterase would promote the conversion of acetylcholine into choline – thereby lowering acetylcholine after manipulated biting. In turn, additional choline in the fungus can be used for cellular processes, such as phosphatidylcholine biosynthesis. Speculatively, *Ophiocordyceps* may require increased cell-membrane choline-derived components used during cell proliferation and membrane remodeling for structures such as lipid rafts or transmembrane proteins important during infection and manipulation.

During heightened diseased activity, physiological stresses in the ant, especially in muscle and neural tissues, may be assuaged by the production of carnosine. Carnosine was only distinctly detected in manipulated samples and not in healthy ants. This is in line with carnosine not being reported outside of vertebrates and some mollusks. Although the *O. camponoti-floridani* genome contains more genes with similar domain structure to known carnosine synthases than the ant genome, we found no satisfying candidate gene to produce the enzyme for carnosine synthesis. Catalysis of carnosine production may use ant or fungal enzymes highly dissimilar from canonical carnosine synthases. Alternatively, other microbes in the host or fungus could contribute to its production.

Metabolism of ecdysteroids and juvenile hormone appeared to change during manipulation. These hormones have major roles in development, but also correlate to behavioral profiles in adult

insects. In baculovirus, inhibited 20-hydroxyecdysone activity has been associated with summiting disease of caterpillars in some cases. Manipulated ants lowly expressed an enzyme to produce 20-hydroxyecdysone, a compound we possibly detected to be reduced during manipulation (compound match based on Mummichog). Meanwhile, the fungus upregulated a gene putatively encoding a kinase that could inhibit ecdysteroids. Genetic and metabolic signals for juvenile hormone were mixed. Inactive juvenile hormone forms and a compound used in juvenile hormone synthesis were both putatively reduced in manipulated ants (matches based on Mummichog). Host genes involved both in juvenile hormone biosynthesis and inactivation were downregulated during manipulation. Changes in juvenile hormone metabolism seem apparent, but it is difficult to conclude exactly how at this time.

We have proposed new or further developed existing hypotheses on the mechanistic basis of infection and manipulation of *C. flordianus* ants by *O. camponoti-floridani* fungi using a multiomic approach. We combined earlier genomic and transcriptomic work with this current metabolomic work spanning three LC-MS/MC chemistries. We hypothesize that altered metabolism of the neurotransmitters, dopamine, serotonin, octopamine, and acetylcholine may be proximate causes of infected ant behaviors. Glutamate and GABA could also be implicated, but the data are less robust for these compounds. In turn, the fungus may suppress ant immunity and scavenge host metabolites for its own use. The fungus could also promote protective effects mediated by metabolites such as carnosine, kynurenic acid (via increased kynurenine synthesis), or ergothioneine to ensure their heavily diseased host can perform necessary manipulated behaviors at the end of life.

By inducing changes in direct regulators of behavior (neurotransmitters) that are used to control activity in healthy ants, the fungus may be impinging upon existing host systems to modify behavior rather than forcibly introducing novel pathways. Indeed, many of the hallmark phenotypes of infection by ant-manipulating *Ophiocordyceps* are not so dissimilar from activities influenced by levels of dopamine, serotonin, octopamine, and acetylcholine in eusocial insects: foraging/locomotor behavior (i.e.,

summiting and hyperactivity), sociality (i.e., wandering and reduced communication), and the biting/aggression (the final "death grip" bite). Changes in social behavior could not only be a symptom of disease, but contribute to it as well. As socially isolated infected ants may less frequently exchange trophallactic fluid with nestmates, these infected individuals would lose an important source of nutrition, communication, and hormones (Leboeuf *et al.* 2016). How exactly the fungus may dysregulate physiological pathways that influence behavior (e.g., juvenile hormone metabolism), to what degree some level of dysregulation is typical in many diseases, and if the fungus may take advantage of these processes, is still unclear.

These hypotheses can be further investigated by functional tests (e.g., gene knockouts or dosing ants with metabolites) and LC-MS/MS validations of key compounds using chemical standards. Further investigations specifically into the lipids dataset may benefit from different analytical approaches. Lipids are distinctly different molecules than many of the compounds measured in the biogenic amines and polyphenol datasets. Whereas these two datasets produced many pathways and annotations interesting for our discussion of manipulated behavior, lipid features were highlighted less frequently. Additionally, novel, poorly described, or low abundance compounds (below the DDA MS/MS threshold) may have been missed in our broad bioinformatic approaches. Searching individual feature chromatograph data for signals of compounds similar to predicted fungal secondary metabolites or mycotoxins from genomic data could be a fruitful endeavor. But those searches will be largely limited by databases and the model systems that populate them. Outside of metabolomic perspective, single protein effectors and other mechanisms, such as RNAs, could be critical during the infection and manipulation of hosts. A full picture of manipulation at the molecular level will need to integrate metabolomic studies such as this one, but also expand outside of them.

Acknowledgments

We would like to thank Sophia Vermeulen for assisting with testing fungal strain OJ2.1 and, with Biplabendu Das, their help with ant infections and observations. We also thank Devin Burris for help with ant monitoring. Jordan Dowell provided insightful discussions on LC-MS/MS methods and interpretation for which we are grateful for. The Genetics Society of America supported sharing of this work with a travel award. Research funding for this project came from NSF (NSF-CAREER IOS-1941546). The expected authorship team for publication of this work is Ian Will, Geoff Attardo, and Charissa de Bekker. Supplemental data files are available upon request.

CHAPTER FIVE: CONCLUSIONS

The ant-manipulating *Ophiocordyceps* fungi are naturally evolved "neurobiologists" capable of modifying the behavior of their hosts in a manner that human biologists do not yet fully understand and cannot replicate (Adamo *et al.* 2013; de Bekker *et al.* 2021). *Ophiocordyceps camponoti-floridani* induces a summit disease in *Camponotus floridanus* ants. As the host dies at an elevated position it offers a starting point for new fungal growth and transmission. Understanding the mechanisms of how this parasitic manipulation operates can inform efforts to improve our knowledge of the molecular basis of animal behavior, undescribed bio- and neuro-active compounds, and how to integrate a growing field of parasitic manipulation studies. Mechanistic hypotheses and observations of manipulation in ant-manipulating *Ophiocordyceps*, largely from *Ophiocordyceps kimflemingiae*, are based on genomic, transcriptomic, metabolomic, and histological data (de Bekker *et al.* 2014b, 2015, 2017; Wichadakul *et al.* 2015; Fredericksen *et al.* 2017; Kobmoo *et al.* 2018; Mangold *et al.* 2019; Zheng *et al.* 2019; Loreto and Hughes 2019). By undertaking complementary, updated explorations in *O. camponoti-floridani*, we aimed to refine existing hypotheses and develop new ones.

We produced multiple large datasets – three based on physical sampling and a fourth based on bioinformatic predictions. First, we generated genomic sequence data of *O. camponoti-floridani* using a combination of short-read Illumina and long-read Nanopore technologies. We then assembled the first published genome of *O. camponoti-floridani*. Second, we created a transcriptomic dataset with coverage of both host and parasite during control conditions, active manipulated behavior, and death of the moribund, manipulated host. We used this RNAseq data to hypothesize key effectors and pathways that might play a role in producing manipulated behavior. Third, we used these genetic data to build an interactome of computationally predicted host-parasite protein-protein interactions (PPIs). These data complemented the RNAseq-based results and highlighted other possible parasite effector and host proteins. Lastly, in an independent experiment from RNAseq data collection, we analyzed untargeted

metabolomics data with three different chromatography chemistries on both *C. floridanus* and mixed-metabolome (fungus and ant) samples from actively manipulated hosts. With this fourth dataset, we began the multiomic integrative work of uniting genetic and chemical signals to develop hypotheses supported by multiple types of molecular evidence from independent experiments.

Our explorations of these large datasets offered a wealth of proteins, metabolites, and molecular pathways that could contribute to infection and manipulation of *C. floridanus*. Hypotheses supported by a single dataset are certainly plausible; as some mechanisms of manipulation may only have been clearly detectable by one of our approaches or, simply by chance, these sweeping bioinformatic analyses failed to find certain signals in all cases. However, when we can connect supporting evidence from multiple experiments and data types, these produce our most robust hypotheses. We propose three general mechanistic avenues linking molecular perturbations to observed phenotypes: (*i*) direct effects on neurotransmission and signaling and sensory systems, (*ii*) indirect effects via behavior-modulating foraging/feeding, circadian clocks, locomotion, and insect hormone pathways, and (*iii*) tissue destruction and immunosuppression (Fig. 21). These groups have links to each other and do not function in isolation, but generally characterize many of the molecular patterns we observed. These three branches of manipulation mechanisms are similar to how they have been conceived of elsewhere, indicating commonalities among parasitic manipulations (Lafferty and Shaw 2013; de Bekker *et al.* 2021).

Neurotransmission and signaling and sensory systems. Multiple neurotransmitters are used by insect neurons to control behavior, making them potential proximal drivers of manipulated and infected phenotypes (Osborne 1996). We found changes in host gene expression and compound abundances related to metabolism or reception of dopamine, serotonin, octopamine, acetylcholine, and perhaps glutamate and GABA (Fig. 21). Furthermore, not only could neurotransmission be a functional output of dysregulated “upstream” host physiology leading to behavioral changes, neuronal function and signaling

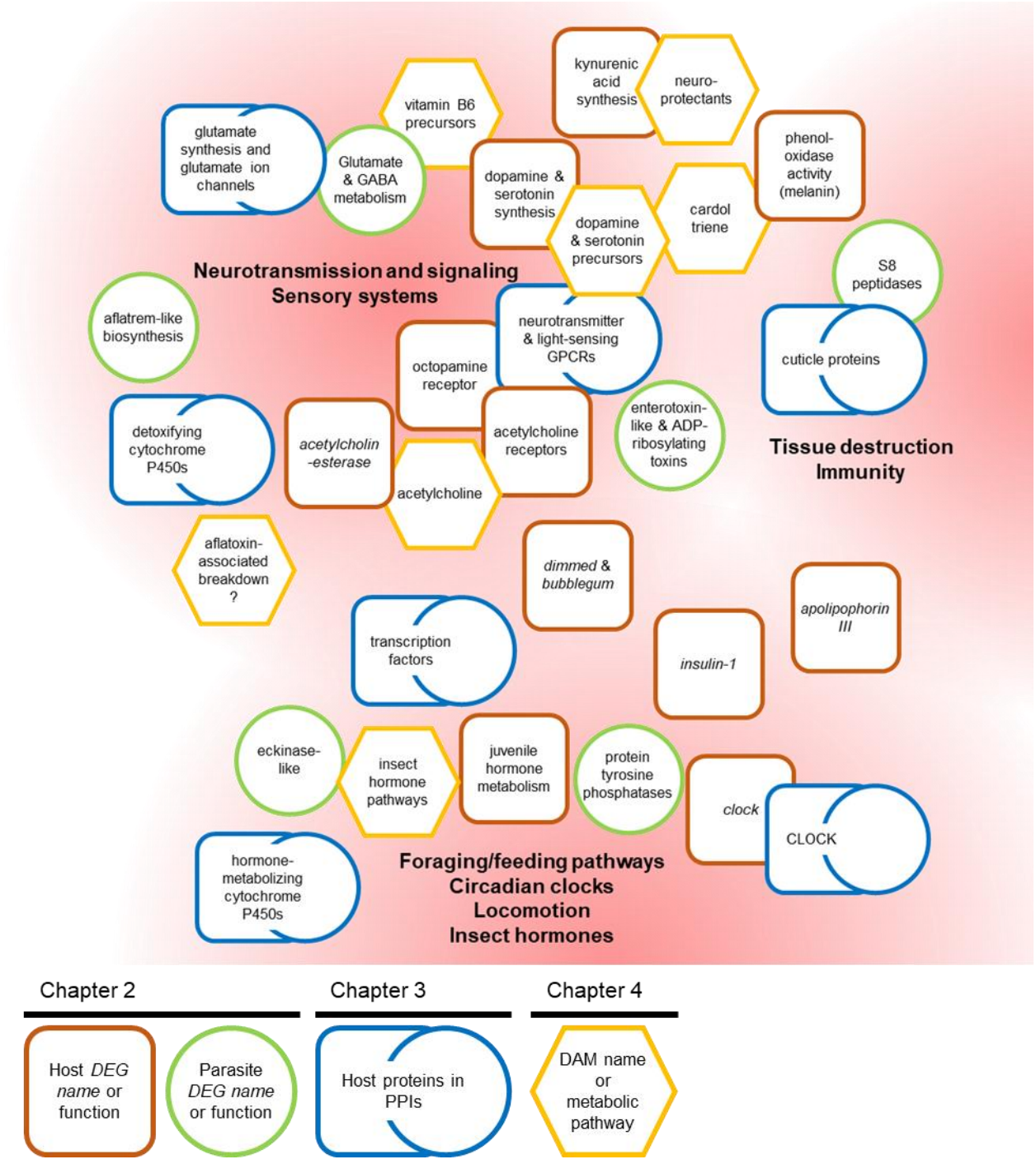

Figure 21. Brief summary of findings and conceptual clustering, across datatypes.

We highlight a selection of the individual molecules and mechanisms discussed that are *Camponotus* differentially expressed genes (DEGs) (brown squares), *Ophiocordyceps* DEGs (green circles), host proteins in cross-species PPIs

(combined blue squares and circles), or mixed-organism differentially abundant metabolites (DAMs) (yellow hexagons) during behavioral manipulation. We loosely clustered mechanisms by their relationships to each other and how we hypothesize they relate to the three main branches of manipulation processes proposed (red auras and bold text).

appear to be directly targeted by the fungus. We hypothesized an aflatrem-like *Ophiocordyceps* metabolite to dysregulate neuronal function, possibly producing hyperactivity and convulsions during the late phase of infection (Fig. 21). We also genomically predicted that *Ophiocordyceps* produces other secondary metabolites that could act as mycotoxins to dysregulate host neurophysiology. The analytical approach used for our metabolomic data was not likely to immediately detect such putative mycotoxins unless they were already well documented metabolites. However, further investigation of these data may allow us to speculate if compounds in the same class as known mycotoxins are produced during infection. Although not substantiated by our PPI predictions, the strong genomic and transcriptomic signals for enterotoxin-like proteins that possibly dysregulate cellular signaling related to neurotransmission pathways also suggests fungal interference with neuronal function (Fig. 21). Protein interaction predictions did, however, provide numerous putative host neurotransmitter GPCRs targeted by fungal proteins. These receptors include ones for the neurotransmitters listed above, but also many other neuropeptides (as well as light) (Fig. 21). Support from predicted PPIs also suggests that the fungus can dysregulate transcription factors implicated in regulating neuronal maintenance and gravity or light sensing functions (Fig. 21). How activity of any one host GPCR or transcription factor changes remains unclear, but multiple PPIs support that the parasite is interfering with these pathways. Fungal metabolism of host neurotransmitters and their precursors may also play a role. If *Ophiocordyceps* cells scavenge metabolites from or provide metabolites to host cells, this exchange may modulate host functions related to glutamate, GABA, and acetylcholine or vitamin B6 mediated neurotransmitter synthesis (e.g.,

dopamine, serotonin, and GABA). Similarly, *Ophiocordyceps* secreted tyrosinases and cardol triene could dysregulate dopamine/melanin precursor levels (Fig. 21).

Foraging/feeding, circadian clocks, locomotion, and insect hormone pathways. Sick ants, and other animals, behave differently than their healthy counterparts as a consequence of their physiological status and as a targeted disease response (de Bekker *et al.* 2018). Similarly, the fungal parasite may be eliciting these responses as an effect of infection but also tapping into preexisting behavioral pathways to manipulate host activity. Nutritional state and caste-task behaviors are tied to activity levels, locomotion, and foraging (Ament *et al.* 2008; Libbrecht *et al.* 2013; Opachaloemphan *et al.* 2018; Chandra *et al.* 2018; LeBoeuf *et al.* 2018). *Camponotus* infected by *Ophiocordyceps* altered gene expression of putative insulin and lipid metabolism genes related to nutritional signaling. Additionally, we found metabolomic signals related to hormone biosynthesis pathways and differentially expressed juvenile hormone metabolism genes (Fig. 21). The fungus may upregulate transcription of an ecdysteroid inactivating protein and target multiple host cytochrome P450s by PPIs, which broadly speaking, can participate in hormone metabolism (Fig. 21). With links to feeding and forager behavior, hormone signaling connects to locomotor activity in ants. Foraging *C. flordidanus* also operate in a circadian manner, with daily peaks in foraging and locomotor behavior (Trinh *et al.* 2021; de Bekker and Das 2022; Das and de Bekker 2022). Changes in host gene expression of a core clock gene and multiple predicted host-pathogen PPIs involving this gene may represent manipulation of host circadian rhythm and downstream clock-controlled behaviors (Fig. 21). Protein tyrosine phosphatase has been hypothesized to operate at the intersection of these molecular circuits, possibly involving juvenile hormone, the circadian clock, and foraging-regulating molecules in baculovirus to induce enhanced locomotor activity (van Houte *et al.* 2013) (Fig. 21). The upregulation of fungal secreted protein tyrosine phosphatases predicted in many PPIs offers clues that *Ophiocordyceps* could employ a similar strategy. Furthermore, a number of PPIs

involved host transcription factors regulating processes including insect hormone function, locomotion, and circadian rhythms (Fig. 21).

Immunity and tissue destruction. As *Ophiocordyceps* colonizes its host, it destroys tissue and overcomes the immune system (Hughes *et al.* 2011; Fredericksen *et al.* 2017; Mangold *et al.* 2019). Undoubtedly part of killing and consuming the ant, these processes may relate to infection phenotypes and have roles in manipulation of *Camponotus* as well. To subvert host immunity, the fungus appears to secrete cardol triene, a metabolite capable of suppressing tyrosinase activity (and likely insect phenoloxidases), a necessary element in the beginning of melanin synthesis used for host immune responses (Fig. 21). In turn, this would leave an excess of precursor molecules shared with the biosynthetic pathway for dopamine. Speculatively, secreted fungal tyrosinases may be interacting with host melanin precursors rendering them unusable by host immunity. Upregulated serine peptidases, and PPIs involving them, indicated that the fungus is degrading host cuticular proteins (Fig. 21). In addition to breaching certain tissue compartments or body segments, this activity could also detach musculature. We predicted these fungal peptidases to be in PPIs with host kinesin; kinesin inactivation would dysregulate cellular processes, including vesicle transport within neurons. Unfettered tissue destruction would likely lead to premature host death and removal of key tissues (e.g., brain and mandible or leg muscles) required for successful summiting and biting. But, if tightly controlled until once the host has latched onto a summit position, destroying antagonist muscles needed to release from summiting could lock the manipulated host in place.

Future directions. Many open questions remain, both in the presented data and behavioral manipulation at large. For both the PPI and metabolomic datasets, more detailed analysis of the data can improve the specificity of our hypothesized mechanisms of infection and manipulation. The PPI data have only been explored in a preliminary fashion focused on signals with the clearest links to manipulation. Some functional enrichments and PPIs have yet to be rigorously considered. Furthermore, individual PPIs

should be vetted for plausibility and to suggest the specific effect of the interaction (e.g., increased or decreased activity of the host protein). With our metabolomics data, two main explorations can still be better developed. The lipidomics data were not commonly linked to KEGG pathways in our enrichment analyses. Getting the best use of these data could require different approaches. The lipid data had the most annotated compounds as well, but the nature of these annotations was not very amenable to timely and specific research in the literature (i.e., a lipid class and carbon-chain length is given). Also, we have relied on the annotations provided by the core facility – although we believe them to be reliable, they did not entail a deep dive into the data searching for specific compounds we are interested in measuring (e.g., dopamine or the predicted aflatrem-like toxin). We can return to the raw chromatograph data and consider more focused approaches in determining if certain compounds are likely represented in our data.

Functional tests are the critical future direction in validating any of these proposed effectors and mechanisms. Genetic manipulations (e.g., knockouts or overexpression), RNAi, and drug dosing are all reasonable methods to test behavioral effects. To this end, we have piloted approaches for genetic transformation of *O. camponoti-floridani*. Our results are still preliminary and poorly reproducible, but in some instances we have generated genetically modified strains using an *Agrobacterium* mediated integration of donor DNA. We have also heterologously expressed a top candidate effector, an enteroxin-like gene, in the generalist entomopathogen *Cordyceps bassiana*. Pilot studies using this knock-in approach have begun (Burris 2022). If heterologous expression of this gene generate behavioral changes in infected *Camponotus* remains inconclusive until further experiments can be performed. Other lab members have spearheaded the first compound-dosing experiments, treating ants with aflatrem and observing for changes in locomotor function and activity levels. Biochemical assays, *in vitro* cell culture responses, and targeted metabolomics could also be important steps in gathering real-world evidence to test hypotheses centered on predicted protein-binding, receptor activation, or predicted fungal secondary metabolites. Candidate mechanism testing by removing or adding any single element in isolation is

technically practical, but these experiments will have to contend with the biological reality that manipulation is likely a multilayered interlinked process that may not be easily dissected by such approaches. Both the parasite and host could have functional redundancies in the pathways underlying manipulation. There may be few, if any, effectors or targets that are wholly sufficient or necessary to produce certain aspects of manipulation. However, such efforts are likely where we must begin, and we propose that some of our hypothesized mechanisms will be biologically significant and produce, even partial, changes in host responses and behavior when tested.

APPENDIX A: CLIMATE AND HOUSING CONDITIONS DURING INFECTION EXPERIMENT

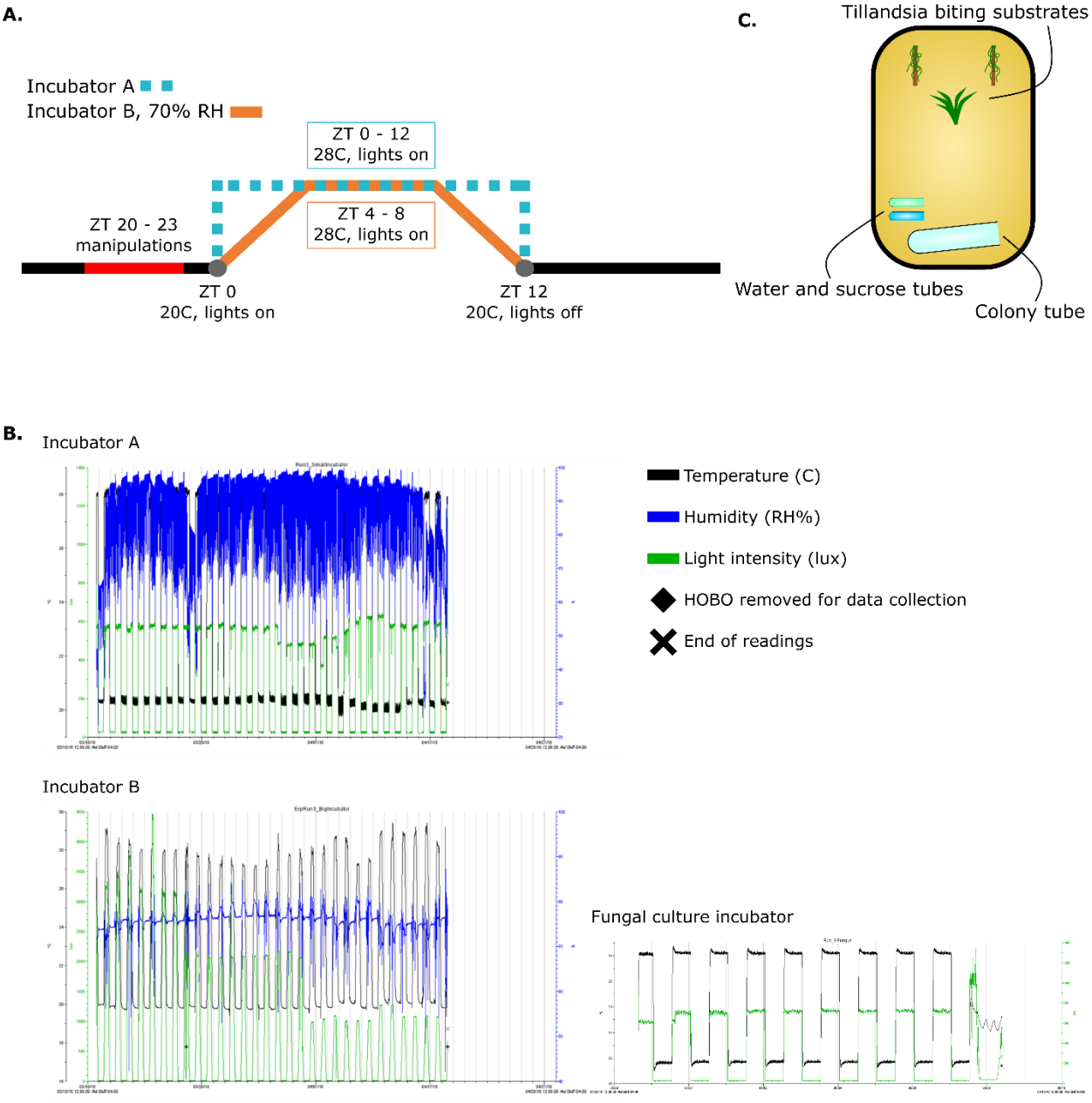

Climate and housing conditions during the infection experiment. A) Incubator climate cycle settings. Incubator B included a constant humidity at 70% RH. B) Climate data for the duration of the experiment from incubator A, B, and the incubator used to culture fungi. C) Schematic of ant infection experiment enclosure, 33 cm x 22 cm.

APPENDIX B: UNSUPERVISED DENDROGRAM CLUSTERING OF BIOLOGICAL REPLICATES BASED ON NORMALIZED GENE EXPRESSION LEVELS (RPKM)

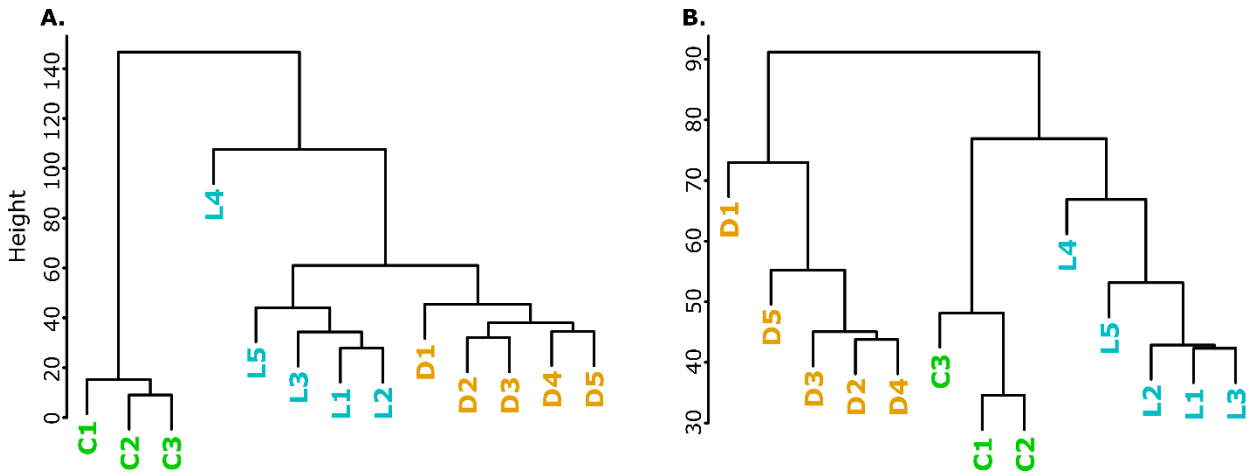

Control (green, C1 – C3), live manipulation (blue, L1 – L5), and dead manipulated (orange, D1 – D5) samples largely cluster into their defined biological groups. A) Dendrogram of O. camponoti-floridani transcriptome data. The clustering of replicates indicates that fungi that actively interact with their host have more similar gene expression profiles to each other than to fungal growth under pre-infection conditions. B) Dendrogram of C. floridanus transcriptome data. The clustering of replicates indicates that living ants, whether healthy or manipulated, are more similar to each other than to recently expired ants after manipulation.

APPENDIX C: CHAPTER 1 ADDITIONAL RESULTS AND DISCUSSION

Pathogen-Host Interaction database annotations

We also compared DEGs upregulated and downregulated during manipulation using the Pathogen-Host Interaction (PHI) database (Urban *et al.* 2017). We counted PHI descriptions that contained any annotation other than "unaffected_pathogenicity" as genes putatively involved in virulence and manipulation. Upregulated genes comprised 57 hits with pathogenicity annotations, while only 22 were present in the downregulated gene set. In both cases, numerous gene products without PHI annotation results were present (201 upregulated, 32 downregulated). Of these genes absent in the PHI database, 54 genes in the upregulated set putatively encoded secreted proteins (i.e., SignalP annotation), whereas only 4 such genes were present in the downregulated group. These genes, that lack PHI database annotation but are part of the secretome, could contain novel undescribed fungal effectors that are relevant to *Ophiocordyceps-Camponotus* interactions.

Host gene expression patterns related to tissue destruction and nutrition.

The expression levels of three ant myogenesis-regulating glycosidase genes, decreased from healthy control ants, to live manipulated, and further to dead manipulated ants, as well as a gene annotated as "actin, muscle" (10-fold decrease from control to live manipulation). However, its homolog in *C. castaneus*, followed the opposite expression pattern.

In starved *Drosophila* flies, lipase 3, an enzyme involved in fat metabolism, was found to be up-regulated (Zinke *et al.* 1999). Similarly, we identified an upregulated lipase 3 gene (2-fold increase from control to live manipulation) in ants sampled during manipulation. However, an additional four lipase 3 genes and an overrepresentation of the GO term "lipid metabolic process" among the downregulated subset of genes suggested that overall lipid metabolism might be diminishing in manipulated ants.

As we note changes in gene expression not in line with reports in other insects (i.e., lipase 3, apolipophorin III, and cytochrome P450 4C1), this could mean that the ants' energy reserves have been

fully depleted at our nearly terminal time points of sampling. Alternatively, genetic starvation mechanisms are different in ants compared to flies and cockroaches, or the fungal parasite has disrupted the ants' typical starvation responses.

We found putatively secreted metalloprotease encoding genes upregulated during live manipulation that could be involved in infection and affect host IIS pathways. These genes carried PFAM PF05572|Peptidase_M43 annotations and additional MEROPS protease annotations. Genes with MEROPS M43.002 putatively function similarly to *mep1*, which assists fungi to counteract mammalian immune systems (Hung *et al.* 2005; Shende *et al.* 2018). Putative *mep1* genes in *O. camponoti-floridani* were upregulated during live manipulation relative to both culture and dead manipulated samples (Fig. 7). One homologous *mep1* metalloprotease was also significantly upregulated during manipulation in *O. kimflemingiae* (i.e., 71-fold increase from culture to live manipulation in *O. camponoti-floridani*, 3-fold in *O. kimflemingiae*) (de Bekker *et al.* 2015).

Other M43 annotations present in the *O. camponoti-floridani* genome predicted the presence of ulilysins (MEROPS M43.007) and pappalysins (MEROPS M43.004 or M43.005). Ulilysins and pappalysins are known to interact with IGF binding proteins that regulate levels of free IGF (Tallant *et al.* 2007). Two M43 metalloproteases carrying both ulilysin and pappalysin MEROPS annotations were upregulated from culture to manipulation in *O. camponoti-floridani* but not in *O. kimflemingiae*.

Dysregulation of odor detection.

Two putative odorant receptor genes in *C. floridanus* were differentially expressed from control to live manipulation (i.e., upregulated *or1* and downregulated *or4*-like). Homologs of these genes have been proposed to encode for pheromone receptors in moths (Grosse-Wilde *et al.* 2011; Wicher *et al.* 2017). Other genes possibly associated with odor communication were also downregulated from control to live manipulation in *C. floridanus*. One of these genes was a putative *sensory neuron membrane*

protein 1 (17-fold decrease), which is involved in the detection of lipid-derived pheromones in pheromone-sensing antennal neurons (Pregitzer *et al.* 2014). We additionally detected two putatively encoding acyl-CoA Delta(11) desaturases (16- and 4-fold downregulated), which are key enzymes in the synthesis of pheromones in moths (Choi *et al.* 2002) and may speculatively play a role in chemical communication of ants as well. A homolog to the 16-fold downregulated acyl-CoA Delta(11) desaturase was also reduced in expression in *C. castaneus* (1.8-fold decrease) but does not meet our DEG threshold requirements (de Bekker *et al.* 2015).

Among the 11 differentially expressed PBP and general-OBP (GOBP) domain containing genes, four were annotated to putatively encode pheromone binding protein Gp9. Variation in *Gp9* influences colony dynamics and behavior by regulating queen number in colonies of fire ants (Ross 1997; Ross and Keller 1998; Krieger and Ross 2002; Gotzek and Ross 2007; Gotzek *et al.* 2007). Three of these *Gp9*-like genes were significantly upregulated from control to live manipulation in *C. floridanus*, while the fourth was down-regulated. Although the expression profiles of *C. castaneus* homologs did not match in this case, relatable patterns of odorant receptor and OBP dysregulation were found in manipulated *C. castaneus* (de Bekker *et al.* 2015).

Fungal serine proteases are upregulated during manipulated biting behavior.

The presence of an evolutionarily recent group of subtilases with unclear function that lack I9 domains may be associated with niche adaptation in the Entomophtoromycotina, fungal entomopathogens distantly related to *Ophiocordyceps*. Among the Entomophthoromycotina, the insect manipulating *Entomophthora muscae* and *Pandora formicae* have I9-lacking subtilases, albeit not exclusively (Arnesen *et al.* 2018). These subtilases have been suggested to represent hallmarks of niche specialization (Arnesen *et al.* 2018). A comparison of this protease group to subtilases of Ascomycetes demonstrated a notable dissimilarity. However, the representative of *Ophiocordyceps* in that analysis was a lepidopteran parasite

outside the *O. unilateralis* species complex, *Ophiocordyceps sinesis* (Arnesen *et al.* 2018). Of the differentially expressed S8A subtilases in *O. camponoti-floridani*, two lacked inhibitor I9 domains (one with 38-fold increase, the other increasing from 0 RPKM to 4 RPKM).

Fungal secondary metabolites involved in manipulation and infection.

Cluster 12 is predicted to synthesize a compound similar to the polyketide citrinin. This mycotoxin is lethal to insects with nephrotoxic effects on Malpighian tubules, which perform kidney-like functions (Dowd 1989). Cluster 12 contains a backbone PKS that is a putative homolog to the citrinin PKS gene citS of *Monascus ruber* (BLASTp E-value = 4.49e-120) (He and Cox 2016). Additionally, genes in this cluster had high BLASTp matches to CitA and CitE that also participate in citrinin synthesis (E-value = 1.68e-60 and 1.56e-14 respectively). One cluster 12 gene was present in the manipulation correlated fungal WGCNA module F1 and two were present in F2. However, no suitable matches were found within this cluster for the remaining cluster synthesis genes *citC*, *citD*, or *citB*. Although, these genes did have hits elsewhere in the genome. Of these putative citrinin synthesis homologs, only *citA* appeared differentially expressed, being upregulated during manipulation and host death in both *O. camponoti-floridani* and *O. kimflemingiae*. Possibly, cluster 12 genes are active and play an earlier role in infection than our sampling regime was able to capture.

APPENDIX D: ANT PC1 TOP 20 GENES

Genes are ranked by loading value in descending order (0.099 – 0.063). For every gene, normalized expression values were highest in control samples and lowest in dead manipulated samples. Column “Homolog” refers to presence of a homolog between the current *C. floridanus* assembly and proteins annotated in de Bekker et al. (2015) with similar RNAseq normalized expression patterns to our study. Comments related to putative functions are from Uniprot (Bateman 2019) and Interpro (Finn *et al.* 2017).

BLAST	**PFAM**	**Homolog**	**Comments**
uncharacterized LOC105257597	PF00026|Eukaryotic aspartyl protease, PF00026|Eukaryotic aspartyl protease	no	Lysosome activity
protein CREG1	PF13883|Pyridoxamine 5'-phosphate oxidase	no	Control of cell growth and apoptosis
lysosomal aspartic protease	PF00026|Eukaryotic aspartyl protease	yes	Lysosome activity
myogenesis-regulating glycosidase-like	PF01055|Glycosyl hydrolases family 31	no	Muscle related via interaction with IGF2, jaw adductors known to be hypercontracted and degraded
lysosomal aspartic protease	PF00026|Eukaryotic aspartyl protease	no	Lysosome activity
NA	NA	no	
alpha-amylase 1	PF00128|Alpha amylase, catalytic domain, PF02806|Alpha amylase, C-terminal all-beta domain	no	Starch catabolism, may suggest reduction in food intake
venom acid phosphatase Acph-1	PF00328|Histidine phosphatase superfamily (branch 2)	no	Possibly a non-venom acid phosphatase associated with lysosomes, as *acph-1* is

			associated with venom glands absent in ant heads
NA	NA	no	
regucalcin	PF08450|SMP-30/Gluconolactonase/LRE-like region	no	Modulates calcium dependent processes and signaling
alpha-amylase A-like	PF02806|Alpha amylase, C-terminal all-beta domain, PF00128|Alpha amylase, catalytic domain	yes	Starch catabolism, may suggest reduction in food intake
uncharacterized LOC105253145	PF00135|Carboxylesterase family	no	
venom acid phosphatase Acph-1-like	PF00328|Histidine phosphatase superfamily (branch 2)	no	Possibly a non-venom acid phosphatase associated with lysosomes, as *acph-1* is associated with venom glands absent in ant heads
uncharacterized LOC105250203	PF07464|Apolipophorin-III precursor (apoLp-III)	yes	Fat body and lipid regulation, possibly link to starvation/hunger signaling
NA	NA	no	
pheromone-binding protein Gp-9-like	PF01395|PBP/GOBP family	no	Odorant binding
troponin C-like	PF13499|EF-hand domain pair; PF13833|EF-hand domain pair	no	
cytochrome P450 4g15-like	PF00067|Cytochrome P450	no	Steroid synthesis

actin, muscle	PF00022|Actin	no	Muscle related, jaw adductors known to be hypercontracted and degraded
uncharacterized LOC105258464	PF01395|PBP/GOBP family	no	Odorant binding

APPENDIX E: ANT PC2 TOP 20 GENES

Genes are ranked by loading value in descending order (0.098 - 0.054). Column “Homolog” refers to presence of a homolog between the current *C. floridanus* assembly and proteins annotated in de Bekker et al. (2015) with corresponding RNAseq data displaying similar patterns to our study. Comments related to putative functions are from Uniprot (Bateman 2019) and Interpro (Finn *et al.* 2017).

BLAST	**PFAM**	**Homolog**	**Comments**
NA	NA	no	
NA	NA	no	
uncharacterized LOC105253145	PF00135|Carboxylesterase family	no	
uncharacterized LOC105254189	PF13639|Ring finger domain	yes	
cytochrome P450 9e2	PF00067|Cytochrome P450	no	
sialin	NAPF07690|Major Facilitator Superfamily	yes	
uncharacterized LOC105251735	NA	yes	
pheromone-binding protein Gp-9-like	PF01395|PBP/GOBP family	no	Odorant binding
NA	NA	no	
uncharacterized LOC112639471	PF15430|Single domain von Willebrand factor type C	no	Response to infection and changes in nutritional status, especially in arthropods.
protein CREG1	PF13883|Pyridoxamine 5'-phosphate oxidase	no	Control of cell growth and apoptosis
defensin	PF01097|Arthropod defensin	no	Arthropod immunity, especially against bacteria

uncharacterized LOC112639414	PF01395|PBP/GOBP family	no	Odorant binding
2-amino-3-ketobutyrate coenzyme A ligase, mitochondrial-like	PF00155|Aminotransferase class I and II	no	
uncharacterized LOC105255569	PF13445|RING-type zinc-finger, PF00240|Ubiquitin family	no	
regucalcin	PF08450|SMP-30/Gluconolactonase/LRE-like region	no	Modulates calcium dependent processes and signaling
ankyrin-1	PF07525|SOCS box, PF00023|Ankyrin repeat, PF12796|Ankyrin repeat	yes	
protein CREG1	PF13883|Pyridoxamine 5'-phosphate oxidase	yes	Control of cell growth and apoptosis
cytochrome P450 4C1-like	PF00067|Cytochrome P450	no	JH interacting, starvation response (Lu *et al.* 1999)
WEB family protein At4g27595, chloroplastic	NA	no	Most BLAST results lacked meaningful annotations

APPENDIX F: FUNGAL PC1 TOP 20 GENES

Genes are ranked by highest to lowest loading value (0.084 – 0.062). All have homologs in *O. kimflemingiae* with peak RPKM during live manipulation (de Bekker *et al.* 2015). Comments related to putative functions are from Uniprot (Bateman 2019) and Interpro (Finn *et al.* 2017).

BLAST	**PFAM**	**Secretion**	**Comments**
MFS transporter	PF07690|MFS_1		Small solute transporter
protein kinase domain protein		SignalP, SSP	
aromatic prenyl transferase	PF11991|Trp_DMAT		Cluster 18 (aflatrem)
GPI anchored serine-rich protein			
G-protein coupled receptor protein	PF00002|7tm_2		
SCP-like extracellular protein	PF00188|CAP	SignalP	Cysteine-rich secretory proteins, antigen 5, and pathogenesis-related 1 protein
alpha-ketoglutarate-dependent taurine dioxygenase	PF02668|TauD		
putative enterotoxin	PF01375|Enterotoxin_a	SignalP	Highly expressed and most homologous enterotoxin
amidohydrolase family protein	PF04909|Amidohydro_2		
P450 monooxygenase	PF00067|p450		Cluster 18 (aflatrem)
prenyl transferase	PF00348|polyprenyl_synt		Cluster 18 (aflatrem)
P450 monooxygenase	PF01494|FAD_binding_3, PF00067|p450		Cluster 18 (aflatrem)
beta-lactamase family protein	PF11954|DUF3471, PF00144|Beta-lactamase		Antibiotic resistance

P450 monooxygenase	PF00067|p450		Cluster 18 (aflatrem)
hypothetical protein CDD80_6012		SignalP, SSP	
hypothetical protein CDD80_6620		SignalP, SSP	
tyrosinase 2	PF00264|Tyrosinase	SignalP	Associated with melanin production, stress and immune interactions
carbohydrate-binding module family 19 protein			
AtmB protein			Cluster 18 (aflatrem)
Pyruvate/Phosphoenolpyruvate kinase	PF13714|PEP_mutase, PF00463|ICL		

APPENDIX G: WGCNA OF ANT NORMALIZED GENE EXPRESSION DATA CORRELATED TO SAMPLE TYPE

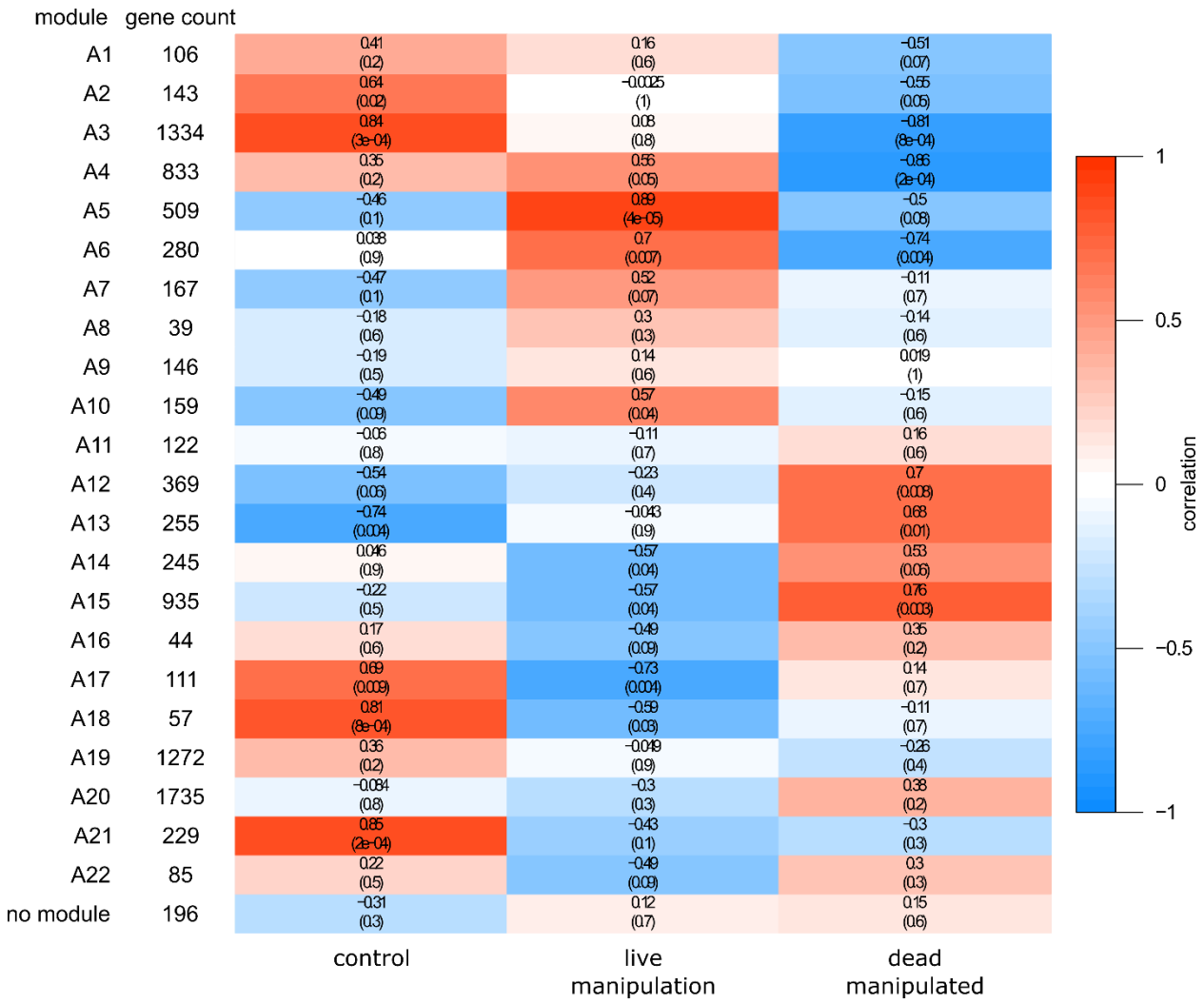

Correlation values are the top value in each cell, the p-values are in parentheses below.

APPENDIX H: ANT GENES LEADING TO ENRICHMENT OF THE RHODOPSIN FAMILY 7 TRANSMEMBRANE PFAM DOMAIN IN ANT WGCNA MODULES A14 AND A15

Some of these genes are putatively involved in light sensing as rhodopsin, but many BLAST annotations seemingly indicate diverse cell signaling functions related to neurotransmitters. 5-hydroxtryptamine is synonymous with serotonin.

BLAST annotation
5-hydroxytryptamine receptor 1
5-hydroxytryptamine receptor 2A
5-hydroxytryptamine receptor 2B
adenosine receptor A2b
allatostatin-A receptor
alpha-2A adrenergic receptor
cholecystokinin receptor type A
dopamine D2-like receptor
dopamine receptor 1
dopamine receptor 2
G-protein coupled receptor 52
lutropin-choriogonadotropic hormone receptor
melatonin receptor type 1B
muscarinic acetylcholine receptor DM1
neuropeptide CCHamide-2 receptor
neuropeptide FF receptor 1
neuropeptides capa receptor
octopamine receptor beta-1R
octopamine receptor beta-3R
opsin, ultraviolet-sensitive
probable G-protein coupled receptor B0563.6

pyrokinin-1 receptor

somatostatin receptor type 2

tachykinin-like peptides receptor 99D

trace amine-associated receptor 2-like

tyramine receptor 1

uncharacterized

uncharacterized

uncharacterized

APPENDIX I: ANT GENES LEADING TO ENRICHMENT OF IMMUNOGLOBULIN PFAM DOMAINS IN ANT WGCNA MODULES A14 AND A15

Many of these genes have developmental and functional associations with neuronal tissues (but not always exclusively).

BLAST annotation	Neuron associated	References
basement membrane-specific heparan sulfate proteoglycan core protein	yes	(Lindner *et al.* 2007; Cho *et al.* 2012)
cell adhesion molecule 2	-	
Down syndrome cell adhesion molecule-like protein Dscam2	yes	(Clandinin and Zipursky 2002; Lah *et al.* 2014)
follistatin-related protein 5	yes	(Bickel *et al.* 2008; Pentek *et al.* 2009)
hemicentin-2	-	
igLON family member 5	yes	(Carrillo *et al.* 2015)
immunoglobulin domain-containing protein oig-4	yes	(Rapti *et al.* 2011; Sengupta *et al.* 2019)
inactive tyrosine-protein kinase 7	-	
irregular chiasm C-roughest protein	yes (esp. antennae)	(Ramos *et al.* 1993; Venugopala Reddy *et al.* 1999)
lachesin	yes	(Karlstrom *et al.* 1993; Strigini *et al.* 2006)
leucine-rich repeat-containing protein 24	yes	(Dolan *et al.* 2007; Carrillo *et al.* 2015)

leucine-rich repeat-containing protein 4	yes	(Dolan *et al.* 2007; Carrillo *et al.* 2015)
neogenin	yes	(Wilson and Key 2007)
nephrin	yes (mammal) nephrocytes (insect)	(Zhuang *et al.* 2009; Li *et al.* 2011)
netrin receptor UNC5C	yes	(Keleman and Dickson 2001; Kang *et al.* 2019)
neuroglian	yes	(Godenschwege and Murphey 2009; Goossens *et al.* 2011)
neurotrimin	yes (mammal)	(Krizsan-Agbas *et al.* 2008; Sanz *et al.* 2015)
neurotrimin-like	yes	(Krizsan-Agbas *et al.* 2008; Sanz *et al.* 2015)
obscurin	- (muscle)	(Katzemich *et al.* 2012, 2015)
opioid-binding protein/cell adhesion molecule homolog	yes (mammal)	(Miyata *et al.* 2003; Reed *et al.* 2007)
peroxidasin	-	
protein borderless	yes	(Shaw *et al.* 2019)

protogenin	yes	(Wong *et al.* 2010; Yu *et al.* 2013)
T-lymphocyte activation antigen CD86	-	
tyrosine-protein phosphatase Lar	yes	(Sethi *et al.* 2010; Agrawal and Hardin 2016)
zwei Ig domain protein zig-8	yes	(Bénard *et al.* 2012; Cheng *et al.* 2019)

APPENDIX J: WGCNA OF FUNGAL NORMALIZED GENE EXPRESSION DATA CORRELATED TO SAMPLE TYPE

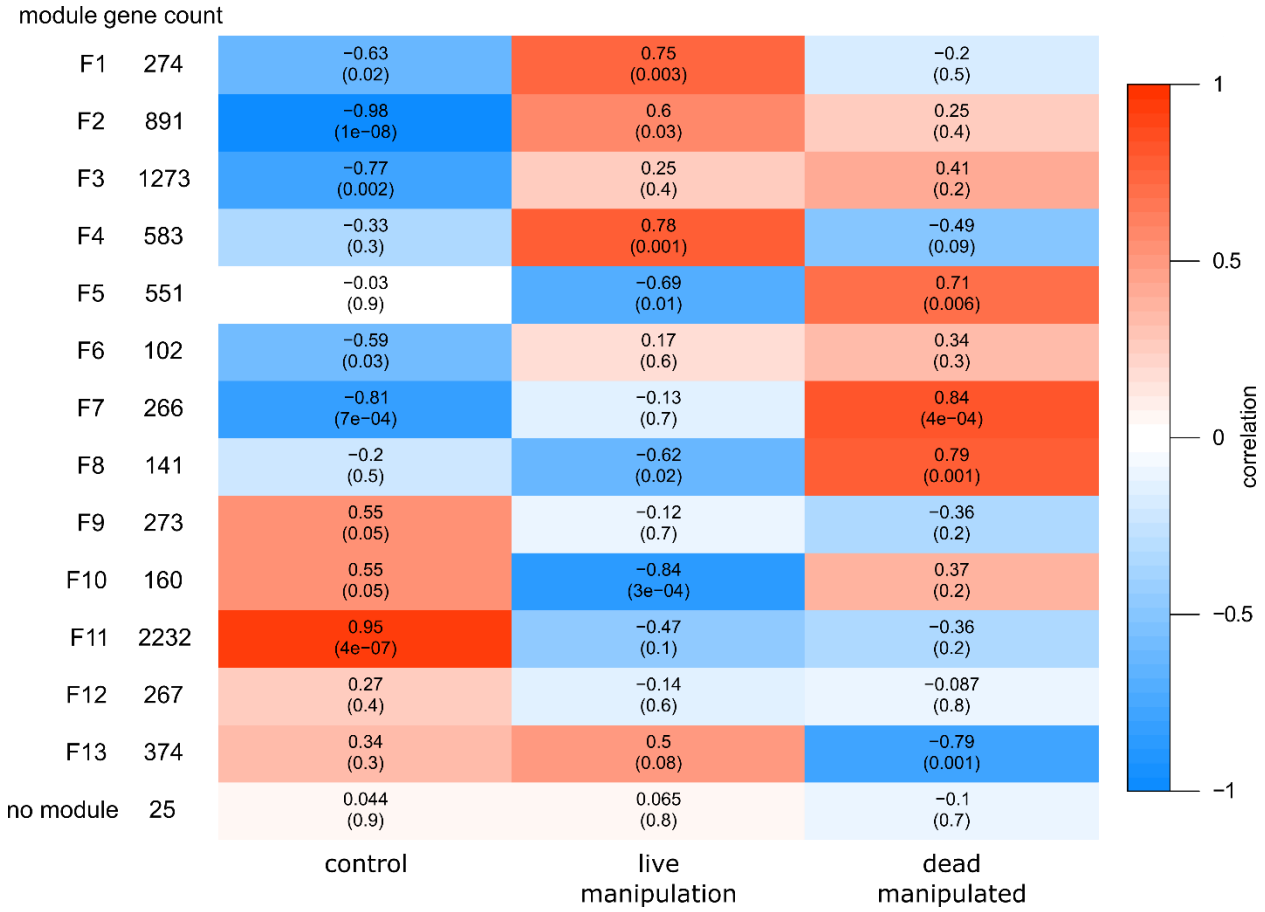

Correlation values are the top value in each cell, the p-values are in parentheses below.

APPENDIX K: PUTATIVELY SECRETED PROTEINS ARE TRANSCRIBED DURING MANIPULATION, BUT MANY GENES LACK FUNCTIONAL PFAM DOMAIN ANNOTATION

	SignalP		SSP	
	Total	**PFAM**	**Total**	**PFAM**
Genome	801	409	271	52
Upregulated	77	39	31	6
Upregulated from culture	239	129	85	19

APPENDIX L: CARNOSINE SYNTHASE PROTEIN ALIGNMENT

One of the fungal genes possibly related to carnosine synthase contained only the two ATP-grasp and one ligase domains. This gene has been annotated as a glutathione synthetase ATP-binding domain-like protein (Will *et al.* 2020), however BLASTp searches against the NCBI nr database displayed mixed results. This annotation largely reflects glutathione synthetase being the most common BLAST description in the top 20 BLASTp hits, discounting "hypothetical protein" and "uncharacterized protein" descriptions. However, the top glutathione synthetase hit only had a 36% pairwise identity to this gene (e-value = 5E-123). Other BLAST descriptions were carnosine synthase 1 (top hit 46% pairwise identity, e-value = 2E-175) and ATP-grasp domain-containing protein (top hit 54% pairwise identity, e-value = 9E-111). Although there were hits to putative carnosine synthase 1 genes from two fungi, those annotations were not investigated past initial high-throughput genome annotation (Yin *et al.* 2015; Smit *et al.* 2016). Following (Drozak *et al.* 2010), we aligned the C-terminal 450 amino acids of the protein sequences of this *O. camponoti-floridani* gene and carnosine synthase or putative ancestral genes from chicken, oyster, and the four bacteria used in (Drozak *et al.* 2010) (Appx. L Fig. 1A). We additionally included two random *O. camponoti-flordani* sequences of the same length as the candidate gene (658 amino acids) as estimates of pairwise identity found at random (Appx. L Fig. 1B). The animal carnosine synthases had 40% pairwise identity and the bacterial sequences had 25-46% among each other. Compared to these proteins, the candidate *O. camponoti-floridani* protein had 13-17% pairwise identity, which was similar to the range between the animal and bacterial sequences 15-19%. Most dissimilar from the rest, the two *O. camponti-floridani* "random genes" had 7-11% pairwise identity to any other sequences tested (Appx. L Fig. 1B). The candidate *O. camponoti-floridani* gene was also not a DEG during manipulation, but rather consistently and lowly expressed. Despite limited evidence regarding carnosine synthase activity by this *O. camponoti-floridani* protein, it appears to be a stronger candidate than any protein encoded in the ant genome. As carnosine was not detected above our data quality criteria and there are no ant genes

annotated with domains in a manner possibly linked to carnosine synthase, the fungus remains the more likely organism producing carnosine.

A

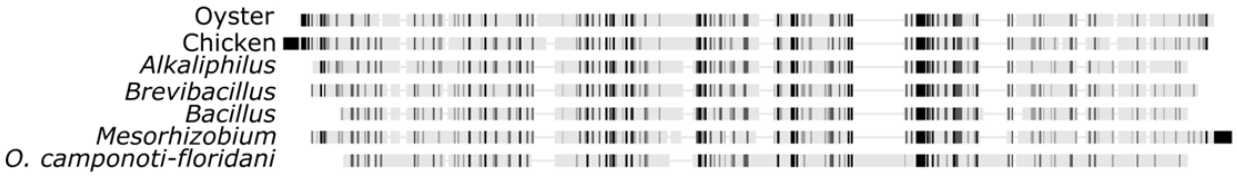

B

	Oyster	Chicken	*A. m.*	*B. b.*	*B. m.*	*M. o.*	*O. c.* (1)	*O. c.* (2)	*O. c.* (3)
Oyster									
Chicken	40.397								
Alkaliphilus metalliredigens	15.367	17.716							
Brevibacillus brevis	14.612	18.119	30.31						
Bacillus mycoides	15.144	18.357	32.01	45.96					
Mesorhizobium opportunistum	14.597	19.121	24.941	29.524	27.889				
***O. camponoti-floridani* (1)**	14.465	17.089	16.702	16.667	13.889	12.903			
***O. camponoti-floridani* (2)**	6.963	10.557	7.937	10.621	8.842	10.621	7.353		
***O. camponoti-floridani* (3)**	8.039	8.4	8.932	9.595	7.175	8.853	7.863	6.1	

Appendix 12 Figure 1. Protein sequence alignment of the C-terminal 450 amino acids of animal carnosine synthases, putative ancestral-like bacteria proteins, and an *O. camponoti-floridani* candidate protein.
(A) MAFFT alignments of the protein sequences showing 100% similarity (black), > 80% (dark gray), > 60% (light gray), and < 60% (faint shading). (B) Pairwise identities for the sequences aligned in (A), with higher identity colored red and lower as blue. The *O. camponoti-floridani* candidate had similar pairwise identity to the animal carnosine synthases as the putative ancestral sequences from the bacteria. Sequence *O. camponoti-floridani* (1) is the candidate and (2-3) are from genes selected at random with the same length as (1). GenBank accessions are as follows: Oyster (DAA12499.1), Chicken (NP_001166064.1), *A. metallredigens* (WP_012063195.1), *B. brevis* (WP_015893420.1), *B. mycoides* (ZP_04160564.1), *M. opportunistum* (ZP_05810115.1), *O. camponoti-floridani* (1) (KAF4585988.1), *O. camponoti-floridani* (2) (KAF4585763.1), and *O. camponoti-floridani* (3) (KAF4584313.1).

REFERENCES

Ables, E. T., K. E. Bois, C. A. Garcia, and D. Drummond-Barbosa, 2015 Ecdysone response gene E78 controls ovarian germline stem cell niche formation and follicle survival in Drosophila. Dev. Biol. 400: 33.

Acharjee, A., J. Larkman, Y. Xu, V. R. Cardoso, and G. V. Gkoutos, 2020 A random forest based biomarker discovery and power analysis framework for diagnostics research. BMC Med. Genomics 13: 1–14.

Adamo, S. A., 2008 Norepinephrine and octopamine: linking stress and immune function across phyla. ISJ 5: 12–19.

Adamo, S. A., 2019 Turning your victim into a collaborator: exploitation of insect behavioral control systems by parasitic manipulators. Curr. Opin. Insect Sci. 33: 25–29.

Adamo, S. A., A. Bartlett, J. Le, N. Spencer, and K. Sullivan, 2010 Illness-induced anorexia may reduce trade-offs between digestion and immune function. Anim. Behav. 79: 3–10.

Adamo, S. A., C. E. Linn, and N. E. Beckage, 2013 Parasites: evolution's neurobiologists. J. Exp. Biol. 216: 3–10.

Agrawal, P., and P. E. Hardin, 2016 The Drosophila Receptor Protein Tyrosine Phosphatase LAR Is Required for Development of Circadian Pacemaker Neuron Processes That Support Rhythmic Activity in Constant Darkness But Not during Light/Dark Cycles. J. Neurosci. 36: 3860–70.

Aguilar, R., J. L. Maestro, L. Vilaplana, N. Pascual, M. D. Piulachs *et al.*, 2003 Allatostatin gene expression in brain and midgut, and activity of synthetic allatostatins on feeding-related processes in the cockroach Blattella germanica. Regul. Pept. 115: 171–177.

Alecu, I., and S. A. L. Bennett, 2019 Dysregulated lipid metabolism and its role in α-synucleinopathy in Parkinson's disease. Front. Neurosci. 13: 328.

Almagro Armenteros, J. J., K. D. Tsirigos, C. K. Sønderby, T. N. Petersen, O. Winther *et al.*, 2019

SignalP 5.0 improves signal peptide predictions using deep neural networks. Nat. Biotechnol. 37: 420–423.

Altschul, S. F., W. Gish, W. Miller, E. W. Myers, and D. J. Lipman, 1990 Basic local alignment search tool. J. Mol. Biol. 215: 403–410.

Ament, S. A., M. Corona, H. S. Pollock, and G. E. Robinson, 2008 Insulin signaling is involved in the regulation of worker division of labor in honey bee colonies. Proc. Natl. Acad. Sci. U. S. A. 105: 4226–31.

Ament, S. A., Y. Wang, and G. E. Robinson, 2010 Nutritional regulation of division of labor in honey bees: toward a systems biology perspective. Wiley Interdiscip. Rev. Syst. Biol. Med. 2: 566–576.

Ammari, M. G., C. R. Gresham, F. M. McCarthy, and B. Nanduri, 2016 HPIDB 2.0: a curated database for host–pathogen interactions. Database 2016: 103.

Andersen, S. B., M. Ferrari, H. C. Evans, S. L. Elliot, J. J. Boomsma *et al.*, 2012 Disease dynamics in a specialized parasite of ant societies (J. A. R. Marshall, Ed.). PLoS One 7: e36352.

Andersen, S. B., S. Gerritsma, K. M. Yusah, D. Mayntz, N. L. Hywel-Jones *et al.*, 2009 The Life of a Dead Ant: The Expression of an Adaptive Extended Phenotype. Am. Nat. 174: 424–433.

Andrews, R. K., and M. C. Berndt, 2000 Snake venom modulators of platelet adhesion receptors and their ligands. Toxicon 38: 775–791.

Andriolli, F. S., N. K. Ishikawa, R. Vargas-Isla, T. S. Cabral, C. de Bekker *et al.*, 2019 Do zombie ant fungi turn their hosts into light seekers? Behav. Ecol. 30: 609–616.

Aonuma, H., and T. Watanabe, 2012 Changes in the content of brain biogenic amine associated with early colony establishment in the Queen of the ant, Formica japonica. PLoS One 7: e43377–e43377.

Araújo, J. P. M., H. C. Evans, R. Kepler, and D. P. Hughes, 2018 Zombie-ant fungi across continents: 15 new species and new combinations within Ophiocordyceps. I. Myrmecophilous hirsutelloid species. Stud. Mycol.

Araújo, J. P. M., and D. P. Hughes, 2019 Zombie-Ant Fungi Emerged from Non-manipulating, Beetle-Infecting Ancestors. Curr. Biol.

Arnesen, J. A., J. Małagocka, A. Gryganskyi, I. V Grigoriev, K. Voigt *et al.*, 2018 Early Diverging Insect-Pathogenic Fungi of the Order Entomophthorales Possess Diverse and Unique Subtilisin-Like Serine Proteases. G3 8: 3311–3319.

Ashburner, M., C. A. Ball, J. A. Blake, D. Botstein, H. Butler *et al.*, 2000 Gene Ontology: tool for the unification of biology. Nat. Genet. 25: 25–29.

Barchuk, A. R., A. S. Cristino, R. Kucharski, L. F. Costa, Z. L. P. Simões *et al.*, 2007 Molecular determinants of caste differentiation in the highly eusocial honeybee Apis mellifera. BMC Dev. Biol. 7: 70.

Bartzis, G., J. Deelen, J. Maia, W. Ligterink, H. W. M. Hilhorst *et al.*, 2017 Estimation of metabolite networks with regard to a specific covariable: applications to plant and human data. Metabolomics 13: 129.

Bateman, A., 2019 UniProt: a worldwide hub of protein knowledge. Nucleic Acids Res. 47: D506–D515.

Bateman, A., M. J. Martin, S. Orchard, M. Magrane, R. Agivetova *et al.*, 2021 UniProt: the universal protein knowledgebase in 2021. Nucleic Acids Res. 49: D480–D489.

Batrakov, S. G., I. V. Konova, V. I. Sheichenko, S. E. Esipov, and L. A. Galanina, 2001 Two unusual glycerophospholipids from a filamentous fungus, Absidia corymbifera. Biochim. Biophys. Acta - Mol. Cell Biol. Lipids 1531: 169–177.

Baumel, B. S., P. M. Doraiswamy, M. Sabbagh, and R. Wurtman, 2021 Potential Neuroregenerative and Neuroprotective Effects of Uridine/Choline-Enriched Multinutrient Dietary Intervention for Mild Cognitive Impairment: A Narrative Review. Neurol. Ther. 10: 43–60.

Beckerson, W. C., R. C. Rodríguez De La Vega, F. E. Hartmann, M. Duhamel, T. Giraud *et al.*, 2019 Cause and effectors: Whole-genome comparisons reveal shared but rapidly evolving effector sets

among host-specific plant-castrating fungi. MBio 10:.

Beckstead, R. B., G. Lam, and C. S. Thummel, 2007 Specific transcriptional responses to juvenile hormone and ecdysone in Drosophila. Insect Biochem. Mol. Biol. 37: 570–8.

de Bekker, C., 2019 Ophiocordyceps–ant interactions as an integrative model to understand the molecular basis of parasitic behavioral manipulation. Curr. Opin. Insect Sci. 33: 19–24.

de Bekker, C., W. C. Beckerson, and C. Elya, 2021 Mechanisms behind the Madness: How Do Zombie-Making Fungal Entomopathogens Affect Host Behavior To Increase Transmission? (D. A. Garsin, Ed.). MBio.

de Bekker, C., and B. Das, 2022 Hijacking time: How Ophiocordyceps fungi could be using ant host clocks to manipulate behavior. Parasite Immunol. 44: e12909.

de Bekker, C., M. Merrow, and D. P. Hughes, 2014a From behavior to mechanisms: An integrative approach to the manipulation by a parasitic fungus (Ophiocordyceps unilateralis s.l.) of its host ants (Camponotus spp.). Integr. Comp. Biol. 52: 166–176.

de Bekker, C., R. A. Ohm, H. C. Evans, A. Brachmann, and D. P. Hughes, 2017a Ant-infecting Ophiocordyceps genomes reveal a high diversity of potential behavioral manipulation genes and a possible major role for enterotoxins. Sci. Rep. 7: 12508.

de Bekker, C., R. A. Ohm, R. G. Loreto, A. Sebastian, I. Albert *et al.*, 2015 Gene expression during zombie ant biting behavior reflects the complexity underlying fungal parasitic behavioral manipulation. BMC Genomics 16: 620.

de Bekker, C., L. E. Quevillon, P. B. Smith, K. R. Fleming, D. Ghosh *et al.*, 2014b Species-specific Ant Brain Manipulation by a Specialized Fungal Parasite. BMC Evol. Biol. 14: 166.

de Bekker, C., I. Will, B. Das, and R. M. Adams, 2018 The ants (Hymenoptera: Formicidae) and their parasites: effects of parasitic manipulations and host responses on ant behavioral ecology. Myrmecological News 28: 1–24.

de Bekker, C., I. Will, D. P. Hughes, A. Brachmann, and M. Merrow, 2017b Daily rhythms and enrichment patterns in the transcriptome of the behavior-manipulating parasite Ophiocordyceps kimflemingiae. PLoS One 12:.

Bellia, F., G. Vecchio, S. Cuzzocrea, V. Calabrese, and E. Rizzarelli, 2011 Neuroprotective features of carnosine in oxidative driven diseases. Mol. Aspects Med. 32: 258–266.

Ben-Shahar, Y., H.-T. Leung, W. L. Pak, M. B. Sokolowski, and G. E. Robinson, 2003 cGMP-dependent changes in phototaxis: a possible role for the foraging gene in honey bee division of labor. J. Exp. Biol. 206: 2507–15.

Ben-Shahar, Y., A. Robichon, M. B. Sokolowski, and G. E. Robinson, 2002 Influence of gene action across different time scales on behavior. Science (80-.). 296: 741–744.

Bénard, C. Y., C. Blanchette, J. Recio, and O. Hobert, 2012 The Secreted Immunoglobulin Domain Proteins ZIG-5 and ZIG-8 Cooperate with L1CAM/SAX-7 to Maintain Nervous System Integrity (A. D. Chisholm, Ed.). PLoS Genet. 8: e1002819.

van den Berg, M. J., and G. Ziegelberger, 1991 On the function of the pheromone binding protein in the olfactory hairs of Antheraea polyphemus. J. Insect Physiol. 37: 79–85.

Bickel, D., R. Shah, S. C. Gesualdi, and T. E. Haerry, 2008 Drosophila Follistatin exhibits unique structural modifications and interacts with several TGF-β family members. Mech. Dev. 125: 117–129.

Bjorum, S. M., R. A. Simonette, R. Alanis, J. E. Wang, B. M. Lewis *et al.*, 2013 The Drosophila BTB Domain Protein Jim Lovell Has Roles in Multiple Larval and Adult Behaviors. PLoS One 8: 61270.

Bloch, G., A. Hefetz, and K. Hartfelder, 2000 Ecdysteroid titer, ovary status, and dominance in adult worker and queen bumble bees (Bombus terrestris). J. Insect Physiol. 46: 1033–1040.

Bok, J. W., and N. P. Keller, 2004 LaeA, a Regulator of Secondary Metabolism in Aspergillus spp. Eukaryot. Cell 3: 527.

Boldyrev, A. A., G. Aldini, and W. Derave, 2013 Physiology and pathophysiology of carnosine. Physiol. Rev. 93: 1803–1845.

Bonasio, R., G. Zhang, C. Ye, N. S. Mutti, X. Fang *et al.*, 2010 Genomic comparison of the ants Camponotus floridanus and Harpegnathos saltator. Science (80-.). 329: 1068–1071.

Boulay, R., V. Soroker, E. J. Godzinska, A. Hefetz, and A. Lenoir, 2000 Octopamine reverses the isolation-induced increase introphallaxis in the carpenter ant Camponotus Fellah. Journgal Exp. Biol. 203: 513–520.

Brent, C., C. Peeters, V. Dietmann, R. Crewe, and E. Vargo, 2006 Hormonal correlates of reproductive status in the queenless ponerine ant, Streblognathus peetersi. J. Comp. Physiol. A 192: 315–320.

Brown, D. W., T. H. Adams, N. P. Keller, D. W. Udwary, and C. A. Townsend, 1996 Aspergillus has distinct fatty acid synthases for primary and secondary metabolism. Proc. Natl. Acad. Sci. U. S. A. 93: 14873–7.

Burrows, M., and G. P. Sutton, 2012 Locusts use a composite of resilin and hard cuticle as an energy store for jumping and kicking. J. Exp. Biol. 215: 3501–3512.

Bushnell, B., 2019 BBMap.

Cardoso Neto, J. A., L. C. Leal, and F. B. Baccaro, 2019 Temporal and spatial gradients of humidity shape the occurrence and the behavioral manipulation of ants infected by entomopathogenic fungi in Central Amazon. Fungal Ecol. 42: 100871.

Carillo, P., 2018 GABA shunt in durum wheat. Front. Plant Sci. 9: 100.

Carlson, M. R. J., B. Zhang, Z. Fang, P. S. Mischel, S. Horvath *et al.*, 2006 Gene connectivity, function, and sequence conservation: Predictions from modular yeast co-expression networks. BMC Genomics 7: 1–15.

Carrillo, R. A., E. Özkan, K. P. Menon, S. Nagarkar-Jaiswal, P.-T. Lee *et al.*, 2015 Control of Synaptic Connectivity by a Network of Drosophila IgSF Cell Surface Proteins. Cell 163: 1770–1782.

Cassilly, C. D., and T. B. Reynolds, 2018 PS, It's Complicated: The Roles of Phosphatidylserine and Phosphatidylethanolamine in the Pathogenesis of Candida albicans and Other Microbial Pathogens. J. Fungi 4:.

Cen, K., B. Li, Y. Lu, S. Zhang, and C. Wang, 2017 Divergent LysM effectors contribute to the virulence of Beauveria bassiana by evasion of insect immune defenses. PLOS Pathog. 13: e1006604.

Ceriani, M. F., J. B. Hogenesch, M. Yanovsky, S. Panda, M. Straume *et al.*, 2002 Genome-wide expression analysis in Drosophila reveals genes controlling circadian behavior. J. Neurosci. 22: 9305–19.

Chandra, V., I. Fetter-Pruneda, P. R. Oxley, A. L. Ritger, S. K. McKenzie *et al.*, 2018 Social regulation of insulin signaling and the evolution of eusociality in ants. Science (80-.). 361: 398–402.

Chang, H., Y. Liu, T. Yang, P. Pelosi, S. Dong *et al.*, 2015 Pheromone binding proteins enhance the sensitivity of olfactory receptors to sex pheromones in Chilo suppressalis. Sci. Rep. 5: 13093.

Chatr-aryamontri, A., A. Ceol, L. M. Palazzi, G. Nardelli, M. V. Schneider *et al.*, 2007 MINT: the Molecular INTeraction database. Nucleic Acids Res. 35: D572.

Chen, M., C. J.-T. Ju, G. Zhou, X. Chen, T. Zhang *et al.*, 2019 Multifaceted protein–protein interaction prediction based on Siamese residual RCNN. Bioinformatics 35: i305–i314.

Cheng, Y. C., M. C. Chiang, H. Y. Shih, T. L. Ma, T. H. Yeh *et al.*, 2015 The transcription factor hairy/E(spl)-related 2 induces proliferation of neural progenitors and regulates neurogenesis and gliogenesis. Dev. Biol. 397: 116–128.

Cheng, Q., and C. A. Michels, 1989 The maltose permease encoded by the MAL61 gene of Saccharomyces cerevisiae exhibits both sequence and structural homology to other sugar transporters. Genetics 123: 477–484.

Cheng, S., Y. Park, J. D. Kurleto, M. Jeon, K. Zinn *et al.*, 2019 Family of neural wiring receptors in bilaterians defined by phylogenetic, biochemical, and structural evidence. Proc. Natl. Acad. Sci. U.

S. A. 116: 9837–9842.

Cheng, Q., H. Wang, B. Xu, S. Zhu, L. Hu *et al.*, 2014 Discovery of a novel small secreted protein family with conserved N-terminal IGY motif in Dikarya fungi. BMC Genomics 15: 1–12.

Chetouhi, C., J. Panek, L. Bonhomme, H. ElAlaoui, C. Texier *et al.*, 2015 Cross-talk in host–parasite associations: What do past and recent proteomics approaches tell us? Infect. Genet. Evol. 33: 84–94.

Chiariello, M., J. P. Vaqué, P. Crespo, and J. S. Gutkind, 2010 Activation of Ras and Rho GTPases and MAP Kinases by G-Protein-Coupled Receptors. Methods Mol. Biol. 661: 137–150.

Cho, J. Y., K. Chak, B. J. Andreone, J. R. Wooley, and A. L. Kolodkin, 2012 The extracellular matrix proteoglycan perlecan facilitates transmembrane semaphorin-mediated repulsive guidance. Genes Dev. 26: 2222–35.

Choi, M.-Y., K. S. Han, K. S. Boo, and R. A. Jurenka, 2002 Pheromone biosynthetic pathways in the moths Helicoverpa zea and Helicoverpa assulta. Insect Biochem. Mol. Biol. 32: 1353–1359.

Choi, M.-Y., R. K. Vander Meer, M. Coy, and M. E. Scharf, 2012 Phenotypic impacts of PBAN RNA interference in an ant, Solenopsis invicta, and a moth, Helicoverpa zea. J. Insect Physiol. 58: 1159–1165.

Christianson, J. C., T. A. Shaler, R. E. Tyler, and R. R. Kopito, 2008 OS-9 and GRP94 deliver mutant α1-antitrypsin to the Hrd1-SEL1L ubiquitin ligase complex for ERAD. Nat. Cell Biol. 10: 272.

Chung, T. Y., P. F. Sun, J. I. Kuo, Y. I. Lee, C. C. Lin *et al.*, 2017 Zombie ant heads are oriented relative to solar cues. Fungal Ecol. 25: 22–28.

Clandinin, T. R., and S. L. Zipursky, 2002 Making Connections in the Fly Visual System. Neuron 35: 827–841.

Clay, K., and G. P. Cheplick, 1989 Effect of ergot alkaloids from fungal endophyte-infected grasses on fall armyworm (Spodoptera frugiperda). J. Chem. Ecol. 15: 169–182.

Cole, G. T., S. Zhu, S. Pan, L. Yuan, D. Kruse *et al.*, 1989 Isolation of antigens with proteolytic activity

from Coccidioides immitis. Infect. Immun. 57: 1524.

Coleman, C. M., and W. S. Neckameyer, 2005 Serotonin synthesis by two distinct enzymes in Drosophila melanogaster. Arch. Insect Biochem. Physiol. 59: 12–31.

Colín-González, A. L., P. D. Maldonado, and A. Santamaría, 2013 3-Hydroxykynurenine: An intriguing molecule exerting dual actions in the Central Nervous System. Neurotoxicology 34: 189–204.

Colovic, M. B., D. Z. Krstic, T. D. Lazarevic-Pasti, A. M. Bondzic, and V. M. Vasic, 2013 Acetylcholinesterase Inhibitors: Pharmacology and Toxicology. Curr. Neuropharmacol. 11: 315.

Conesa, A., S. Gotz, J. M. Garcia-Gomez, J. Terol, M. Talon *et al.*, 2005 Blast2GO: a universal tool for annotation, visualization and analysis in functional genomics research. Bioinformatics 21: 3674–3676.

Cooper, R. ., and W. . Neckameyer, 1999 Dopaminergic modulation of motor neuron activity and neuromuscular function in Drosophila melanogaster. Comp. Biochem. Physiol. Part B Biochem. Mol. Biol. 122: 199–210.

Corona, M., R. Libbrecht, and D. E. Wheeler, 2016 Molecular mechanisms of phenotypic plasticity in social insects. Curr. Opin. Insect Sci. 13: 55–60.

Corona, M., R. Libbrecht, Y. Wurm, O. Riba-Grognuz, R. A. Studer *et al.*, 2013 Vitellogenin Underwent Subfunctionalization to Acquire Caste and Behavioral Specific Expression in the Harvester Ant Pogonomyrmex barbatus (J. Zhang, Ed.). PLoS Genet. 9: e1003730.

Corona, M., R. A. Velarde, S. Remolina, A. Moran-Lauter, Y. Wang *et al.*, 2007 Vitellogenin, juvenile hormone, insulin signaling, and queen honey bee longevity. Proc. Natl. Acad. Sci. U. S. A. 104: 7128–7133.

Csata, E., and A. Dussutour, 2019 Nutrient regulation in ants (Hymeno ptera: Formicidae): a review. Myrmecological News 29: 111–124.

Dakshinamurti, K., S. Dakshinamurti, M. P. Czubryt, K. Dakshinamurti, S. Dakshinamurti *et al.*, 2017

Vitamin B6: Effects of Deficiency, and Metabolic and Therapeutic Functions. Handb. Famine, Starvation, Nutr. Deprivation 1–23.

Darlington, T. K., K. Wager-Smith, M. F. Ceriani, D. Staknis, N. Gekakis *et al.*, 1998 Closing the circadian loop: CLOCK-induced transcription of its own inhibitors per and tim. Science (80-.). 280: 1599–603.

Darwiche, R., A. Kelleher, E. M. Hudspeth, R. Schneiter, and O. A. Asojo, 2016 Structural and functional characterization of the CAP domain of pathogen-related yeast 1 (Pry1) protein. Sci. Reports 2016 61 6: 1–10.

Das, B., 2022 timecourseRnaseq: Analyses And Visualisation Of Timecourse RNASeq Data.

Das, S., 2016 Vertebrate hormones in insects: The role of estrogen in silkworm – A review. Turkish J. Zool. 40: 297–302.

Das, B., and C. de Bekker, 2022 Time-course RNASeq of Camponotus floridanus forager and nurse ant brains indicate links between plasticity in the biological clock and behavioral division of labor. BMC Genomics 23: 1–23.

Daubner, S. C., T. Le, and S. Wang, 2011 Tyrosine hydroxylase and regulation of dopamine synthesis. Arch. Biochem. Biophys. 508: 1–12.

David, J. C., and H. Verron, 1982 Locomotor behavior in relation to octopamine levels in the ant Lasius niger. Experientia 38: 650–651.

Davies, R. G., 1988 Insect structure and function. Outlines Entomol. 7–96.

Dawaliby, R., C. Trubbia, C. Delporte, C. Noyon, J. M. Ruysschaert *et al.*, 2016 Phosphatidylethanolamine Is a Key Regulator of Membrane Fluidity in Eukaryotic Cells. J. Biol. Chem. 291: 3658.

Delaney, S. J., D. C. Hayward, F. Barleben, K. F. Fischbach, and G. L. G. Miklos, 1991 Molecular cloning and analysis of small optic lobes, a structural brain gene of Drosophila melanogaster. Proc.

Natl. Acad. Sci. U. S. A. 88: 7214–7218.

Dempsey, D. R., A. M. Carpenter, S. R. Ospina, and D. J. Merkler, 2015 Probing the Chemical Mechanism and Critical Regulatory Amino Acid Residues of Drosophila melanogaster Arylalkylamine N-acyltransferase Like 2. Insect Biochem. Mol. Biol. 66: 1.

Dempsey, D. R., K. A. Jeffries, J. D. Bond, A. M. Carpenter, S. Rodriguez-Ospina *et al.*, 2014 Mechanistic and structural analysis of Drosophila melanogaster arylalkylamine N-acetyltransferases. Biochemistry 53: 7777–7793.

Diez, L., P. Lejeune, and C. Detrain, 2014 Keep the nest clean: survival advantages of corpse removal in ants. Biol. Lett. 10:.

Ding, Y., R. M. Williams, and D. H. Sherman, 2008 Molecular Analysis of a 4-Dimethylallyltryptophan Synthase from *Malbranchea aurantiaca*. J. Biol. Chem. 283: 16068–16076.

Dohlman, H. G., and S. L. Campbell, 2019 Regulation of large and small G proteins by ubiquitination. J. Biol. Chem. 294: 18613–18623.

Dolan, E., B. Saunders, R. C. Harris, J. E. P. W. Bicudo, D. J. Bishop *et al.*, 2019 Comparative physiology investigations support a role for histidine-containing dipeptides in intracellular acid–base regulation of skeletal muscle. Comp. Biochem. Physiol. Part A Mol. Integr. Physiol. 234: 77–86.

Dolan, J., K. Walshe, S. Alsbury, K. Hokamp, S. O'Keeffe *et al.*, 2007 The extracellular Leucine-Rich Repeat superfamily; a comparative survey and analysis of evolutionary relationships and expression patterns. BMC Genomics 8: 320.

Dolezal, A. G., C. S. Brent, B. Hölldobler, and G. V. Amdam, 2012 Worker division of labor and endocrine physiology are associated in the harvester ant, Pogonomyrmex californicus. J. Exp. Biol. 215: 454–460.

Douglas, A. E., 2017 The B vitamin nutrition of insects: the contributions of diet, microbiome and horizontally acquired genes. Curr. Opin. Insect Sci. 23: 65–69.

Dowd, P. F., 1989 Toxicity of Naturally Occurring Levels of the Penicillium Mycotoxins Citrinin., Ochratoxin A, and Penicillic Acid to the Corn Earworm., Heliothis zea, and the Fall Armyworm, Spodoptera frugiperda (Lepidoptera: Noctuidae). Environ. Entomol. 18: 24–29.

Drozak, J., M. Veiga-da-Cunha, D. Vertommen, V. Stroobant, and E. Van Schaftingen, 2010 Molecular Identification of Carnosine Synthase as ATP-grasp Domain-containing Protein 1 (ATPGD1). J. Biol. Chem. 285: 9346.

Dubovskii, I. M., E. V. Grizanova, E. A. Chertkova, I. A. Slepneva, D. A. Komarov *et al.*, 2010 Generation of reactive oxygen species and activity of antioxidants in hemolymph of the moth larvae Galleria mellonella (L.) (Lepidoptera: Piralidae) at development of the process of encapsulation. J. Evol. Biochem. Physiol. 2010 461 46: 35–43.

Van Ekert, E., R. G. Shatters, P. Rougé, C. A. Powell, G. Smagghe *et al.*, 2015 Cloning and expressing a highly functional and substrate specific farnesoic acid o-methyltransferase from the Asian citrus psyllid (Diaphorina citri Kuwayama). FEBS Open Bio 5: 264–275.

Elya, C., T. C. Lok, Q. E. Spencer, H. McCausland, C. C. Martinez *et al.*, 2018 Robust manipulation of the behavior of Drosophila melanogaster by a fungal pathogen in the laboratory. Elife 7: 1–34.

Evans, H. C., S. L. Elliot, D. P. Hughes, L. Rosa, and S. Ribeiro, 2011 Hidden diversity behind the zombie-ant fungus ophiocordyceps unilateralis: Four new species described from carpenter ants in Minas Gerais, Brazil (C. Moreau, Ed.). PLoS One 6: e17024.

Feldman, D., O. Yarden, and Y. Hadar, 2020 Seeking the Roles for Fungal Small-Secreted Proteins in Affecting Saprophytic Lifestyles. Front. Microbiol. 11: 455.

Feng, P., Y. Shang, K. Cen, and C. Wang, 2015 Fungal biosynthesis of the bibenzoquinone oosporein to evade insect immunity. Proc. Natl. Acad. Sci. U. S. A. 112: 11365–11370.

Ferguson, S. T., K. Y. Park, A. A. Ruff, I. Bakis, and L. J. Zwiebel, 2020 Odor coding of nestmate recognition in the eusocial ant Camponotus floridanus. J. Exp. Biol.

Fiehn Lab, 2020 ESI-MS-adducts-2020.

Figueiredo, J., M. Sousa Silva, and A. Figueiredo, 2018 Subtilisin-like proteases in plant defence: the past, the present and beyond. Mol. Plant Pathol. 19: 1017–1028.

Finetti, L., T. Roeder, G. Calò, and G. Bernacchia, 2021 The Insect Type 1 Tyramine Receptors: From Structure to Behavior. Insects 12: 315.

Finn, R. D., T. K. Attwood, P. C. Babbitt, A. Bateman, P. Bork *et al.*, 2017 InterPro in 2017—beyond protein family and domain annotations. Nucleic Acids Res. 45: D190–D199.

Finn, R. D., A. Bateman, J. Clements, P. Coggill, R. Y. Eberhardt *et al.*, 2014 Pfam: the protein families database. Nucleic Acids Res. 42: D222–D230.

Fischbach, K. F., and M. Heisenberg, 1981 Structural brain mutant of Drosophila melanogaster with reduced cell number in the medulla cortex and with normal optomotor yaw response. Proc. Natl. Acad. Sci. U. S. A. 78: 1105–1109.

Fischer, R., and N. Requena, 2022 Small-secreted proteins as virulence factors in nematode-trapping fungi. Trends Microbiol.

Fournier, D., J.-M. Bride, F. Hoffmann, and F. Karch, 1992 Acetylcholinesterase TWO TYPES OF MODIFICATIONS CONFER RESISTANCE TO INSECTICIDE. J. Biol. Chem. 267: 14270–14274.

Fredericksen, M. A., Y. Zhang, M. L. Hazen, R. G. Loreto, C. A. Mangold *et al.*, 2017 Three-dimensional visualization and a deep-learning model reveal complex fungal parasite networks in behaviorally manipulated ants. Proc. Natl. Acad. Sci. 114: 201711673.

Friedman, D. A., A. Pilko, D. Skowronska-Krawczyk, K. Krasinska, J. W. Parker *et al.*, 2018 The Role of Dopamine in the Collective Regulation of Foraging in Harvester Ants. iScience 8: 283.

Gaderer, R., K. Bonazza, and V. Seidl-Seiboth, 2014 Cerato-platanins: a fungal protein family with intriguing properties and application potential. Appl. Microbiol. Biotechnol. 98: 4795.

Gallagher, R. T., and A. D. Hawkes, 1986 The potent tremorgenic neurotoxins lolitrem B and aflatrem: A comparison of the tremor response in mice. Experientia 42: 823–825.

Gant, D. B., R. J. Cole, J. J. Valdes, M. E. Eldefrawi, and A. T. Eldefrawi, 1987 Action of tremorgenic mycotoxins on GABAA receptor. Life Sci. 41: 2207–2214.

Gao, Q., K. Jin, S.-H. Ying, Y. Zhang, G. Xiao *et al.*, 2011 Genome sequencing and comparative transcriptomics of the model entomopathogenic fungi Metarhizium anisopliae and M. acridum. PLoS Genet. 7: e1001264.

García-Bellido, A., and J. F. De Celis, 2009 The Complex Tale of the achaete–scute Complex: A Paradigmatic Case in the Analysis of Gene Organization and Function During Development. Genetics 182: 631.

Gasparetti, C., E. Nordlund, J. Jänis, J. Buchert, and K. Kruus, 2012 Extracellular tyrosinase from the fungus Trichoderma reesei shows product inhibition and different inhibition mechanism from the intracellular tyrosinase from Agaricus bisporus. Biochim. Biophys. Acta - Proteins Proteomics 1824: 598–607.

Gauthier, M., 2010 *Insect Nicotinic Acetylcholine Receptors: State of the Art on Insect Nicotinic Acetylcholine Receptor Function in Learning and Memory* (S. Hervé Thany, Ed.).

Gelderblom, W. C. A., P. G. Thiel, and K. J. van der Merwe, 1988 The chemical and enzymatic interaction of glutathione with the fungal metabolite, fusarin C. Mutat. Res. Mol. Mech. Mutagen. 199: 207–214.

Geun, S. K., M. Nalini, Y. Kim, and D. W. Lee, 2009 Octopamine and 5-hydroxytryptamine mediate hemocytic phagocytosis and nodule formation via eicosanoids in the beet armyworm, Spodoptera exigua. Arch. Insect Biochem. Physiol. 70: 162–176.

Gillis, J., and P. Pavlidis, 2012 “Guilt by Association” Is the Exception Rather Than the Rule in Gene Networks. PLOS Comput. Biol. 8: e1002444.

Godenschwege, T. A., and R. K. Murphey, 2009 Genetic interaction of Neuroglian and Semaphorin1a during guidance and synapse formation. J. Neurogenet. 23: 147–55.

González-Santoyo, I., and A. Córdoba-Aguilar, 2012 Phenoloxidase: a key component of the insect immune system. Entomol. Exp. Appl. 142: 1–16.

Goossens, T., Y. Y. Kang, G. Wuytens, P. Zimmermann, Z. Callaerts-Végh *et al.*, 2011 The Drosophila L1CAM homolog Neuroglian signals through distinct pathways to control different aspects of mushroom body axon development. Development 138: 1595–605.

Gorman, M. J., and Y. Arakane, 2010 Tyrosine hydroxylase is required for cuticle sclerotization and pigmentation in Tribolium castaneum. Insect Biochem. Mol. Biol. 40: 267–273.

Gotzek, D., and K. G. Ross, 2007 Genetic regulation of colony social organization in fire ants: an integrative overview. Q. Rev. Biol. 82: 201–26.

Gotzek, D., D. D. Shoemaker, and K. G. Ross, 2007 Molecular variation at a candidate gene implicated in the regulation of fire ant social behavior. PLoS One 2: e1088.

Gracia, E. S., C. De Bekker, E. M. Hanks, and D. P. Hughes, 2018 Within the fortress: A specialized parasite is not discriminated against in a social insect society. PLoS One 13:.

Grosse-Wilde, E., L. S. Kuebler, S. Bucks, H. Vogel, D. Wicher *et al.*, 2011 Antennal transcriptome of Manduca sexta. Proc. Natl. Acad. Sci. U. S. A. 108: 7449–54.

Grünewald, B., and P. Siefert, 2019 Acetylcholine and Its Receptors in Honeybees: Involvement in Development and Impairments by Neonicotinoids. Insects 10:.

Gui, Z., C. Hou, T. Liu, G. Qin, M. Li *et al.*, 2009 Effects of Insect Viruses and Pesticides on Glutathione *S*-Transferase Activity and Gene Expression in *Bombyx mori*. J. Econ. Entomol. 102: 1591–1598.

Guo, Z., J. Qin, X. Zhou, and Y. Zhang, 2018 Insect Transcription Factors: A Landscape of Their Structures and Biological Functions in Drosophila and beyond. Int. J. Mol. Sci. 19:.

Gupta, S. K., M. Kupper, C. Ratzka, H. Feldhaar, A. Vilcinskas *et al.*, 2015 Scrutinizing the immune

defence inventory of Camponotus floridanus applying total transcriptome sequencing. BMC Genomics 16: 1–21.

Gupta, S. K., M. Srivastava, Ö. Osmanoglu, and T. Dandekar, 2020 Genome-wide inference of the Camponotus floridanus protein-protein interaction network using homologous mapping and interacting domain profile pairs. Sci. Rep. 10: 2334.

Häcker, U., E. Kaufmann, C. Hartmann, G. Jürgens, W. Knöchel *et al.*, 1995 The Drosophila fork head domain protein crocodile is required for the establishment of head structures. EMBO J. 14: 5306.

Hafer-Hahmann, N., 2019 Experimental evolution of parasitic host manipulation. Proc. R. Soc. B Biol. Sci. 286: 20182413.

Halaouli, S., M. Asther, J. C. Sigoillot, M. Hamdi, and A. Lomascolo, 2006 Fungal tyrosinases: New prospects in molecular characteristics, bioengineering and biotechnological applications. J. Appl. Microbiol. 100: 219–232.

Hamanaka, Y., D. Park, P. Yin, S. P. Annangudi, T. N. Edwards *et al.*, 2010 Transcriptional Orchestration of the Regulated Secretory Pathway in Neurons by the bHLH protein DIMM. Curr. Biol. 20: 9–18.

Han, Q., T. Cai, D. A. Tagle, H. Robinson, and J. Li, 2008 Substrate specificity and structure of human aminoadipate aminotransferase/kynurenine aminotransferase II. Biosci. Rep. 28: 205.

Han, Y., S. van Houte, G. F. Drees, M. M. van Oers, and V. I. D. Ros, 2015 Parasitic Manipulation of Host Behaviour: Baculovirus SeMNPV EGT Facilitates Tree-Top Disease in Spodoptera exigua Larvae by Extending the Time to Death. Insects 6: 716–31.

Han, Y., S. van Houte, M. M. van Oers, and V. I. D. Ros, 2018 Timely trigger of caterpillar zombie behaviour: temporal requirements for light in baculovirus-induced tree-top disease. Parasitology 145: 822–827.

Hang, J., and M. Dasso, 2002 Association of the Human SUMO-1 Protease SENP2 with the Nuclear Pore

*. J. Biol. Chem. 277: 19961–19966.

He, Y., and R. J. Cox, 2016 The molecular steps of citrinin biosynthesis in fungi. Chem. Sci. 7: 2119–2127.

Hebert, F. O., L. Phelps, I. Samonte, M. Panchal, S. Grambauer *et al.*, 2015 Identification of candidate mimicry proteins involved in parasite-driven phenotypic changes. Parasit. Vectors 8: 225.

Heil, M., 2016 Host Manipulation by Parasites: Cases, Patterns, and Remaining Doubts. Front. Ecol. Evol. 4: 80.

Helluy, S., 2013 Parasite-induced alterations of sensorimotor pathways in gammarids: collateral damage of neuroinflammation? J. Exp. Biol. 216: 67–77.

Helluy, S., and J. C. Holmes, 1990 Serotonin, octopamine, and the clinging behavior induced by the parasite Polymorphus paradoxus (Acanthocephala) in Gammarus lacustris (Crustacea). Can. J. Zool. 68: 1214–1220.

Hennessy, F., W. S. Nicoll, R. Zimmermann, M. E. Cheetham, and G. L. Blatch, 2005 Not all J domains are created equal: Implications for the specificity of Hsp40–Hsp70 interactions. Protein Sci. 14: 1697–1709.

Herbison, R. E. H., 2017 Lessons in Mind Control: Trends in Research on the Molecular Mechanisms behind Parasite-Host Behavioral Manipulation. Front. Ecol. Evol. 5: 102.

Herbison, R., S. Evans, J. F. Doherty, M. Algie, T. Kleffmann *et al.*, 2019 A molecular war: convergent and ontogenetic evidence for adaptive host manipulation in related parasites infecting divergent hosts. Proc. R. Soc. B Biol. Sci. 286: 20191827.

Hergarden, A. C., T. D. Tayler, and D. J. Anderson, 2012 Allatostatin-A neurons inhibit feeding behavior in adult Drosophila. Proc. Natl. Acad. Sci. U. S. A. 109: 3967–3972.

Hermjakob, H., L. Montecchi-Palazzi, C. Lewington, S. Mudali, S. Kerrien *et al.*, 2004 IntAct: an open source molecular interaction database. Nucleic Acids Res. 32: D452.

Hintermann, E., P. Jenö, and U. A. Meyer, 1995 Isolation and characterization of an arylalkylamine N-acetyltransferase from Drosophila melanogaster. FEBS Lett. 375: 148–150.

Hite, J. L., A. C. Pfenning, and C. E. Cressler, 2019 Starving the Enemy? Feeding Behavior Shapes Host-Parasite Interactions. Trends Ecol. Evol.

Hoff, K. J., S. Lange, A. Lomsadze, M. Borodovsky, and M. Stanke, 2016 BRAKER1: Unsupervised RNA-Seq-Based Genome Annotation with GeneMark-ET and AUGUSTUS. Bioinformatics 32: 767–769.

Hogenhout, S. A., R. A. L. Van Der Hoorn, R. Terauchi, and S. Kamoun, 2009 Emerging concepts in effector biology of plant-associated organisms. Mol. Plant-Microbe Interact. 22: 115–122.

Hölldobler, B., and E. O. Wilson, 1990 *The Ants*. Belknap Press of Harvard University Press, Cambridge, MA.

Hoover, K., M. Grove, M. Gardner, D. P. Hughes, J. McNeil *et al.*, 2011 A Gene for an Extended Phenotype. Science (80-.). 333: 1401–1401.

Hosokawa, M., 2008 Structure and Catalytic Properties of Carboxylesterase Isozymes Involved in Metabolic Activation of Prodrugs. Molecules 13: 412.

van Houte, S., M. M. van Oers, Y. Han, J. M. Vlak, V. I. D. Ros *et al.*, 2014a Baculovirus infection triggers a positive phototactic response in caterpillars to induce 'tree-top' disease. Biol. Lett. 10: 20140680.

van Houte, S., V. I. D. Ros, T. G. Mastenbroek, N. J. Vendrig, K. Hoover *et al.*, 2012 Protein Tyrosine Phosphatase-Induced Hyperactivity Is a Conserved Strategy of a Subset of BaculoViruses to Manipulate Lepidopteran Host Behavior (C. Breuker, Ed.). PLoS One 7: e46933.

van Houte, S., V. I. D. Ros, and M. M. van Oers, 2014b Hyperactivity and tree-top disease induced by the baculovirus AcMNPV in Spodoptera exigua larvae are governed by independent mechanisms. Naturwissenschaften 101: 347–350.

van Houte, S., V. I. D. Ros, and M. M. van Oers, 2013 Walking with insects: Molecular mechanisms behind parasitic manipulation of host behaviour. Mol. Ecol. 22: 3458–3475.

Hoxmeier, J. C., B. D. Thompson, C. D. Broeckling, P. Small, B. D. Foy *et al.*, 2015 Analysis of the metabolome of Anopheles gambiae mosquito after exposure to Mycobacterium ulcerans. Sci. Reports 2015 51 5: 1–8.

Huang, Y., B. Niu, Y. Gao, L. Fu, and W. Li, 2010 CD-HIT Suite: a web server for clustering and comparing biological sequences. Bioinformatics 26: 680–682.

Huang, Y., L. Su, and J. Wu, 2016 Pyridoxine Supplementation Improves the Activity of Recombinant Glutamate Decarboxylase and the Enzymatic Production of Gama-Aminobutyric Acid. PLoS One 11: e0157466.

Hughes, D. P., S. B. Andersen, N. L. Hywel-Jones, W. Himaman, J. Billen *et al.*, 2011 Behavioral mechanisms and morphological symptoms of zombie ants dying from fungal infection. BMC Ecol. 11: 13.

Hung, C.-Y., K. R. Seshan, J.-J. Yu, R. Schaller, J. Xue *et al.*, 2005 A metalloproteinase of Coccidioides posadasii contributes to evasion of host detection. Infect. Immun. 73: 6689–703.

Hunt, M., N. De Silva, T. D. Otto, J. Parkhill, J. A. Keane *et al.*, 2015 Circlator: automated circularization of genome assemblies using long sequencing reads. Genome Biol. 16: 294.

Hunter, S., R. Apweiler, T. K. Attwood, A. Bairoch, A. Bateman *et al.*, 2009 InterPro: the integrative protein signature database. Nucleic Acids Res. 37: D211–D215.

Iga, M., and H. Kataoka, 2012 Recent Studies on Insect Hormone Metabolic Pathways Mediated by Cytochrome P450 Enzymes. Biol. Pharm. Bull. 35: 838–843.

Ingram, K. K., L. Kleeman, and S. Peteru, 2011 Differential regulation of the foraging gene associated with task behaviors in harvester ants. BMC Ecol. 11: 19.

Itzhaki, Z., E. Akiva, Y. Altuvia, and H. Margalit, 2006 Evolutionary conservation of domain-domain

interactions. Genome Biol. 7:.

Iwanicki, N. S. A., I. Delalibera, J. Eilenberg, and H. H. de Fine Licht, 2020 Comparative RNAseq Analysis of the Insect-Pathogenic Fungus Metarhizium anisopliae Reveals Specific Transcriptome Signatures of Filamentous and Yeast-Like Development. G3 Genes|Genomes|Genetics 10: 2141–2157.

Joardar, V., N. F. Abrams, J. Hostetler, P. J. Paukstelis, S. Pakala *et al.*, 2012 Sequencing of mitochondrial genomes of nine Aspergillus and Penicillium species identifies mobile introns and accessory genes as main sources of genome size variability. BMC Genomics 13: 698.

Johansen, J., M. E. Halpern, K. M. Johansen, and H. Keshishian, 1989 Stereotypic morphology of glutamatergic synapses on identified muscle cells of Drosophila larvae. J. Neurosci. 9: 710.

Jones, W. D., T.-A. T. Nguyen, B. Kloss, K. J. Lee, and L. B. Vosshall, 2005 Functional conservation of an insect odorant receptor gene across 250 million years of evolution. Curr. Biol. 15: R119–R121.

Joshi, L., R. J. St. Leger, and M. J. Bidochka, 1995 Cloning of a cuticle-degrading protease from the entomopathogenic fungus, *Beauveria bassiana*. FEMS Microbiol. Lett. 125: 211–217.

Jukić, I., N. Kolobarić, A. Stupin, A. Matić, N. Kozina *et al.*, 2021 Carnosine, Small but Mighty—Prospect of Use as Functional Ingredient for Functional Food Formulation. Antioxidants 2021, Vol. 10, Page 1037 10: 1037.

Jurenka, R., and T. Nusawardani, 2011 The pyrokinin/ pheromone biosynthesis-activating neuropeptide (PBAN) family of peptides and their receptors in Insecta: evolutionary trace indicates potential receptor ligand-binding domains. Insect Mol. Biol. 20: 323–334.

Kachman, M., H. Habra, W. Duren, J. Wigginton, P. Sajjakulnukit *et al.*, 2020 Deep annotation of untargeted LC-MS metabolomics data with Binner. Bioinformatics 36: 1801–1806.

Kamhi, J. F., S. Arganda, C. S. Moreau, and J. F. A. Traniello, 2017 Origins of aminergic regulation of behavior in complex insect social systems. Front. Syst. Neurosci. 11: 74.

Kamimura, M., H. Saito, R. Niwa, T. Niimi, K. Toyoda *et al.*, 2012 Fungal ecdysteroid-22-oxidase, a new tool for manipulating ecdysteroid signaling and insect development. J. Biol. Chem. 287: 16488–98.

Kamita, S. G., K. Nagasaka, J. W. Chua, T. Shimada, K. Mita *et al.*, 2005 A protein tyrosine phosphatase-like protein from baculovirus has RNA 5'-triphosphatase and diphosphatase activities. PNAS 95: 9808–9812.

Kandel, S. E., and J. N. Lampe, 2014 Role of Protein–ProteinInteractions in CytochromeP450-Mediated Drug Metabolism and Toxicity. Chem. Res. Toxicol. 27: 1474.

Kanehisa, M., and S. Goto, 2000 KEGG: Kyoto Encyclopedia of Genes and Genomes. Nucleic Acids Res. 28: 27.

Kang, H., J. Zhao, X. Jiang, G. Li, W. Huang *et al.*, 2019 Drosophila Netrin-B controls mushroom body axon extension and regulates courtship-associated learning and memory of a Drosophila fragile X syndrome model. Mol. Brain 12: 52.

Karlstrom, R. O., L. P. Wilder, and M. J. Bastiani, 1993 Lachesin: an immunoglobulin superfamily protein whose expression correlates with neurogenesis in grasshopper embryos. Development 118:.

Kassambara, A., M. Kosinski, P. Biecek, and S. Fabian, 2019 Drawing Survival Curves using "ggplot2" [R package survminer version 0.4.4].

Kathirithamby, J., A. Hayward, D. P. Mcmahon, R. S. Ferreira, R. Andreazze *et al.*, 2010 Conspecifics of a heterotrophic heteronomous species of Strepsiptera (Insecta) are matched by molecular characterization. Syst. Entomol. 35: 234–242.

Katoh, K., K. Misawa, K. I. Kuma, and T. Miyata, 2002 MAFFT: a novel method for rapid multiple sequence alignment based on fast Fourier transform. Nucleic Acids Res. 30: 3059–3066.

Katsuma, S., Y. Koyano, W. K. Kang, R. Kokusho, S. G. Kamita *et al.*, 2012 The baculovirus uses a captured host phosphatase to induce enhanced locomotory activity in host caterpillars (D. S. Schneider, Ed.). PLoS Pathog. 8: e1002644.

Katzemich, A., N. Kreisköther, A. Alexandrovich, C. Elliott, F. Schöck *et al.*, 2012 The function of the M-line protein obscurin in controlling the symmetry of the sarcomere in the flight muscle of Drosophila. J. Cell Sci. 125: 3367–79.

Katzemich, A., R. J. H. West, A. Fukuzawa, S. T. Sweeney, M. Gautel *et al.*, 2015 Binding partners of the kinase domains in Drosophila obscurin and their effect on the structure of the flight muscle. J. Cell Sci. 128: 3386–97.

Keleman, K., and B. J. Dickson, 2001 Short- and Long-Range Repulsion by the Drosophila Unc5 Netrin Receptor. Neuron 32: 605–617.

Khaldi, N., F. T. Seifuddin, G. Turner, D. Haft, W. C. Nierman *et al.*, 2010 SMURF: Genomic mapping of fungal secondary metabolite clusters. Fungal Genet. Biol. 47: 736–741.

Khan, N. A., Y. Wang, K. J. Kim, J. W. Chung, C. A. Wass *et al.*, 2002 Cytotoxic necrotizing factor-1 contributes to Escherichia coli K1 invasion of the central nervous system. J. Biol. Chem. 277: 15607–12.

Kim, D., B. Langmead, and S. L. Salzberg, 2015 HISAT: a fast spliced aligner with low memory requirements. Nat. Methods 12: 357–360.

Kind, T., K. H. Liu, D. Y. Lee, B. Defelice, J. K. Meissen *et al.*, 2013 LipidBlast in silico tandem mass spectrometry database for lipid identification. Nat. Methods 2013 108 10: 755–758.

Kiuchi, M., H. Yasui, S. Hayasaka, and M. Kamimura, 2003 Entomogenous fungusNomuraea rileyi inhibits host insect molting by C22-oxidizing inactivation of hemolymph ecdysteroids. Arch. Insect Biochem. Physiol. 52: 35–44.

Klinman, E., and E. L. F. Holzbaur, 2018 Walking Forward with Kinesin. Trends Neurosci. 41: 555–556.

Knaus, H.-G., O. B. McManus, S. H. Lee, W. A. Schmalhofer, M. Garcia-Calvo *et al.*, 1994 Tremorgenic Indole Alkaloids Potently Inhibit Smooth Muscle High-Conductance Calcium-Activated Potassium Channels. Biochemistry 33: 5819–5828.

Kobmoo, N., S. Mongkolsamrit, K. Tasanathai, D. Thanakitpipattana, and J. J. Luangsa-Ard, 2012 Molecular phylogenies reveal host-specific divergence of Ophiocordyceps unilateralis sensu lato following its host ants. Mol. Ecol. 21: 3022–3031.

Kobmoo, N., D. Wichadakul, N. Arnamnart, R. C. Rodríguez De La Vega, J.-J. J. Luangsa-ard *et al.*, 2018 A genome scan of diversifying selection in Ophiocordyceps zombie-ant fungi suggests a role for enterotoxins in co-evolution and host specificity. Mol. Ecol. 27: 3582–3598.

Kohlmeier, P., B. Feldmeyer, and S. Foitzik, 2018 Vitellogenin-like A–associated shifts in social cue responsiveness regulate behavioral task specialization in an ant. PLOS Biol. 16: e2005747.

Komatsu, H., M. Maruyama, S. Yao, T. Shinohara, K. Sakuma *et al.*, 2014 Anatomical Transcriptome of G Protein-Coupled Receptors Leads to the Identification of a Novel Therapeutic Candidate GPR52 for Psychiatric Disorders. PLoS One 9:.

Koren, S., B. P. Walenz, K. Berlin, J. R. Miller, N. H. Bergman *et al.*, 2017 Canu: scalable and accurate long-read assembly via adaptive k-mer weighting and repeat separation. Genome Res. 27: 722–736.

Korneta, I., M. Magnus, and J. M. Bujnicki, 2012 Structural bioinformatics of the human spliceosomal proteome. Nucleic Acids Res. 40: 7046–7065.

Krasnoff, S. B., C. H. Sommers, Y.-S. Moon, B. G. G. Donzelli, J. D. Vandenberg *et al.*, 2006 Production of Mutagenic Metabolites by Metarhizium anisopliae. J. Agric. Food Chem. 54: 7083–7088.

Krasnoff, S. B., D. W. Watson, D. M. Gibson, and E. C. Kwan, 1995 Behavioral effects of the entomopathogenic fungus, Entomophthora muscae on its host Musca domestica: Postural changes in dying hosts and gated pattern of mortality. J. Insect Physiol. 41: 895–903.

Kravats, A. N., S. M. Doyle, J. R. Hoskins, O. Genest, E. Doody *et al.*, 2017 Interaction of E. coli Hsp90 with DnaK Involves the DnaJ Binding Region of DnaK. J. Mol. Biol. 429: 858–872.

Krieger, M. J. B., and K. G. Ross, 2002 Identification of a major gene regulating complex social behavior. Science (80-.). 295: 328–32.

Krizsan-Agbas, D., T. Pedchenko, and P. G. Smith, 2008 Neurotrimin is an estrogen-regulated determinant of peripheral sympathetic innervation. J. Neurosci. Res. 86: 3086–3095.

Krnjević, K., 2010 When and why amino acids? J. Physiol. 588: 33–44.

Krogh, A., B. Larsson, G. von Heijne, and E. L. . Sonnhammer, 2001 Predicting transmembrane protein topology with a hidden markov model: application to complete genomes. J. Mol. Biol. 305: 567–580.

Kumagai, H., T. Kunieda, K. Nakamura, Y. Matsumura, M. Namiki *et al.*, 2020 Developmental stage-specific distribution and phosphorylation of Mblk-1, a transcription factor involved in ecdysteroid-signaling in the honey bee brain. Sci. Rep. 10:.

Kumar, S., and N. S. Punekar, 1997 The metabolism of 4-aminobutyrate (GABA) in fungi. Mycol. Res. 101: 403–409.

Kursa, M. B., and W. R. Rudnicki, 2010 Feature Selection with the Boruta Package. J. Stat. Softw. 36: 1–13.

Kurtz, S., A. Phillippy, A. L. Delcher, M. Smoot, M. Shumway *et al.*, 2004 Versatile and open software for comparing large genomes. Genome Biol. 5: R12.

Lafferty, K. D., and A. M. Kuris, 2012 Ecological consequences of manipulative parasites (D. P. Hughes, J. Brodeur, & F. Thomas, Eds.). Host Manip. by parasites 158–168.

Lafferty, K. D., and J. C. Shaw, 2013 Comparing mechanisms of host manipulation across host and parasite taxa. J. Exp. Biol. 216: 56–66.

Da Lage, J.-L., 2018 The Amylases of Insects. Int. J. insect Sci. 10: 1179543318804783.

Lah, G. J., J. S. S. Li, and S. S. Millard, 2014 Cell-Specific Alternative Splicing of Drosophila Dscam2 Is Crucial for Proper Neuronal Wiring. Neuron 83: 1376–1388.

Langfelder, P., and S. Horvath, 2008 WGCNA: an R package for weighted correlation network analysis. BMC Bioinformatics 9: 559.

LeBoeuf, A. C., A. B. Cohanim, C. Stoffel, C. S. Brent, P. Waridel *et al.*, 2018 Molecular evolution of juvenile hormone esterase-like proteins in a socially exchanged fluid. Sci. Rep. 8: 17830.

Leboeuf, A. C., P. Waridel, C. S. Brent, A. N. Gonçalves, L. Menin *et al.*, 2016 Oral transfer of chemical cues, growth proteins and hormones in social insects. Elife 5:.

Lechner, M., S. Findeiß, L. Steiner, M. Marz, P. F. Stadler *et al.*, 2011 Proteinortho: Detection of (Co-)orthologs in large-scale analysis. BMC Bioinformatics 12: 1–9.

Lee, Y. S., Y. S. Park, S. Nam, S. J. Suh, J. Lee *et al.*, 2000 Characterization of GAR-2, a Novel G Protein-Linked Acetylcholine Receptor from Caenorhabditis elegans. J. Neurochem. 75: 1800–1809.

Lefèvre, T., S. A. Adamo, D. G. Biron, D. Missé, D. Hughes *et al.*, 2009 Invasion of the body snatchers: the diversity and evolution of manipulative strategies in host-parasite interactions. Adv. Parasitol. 68: 45–83.

Lengyel, F., S. A. Westerlund, and M. Kaib, 2006 Juvenile Hormone III Influences Task-Specific Cuticular Hydrocarbon Profile Changes in the Ant Myrmicaria eumenoides. J. Chem. Ecol. 33: 167–181.

Li, H., 2018 Minimap2: pairwise alignment for nucleotide sequences (I. Birol, Ed.). Bioinformatics 34: 3094–3100.

Li, M., S. Armelloni, M. Ikehata, A. Corbelli, M. Pesaresi *et al.*, 2011 Nephrin expression in adult rodent central nervous system and its interaction with glutamate receptors. J. Pathol. 225: 118–128.

Li, Y., J. Hoffmann, Y. Li, F. Stephano, I. Bruchhaus *et al.*, 2016 Octopamine controls starvation resistance, life span and metabolic traits in Drosophila. Sci. Rep. 6: 35359.

Li, S., Y. Park, S. Duraisingham, F. H. Strobel, N. Khan *et al.*, 2013 Predicting Network Activity from High Throughput Metabolomics. PLOS Comput. Biol. 9: e1003123.

Li, Z., and D. E. Vance, 2008 Thematic Review Series: Glycerolipids. Phosphatidylcholine and choline homeostasis. J. Lipid Res. 49: 1187–1194.

Libbrecht, R., M. Corona, F. Wende, D. O. Azevedo, J. E. Serrão *et al.*, 2013 Interplay between insulin signaling, juvenile hormone, and vitellogenin regulates maternal effects on polyphenism in ants. Proc. Natl. Acad. Sci. U. S. A. 110: 11050–5.

Libersat, F., and R. Gal, 2014 Wasp Voodoo Rituals, Venom-Cocktails, and the Zombification of Cockroach Hosts. Integr. Comp. Biol. 54: 129–142.

Libersat, F., M. Kaiser, and S. Emanuel, 2018 Mind Control: How Parasites Manipulate Cognitive Functions in Their Insect Hosts. Front. Psychol. 9: 572.

Lin, C.-F., C.-L. Chen, W.-C. Huang, Y.-L. Cheng, C.-Y. Hsieh *et al.*, 2010 Different types of cell death induced by enterotoxins. Toxins (Basel). 2: 2158–76.

Lin, W. J., Y. I. Lee, S. L. Liu, C. C. Lin, T. Y. Chung *et al.*, 2020 Evaluating the tradeoffs of a generalist parasitoid fungus, Ophiocordyceps unilateralis, on different sympatric ant hosts. Sci. Rep. 10:.

Lin, W., Y. Yu, P. Zhou, J. Zhang, L. Dou *et al.*, 2015 Identification and Knockdown of the Olfactory Receptor (OrCo) in Gypsy Moth, Lymantria dispar. Int. J. Biol. Sci. 11: 772–80.

Lin, R., X. Zhang, B. Xin, M. Zou, Y. Gao *et al.*, 2019 Genome sequence of Isaria javanica and comparative genome analysis insights into family S53 peptidase evolution in fungal entomopathogens. Appl. Microbiol. Biotechnol. 1–18.

Lindner, J. R., P. R. Hillman, A. L. Barrett, M. C. Jackson, T. L. Perry *et al.*, 2007 The Drosophila Perlecan gene trol regulates multiple signaling pathways in different developmental contexts. BMC Dev. Biol. 7: 121.

Liu, L., M. Downs, J. Guidry, and E. J. Wojcik, 2021 Inter-organelle interactions between the ER and mitotic spindle facilitates Zika protease cleavage of human Kinesin-5 and results in mitotic defects. iScience 24: 102385.

Liu, Y., J. Luo, and D. R. Nässel, 2016 The Drosophila Transcription Factor Dimmed Affects Neuronal Growth and Differentiation in Multiple Ways Depending on Neuron Type and Developmental

Stage. Front. Mol. Neurosci. 9: 97.

Loaiza, C. D., N. Duhan, M. Lister, and R. Kaundal, 2021 In silico prediction of host–pathogen protein interactions in melioidosis pathogen Burkholderia pseudomallei and human reveals novel virulence factors and their targets. Brief. Bioinform. 22: 1–18.

Locht, C., J. M. Keith, C. Locht, and J. M. Keith, 1986 Pertussis Toxin Gene : Nucleotide Sequence and Genetic Organization. Science (80-.). 232: 1258–1264.

Loman, N. J., J. Quick, and J. T. Simpson, 2015 A complete bacterial genome assembled de novo using only nanopore sequencing data. Nat. Methods 12: 733–735.

Loreto, R. G., J. P. M. Araújo, R. M. Kepler, K. R. Fleming, C. S. Moreau *et al.*, 2018 Evidence for convergent evolution of host parasitic manipulation in response to environmental conditions. Evolution (N. Y). 211144.

Loreto, R. G., S. L. Elliot, M. L. R. Freitas, T. M. Pereira, and D. P. Hughes, 2014 Long-term disease dynamics for a specialized parasite of ant societies: a field study (N. Chaline, Ed.). PLoS One 9: e103516.

Loreto, R. G., and D. P. Hughes, 2019 The metabolic alteration and apparent preservation of the zombie ant brain. J. Insect Physiol. 118: 103918.

Lovett, B., R. J. St. Leger, and H. H. de Fine Licht, 2020 Going gentle into that pathogen-induced goodnight. J. Invertebr. Pathol. 174: 107398.

Lu, K.-H., J. Y. Bradfield, and L. L. Keeley, 1999 Juvenile hormone inhibition of gene expression for cytochrome P4504C1 in adult females of the cockroach, Blaberus discoidalis. Insect Biochem. Mol. Biol. 29: 667–673.

Lucas, C., and M. B. Sokolowski, 2009 Molecular basis for changes in behavioral state in ant social behaviors. Proc. Natl. Acad. Sci. U. S. A. 106: 6351–6.

Luo, J., Y. Liu, and D. R. Nässel, 2013 Insulin/IGF-Regulated Size Scaling of Neuroendocrine Cells

Expressing the bHLH Transcription Factor Dimmed in Drosophila (P. H. Taghert, Ed.). PLoS Genet. 9: e1004052.

Ma, S., Q. Song, H. Tao, A. Harrison, S. Wang *et al.*, 2019 Prediction of protein–protein interactions between fungus (Magnaporthe grisea) and rice (Oryza sativa L.). Brief. Bioinform. 20: 448–456.

Mangmool, S., and H. Kurose, 2011 G(i/o) protein-dependent and -independent actions of Pertussis Toxin (PTX). Toxins (Basel). 3: 884–99.

Mangold, C. A., M. J. Ishler, R. G. Loreto, M. L. Hazen, and D. P. Hughes, 2019 Zombie ant death grip due to hypercontracted mandibular muscles. J. Exp. Biol. 222: jeb200683.

Mannino, M. C., C. Huarte-Bonnet, B. Davyt-Colo, N. Pedrini, M. C. Mannino *et al.*, 2019 Is the Insect Cuticle the only Entry Gate for Fungal Infection? Insights into Alternative Modes of Action of Entomopathogenic Fungi. J. Fungi 5: 33.

Mantas, I., M. Saarinen, Z. Q. D. Xu, and P. Svenningsson, 2021 Update on GPCR-based targets for the development of novel antidepressants. Mol. Psychiatry 2021 271 27: 534–558.

Marie, B., E. Pym, S. Bergquist, and G. W. Davis, 2010 Synaptic Homeostasis Is Consolidated by the Cell Fate Gene gooseberry, a Drosophila pax3/7 Homolog. J. Neurosci. 30: 8071–8082.

Matyash, V., G. Liebisch, T. V. Kurzchalia, A. Shevchenko, and D. Schwudke, 2008 Lipid extraction by methyl-tert-butyl ether for high-throughput lipidomics. J. Lipid Res. 49: 1137–1146.

Mersch, D. P., A. Crespi, and L. Keller, 2013 Tracking individuals shows spatial fidelity is a key regulator of ant social organization. Science 340: 1090–3.

Meunier, N., Y. H. Belgacem, and J.-R. Martin, 2007 Regulation of feeding behaviour and locomotor activity by takeout in Drosophila. J. Exp. Biol. 210: 1424–34.

Michaeli, S., and H. Fromm, 2015 Closing the loop on the GABA shunt in plants: Are GABA metabolism and signaling entwined? Front. Plant Sci. 6: 419.

Michalkova, V., J. B. Benoit, B. L. Weiss, G. M. Attardo, and S. Aksoy, 2014 Vitamin B6 Generated by

Obligate Symbionts Is Critical for Maintaining Proline Homeostasis and Fecundity in Tsetse Flies. Appl. Environ. Microbiol. 80: 5844.

Min, K. T., and S. Benzer, 1999 Preventing neurodegeneration in the Drosophila mutant bubblegum. Science (80-.). 284: 1985–8.

Miyata, S., K. Taguchi, and S. Maekawa, 2003 Dendrite-associated opioid-binding cell adhesion molecule localizes at neurosecretory granules in the hypothalamic magnocellular neurons. Neuroscience 122: 169–181.

Mongkolsamrit, S., N. Kobmoo, K. Tasanathai, A. Khonsanit, W. Noisripoom *et al.*, 2012 Life cycle, host range and temporal variation of Ophiocordyceps unilateralis/Hirsutella formicarum on Formicine ants. J. Invertebr. Pathol. 111: 217–224.

Moore, J., 2013 An overview of parasite-induced behavioral alterations - and some lessons from bats. J. Exp. Biol. 216: 11–7.

Moore, J., 1995 The behavior of parazitized animals. When an ant... is not an ant. Bioscience 45: 89–96.

Moreno-Salinas, A. L., M. Avila-Zozaya, P. Ugalde-Silva, D. A. Hernández-Guzmán, F. Missirlis *et al.*, 2019 Latrophilins: A neuro-centric view of an evolutionary conserved adhesion g protein-coupled receptor subfamily. Front. Neurosci. 13: 700.

Murali, T., S. Pacifico, J. Yu, S. Guest, G. G. Roberts *et al.*, 2011 DroID 2011: a comprehensive, integrated resource for protein, transcription factor, RNA and gene interactions for Drosophila. Nucleic Acids Res. 39: D736–D743.

Muscedere, M. L., N. Johnson, B. C. Gillis, J. F. Kamhi, and J. F. A. Traniello, 2012 Serotonin modulates worker responsiveness to trail pheromone in the ant Pheidole dentata. J. Comp. Physiol. A Neuroethol. Sensory, Neural, Behav. Physiol. 198: 219–227.

Nässel, D. R., and M. J. Williams, 2014 Cholecystokinin-Like Peptide (DSK) in Drosophila, Not Only for Satiety Signaling. Front. Endocrinol. (Lausanne). 5:.

Neckameyer, W. S., C. M. Coleman, S. Eadie, and S. F. Goodwin, 2007 Compartmentalization of neuronal and peripheral serotonin synthesis in Drosophila melanogaster. Genes, Brain Behav. 6: 756–769.

Neckameyer, W. S., and K. White, 1992 A single locus encodes both phenylalanine hydroxylase and tryptophan hydroxylase activities in Drosophila. J. Biol. Chem. 267: 4199–4206.

Nelson, C. M., K. E. Ihle, M. K. Fondrk, R. E. Page, G. V Amdam *et al.*, 2007 The gene vitellogenin has multiple coordinating effects on social organization. PLoS Biol. 5: e62.

Nicholson, M. J., A. Koulman, B. J. Monahan, B. L. Pritchard, G. A. Payne *et al.*, 2009 Identification of two aflatrem biosynthesis gene loci in Aspergillus flavus and metabolic engineering of Penicillium paxilli to elucidate their function. Appl. Environ. Microbiol. 75: 7469–81.

Niehaus, E.-M., K. Kleigrewe, P. Wiemann, L. Studt, C. M. K. Sieber *et al.*, 2013 Genetic Manipulation of the Fusarium fujikuroi Fusarin Gene Cluster Yields Insight into the Complex Regulation and Fusarin Biosynthetic Pathway. Chem. Biol. 20: 1055–1066.

Nižňanský, Ľ., S. Kryštofová, P. Vargovič, M. Kaliňák, M. Šimkovič *et al.*, 2013 Glutamic acid decarboxylase gene disruption reveals signalling pathway(s) governing complex morphogenic and metabolic events in Trichoderma atroviride. Antonie van Leeuwenhoek, Int. J. Gen. Mol. Microbiol. 104: 793–807.

Norman, V. C., and W. O. H. Hughes, 2016 Behavioural effects of juvenile hormone and their influence on division of labour in leaf-cutting ant societies. J. Exp. Biol. 219: 8–11.

Nosanchuk, J. D., and A. Casadevall, 2006 Impact of melanin on microbial virulence and clinical resistance to antimicrobial compounds. Antimicrob. Agents Chemother. 50: 3519–3528.

Nosanchuk, J. D., R. E. Stark, and A. Casadevall, 2015 Fungal melanin: What do we know about structure? Front. Microbiol. 6: 1463.

O'Connell, K., J. Gannon, P. Doran, and K. Ohlendieck, 2008 Reduced expression of sarcalumenin and

related Ca2+-regulatory proteins in aged rat skeletal muscle. Exp. Gerontol. 43: 958–961.

O'Reilly, D. R., 1995 Baculovirus-encoded ecdysteroid UDP-glucosyltransferases. Insect Biochem. Mol. Biol. 25: 541–550.

O'Reilly, D. R., and L. K. Miller, 1989 A Baculovirus Blocks Insect Molting by Producing Ecdysteroid UDP-Glucosyl Transferase. Science (80-.). 245: 1110–1112.

Olombrada, M., E. Herrero-Galán, D. Tello, M. Oñaderra, J. G. Gavilanes *et al.*, 2013 Fungal extracellular ribotoxins as insecticidal agents. Insect Biochem. Mol. Biol. 43: 39–46.

Opachaloemphan, C., H. Yan, A. Leibholz, C. Desplan, and D. Reinberg, 2018 Recent Advances in Behavioral (Epi)Genetics in Eusocial Insects. Annu. Rev. Genet. 52: 489–510.

Osborne, A. R., T. A. Rapoport, and B. Van Den Berg, 2005 Protein translocation by the Sec61/SecY channel. http://dx.doi.org/10.1146/annurev.cellbio.21.012704.133214 21: 529–550.

Osborne, K. A., A. Robichon, E. Burgess, S. Butland, R. A. Shaw *et al.*, 1997 Natural Behavior Polymorphism Due to a cGMP-Dependent Protein Kinase of Drosophila. Science (80-.). 277: 834–836.

Oughtred, R., J. Rust, C. Chang, B. J. Breitkreutz, C. Stark *et al.*, 2021 The BioGRID database: A comprehensive biomedical resource of curated protein, genetic, and chemical interactions. Protein Sci. 30: 187.

Pan, C., Z. Liao, J. He, Z. Gu, C. Wang *et al.*, 2021 Carnosine concentration and expression profiles of carnosine related genes in Mytilus after beta-alanine injection. J. Oceanol. Limnol. 2021 1–14.

Panaccione, D. G., and S. L. Arnold, 2017 Ergot alkaloids contribute to virulence in an insect model of invasive aspergillosis. Sci. Rep. 7: 8930.

Pang, Z., J. Chong, G. Zhou, D. A. De Lima Morais, L. Chang *et al.*, 2021 MetaboAnalyst 5.0: narrowing the gap between raw spectra and functional insights. Nucleic Acids Res. 49: W388–W396.

Park, J., J. Park, S. Jang, S. Kim, S. Kong *et al.*, 2008 FTFD: an informatics pipeline supporting

phylogenomic analysis of fungal transcription factors. Bioinformatics 24: 1024–1025.

Parkinson, N., C. Conyers, and I. Smith, 2002a A venom protein from the endoparasitoid wasp Pimpla hypochondriaca is similar to snake venom reprolysin-type metalloproteases. J. Invertebr. Pathol. 79: 129–131.

Parkinson, N., E. H. Richards, C. Conyers, I. Smith, and J. P. Edwards, 2002b Analysis of venom constituents from the parasitoid wasp Pimpla hypochondriaca and cloning of a cDNA encoding a venom protein. Insect Biochem. Mol. Biol. 32: 729–735.

Pawson, T., and P. Nash, 2003 Assembly of cell regulatory systems through protein interaction domains. Science (80-.). 300: 445–452.

Penick, C. A., J. Liebig, and C. S. Brent, 2011 Reproduction, dominance, and caste: endocrine profiles of queens and workers of the ant Harpegnathos saltator. J. Comp. Physiol. A 197: 1063–1071.

Pentek, J., L. Parker, A. Wu, and K. Arora, 2009 Follistatin preferentially antagonizes activin rather than BMP signaling in *Drosophila*. genesis 47: 261–273.

Petryk, A., J. T. Warren, G. Marqués, M. P. Jarcho, L. I. Gilbert *et al.*, 2003 Shade is the Drosophila P450 enzyme that mediates the hydroxylation of ecdysone to the steroid insect molting hormone 20-hydroxyecdysone. Proc. Natl. Acad. Sci. U. S. A. 100: 13773–13778.

Pflüger, H. J., and C. Duch, 2011 Dynamic neural control of insect muscle metabolism related to motor behavior. Physiology 26: 293–303.

Piao, S., Y. L. Song, H. K. Jung, Y. P. Sam, W. P. Ji *et al.*, 2005 Crystal structure of a clip-domain serine protease and functional roles of the clip domains. EMBO J. 24: 4404.

Platten, M., E. A. A. Nollen, U. F. Röhrig, F. Fallarino, and C. A. Opitz, 2019 Tryptophan metabolism as a common therapeutic target in cancer, neurodegeneration and beyond. Nat. Rev. Drug Discov. 2019 185 18: 379–401.

Podlevsky, J. D., C. J. Bley, R. V Omana, X. Qi, and J. J.-L. Chen, 2008 The telomerase database.

Nucleic Acids Res. 36: D339-43.

Pokotylo, I., P. Pejchar, M. Potocký, D. Kocourková, Z. Krčková *et al.*, 2013 The plant non-specific phospholipase C gene family. Novel competitors in lipid signalling. Prog. Lipid Res. 52: 62–79.

Pontoppidan, M. B., W. Himaman, N. L. Hywel-Jones, J. J. Boomsma, and D. P. Hughes, 2009 Graveyards on the move: The spatio-temporal distribution of dead ophiocordyceps-infected ants (A. Dornhaus, Ed.). PLoS One 4: e4835.

Poulin, R., and F. Maure, 2015 Host Manipulation by Parasites: A Look Back Before Moving Forward. Trends Parasitol. 31: 563–570.

Prandovszky, E., E. Gaskell, H. Martin, J. P. Dubey, J. P. Webster *et al.*, 2011 The Neurotropic Parasite Toxoplasma Gondii Increases Dopamine Metabolism. PLoS One 6: e23866.

Pregitzer, P., M. Greschista, H. Breer, and J. Krieger, 2014 The sensory neurone membrane protein SNMP1 contributes to the sensitivity of a pheromone detection system. Insect Mol. Biol. 23: 733–742.

Punzo, F., and D. F. Williams, 1994 Free amino acids and biogenic amines in the brain of the carpenter ant, Campanotus floridanus (Buckley) (Hymenoptera, Formicidae). Comp. Biochem. Physiol. Part C Pharmacol. 107: 387–392.

R Core Team, 2014 R: A language and environment for statistical computing. R Foundation for Statistical Computing.

R Core Team, 2021 R: A language and environment for statistical computing.

Ragionieri, L., B. Özbagci, S. Neupert, Y. Salts, M. Davidovitch *et al.*, 2017 Identification of mature peptides from pban and capa genes of the moths Heliothis peltigera and Spodoptera littoralis. Peptides 94: 1–9.

Ramirez, J. L., E. J. Muturi, C. Dunlap, and A. P. Rooney, 2018 Strain-specific pathogenicity and subversion of phenoloxidase activity in the mosquito Aedes aegypti by members of the fungal

entomopathogenic genus Isaria. Sci. Reports 2018 81 8: 1–12.

Ramos, R. G. P., G. L. Igloi, B. Lichte, U. Baumann, D. Maier *et al.*, 1993 The irregular chiasm C-roughest locus of Drosophila, which affects axonal projections and programmed cell death, encodes a novel immunoglobulin-like protein. Genes Dev. 7: 2533–2547.

Rapti, G., J. Richmond, and J.-L. Bessereau, 2011 A single immunoglobulin-domain protein required for clustering acetylcholine receptors in C. elegans. EMBO J. 30: 706–18.

Raschle, T., D. Arigoni, R. Brunisholz, H. Rechsteiner, N. Amrhein *et al.*, 2007 Reaction Mechanism of Pyridoxal 5′-Phosphate Synthase: Detection of an enzyme-bound chromophoric intermediate. J. Biol. Chem. 282: 6098–6105.

Rashmi, D., R. Zanan, S. John, K. Khandagale, and A. Nadaf, 2018 γ-Aminobutyric Acid (GABA): Biosynthesis, Role, Commercial Production, and Applications. Stud. Nat. Prod. Chem. 57: 413–452.

Ratzka, C., C. Liang, T. Dandekar, R. Gross, and H. Feldhaar, 2011 Immune response of the ant Camponotus floridanus against pathogens and its obligate mutualistic endosymbiont. Insect Biochem. Mol. Biol. 41: 529–536.

Rawlings, N. D., M. Waller, A. J. Barrett, and A. Bateman, 2014 *MEROPS* : the database of proteolytic enzymes, their substrates and inhibitors. Nucleic Acids Res. 42: D503–D509.

Reed, J. E., J. R. Dunn, D. G. du Plessis, E. J. Shaw, P. Reeves *et al.*, 2007 Expression of cellular adhesion molecule “OPCML” is down-regulated in gliomas and other brain tumours. Neuropathol. Appl. Neurobiol. 33: 77–85.

Ren, G. R., F. Hauser, K. F. Rewitz, S. Kondo, A. F. Engelbrecht *et al.*, 2015 CCHamide-2 Is an Orexigenic Brain-Gut Peptide in Drosophila. PLoS One 10: e0133017.

Rivera-Perez, C., M. Nouzova, M. E. Clifton, E. M. Garcia, E. LeBlanc *et al.*, 2013 Aldehyde Dehydrogenase 3 Converts Farnesal into Farnesoic Acid in the Corpora Allata of Mosquitoes. Insect Biochem. Mol. Biol. 43: 675.

Rodríguez-Navarro, S., B. Llorente, M. Teresa Rodríguez-Manzaneque, A. Ramne, G. Uber *et al.*, 2002 Yeast Functional Analysis Report Functional analysis of yeast gene families involved in metabolism of vitamins B 1 and B 6. Yeast 19: 1261–1276.

Roeder, T., 2005 Tyramine AND Octopamine: Ruling Behavior and Metabolism. Annu. Rev. Entomol. 50: 447–477.

Rohlfs, M., and A. C. L. Churchill, 2011 Fungal secondary metabolites as modulators of interactions with insects and other arthropods. Fungal Genet. Biol. 48: 23–34.

Ros, V. I. D., S. van Houte, L. Hemerik, and M. M. van Oers, 2015 Baculovirus-induced tree-top disease: how extended is the role of *egt* as a gene for the extended phenotype? Mol. Ecol. 24: 249–258.

Ross, K. G., 1997 Multilocus evolution in fire ants: effects of selection, gene flow and recombination. Genetics 145: 961–74.

Ross, K. G., and L. Keller, 1998 Genetic control of social organization in an ant. Proc. Natl. Acad. Sci. 95: 14232–14237.

Rossi, F., R. Miggiano, D. M. Ferraris, and M. Rizzi, 2019 The synthesis of kynurenic acid in mammals: An updated kynurenine aminotransferase structural KATalogue. Front. Mol. Biosci. 6: 7.

RStudio Team, 2015 RStudio: Integrated Development for R.

Saha, T. T., S. W. Shin, W. Dou, S. Roy, B. Zhao *et al.*, 2016 Hairy and Groucho mediate the action of juvenile hormone receptor Methoprene-tolerant in gene repression. Proc. Natl. Acad. Sci. U. S. A. 113: E735–E743.

Sakai, T., A. Shiraishi, T. Kawada, S. Matsubara, M. Aoyama *et al.*, 2017 Invertebrate gonadotropin-releasing hormone-related peptides and their receptors: An update. Front. Endocrinol. (Lausanne). 8: 217.

Sakolrak, B., R. Blatrix, U. Sangwanit, and N. Kobmoo, 2018 Experimental infection of the ant Polyrhachis furcata with Ophiocordyceps reveals specificity of behavioural manipulation. Fungal

Ecol. 33: 122–124.

Salwinski, L., C. S. Miller, A. J. Smith, F. K. Pettit, J. U. Bowie *et al.*, 2004 The Database of Interacting Proteins: 2004 update. Nucleic Acids Res. 32: D449.

Sanz, R., G. B. Ferraro, and A. E. Fournier, 2015 IgLON cell adhesion molecules are shed from the cell surface of cortical neurons to promote neuronal growth. J. Biol. Chem. 290: 4330–42.

Sarov-Blat, L., W. V. So, L. Liu, and M. Rosbash, 2000 The Drosophila takeout Gene Is a Novel Molecular Link between Circadian Rhythms and Feeding Behavior. Cell 101: 647–656.

Schardl, C. L., C. A. Young, U. Hesse, S. G. Amyotte, K. Andreeva *et al.*, 2013 Plant-symbiotic fungi as chemical engineers: multi-genome analysis of the clavicipitaceae reveals dynamics of alkaloid loci. PLoS Genet. 9: e1003323.

Schiff, P. L. J., 2006 Ergot and its alkaloids. Am. J. Pharm. Educ. 70: 98.

Schulz, D. J., J. P. Sullivan, and G. E. Robinson, 2002 Juvenile Hormone and Octopamine in the Regulation of Division of Labor in Honey Bee Colonies. Horm. Behav. 42: 222–231.

Schuster-Böckler, B., and A. Bateman, 2007 Reuse of structural domain-domain interactions in protein networks. BMC Bioinformatics 8:.

Schwinghammer, M. A., X. Zhou, S. Kambhampati, G. W. Bennett, and M. E. Scharf, 2011 A novel gene from the takeout family involved in termite trail-following behavior. Gene 474: 12–21.

Scott, J. G., and Z. Wen, 2001 Cytochromes P450 of insects: the tip of the iceberg. Pest Manag. Sci. 57: 958–967.

Selinheimo, E., M. Saloheimo, E. Ahola, A. Westerholm-Parvinen, N. Kalkkinen *et al.*, 2006 Production and characterization of a secreted, C-terminally processed tyrosinase from the filamentous fungus Trichoderma reesei. FEBS J. 273: 4322–4335.

Sengupta, S., L. B. Crowe, S. You, M. A. Roberts, and F. R. Jackson, 2019 A Secreted Ig-Domain Protein Required in Both Astrocytes and Neurons for Regulation of Drosophila Night Sleep. Curr. Biol. 29:

2547-2554.e2.

Sethi, J., B. Zhao, V. Cuvillier-Hot, C. Boidin-Wichlacz, M. Salzet *et al.*, 2010 The receptor protein tyrosine phosphatase HmLAR1 is up-regulated in the CNS of the adult medicinal leech following injury and is required for neuronal sprouting and regeneration. Mol. Cell. Neurosci. 45: 430–438.

Shandala, T., K. Takizawa, and R. Saint, 2003 The dead ringer/retained transcriptional regulatory gene is required for positioning of the longitudinal glia in the Drosophilaembryonic CNS. Development 130: 1505–1513.

Shaw, H. S., S. A. Cameron, W.-T. Chang, and Y. Rao, 2019 The Conserved IgSF9 Protein Borderless Regulates Axonal Transport of Presynaptic Components and Color Vision in Drosophila. J. Neurosci. 39: 6817–6828.

Shaw, J. C., W. J. Korzan, R. E. Carpenter, A. M. Kuris, K. D. Lafferty *et al.*, 2009 Parasite manipulation of brain monoamines in California killifish (Fundulus parvipinnis) by the trematode Euhaplorchis californiensis. Proc. R. Soc. B Biol. Sci. 276: 1137–1146.

Shende, R., S. Sze, W. Wong, S. Rapole, R. Beau *et al.*, 2018 *Aspergillus fumigatus* conidial metalloprotease Mep1p cleaves host complement proteins. J. Biol. Chem. 239: 15538–15555.

Shields, E. J., L. Sheng, A. K. Weiner, B. A. Garcia, and R. Bonasio, 2018 High-Quality Genome Assemblies Reveal Long Non-coding RNAs Expressed in Ant Brains. Cell Rep. 23: 3078–3090.

Shinoda, T., and K. Itoyama, 2003 Juvenile hormone acid methyltransferase: a key regulatory enzyme for insect metamorphosis. Proc. Natl. Acad. Sci. U. S. A. 100: 11986–91.

Shoop, W. L., L. M. Gregory, M. Zakson-Aiken, B. F. Michael, H. W. Haines *et al.*, 2001 Systemic efficacy of nodulisporic acid against fleas on dogs. J. Parasitol. 87: 419–423.

Shyu, P., B. S. H. Ng, N. Ho, R. Chaw, Y. L. Seah *et al.*, 2019 Membrane phospholipid alteration causes chronic ER stress through early degradation of homeostatic ER-resident proteins. Sci. Reports 2019 91 9: 1–15.

Simão, F. A., R. M. Waterhouse, P. Ioannidis, E. V. Kriventseva, and E. M. Zdobnov, 2015 BUSCO: assessing genome assembly and annotation completeness with single-copy orthologs. Bioinformatics 31: 3210–3212.

Simola, D. F., R. J. Graham, C. M. Brady, B. L. Enzmann, C. Desplan *et al.*, 2016 Epigenetic (re)programming of caste-specific behavior in the ant Camponotus floridanus. Science (80-.). 351: aac6633.

Singh, K. D., R. K. Labala, T. B. Devi, N. I. Singh, H. D. Chanu *et al.*, 2017 Biochemical efficacy, molecular docking and inhibitory effect of 2, 3-dimethylmaleic anhydride on insect acetylcholinesterase. Sci. Reports 2017 71 7: 1–11.

Sivachenko, A., H. B. Gordon, S. S. Kimball, E. J. Gavin, J. L. Bonkowsky *et al.*, 2016 Neurodegeneration in a Drosophila model of adrenoleukodystrophy: the roles of the Bubblegum and Double bubble acyl-CoA synthetases. Dis. Model. Mech. 9: 377–87.

Sledzieski, S., R. Singh, L. Cowen, and B. Berger, 2021 D-SCRIPT translates genome to phenome with sequence-based, structure-aware, genome-scale predictions of protein-protein interactions. Cell Syst. 12: 969-982.e6.

Slot, J. C., E. Gluck-Thaler, J. Wideman, and T. Richards, 2019 Metabolic gene clusters, fungal diversity, and the generation of accessory functions. Curr. Opin. Genet. Dev. 59: 17–24.

Smit, S., M. F. L. Derks, S. Bervoets, A. Fahal, W. van Leeuwen *et al.*, 2016 Genome Sequence of Madurella mycetomatis mm55, Isolated from a Human Mycetoma Case in Sudan. Genome Announc. 4:.

Smith, M. M., V. A. Warren, B. S. Thomas, R. M. Brochu, E. A. Ertel *et al.*, 2000 Nodulisporic Acid Opens Insect Glutamate-Gated Chloride Channels: Identification of a New High Affinity Modulator. Biochemistry 39: 5543–5554.

Sondergaard, T. E., F. T. Hansen, S. Purup, A. K. Nielsen, E. C. Bonefeld-Jørgensen *et al.*, 2011 Fusarin

C acts like an estrogenic agonist and stimulates breast cancer cells in vitro. Toxicol. Lett. 205: 116–121.

Sonobe, H., T. Ohira, K. Ieki, S. Maeda, Y. Ito *et al.*, 2006 Purification, kinetic characterization, and molecular cloning of a novel enzyme, ecdysteroid 22-kinase. J. Biol. Chem. 281: 29513–24.

Srivastava, D., R. K. Singh, M. A. Moxley, M. T. Henzl, D. F. Becker *et al.*, 2012 The Three-Dimensional Structural Basis of Type II Hyperprolinemia. J. Mol. Biol. 420: 176–189.

St Leger, R., L. Joshi, M. J. Bidochka, and D. W. Roberts, 1996 Construction of an improved mycoinsecticide overexpressing a toxic protease. Proc. Natl. Acad. Sci. U. S. A. 93: 6349–54.

Stanke, M., M. Diekhans, R. Baertsch, and D. Haussler, 2008 Using native and syntenically mapped cDNA alignments to improve de novo gene finding. Bioinformatics 24: 637–644.

Stankiewicz, M., A. Hamon, R. Benkhalifa, W. Kadziela, B. Hue *et al.*, 199AD Effects of a centipede venom fraction on insect nervous system, a native Xenopus oocyte receptor and on an expressed Drosophila muscarinic receptor. Toxicon 37: 1431–1445.

Stengl, M., and N. W. Funk, 2013 The role of the coreceptor Orco in insect olfactory transduction. J. Comp. Physiol. A 199: 897–909.

Strausbach, P., and E. H. Fischer, 1970 Structure of the binding site of pyridoxal 5'-phosphate to Escherichia coli glutamate decarboxylase. Biochemistry 9: 233–238.

Strigini, M., R. Cantera, X. Morin, M. J. Bastiani, M. Bate *et al.*, 2006 The IgLON protein Lachesin is required for the blood–brain barrier in Drosophila. Mol. Cell. Neurosci. 32: 91–101.

Stuart, J. M., E. Segal, D. Koller, and S. K. Kim, 2003 A gene-coexpression network for global discovery of conserved genetic modules. Science (80-.). 302: 249–255.

Su, L., C. Yang, J. Meng, L. Zhou, and C. Zhang, 2021 Comparative transcriptome and metabolome analysis of Ostrinia furnacalis female adults under UV-A exposure. Sci. Reports | 11: 6797.

Subramanian, A., P. Tamayo, V. K. Mootha, S. Mukherjee, B. L. Ebert *et al.*, 2005 Gene set enrichment

analysis: A knowledge-based approach for interpreting genome-wide expression profiles. Proc. Natl. Acad. Sci. U. S. A. 102: 15545–15550.

Sugumaran, M., and H. Barek, 2016 Critical Analysis of the Melanogenic Pathway in Insects and Higher Animals. Int. J. Mol. Sci. 17:.

Supek, F., M. Bošnjak, N. Škunca, and T. Šmuc, 2011 REVIGO Summarizes and Visualizes Long Lists of Gene Ontology Terms. PLoS One 6: e21800.

Szczuka, A., J. Korczyńska, A. Wnuk, B. Symonowicz, A. Gonzalez Szwacka *et al.*, 2013 The effects of serotonin, dopamine, octopamine and tyramine on behavior of workers of the ant Formica polyctena during dyadic aggression tests. Acta Neurobiol. Exp. (Wars). 73: 495–520.

Sztal, T., H. Chung, S. Berger, P. D. Currie, P. Batterham *et al.*, 2012 A Cytochrome P450 Conserved in Insects Is Involved in Cuticle Formation. PLoS One 7: e36544.

Tallant, C., R. García-Castellanos, A. Marrero, M. Solà, U. Baumann *et al.*, 2007 Substrate specificity of a metalloprotease of the pappalysin family revealed by an inhibitor and a product complex. Arch. Biochem. Biophys. 457: 57–72.

Tang, B., K. Becanovic, P. A. Desplats, B. Spencer, A. M. Hill *et al.*, 2012 Forkhead box protein p1 is a transcriptional repressor of immune signaling in the CNS: implications for transcriptional dysregulation in Huntington disease. Hum. Mol. Genet. 21: 3097.

Tenebaum, D., and B. Maintainer, 2021 KEGGREST: Client-side REST access to the Kyoto Encyclopedia of Genes and Genomes (KEGG).

Thanabalu, T., J. Hindley, J. Jackson-Yap, and C. Berry, 1991 Cloning, sequencing, and expression of a gene encoding a 100-kilodalton mosquitocidal toxin from Bacillus sphaericus SSII-1. J. Bacteriol. 173: 2776–85.

Therneau, T., 2015 A Package for Survival Analysis in S.

Thomas, F., R. Poulin, and J. Brodeur, 2010 Host manipulation by parasites: A multidimensional

phenomenon. Oikos 119: 1217–1223.

Tiwari, V., S. Ambadipudi, and A. B. Patel, 2013 Glutamatergic and GABAergic TCA cycle and neurotransmitter cycling fluxes in different regions of mouse brain. J. Cereb. Blood Flow Metab. 33: 1523.

Trapnell, C., A. Roberts, L. Goff, G. Pertea, D. Kim *et al.*, 2012 Differential gene and transcript expression analysis of RNA-seq experiments with TopHat and Cufflinks. Nat. Protoc. 7: 562–578.

Trienens, M., and M. Rohlfs, 2011 Experimental evolution of defense against a competitive mold confers reduced sensitivity to fungal toxins but no increased resistance in Drosophila larvae. BMC Evol. Biol. 11: 206.

Trinh, T., R. Ouellette, and C. de Bekker, 2021 Getting lost: the fungal hijacking of ant foraging behaviour in space and time. Anim. Behav. 181: 165–184.

Tsentsevitsky, A. N., I. V. Kovyazina, L. F. Nurullin, and E. E. Nikolsky, 2017 Muscarinic cholinoreceptors (M1-, M2-, M3- and M4-type) modulate the acetylcholine secretion in the frog neuromuscular junction. Neurosci. Lett. 649: 62–69.

Tsugawa, H., T. Cajka, T. Kind, Y. Ma, B. Higgins *et al.*, 2015 MS-DIAL: data-independent MS/MS deconvolution for comprehensive metabolome analysis. Nat. Methods 2015 126 12: 523–526.

Turk, V., V. Stoka, O. Vasiljeva, M. Renko, T. Sun *et al.*, 2012 Cysteine cathepsins: From structure, function and regulation to new frontiers. Biochim. Biophys. Acta - Proteins Proteomics 1824: 68–88.

Turner, B., S. Razick, A. L. Turinsky, J. Vlasblom, E. K. Crowdy *et al.*, 2010 iRefWeb: interactive analysis of consolidated protein interaction data and their supporting evidence. Database J. Biol. Databases Curation 2010:.

Urban, M., A. Cuzick, K. Rutherford, A. Irvine, H. Pedro *et al.*, 2017 PHI-base: a new interface and further additions for the multi-species pathogen–host interactions database. Nucleic Acids Res. 45:

D604–D610.

Valdes, J. J., J. E. Cameron, and R. J. Cole, 1985 Aflatrem: a tremorgenic mycotoxin with acute neurotoxic effects. Environ. Health Perspect. 62: 459.

Vandenborre, G., G. Smagghe, B. Ghesquière, G. Menschaert, R. N. Rao *et al.*, 2011 Diversity in Protein Glycosylation among Insect Species. PLoS One 6: e16682.

VanderMolen, K. M., H. A. Raja, T. El-Elimat, and N. H. Oberlies, 2013 Evaluation of culture media for the production of secondary metabolites in a natural products screening program. AMB Express 3: 71.

van der Veen, J. N., J. P. Kennelly, S. Wan, J. E. Vance, D. E. Vance *et al.*, 2017 The critical role of phosphatidylcholine and phosphatidylethanolamine metabolism in health and disease. Biochim. Biophys. Acta - Biomembr. 1859: 1558–1572.

Velarde, R. A., G. E. Robinson, and S. E. Fahrbach, 2009 Coordinated responses to developmental hormones in the Kenyon cells of the adult worker honey bee brain (Apis mellifera L.). J. Insect Physiol. 55: 59–69.

Velarde, R. A., G. E. Robinson, and S. E. Fahrbach, 2006 Nuclear receptors of the honey bee: annotation and expression in the adult brain. Insect Mol. Biol. 15: 583–595.

Venugopala Reddy, G., C. Reiter, S. Shanbhag, K.-F. Fischbach, and V. Rodrigues, 1999 Irregular chiasm-C-roughest, a member of the immunoglobulin superfamily, affects sense organ spacing on the Drosophila antenna by influencing the positioning of founder cells on the disc ectoderm. Dev. Genes Evol. 209: 581–591.

Verlinden, H., 2018 Dopamine signalling in locusts and other insects. Insect Biochem. Mol. Biol. 97: 40–52.

Walhout, A. J. M., R. Sordella, X. Lu, J. L. Hartley, G. F. Temple *et al.*, 2000 Protein interaction mapping in C. elegans Using proteins involved in vulval development. Science (80-.). 287: 116–122.

Walker, B. J., T. Abeel, T. Shea, M. Priest, A. Abouelliel *et al.*, 2014 Pilon: An Integrated Tool for Comprehensive Microbial Variant Detection and Genome Assembly Improvement (J. Wang, Ed.). PLoS One 9: e112963.

Walter, A., U. Korth, M. Hilgert, J. Hartmann, O. Weichel *et al.*, 2004 Glycerophosphocholine is elevated in cerebrospinal fluid of Alzheimer patients. Neurobiol. Aging 25: 1299–1303.

Wang-Eckhardt, L., A. Bastian, T. Bruegmann, P. Sasse, and M. Eckhardt, 2020 Carnosine synthase deficiency is compatible with normal skeletal muscle and olfactory function but causes reduced olfactory sensitivity in aging mice. J. Biol. Chem. 295: 17100–17113.

Wang, Y., H. Jiang, Y. Cheng, C. An, Y. Chu *et al.*, 2017 Activation of Aedes aegypti prophenoloxidase-3 and its role in the immune response against entomopathogenic fungus. Insect Mol. Biol. 26: 552.

Wang, H., H. Peng, W. Li, P. Cheng, and M. Gong, 2021 The Toxins of Beauveria bassiana and the Strategies to Improve Their Virulence to Insects. Front. Microbiol. 12: 2375.

Wang, C., and S. Wang, 2017 Insect Pathogenic Fungi: Genomics, Molecular Interactions, and Genetic Improvements. http://dx.doi.org/10.1146/annurev-ento-031616-035509 62: 73–90.

Wang, D., L. Zou, Q. Jin, J. Hou, G. Ge *et al.*, 2018 Human carboxylesterases: a comprehensive review. Acta Pharm. Sin. B 8: 699–712.

Watford, M., 2008 Glutamine Metabolism and Function in Relation to Proline Synthesis and the Safety of Glutamine and Proline Supplementation. J. Nutr. 138: 2003S-2007S.

Weitekamp, C. A., R. Libbrecht, and L. Keller, 2017 Genetics and Evolution of Social Behavior in Insects. Annu. Rev. Genet. 51: 219–239.

White, T. J., T. Bruns, S. Lee, and J. Taylor, 1990 Amplification and direct sequencing of fungal ribosomal RNA genes for phylogenetics, in *PCR Protocols: A Guide to Methods and Applications*,.

Wichadakul, D., N. Kobmoo, S. Ingsriswang, S. Tangphatsornruang, D. Chantasingh *et al.*, 2015 Insights from the genome of Ophiocordyceps polyrhachis-furcata to pathogenicity and host specificity in

insect fungi. BMC Genomics 16: 881.

Wicher, D., S. Morinaga, L. Halty-deLeon, N. Funk, B. Hansson *et al.*, 2017 Identification and characterization of the bombykal receptor in the hawkmoth Manduca sexta. J. Exp. Biol. 220: 1781–1786.

Wick, R., 2018 Porechop.

Wickham, H., 2016 *ggplot2: Elegant Graphics for Data Analysis*. Springer-Verlag, New York.

Will, I., B. Das, T. Trinh, A. Brachmann, R. A. Ohm *et al.*, 2020 Genetic Underpinnings of Host Manipulation by Ophiocordyceps as Revealed by Comparative Transcriptomics. G3 (Bethesda). 10: 2275–2296.

Williams, C. R., A. Baccarella, J. Z. Parrish, and C. C. Kim, 2016 Trimming of sequence reads alters RNA-Seq gene expression estimates. BMC Bioinformatics 17: 103.

Wilson, N. H., and B. Key, 2007 Neogenin: One receptor, many functions. Int. J. Biochem. Cell Biol. 39: 874–878.

Win, J., A. Chaparro-Garcia, K. Belhaj, D. G. O. Saunders, K. Yoshida *et al.*, 2012 Effector Biology of Plant-Associated Organisms: Concepts and Perspectives. Cold Spring Harb. Symp. Quant. Biol. 77: 235–247.

Wiygul, G., and P. P. Sikorowski, 1991 The effect of a heat-stable enterotoxin isolated from Escherichia coli on pheromone production in fat bodies isolated from male boll weevils. Entomol. Exp. Appl. 60: 305–308.

Wiygul, G., and P. P. Sikorowski, 1986 The effect of staphylococcal enterotoxin B on pheromone production in fat bodies isolated from male boll weevils. J. Invertebr. Pathol. 47: 116–119.

Wolstenholme, A. J., 2012 Glutamate-gated chloride channels. J. Biol. Chem. 287: 40232–40238.

Wong, Y.-H., A.-C. Lu, Y.-C. Wang, H.-C. Cheng, C. Chang *et al.*, 2010 Protogenin Defines a Transition Stage during Embryonic Neurogenesis and Prevents Precocious Neuronal Differentiation. J.

Neurosci. 30: 4428–4439.

Wu, C. Y., I. C. Hu, Y. C. Yang, W. C. Ding, C. H. Lai *et al.*, 2020 An essential role of acetyl coenzyme A in the catalytic cycle of insect arylalkylamine N-acetyltransferase. Commun. Biol. 2020 31 3: 1–12.

Wu, Z., L. Yang, Q. He, and S. Zhou, 2021 Regulatory Mechanisms of Vitellogenesis in Insects. Front. Cell Dev. Biol. 8: 1863.

Wurm, Y., J. Wang, and L. Keller, 2010 Changes in reproductive roles are associated with changes in gene expression in fire ant queens. Mol. Ecol. 19: 1200–1211.

Xiao, G., S.-H. Ying, P. Zheng, Z.-L. Wang, S. Zhang *et al.*, 2012 Genomic perspectives on the evolution of fungal entomopathogenicity in Beauveria bassiana. Sci. Rep. 2: 483.

Xing, X., M. Yan, H. Pang, an Wu, J. Wang *et al.*, 2021 Cytochrome P450s Are Essential for Insecticide Tolerance in the Endoparasitoid Wasp Meteorus pulchricornis (Hymenoptera: Braconidae).

Xu, X., X. Wen, D. M. Veltman, I. Keizer-Gunnink, H. Pots *et al.*, 2017 GPCR-controlled membrane recruitment of negative regulator C2GAP1 locally inhibits Ras signaling for adaptation and long-range chemotaxis. Proc. Natl. Acad. Sci. U. S. A. 114: E10092–E10101.

Yakovlev, I. K., 2018 Effects of Octopamine on Aggressive Behavior in Red Wood Ants. Neurosci. Behav. Physiol. 2018 483 48: 279–288.

Yamamoto, S., and E. S. Seto, 2014 Dopamine dynamics and signaling in Drosophila: an overview of genes, drugs and behavioral paradigms. Exp. Anim. 63: 107–19.

Yamashita, R. A., J. R. Sellers, and J. B. Anderson, 2000 Identification and analysis of the myosin superfamily in Drosophila: a database approach. J. Muscle Res. Cell Motil. 21: 491–505.

Yan, H., C. Opachaloemphan, G. Mancini, H. Yang, M. Gallitto *et al.*, 2017 An engineered orco mutation produces aberrant social behavior and defective neural development in ants. Cell 170: 736.

Yang, Z., Y. Yu, V. Zhang, Y. Tian, W. Qi *et al.*, 2015 Octopamine mediates starvation-induced

hyperactivity in adult Drosophila. Proc. Natl. Acad. Sci. U. S. A. 112: 5219–24.

Yao, Y., X. Cui, I. Al-Ramahi, X. Sun, B. Li *et al.*, 2015 A striatal-enriched intronic GPCR modulates huntingtin levels and toxicity. Elife 4:.

Yao, Y., A. B. Peter, R. Baur, and E. Sigel, 1989 The tremorigen aflatrem is a positive allosteric modulator of the gamma-aminobutyric acidA receptor channel expressed in Xenopus oocytes. Mol. Pharmacol. 35:.

Ye, C., Z. Song, T. Wu, W. Zhang, N. U. Saba *et al.*, 2021 Endocuticle is involved in caste differentiation of the lower termite. Curr. Zool. 67: 489.

Yin, Z., H. Liu, Z. Li, X. Ke, D. Dou *et al.*, 2015 Genome sequence of Valsa canker pathogens uncovers a potential adaptation of colonization of woody bark. New Phytol. 208: 1202–1216.

Yoon, S. J., I. K. Lyoo, C. Haws, T. S. Kim, B. M. Cohen *et al.*, 2009 Decreased Glutamate/Glutamine Levels May Mediate Cytidine's Efficacy in Treating Bipolar Depression: A Longitudinal Proton Magnetic Resonance Spectroscopy Study. Neuropsychopharmacol. 2009 347 34: 1810–1818.

Yu, J., P.-K. Chang, K. C. Ehrlich, J. W. Cary, D. Bhatnagar *et al.*, 2004a Clustered pathway genes in aflatoxin biosynthesis. Appl. Environ. Microbiol. 70: 1253–62.

Yu, X. M., I. Gutman, T. J. Mosca, T. Iram, E. Ozkan *et al.*, 2013 Plum, an immunoglobulin superfamily protein, regulates axon pruning by facilitating TGF-β signaling. Neuron 78: 456–68.

Yu, P., Z. Li, L. Zhang, D. A. Tagle, and T. Cai, 2006 Characterization of kynurenine aminotransferase III, a novel member of a phylogenetically conserved KAT family. Gene 365: 111–118.

Yu, P., N. A. Di Prospero, M. T. Sapko, T. Cai, A. Chen *et al.*, 2004b Biochemical and phenotypic abnormalities in kynurenine aminotransferase II-deficient mice. Mol. Cell. Biol. 24: 6919–30.

Zhang, H., H. Saitoh, and M. J. Matunis, 2002 Enzymes of the SUMO modification pathway localize to filaments of the nuclear pore complex. Mol. Cell. Biol. 22: 6498–6508.

Zhang, J. D., S. Wiemann, M. Carlson, and T. Chiang, 2021 RpsiXML: R interface to PSI-MI 2.5 files.

Zhang, Q.-R. R., W.-H. H. Xu, F.-S. S. Chen, and S. Li, 2005 Molecular and biochemical characterization of juvenile hormone epoxide hydrolase from the silkworm, Bombyx mori. Insect Biochem. Mol. Biol. 35: 153–164.

Zhao, X., M. Yoshida, L. Brotto, H. Takeshima, N. Weisleder *et al.*, 2005 Enhanced resistance to fatigue and altered calcium handling properties of sarcalumenin knockout mice. Physiol. Genomics 23: 72–78.

Zheng, S., R. Loreto, P. Smith, A. Patterson, D. Hughes *et al.*, 2019 Specialist and Generalist Fungal Parasites Induce Distinct Biochemical Changes in the Mandible Muscles of Their Host. Int. J. Mol. Sci. 20:.

Zheng, P., Y. Xia, G. Xiao, C. Xiong, X. Hu *et al.*, 2011 Genome sequence of the insect pathogenic fungus Cordyceps militaris, a valued traditional Chinese medicine. Genome Biol. 12: R116.

Zhou, Y.-L., X.-Q. Zhu, S.-H. Gu, H. Cui, Y.-Y. Guo *et al.*, 2014 Silencing in Apolygus lucorum of the olfactory coreceptor Orco gene by RNA interference induces EAG response declining to two putative semiochemicals. J. Insect Physiol. 60: 31–39.

Zhuang, J. X., Y. H. Hu, M. H. Yang, F. J. Liu, L. Qiu *et al.*, 2010 Irreversible Competitive Inhibitory Kinetics of Cardol Triene on Mushroom Tyrosinase. J. Agric. Food Chem. 58: 12993–12998.

Zhuang, S., H. Shao, F. Guo, R. Trimble, E. Pearce *et al.*, 2009 Sns and Kirre, the Drosophila orthologs of Nephrin and Neph1, direct adhesion, fusion and formation of a slit diaphragm-like structure in insect nephrocytes. Development 136: 2335–44.

Zinke, I., C. Kirchner, L. C. Chao, M. T. Tetzlaff, and M. J. Pankratz, 1999 Suppression of food intake and growth by amino acids in Drosophila: the role of pumpless, a fat body expressed gene with homology to vertebrate glycine cleavage system. Development 126: 5275–5284.